UNIVERSIDADE FEDERAL DO RIO GRANDE DO SUL

INSTITUTO DE CIÊNCIAS BÁSICAS DA SAÚDE

PROGRAMA DE PÓS-GRADUAÇÃO EM CIÊNCIAS BIOLÓGICAS:

BIOQUÍMICA

EFEITOS DO ÁCIDO QUINOLÍNICO SOBRE A HOMEOSTASE DO CITOESQUELETO DE CÉREBRO DE RATOS JOVENS: ÊNFASE NAS VIAS DE SINALIZAÇÃO. ASPECTOS NEUROQUÍMICOS, HISTOLÓGICOS E MORFOLÓGICOS DO DANO CELULAR

Paula Pierozan

Porto Alegre

2014

UNIVERSIDADE FEDERAL DO RIO GRANDE DO SUL

INSTITUTO DE CIÊNCIAS BÁSICAS DA SAÚDE

PROGRAMA DE PÓS-GRADUAÇÃO EM CIÊNCIAS BIOLÓGICAS:

BIOQUÍMICA

EFEITOS DO ÁCIDO QUINOLÍNICO SOBRE A HOMEOSTASE DO CITOESQUELETO DE CÉREBRO DE RATOS JOVENS: ÊNFASE NAS VIAS DE SINALIZAÇÃO. ASPECTOS NEUROQUÍMICOS, HISTOLÓGICOS E MORFOLÓGICOS DO DANO CELULAR

Paula Pierozan

Orientadora: Prof[a] Dr[a] Regina Pessoa-Pureur

Co-Orientador: Prof. Dr. Moacir Wajner

Tese apresentada ao Programa de Pós-Graduação em Ciências Biológicas – Bioquímica da Universidade Federal do Rio Grande do Sul, como requisito parcial à obtenção do grau de Doutor em Bioquímica.

Porto Alegre

2014

AGRADECIMENTOS

Aos meus pais, pelo incentivo, apoio, compreensão das minhas escolhas e caminhos, e pelo imenso amor e carinho que me dedicaram a vida toda. Obrigada por terem me dado um exemplo de caráter e honestidade.

Ao meu irmão, por todos os momentos dedicados a me aconselhar e apoiar.

Ao Rodrigo, pela compreensão nos momentos difíceis, pelo companheirismo e pelo amor. Essa caminhada seria muito mais difícil sem ti ao meu lado.

Á Regui, por todos os ensinamentos, oportunidades, orientação deste trabalho e ajuda no crescimento dos meus conhecimentos científicos. Muito obrigada pela amizade e carinho que sempre dedicaste a mim.

À Ariane, por ter me recebido de braços abertos no lab, ter me ensinado tudo sobre fosforilação de proteínas e por ser um exemplo para mim como profissional e pessoa.

Ás meninas do lab 31, por toda a ajuda nesses anos, pela amizade e momentos compartilhados.

Aos funcionários do Departamento de Bioquímica, por toda a ajuda no desenvolvimento deste trabalho.

Ao CNPQ, pela bolsa concedida.

ÍNDICE

PARTE I

PARTE II

PARTE I

RESUMO

O ácido quinolínico (QUIN) é um metabólito implicado na patologia de diversas doenças neurodegenerativas, sendo que a injeção intraestriatal com QUIN é um modelo bastante utilizado para o estudo da doença de Huntington (DH). A DH envolve manifestações cognitivas, motoras e neuropsiquiátricas, sendo que a forma juvenil da doença (DHJ) tem uma progressão dos sintomas muito mais rápida e é bem menos estudada que a forma adulta. No presente trabalho desenvolvemos um modelo animal da DHJ, além de utilizarmos abordagens *ex vivo* e estudos *in vitro* com o objetivo de avaliar os efeitos do QUIN sobre a homeostase do citoesqueleto, as vias de sinalização direcionadas ao equilíbrio de fosforilação/desfosforilação dos filamentos intermediários (FI) de astrócitos e neurônios e a participação do citoesqueleto das células neurais sobre o dano celular no estriado, cortex cerebral e hipocampo de ratos jovens. Também foram avaliados parâmetros comportamentais no estudo *in vivo*. Para o estudo *in vivo*, os ratos foram submetidos a uma injeção intraestriatal de QUIN (150 nmol) ou solução salina (controles) e os parâmetros bioquímicos e comportamentais foram avaliados 1, 7, 14 e 21 dias após a injeção. Para o estudo *ex vivo*, foram utilizadas fatias de estriado tratadas com QUIN (100 µM) ou tampão fisiológico (controles) durante 50 min e ferramentas farmacológicas foram utilizadas para estudar as vias de sinalização envolvidas nos efeitos causados pela neurotoxina no citoesqueleto. Os estudos *in vitro* foram desenvolvidos utilizando astrócitos e neurônios estriatais em cultura primária, onde as células foram tratadas com QUIN (10-500 µM) ou apenas com veículo (controles) por 24 h. Os resultados mostraram que os ratos injetados com QUIN apresentaram uma diminuição da captação de glutamato e um aumento na captação de Ca^{2+} logo após a infusão. Estes efeitos causaram alteração na fosforilação dos FI, propagaram-se do estriado para o córtex cerebral e hipocampo e foram acompanhados de gliose reativa e neurodegeneração no estriado e córtex, mas não no hipocampo. Além disso, os animais apresentaram déficit cognitivo que precedeu as alterações motoras, o que é uma característica da DHJ. O estudo *ex vivo* mostrou que o QUIN causou hiperfosforilação das subunidades dos neurofilamentos (NF) e da proteína glial fibrilar ácida (GFAP), FI de neurônios e astrócitos, respectivamente. Esses efeitos foram dependentes da ativação de receptores glutamatérgicos ionotrópicos e metabotrópicos, do influxo de Ca^{2+} através de canais de Ca^{2+} dependentes de voltagem (VDCC) e da ativação de cinases dependentes e independentes de segundos mensageiros. Além disso, o estudo *in vitro* mostrou que a alteração da fosforilação dos FI neurais é acompanhada de reorganização do citoesqueleto neuronal e astroglial por mecanismos envolvendo Ca^{2+}. Os efeitos sobre o citoesqueleto neuronal foram totalmente revertidos pelo meio condicionado de astrócitos tratados com QUIN. Ainda, o estudo em co-cultura astrócito/neurônio mostrou que há uma proteção recíproca contra os efeitos do QUIN. O conjunto dos nossos dados evidencia que o dano excitotóxico causado pelo QUIN, através do aumento do influxo de Ca^{2+} para o citoplasma, pode ser um dos principais responsáveis pela desregulação das cascatas de sinalização intracelulares direcionadas para o citoesqueleto, sendo então o citoesqueleto neural um importante alvo para as ações do QUIN no cérebro de ratos jovens. A formação de um quadro de excitotoxicidade, o rompimento da homeostase do citoesqueleto e a alteração tecidual e celular parecem ser etapas iniciais no dano causado pelo QUIN e podem estar relacionados com os déficits comportamentais observados nos animais. Acreditamos que esses resultados são relevantes para a compreensão dos mecanismos moleculares envolvidos na neurotoxicidade causada pelo QUIN em animais jovens e esperamos que a continuidade desse estudo possa contribuir ainda mais para o estudo das bases moleculares da DHJ.

ABSTRACT

Quinolinic acid (QUIN) is a neuroactive metabolite considered to be involved in neurodegenerative disorders, and the intrastriatal injection of QUIN is a commonly used model for the study of HD. The disease involves cognitive, motor and neuropsychiatric manifestations, and the juvenile form of the disease (JHD) has a more rapid progression of symptoms and is much less studied. In the present work we developed an animal model of JHD and ex vivo and in vitro approaches to evaluate the effects of QUIN on the homeostasis of the cytoskeleton, signaling pathways targeting the phosphorylation/dephosphorylation equilibrium of astrocyte and neuron intermediate filaments (IF) and the involvement of the cytoskeleton of neural cells on cell damage in the striatum, cerebral cortex and hippocampus of young rats. Behavioral parameters were also evaluated on *in vivo* study. For the *in vivo* study, rats were subjected to an instrastriatal injection of QUIN (150 nmol) or saline (controls) and the biochemical and behavioral parameters were evaluated 1, 7, 14 and 21 days after injection. For *ex vivo* study, striatal slices treated with QUIN (100 µM) or buffer (control) for 50 min and pharmacological approaches were used to study the signaling pathways involved in the effects caused by the neurotoxin on cytoskeleton. *In vitro* studies were developed using striatal neurons and astrocytes in primary culture, where cells were treated with QUIN (10-500 mM) or vehicle only (controls) for 24 h. The results showed that rats injected with QUIN showed a decrease in uptake of glutamate and increased uptake of Ca^{2+} after infusion. These effects caused alterations in the phosphorylation of IFs that propagated from striatum to cerebral cortex and hippocampus and were accompanied by reactive gliosis and neurodegeneration in cortex and striatum but not in hippocampus. Furthermore, the animals showed cognitive deficits that preceded motor changes, which is a characteristic of JHD. *Ex vivo* studies showed that QUIN caused hyperphosphorylation of neurofilament subunits (NF) and glial fibrillary acidic protein (GFAP), IF of neurons and astrocytes, respectively. These effects were dependent on the activation of ionotropic and metabotropic glutamate receptors, Ca^{2+} influx through voltage-dependent Ca^{2+} (VDCC) and the kinase-dependent and independent of activation of second messengers. Moreover, *in vitro* studies showed that the change in phosphorylation of neural IFs is accompanied by reorganization of the neuronal and astroglial cytoskeleton by mechanisms involving Ca^{2+}. The effects on the neuronal cytoskeleton were completely reversed by the conditioned medium of astrocytes treated with QUIN. Also, the study with co-cultured astrocyte-neuron showed that there is a mutual protection against the effects of QUIN. The set of our data shows that the excitotoxic damage caused by QUIN by increasing the influx of Ca^{2+} into the cytoplasm can be a major contributor to the misregulation of cascades of intracellular signaling directed to the cytoskeleton, making the cytoskeleton an important target for the actions of QUIN in brain of young rats. The formation of excitotoxicity, the disruption of cytoskeletal homeostasis and changes in cell tissue appear to be steps in the initial damage caused by QUIN and may be associated with behavioral deficits observed in the animals. We believe that these findings have contributed to a better understanding of the molecular mechanisms involved in the neurotoxicity caused by QUIN in young rats and we expect that the continuation of this study can contribute to the better understanding of the molecular basis of JHD.

LISTA DE ABREVIATURAS

3-HAO	Enzima ácido 3-hidroxiantranílico
AC	Adenilato ciclase
AMPA	Ácido α-amino-3-hidroxi-5-metil-4-isoxazolepropiônico
BDNF	Fator neurotrófico derivado do cérebro
Ca^{2+}	Cálcio
Cdk5	Cinase dependente de ciclina 5
CNF	Fator de crescimento ciliar
DAG	Diacilglicerol
DARPP-32	Fosfoproteína regulada por dopamine e AMPc
DH	Doença de Huntington
DHJ	Doença de Huntington Juvenil
GFAP	Proteína glial fibrilar ácida
IDO	Indoleamina 2,3-dioxigenase
iGluR	Receptor glutamatérgico ionotrópico
IP3	Inositol trifosfato
FGF	Fator de crescimento de fibroblastos
FI	Filamentos Intermediários
MAP2	Proteína associada ao microtúbulo 2
MAPK	Proteína cinase ativada por mitógeno
mGluR	Receptor glutamatérgico metabotrópico
MF	Microfilamentos
MT	Microtúbulos

NEM	Neurônios espinhais médios
NF	Neurofilamentos
NFH	Neurofilamento de alto peso molecular
NFL	Neurofilamento de médio peso molecular
NFM	Neurofilamento de médio peso molecular
NMDA	N-metil-D-aspartato
nNOS	Óxido nítrico sintase neuronal
NT	Neurotransmissor
PLC	Fosfolipase C
PKA	Proteína cinase A
PKC	Proteína cinase C
PKCaMII	Proteína cinase dependente de cálcio e calmodulina
PP1	Proteína fosfatase 1
PP2A	Proteína fosfatase 2A
PP2B	Proteína fosfatase 2B
QPRT	Quinolinato fosforribosiltransferase
QUIN	Ácido quinolínico
RE	Retículo endoplasmático
RQ	Rota das quinureninas
SNC	Sistema Nervoso Central
SNP	Sistema Nervoso Periférico
VDCC	Canal de cálcio voltagem-dependente
VIM	Vimentina

LISTA DE FIGURAS E TABELAS

1. INTRODUÇÃO

1.1. BIOSSÍNTESE DO ÁCIDO QUINOLÍNICO - ROTA DAS QUINURENINAS

O triptofano é um aminoácido essencial que possui funções biológicas importantes. Nos mamíferos, cerca de 90% do triptofano da dieta é metabolizado através da rota das quinureninas (RQ) (Figura 1) (Schwarcz et al., 2012). A RQ é a maior fonte de nicotinamida-adenina dinucleotídeo (NAD^+), um cofator importante para a respiração celular, produção de ATP, reparo ao DNA e regulação da transcrição gênica (Anderson et al., 2002, Massudi et al., 2012). No SNC, essa rota ocorre nos astrócitos, macrófagos ativados e na microglia (Ruddick et al., 2006). Estudos demonstraram que os metabólitos da RQ participam de funções cerebrais normais como moduladores da neurotransmissão glutamatérgica. Porém, muitos grupos de pesquisa têm estudado as ações destes metabólitos na fisiopatologia de diversas doenças neurodegenerativas e imunológicas (Schwarcz et al., 2012, Stone et al., 2013).

A RQ é formada por uma sequência de enzimas principalmente gliais e seus metabólitos estão presentes normalmente em concentrações nanomolares no cérebro de mamíferos. A enzima regulatória mais importante da via no SNC é a indoleamina 2,3-dioxigenase (IDO) (Schwarcz et al., 2012). Vários estudos têm demonstrado que o interferon c e b, fator de necrose tumoral, peptídeo β-amilóide, entre outros, podem aumentar a expressão celular da IDO, com consequente aumento na produção de seus metabólitos (Takikawa et al., 1986, Heyes et al., 1997, Pemberton et al., 1997, Smith et al., 2001). A RQ produz vários intermediários com funções neuroativas, como o ácido quinurênico, um antagonista de receptores NMDA, a 3-hidroxiquinurenina, que possui

propriedades pró-oxidantes, e o ácido quinolínico (QUIN), um agonista de receptores NMDA (Schwarcz et al., 2012). Entre estes metabólitos, o QUIN é considerado o mais importante em termos de neurotoxicidade.

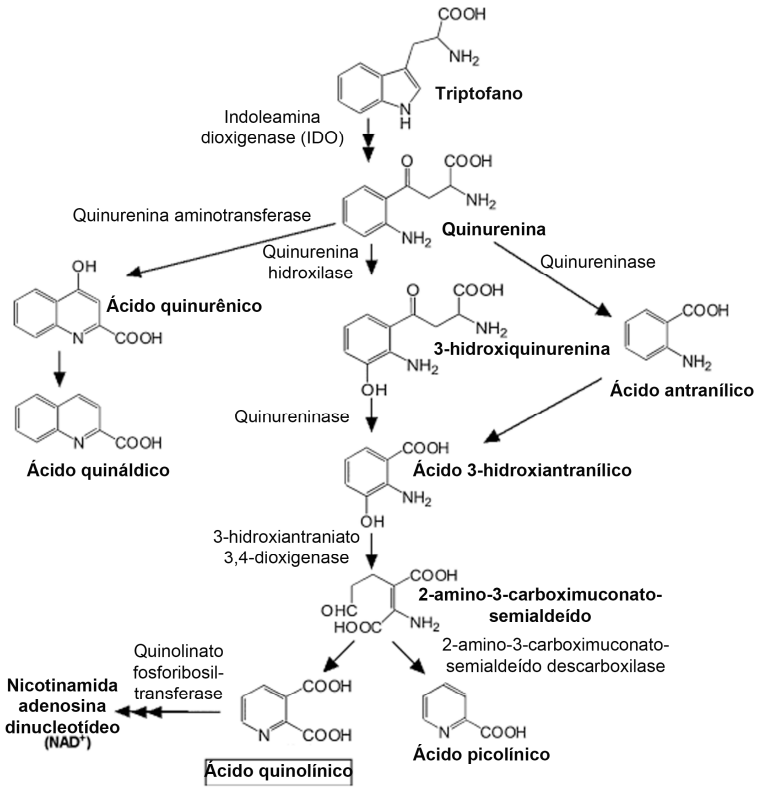

Figura 1. Via das kinureninas (adaptado de Guillemin *et al*, 2012).

1.1.2. NEUROTOXICIDADE PRODUZIDA PELO ÁCIDO QUINOLÍNICO (QUIN)

O padrão de toxicidade que o QUIN exerce é consideravelmente complexo, com muitos mecanismos potencialmente envolvidos. Em um primeiro momento, ele exerce excessiva ativação de receptores N-metil-D-aspartato (NMDA), especificamente os subtipos NR2A e NR2B, causando uma entrada excessiva de Ca^{2+} em neurônios e astrócitos. Como consequência do aumento de Ca^{2+}, há disfunção mitocondrial, diminuição dos níveis de ATP, liberação de citocromo *c* e estresse oxidativo. Estes

efeitos são dependentes de ativação primária de receptores glutamatérgicos e produção de radicais livres, além da inibição da atividade de diversas enzimas da cadeia de respiração celular (Perez-De La Cruz et al., 2007).

O QUIN também causa aumento de liberação de glutamato pelos neurônios e inibe sua recaptação pelos astrócitos (Tavares et al., 2008). Além disso, ele limita o ciclo glutamato-glutamina em astrócitos por diminuir a atividade da enzima glutamina sintetase (Ting et al., 2009), aumentando a concentração de glutamato no microambiente e causando excitotoxicidade. Outro mecanismo importante de neurotoxicidade causada pelo QUIN é a peroxidação lipídica, através da formação de um complexo QUIN-Fe^{2+} que desencadeia a formação de espécies reativas de oxigênio (Goda et al., 1996, Stipek et al., 1997), além de modificar o perfil de diversos antioxidantes endógenos (Perez-De La Cru et al., 2013) .

Durante os processos neuroinflamatórios que ocorrem em diversas doenças do SNC, o aumento da produção de QUIN é um passo chave que desencadeia uma cascata de eventos que irão contribuir para os efeitos deletérios vistos nessas doenças. O QUIN atua em múltiplos alvos, causando desde excitotoxicidade, estresse oxidativo e dano ao DNA, até alterações morfológicas e na dinâmica do citoesqueleto (Figura 2). Esses múltiplos efeitos vão se refletir na perda de várias funções cognitivas e motoras que podem estar relacionadas com a fisiopatologia observada em várias doenças neurodegenerativas, especialmente a doença de Huntington (DH) (Perez-De La Cruz et al., 2012).

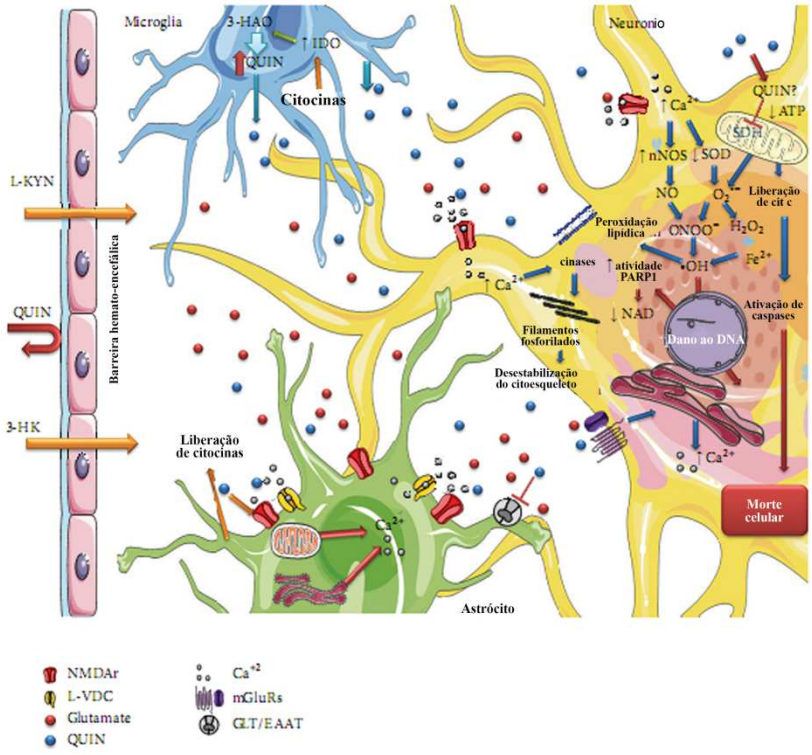

Figura 2. Múltiplos mecanismos que causam toxicidade induzida por QUIN. Um dos principais mecanismos tóxicos se dá pela superativação dos receptores NMDA. Além disso, QUIN aumenta a liberação de glutamato sinaptossomal como uma consequência da inibição da captação de glutamato pelos astrócitos, o que leva a uma superestimulação dos receptores glutamatérgicos. O QUIN pode diminuir a atividade de enzimas antioxidantes, causando produção de espécies reativas de oxigênio e gerando peroxidação lipídica. Ele também pode inibir a atividade de complexos mitocondriais, levando a um déficit energético, ativando caspases e liberando o citocromo c. Todos estes fatores induzem desestabilização do citoesqueleto, dano ao DNA, e morte celular. Adaptado de Perez-de-La-Cruz *et al.* 2012.

1.2. DOENÇA DE HUNTINGTON

A DH é um transtorno neurodegenerativo autossômico dominante caracterizado por uma extensa neurodegeneração no corpo estriado e córtex cerebral, o que resulta em disfunções motoras, cognitivas e neuropsiquiátricas. Ela se manifesta quando o gene da proteína huntintina apresenta um número aumentado de repetições CAG, resultando em uma proteína mutante contendo um sítio amino-terminal alongado, que é formado por várias repetições de glutamina (Munoz-Sanjuan and Bates, 2011). O início dos sintomas é inversamente proporcional ao número de repetições CAG que a proteína apresenta. Quando a proteína apresenta aproximadamente 40 resíduos de glutamina, a doença se

apresenta durante a fase adulta. A doença adulta é caracterizada por alterações motoras, como movimentos repetitivos involuntários, chamados de movimentos coreiformes, além de distúrbios psiquiátricos como agressividade e depressão. Nos estágios finais, aproximadamente 20 anos após o início dos sintomas, os movimentos coreiformes são substituídos por rigidez e bradicinesia, até a morte do paciente (Wang and Qin, 2006).

A forma juvenil da doença (DHJ) ocorre quando a proteína apresenta mais de 60 repetições, e representa cerca de 10% dos pacientes com a DH. A DHJ é caracterizada por uma rápida progressão dos sintomas, sendo que os distúrbios comportamentais normalmente são os primeiros sintomas da doença, precedendo as alterações motoras (Nance and Myers, 2001). Os pacientes apresentam uma rápida deterioração cognitiva, hiperatividade e comportamento desafiador (Gonzalez-Alegre and Afifi, 2006), sendo que estes sintomas progridem rapidamente ao longo dos anos, evoluindo para rigidez muscular, convulsões e perda acentuada das funções cognitivas. A morte do paciente ocorre entre 7 a 10 anos depois (Rasmussen et al., 2000).

O estriado é a principal estrutura cerebral afetada na DH, apresentando pronunciada degeneração dos neurônios espinhais médios (NEM) (Wilson et al., 1990). Mais tardiamente, há a degeneração dos neurônios piramidais das camadas III, V e VI do córtex cerebral (Vonsattel and DiFiglia, 1998). Embora estas duas regiões sejam os principais alvos da doença, um estudo recente mostrou que os pacientes com esse transtorno também apresentam alterações hipocampais (Ransome et al., 2012).

Vários estudos têm demonstrado que a RQ e seus metabólitos estão envolvidos nos mecanismos patológicos na DH. Estudos em cérebros post-mortem revelaram que os níveis de QUIN estão substancialmente elevados nos estágios iniciais da doença, especialmente nas regiões cerebrais que sofrem mais dano, como o corpo estriado e o córtex cerebral (Guidetti et al., 2004). Este aumento, que coincide com a ativação

precoce da microglia, gera concentrações de QUIN claramente capazes de produzir dano excitotóxico.

Modelos animais têm revelado muito a cerca da patogênese da DH e são ferramentas úteis para testar novos alvos terapêuticos. Dentre eles, os modelos genéticos e excitotóxicos são os mais utilizados. Os modelos genéticos apresentam algumas das alterações encontradas na doença humana (Wang and Qin, 2006). Porém, os animais podem desenvolver diabetes e muitos desses modelos transgênicos não apresentam apoptose ou a neurodegeneração corticoestriatal característica da doença (Nance and Myers, 2001; Sathasivam et al., 1999). Por outro lado, a injeção intraestriatal com QUIN induz alterações comportamentais e bioquímicas que mimetizam os achados da DH (Colle et al., 2012; Kalonia et al., 2012; Sadan et al., 2012). Além disso, um estudo pré-clínico mostrou que a administração de QUIN no estriado de ratos causa a morte dos NEM e reproduz várias das alterações comportamentais e bioquímicas vistas na DH (Estrada Sanchez et al., 2008). Deste modo, a injeção intraestriatal com QUIN em ratos adultos se tornou um modelo experimental bastante utilizado para estudar as mudanças patológicas vistas na doença e testar novos tratamentos terapêuticos para a enfermidade. Porém, ainda há poucos estudos sobre as alterações causadas pela injeção com QUIN no cérebro em desenvolvimento. Visto que, apesar do considerável progresso no estudo dos mecanismos deletérios que ocorrem na DH e na DHJ, ainda não há um tratamento efetivo para a prevenção ou diminuição dos sintomas, é de extrema importância o desenvolvimento de novos modelos animais e mais estudos a respeito dos mecanismos de ação fisiopatológicos que ocorrem nesta doença.

1.3. CITOESQUELETO

As células eucarióticas apresentam funções estruturais e mecânicas altamente desenvolvidas, adotando uma grande variedade de formas, para reorganizar seus componentes internos e desenvolver movimentos coordenados e direcionados em resposta ao ambiente. Estas diversas habilidades são dependentes de uma complexa rede de filamentos proteicos que se estende através de todo o citoplasma, denominada citoesqueleto (Alberts et al., 2008). Nos últimos anos, os estudos do citoesqueleto vêm sendo fortemente associados a estudos sobre transdução de sinal. Tornou-se claro que a rede de filamentos do citoesqueleto e as vias de sinalização celular funcionam cooperativamente para gerar um fenótipo adaptado às condições da célula. Quando a célula recebe um sinal, as respostas estruturais comandadas pelo citoesqueleto podem se refletir na formação de novos eixos de polaridade, geração de protrusões, formação ou quebra de contatos, movimentos, divisão, proliferação ou morte. Todos esses eventos envolvem mais de um componente do citoesqueleto, incluindo uma miríade de proteinas associadas, mostrando a complexidade das interações entre as vias de sinalização e o citoesqueleto (Hollenbeck, 2001).

No sistema nervoso central (SNC), os neurônios e as células da glia possuem uma morfologia complexa, relacionada com as suas funções, sendo os componentes do citoesqueleto os principais reponsáveis pela morfologia neural, modificando-se em resposta a uma variedade de sinais extracelulares (Sanchez et al., 2000). Durante a morfogênese neuronal, por exemplo, diferentes proteínas do citoesqueleto se reorganizam para promover a elongação dos neuritos e subsequente estabilização de axônios e dendritos formados (Ludin and Matus, 1993, Letourneau, 1996). Além disso, as proteínas do citoesqueleto têm papel fundamental na criação e manutenção do calibre axonal, bem como no transporte de organelas e substâncias envolvidas na transmissão

sináptica (Kirkpatrick and Brady, 1999) e na organização dos receptores de membrana (Carraway, 2000).

As diversas atividades do citoesqueleto dependem de três tipos de filamentos proteicos: os microfilamentos (MFs), os microtúbulos (MTs) e os filamentos intermediários (FI), (Figura 3). Esses sistemas proteicos são conectados entre si e suas funções são coordenadas por um conjunto de proteínas acessórias, permitindo a participação do citoesqueleto em inúmeras atividades celulares (Alberts et al., 2008). As subunidades constituintes dos MFs e MTs, actina e tubulina respectivamente, são proteínas globulares altamente conservadas. Essas subunidades possuem a característica comum de terem sua dinâmica controlada pela hidrólise de nucleotídeos (Herrmann and Aebi, 2000). Por outro lado, os membros da família dos FIs são compostos por subunidades de proteínas fibrosas específicas de cada tipo celular e sua dinâmica independe da hidrólise de nucleotídios (Fuchs, 1994, Szeverenyi et al., 2008).

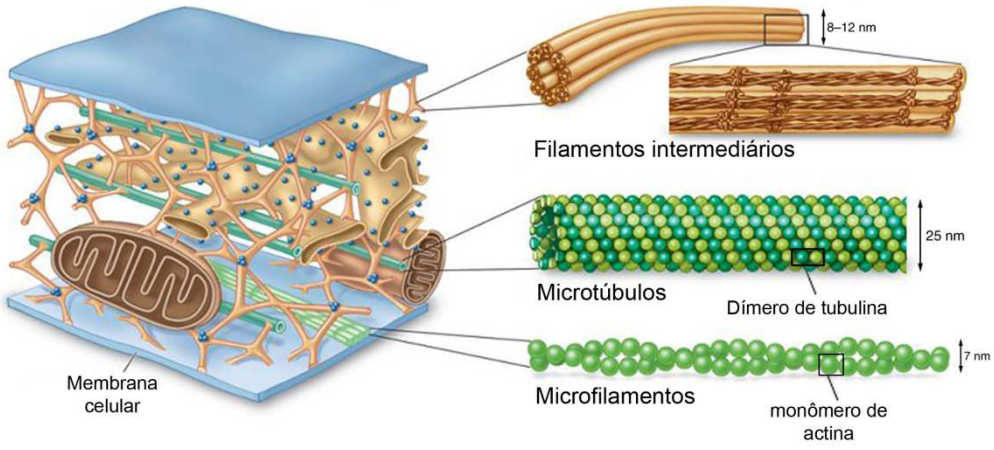

Figura 3. Citoesqueleto das células eucarióticas. O citoesqueleto é constituído por microtúbulos, filamentos intermediários e microfilamentos. Os microfilamentos são formados por uma dupla fita e são responsáveis pela contração muscular, forma da célula e movimentos citoplasmáticos. Os filamentos intermediários são formados por subunidades que formam polímeros, e ajudam na manutenção da forma celular, suportam a extensão das células nervosas e mantém as células unidas. Os microtúbulos são formados por dímeros de α e β-tubulina, e estão associados com o transporte de organelas e cromossomos (adaptado de Snauer Associates, Inc. Publishers).

1.3.1. MICROFILAMENTOS

A actina é uma das mais abundantes e altamente conservadas proteínas das células eucarióticas. Ela é uma proteína globular de 42 kDa que pode sofrer ciclos de auto-associação, gerando um equilíbrio dinâmico entre a forma filamentosa (associada, polimerizada) e a monomérica (desassociada, despolimerizada), através de regulação pela hidrólise de ATP (Campellone and Welch, 2010).

Os MF têm um papel importante na morfologia e motilidade celular, fagocitose, migração, adesão e exocitose/endocitose. Eles são pequenos filamentos flexíveis, situados na região cortical da célula e ancorados à membrana plasmática (Omary et al., 2006). Além disso, eles podem formar tanto estruturas estáveis quanto instáveis dentro da célula. Os MF estáveis formam o coração das microvilosidades e são componentes cruciais do aparato contrátil das células musculares. No entanto, muitos movimentos celulares, como migração e motilidade celular, dependem da dinâmica das estruturas instáveis formadas pelos MF em resposta a estímulos externos (Alberts et al., 2008).

A instabilidade dos filamentos de actina em consequência da hidrólise do ATP em ADP + Pi, é acompanhada por mudanças conformacionais cruciais para o *turnover* destes filamentos. Um *turnover* aumentado dos filamentos de actina é conhecido por promover a longevidade celular, enquanto que a sua estabilização inicia eventos de morte celular, como apoptose (Gourlay and Ayscough, 2005). Além disso, várias evidências mostram que drogas que previnem a polimerização de actina são capazes de alterar várias funções celulares (Alberts et al., 2008) e causar a liberação de espécies reativas de oxigênio, com consequente morte celular (Gourlay and Ayscough, 2005).

1.3.2. FILAMENTOS INTERMEDIÁRIOS

Os filamentos intermediários (FI) são formados pela associação de subunidades fibrosas, formando fibras resistentes encontradas na maioria das células animais. Eles foram denominados intermediários por causa do seu diâmetro (8-10 nm), que está entre o dos MF (7-8 nm) e o dos MT (25 nm) (Alberts et al., 2008). Os FI constituem a família mais diversificada de proteínas do citoesqueleto e são codificados por cerca de 70 genes no genoma humano (Fuchs, 1994), possuindo um alto grau de especificidade celular e sendo frequentemente considerados marcadores de diferenciação celular (Alberts et al., 2008, Eriksson et al., 2009). As subunidades dos FI consistem em um domínio central altamente conservado em α-hélice, e domínios N-terminal e C-terminal variáveis, sendo classificados em seis sub-grupos, de acordo com o tipo celular e o padrão de desenvolvimento (Fuchs, 1994).

Na maioria das células eucarióticas, uma extensa rede de FI circunda o núcleo e se estende para a periferia da célula, interagindo com a membrana plasmática. Eles são particularmente proeminentes no citoplasma de células sujeitas a estresse mecânico, como por exemplo, células epiteliais, axônios neuronais e células musculares (Alberts et al., 2008). No citoplasma, eles provêm sustentação para a mitocôndria, complexo de Golgi, centros de organização dos microtúbulos e outros elementos do citoesqueleto (Green et al., 2005, Herrmann et al., 2007), sendo ancorados em especializações da membrana plasmática, como desmossomos, hemidesmossomos e adesões focais. Essa rede integra e organiza o citoplasma provendo a integridade mecânica que é crucialmente importante para as funções celulares e teciduais (Figura 4). Além disso, os FI estão envolvidos em processos regulatórios, metabólicos e de sinalização celular. Recentemente foi demonstrado que eles possuem efeitos citoprotetores relacionados com a sua capacidade de interagir com vias de sinalização envolvidas na sobrevivência

celular (Eriksson et al., 2009). A natureza dinâmica dos FI é refletida pela sua reorganização em resposta a uma ampla variedade de estímulos fisiológicos, incluindo mitose e apoptose, além de uma variedade de estresses celulares (Omary et al., 2006). Há uma grande lista de desordens genéticas humanas causadas por deficiências nesta rede de organização dos FI, incluindo laminopatias (relacionadas às laminas nucleares, os FI nucleares), miopatias e neuropatias (Magin et al., 2004, Omary et al., 2004).

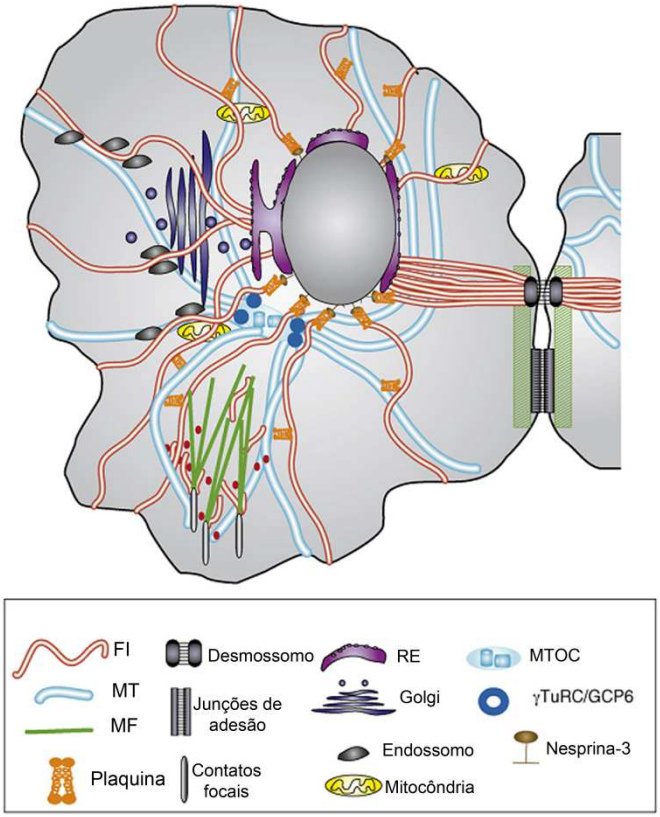

Figura 4. Os FIs são integradores da citoarquitetura. Eles estão ancorados no núcleo e se estendem para o citoplasma, formando pontos de contato na membrana plasmática, associando-se com a mitocôndria, as membranas do complexo de Golgi e o sistema endolisossomal. Os FIs também posicionam os centros de organização dos microtúbulos, influenciando a organização dos MT e as propriedades de suas proteínas transportadoras. Os FI também posicionam os centros de organização dos microtúbulos (MTOCs), através de interações com o complexo γTuRC/GCP6, influenciando a organização dos MT e as propriedades de distribuição das proteínas de membrana (Adaptado de Godsel et al, 2007).

1.3.2.1. NEUROFILAMENTOS

O desenvolvimento e manutenção de um sistema nervoso funcional são dependentes de uma ordenada elaboração e manutenção da matriz axonal, que por sua

vez é dependente da organização do citoesqueleto axonal. Há uma grande variedade de padrões neurais dependendo do tipo celular. Os axônios do Sistema Nervoso Periférico (SNP), por exemplo, excedem 1 metro em comprimento, então não é surpreendente que uma estrutura estável, porém dinâmica, se torne essencial para manter a forma destas células. Esta estrutura é formada pelos FI específicos dos neurônios, os neurofilamentos (NFs) (Koenig, 2009).

Os NFs são um sistema de fibras proteicas altamente estáveis arquitetonicamente. Eles são classificados como FI tipo IV (Fuchs and Cleveland, 1998) e exercem um importante papel estrutural que, junto com as proteínas associadas aos microtúbulos (MAP), formam a rede de sustentação de axônios e dendritos, além de promoverem o crescimento e calibre axonal, consequentemente regulando a velocidade de condução do impulso nervoso (Friede and Samorajski, 1970). Além disso, eles estão envolvidos na diferenciação e regeneração neuronal (Morris and Lasek, 1984).

Os NFs são formados por três subunidades proteicas: a subunidade de baixo peso molecular (NFL) com 68kDa, a subunidade de médio peso molecular (NFM) com 150 kDa e a subunidade de alto peso molecular (NFH) com 200 kDa (Lee and Cleveland, 1996). Originalmente, foi assumido que os NF eram compostos apenas pelas subunidades NFL, NFM e NFH. Porém, estudos indicaram que outras proteínas, como a α-internexina no SNC, e a periferina no SNP, estão co-associadas aos NF (Beaulieu et al., 1999). A extremidade amino-terminal, juntamente com a região em alfa-hélice da subunidade NFL interagem lateralmente e longitudinalmente formando a estrutura propriamente dita do NF, enquanto que a região carboxi-terminal das subunidades NFM e NFH é responsável pelas projeções laterais, que permitem a interação dos NF entre si e com os demais constituintes do citoesqueleto (Gotow et al., 1992).

Acúmulos dos NFs são vistos em uma variedade de doenças neurodegenerativas, como esclerose amiotrófica lateral, doença de Parkinson, e doença de Alzheimer (Bartos

et al., 2012, Su et al., 2012, Puentes et al., 2014). Vários fatores podem levar à agregação anormal dos NFs, incluindo desregulação da expressão gênica, mutações nos NFs e alterações no sistema fosforilante associado ao citoesqueleto (Julien, 1999). Além disso, modelos transgênicos têm suportado a ideia de que este acúmulo aberrante de NFs pode ser a causa da morte dos neurônios afetados, ao invés de ser simplesmente consequência das inúmeras disfunções neurais identificadas nessas doenças (Cote et al., 1993).

1.3.2.2. PROTEINA GLIAL FIBRILAR ÁCIDA E VIMENTINA

A proteína glial fibrilar ácida (GFAP) é o principal FI de astrócitos maduros, e por este motivo é considerada um marcador destas células. A vimentina (vim) é o FI expresso em células mesenquimais, além de ser encontrada nos astrócitos imaturos (Alberts et al., 2008).

O papel estrutural da GFAP em astrócitos é conhecido há bastante tempo. Porém, nos últimos anos, ela tem se mostrado importante em diversas funções astrocitárias, como regeneração após processos patológicos, plasticidade sináptica, gliose reativa, manutenção da forma, migração celular e como alvo de vias de transdução de sinais. Além disso, a GFAP participa de um sofisticado sistema de comunicação entre os astrócitos e neurônios (Middeldorp and Hol, 2011).

Várias doenças apresentam aumento na expressão de GFAP, como a doença de Alzheimer, encefalomielite, esclerose múltipla (Eng and Ghirnikar, 1994) e doença de Alexander (Middeldorp and Hol, 2011). Por outro lado, estudos com animais knockout para a GFAP têm mostrado que falta dessa proteína parece tornar os astrócitos menos eficientes em lidar com estados agudos de injúrias no SNC (Pekny and Pekna, 2004).

O principal mecanismo de regulação dos FI é através da fosforilação de suas subunidades.

1.4. FOSFORILAÇÃO DE PROTEÍNAS

A fosforilação/desfosforilação de proteínas (Figura 5) tem um papel essencial em diversos aspectos da vida celular. Proteínas cinases regulam vias de sinalização e processos celulares que irão mediar o metabolismo, transcrição gênica, progressão do ciclo celular, apoptose, comunicação intercelular, funções neuronais e imunológicas. Em especial, a fosforilação/desfosforilação de proteínas do citoesqueleto é um dos principais mecanismos pós-traducionais que regulam a diferenciação, rearranjo e movimentação do citoesqueleto em resposta a sinais intra e extracelulares (Johnson, 2009).

No SNC, a fosforilação proteica, através de Ser/Thr cinases, é um mecanismo molecular dinâmico de fundamental importância na regulação de muitas funções neuronais, onde diversos sinais produzem efeitos fisiológicos nas células alvo através da regulação do estado de fosforilação de determinadas fosfoproteínas (Ubersax and Ferrell, 2007). Essa modificação covalente regula a função de proteínas em resposta a estímulos extracelulares, chamados primeiros mensageiros, como neurotransmissores, hormônios, fatores tróficos e drogas. Segundos mensageiros típicos, como AMPc, inositol-3-fosfato (IP3) e cálcio (Ca^{+2}), transduzem o sinal a partir do primeiro mensageiro, ativando cascatas de cinases ou fosfatases que, por sua vez, modificam o estado de fosforilação de proteínas intracelulares, regulando as funções neurais. Proteínas alvo são fosforiladas por uma ampla variedade de cinases e os grupamentos fosfato das fosfoproteinas são removidos por fosfatases, traduzindo-se num processo dinâmico capaz de modular uma resposta fisiológica (Helfand et al., 2005).

As proteínas cinases compartilham um domínio catalítico conservado, que catalisa a transferência de um fosfato do ATP para um resíduo de serina, treonina ou tirosina no substrato proteico. As cinases existem em um estado ativo ou inativo e são reguladas por uma variedade de mecanismos que incluem controle por fosforilação, por adição de domínios, por ligação e regulação de subunidades e também por associação proteína-proteína (Johnson, 2009).

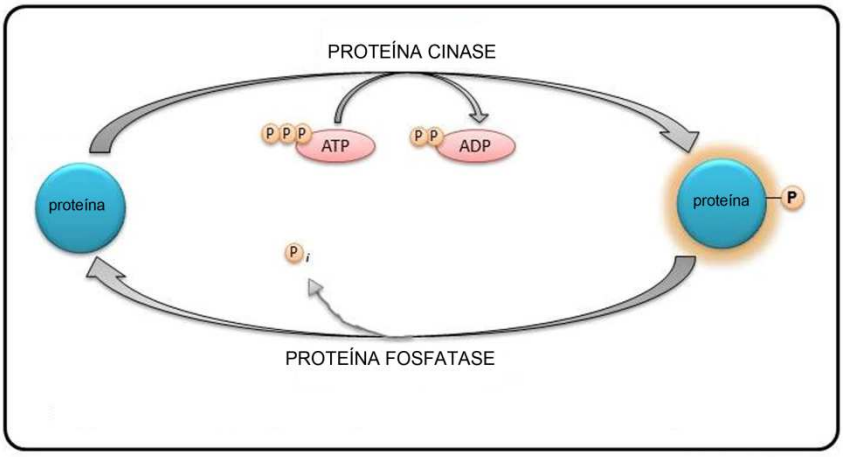

Figura 5. Regulação das proteínas celulares por fosforilação. Proteínas cinases transferem grupos fosfato do ATP para resíduos de serina, treonina ou tirosina em um substrato proteico. A remoção dos grupos fosfato é catalisada por proteínas fosfatases. Adaptado de Purves *et al*. 2005.

1.4.1. FOSFORILAÇÃO COMO MECANISMO REGULATÓRIO DOS FI

A fosforilação/desfosforilação é o principal mecanismo regulatório dos FI e de outras proteínas do citoesqueleto e alterações nos níveis fisiológicos de fosforilação/desfosforilação destas proteinas são consideradas eventos críticos em patologias do SNC (Miller et al., 2002), podendo levar a disfunções neurológicas e morte celular. Um grande número de doenças neurodegenerativas, como doença de Alzheimer, doença de Parkinson e doença de Huntington (DH) são caracterizadas por acúmulo de agregados de filamentos insolúveis no citoplasma das células (Goedert, 1998, Julien, 1999, DiProspero et al., 2004), os quais estão relacionados à desregulação

na atividade de cinases e fosfatases associadas aos FI, constituindo-se num achado comum na neurodegeneração (Petzold, 2005).

Resultados experimentais mostram que as subunidades de FI são altamente fosforiladas nos seus domínios amino e carbóxi-terminais, sendo o domínio amino-terminal fosforilado principalmente por cinases dependentes de segundos mensageiros, como a proteina cinase A (PKA), proteína cinase C (PKC), proteína cinase dependente de Ca^{+2} e calmodulina II (PKCaMII), enquanto que o domínio carbóxi-terminal é fosforilado por cinases independentes de segundos mensageiros, como as proteínas cinases ativadas por mitógenos (MAPK) e a proteína cinase dependente de ciclina 5 (cdk5), o que pode alterar drasticamente a fisiologia destes filamentos (Chang and Goldman, 2004, Sihag et al., 2007, Zamoner et al., 2008, Heimfarth et al., 2012, Pierozan et al., 2012).

As Ser/Thr fosfatases também desempenham um papel importante na manutenção da integridade estrutural dos FI (Eriksson et al. 1992) e sinais que rompem o equilíbrio de ação destas enzimas são capazes de causar um desequilíbrio na homeosatase dos FI. Inúmeros trabalhos de nosso grupo têm mostrado a importância das proteínas fosfatases mediando respostas dos NF e GFAP a diferentes metabólitos e toxinas em modelos animais de doenças metabólicas e neurotoxicidade. As principais Ser/Thr fosfatases associadas à desfosforilação dos FI em células neurais são: proteína fosfatase 1, 2A e 2B, ou calcineurina (Loureiro et al., 2009, Loureiro et al., 2010a, Heimfarth et al., 2012).

O balanço entre as atividades de proteínas cinases e fosfatases é essencial para as funções que os FI desempenham nas células (Goto et al., 1998, Inada et al., 1999), sendo que o estudo dos mecanismos da ação dessas enzimas é de grande importância na compreensão da dinâmica das proteínas do citoesqueleto e de seu envolvimento no funcionamento celular (Inada et al., 1999). Neste contexto, a

fosforilação/desfosforilação do domínio amino-terminal no NFL e NFM tem sido relacionada com a associação\desassociação destas subunidades (Gotow, 2000). Já a fosforilação/desfosforilação do domínio carbóxi-terminal do NFM e NFH regula a interação dos NFs entre si e com outras estruturas do citoesqueleto (Sihag et al., 2007, Shea and Chan, 2008) e está também envolvida na regulação do calibre axonal e da velocidade do transporte através do axônio (Ackerley et al., 2003). Os NF hipofosforilados são transportados mais rapidamente através do axônio que os extensivamente fosforilados (Jung et al., 2000), sendo que o aumento excessivo de sua fosforilação retarda o transporte dos NFs, levando a acúmulos patológicos destas proteínas em regiões proximais ou distais dos axônios, observados em diferentes patologias (Ackerley et al., 2000, Ackerley et al., 2004, Juranek et al., 2013).

A GFAP apresenta seis diferentes sítios de fosforilação identificados, sendo cinco identificados na região amino-terminal e um identificado na região carboxi-terminal (Inagaki et al., 1990, Nakamura et al., 1992). É sabido que a fosforilação da GFAP em resíduos específicos na região amino-terminal está envolvida na regulação da associação entre as suas subunidades. Essa regulação é importante para a redistribuição da GFAP durante o ciclo celular (Ralton et al., 1994). Estudos com mutações na região amino-terminal da GFAP mostraram uma associação anormal entre as suas subunidades *in vitro*, enquanto que mutações na região carboxi-terminal causaram modificação na morfologia do filamento, o que é importante para a sua associação com outras proteínas citoplasmáticas (Pekny et al., 1999).

1.5. SINALIZAÇÃO CELULAR

Para se adaptar às mudanças no ambiente, as células precisam de sinais, que devem ser cuidadosamente regulados e coordenados. Para isto, a sinalização celular

requer tanto moléculas sinalizadoras extracelulares e receptores de proteínas, quanto moléculas sinalizadoras intracelulares, capazes de se ligar e responder de forma integrada, programada e característica (Alberts et al., 2008).

As várias rotas de sinalização intracelular ativadas por receptores de superfície diferem em sua complexidade e modo pelo qual ativam sinais, desencadeando assim uma variedade de respostas biológicas. A ligação de moléculas sinalizadoras aos seus receptores específicos leva à alteração de segundos mensageiros intracelulares, os quais desencadeiam uma série de reações, modificando a atividade de enzimas intermediárias das cascatas de sinalização celular (Alberts et al., 2008).

Existem três famílias de receptores de superfície, cada um deles desencadeando cascatas de transdução de sinais diferentes. Receptores ligados a canais iônicos se abrem ou fecham rapidamente em resposta à ligação ao NT específico. Receptores ligados a proteínas G ativam ou inibem indiretamente enzimas ligadas à membrana plasmática ou canais iônicos. Receptores ligados a enzimas atuam diretamente como enzimas ou estão associados com alguma enzima, que usualmente são proteínas cinases, as quais fosforilam proteínas específicas na cascata de sinalização. Todas essas cascatas são altamente reguladas por fosforilação/desfosforilação de proteínas, interação entre proteínas e alteração nas concentrações de íons intracelulares. (Alberts et al., 2008).

1.5.1. HOMEOSTASE GLUTAMATÉRGICA

O glutamato é o maior neurotransmissor excitatório do SNC. Ele produz mudanças na excitabilidade neuronal, organização sináptica, migração neuronal durante o desenvolvimento e viabilidade neuronal (Meldrum, 2000). As respostas excitatórias desse aminoácido são mediadas por um grande número de receptores de membrana celular. Dois tipos de receptores modulam as ações do glutamato: os receptores

ionotrópicos e os metabotrópicos (Sprengel and Seeburg, 1993, Hollmann and Heinemann, 1994). Os receptores ionotrópicos (iGluR) podem ser distinguidos por suas propriedades farmacológicas e eletrofisiológicas: o receptor N-metil-D-aspartato (NMDA) é um canal altamente permeável ao Ca^{2+}, enquanto que o receptor ácido α-amino-3-hidroxi-5-metil-4-isoxazol-propiônico (AMPA) e o kainato são canais permeáveis principalmente ao sódio (Na^{+}). Os receptores metabotrópicos (mGluR) são acoplados a proteínas G e induzem a ativação de sistemas de segundos mensageiros, como o IP3, causando a liberação de Ca^{2+} do retículo endoplasmático. São conhecidos oito subtipos de receptores metabotrópicos, os quais exercem tanto ações excitatórias quanto inibitórias (Ozawa et al., 1998).

O glutamato do espaço extracelular interage também com iGluR e mGluR de astrócitos iniciando várias respostas nestas células, incluindo a ativação de cascatas de mensageiros intracelulares e a modulação da síntese de proteinas. O influxo de Ca^{2+} causado pela ativação de receptores AMPA astrocitários, por exemplo, regula a manutenção da associação estrutural entre neurônios e astrócitos nas sinapses. A perda da permeabilidade ao Ca^{2+} causa uma retração dos processos gliais, tornando a remoção de glutamato da fenda sináptica menos eficiente (Iino et al., 2001).

Os mecanismos glutamatérgicos estão entre os sinais mais importantes na regulação/desregulação da dinâmica do citoesqueleto neural. Os iGluR e mGluR podem mediar vias de sinalização dependentes de Ca^{2+}, que controlam diretamente o sistema fosforilante associado ao citoesqueleto (Mattson, 1989, Carraway, 2000). Metabólitos ou neurotoxinas são capazes de ativar o sistema glutamatérgico, que por sua vez, ativa cinases e fosfatases dependentes ou independentes de segundos mensageiros, as quais fosforilam/desfosforilam sítios específicos em subunidades dos FI ou proteínas associadas aos filamentos de actina, mediando a reorganização do citoesqueleto e a plasticidade celular (Loureiro et al., 2010a, Pierozan et al., 2012).

Na maioria das células, o Ca^{2+} é o maior sinalizador celular. As concentrações de Ca^{2+} livres no citosol da célula são extremamente baixas ($<10^{-7}$ M), enquanto que as concentrações no espaço extracelular e retículo endoplasmático (RE) são relativamente altas ($\sim10^{-3}$). Por este motivo, há uma tendência à entrada de Ca^{2+} para o citosol através da membrana plasmática e do RE. As concentrações de Ca^{2+} intracelulares são reguladas por vários processos simultâneos, que podem ou colocar o Ca^{2+} para o interior do citosol, ou então retirá-lo para o meio extracelular ou para depósitos intracelulares. Os mecanismos de entrada de Ca^{2+} para o citosol incluem canais localizados na membrana plasmática e no RE. Quando um sinal abre os canais de Ca^{2+} nestas membranas, há uma grande entrada deste íon para o citosol, aumentando drasticamente suas concentrações locais e ativando proteínas responsivas ao Ca^{2+}. Após a ativação das cascatas específicas ativadas por este íon, as concentrações precisam voltar para o seu estado basal. Os mecanismos de retirada de Ca^{2+} incluem Ca^{2+}-ATPases na membrana plasmática e no RE, além de trocadores iônicos que utilizam o gradiente de outros íons para transportar o Ca^{2+} para o meio extracelular. Todos estes mecanismos agem em conjunto para restaurar os níveis basais dentro da célula (Berridge et al., 2000, Montero et al., 2000, Alberts et al., 2008).

As diferentes frequências e intensidades de estímulos extracelulares causam as mais variadas combinações de influxo/liberação de Ca^{2+} por parte de uma célula, gerando uma enorme variedade de perfis de flutuação intracelular de Ca^{2+}, o que constitui um dos mais importantes e complexos padrões de sinalização para a célula. Esta diversidade nos mecanismos de sinalização de Ca^{2+} pode ser vista durante a estimulação de diferentes tipos celulares (Berridge et al., 2000).

Os diversos padrões de liberação de Ca^{2+} controlam muitas funções celulares no SNC, como diferenciação e crescimento, excitabilidade da membrana, exocitose e atividade sináptica (Sattler and Tymianski, 2000). Os neurônios possuem mecanismos

especializados de homeostase do Ca^{2+} para assegurar um alto controle dos níveis citosólicos deste íon. Pequenos aumentos nas concentrações de Ca^{2+} que ocorrem na vizinhança dos canais iônicos ou nos sítios de liberação intracelulares podem ativar enzimas ou canais iônicos próximos. Os neurônios controlam tanto os níveis intracelulares quanto a localização da liberação do Ca^{2+} através da ação combinada entre influxo e liberação, tampões de Ca^{2+} e regulação dos estoques internos deste íon. O influxo de Ca^{2+} extracelular é mediado por canais voltagem-dependentes (VDCC) e por receptores NMDA. A liberação dos estoques internos envolve principalmente liberação de Ca^{+2} do RE induzida por aumento do Ca^{+2} citosólico (*Ca^{2+}-induced Ca^{2+} release*) ou por ativação de canais de Ca^{2+} do RE sensíveis ao IP3 (Konur and Ghosh, 2005). Em condições fisiológicas, estes processos permitem que muitas cascatas de sinalização reguladas pelo Ca^{2+} ocorram independentemente dentro de uma mesma célula. No entanto, o excessivo influxo de Ca^{2+} pela membrana plasmática ou liberação dos estoques intracelulares pode elevá-lo a níveis que excedem a capacidade de ação dos seus mecanismos regulatórios. Isto leva a uma ativação excessiva de processos dependentes de Ca^{2+} que estão normalmente inativos ou operando em baixos níveis, causando danos metabólicos que afetam a viabilidade celular (Tymianski and Tator, 1996, Bootman et al., 2001).

A excitotoxicidade é causada por uma excessiva liberação de glutamato ou por sua reduzida remoção da fenda sináptica (Caudle and Zhang, 2009), o que consequentemente irá causar uma superestimulação dos receptores glutamatérgicos. O aumento de glutamato na fenda sináptica ativa os receptores NMDA, AMPA e os canais L-VDCC causando um aumento do influxo de Ca^{2+} para o citosol. Além disso, a ativação de mGluRs pode estimular a liberação de Ca^{2+} dos estoques internos (Tymianski, 1996). Enzimas ativadas por Ca^{2+}, como proteases, endonucleases e fosfolipases contribuem para a degradação de diferentes componentes celulares e para a

morte neuronal. Um influxo massivo de Ca^{2+} durante a excitotoxicidade causa uma sobrecarga intramitocondrial de Ca^{2+}, alterando sua atividade e prejudicando a produção de ATP. Como consequência, mecanismos de extrusão de Ca^{2+} podem ser prejudicados, levando a um aumento sustentado de Ca^{2+} intracelular (Ali et al., 2006). Outro evento-chave envolvido na excitotoxicidade é a geração de radicais livres como resultado da disfunção mitocondrial e da ativação de enzimas dependentes de Ca^{2+}, tais como a óxido nítrico sintase. Os radicais livres danificam os componentes lipídicos e proteicos da célula, bem como os ácidos nucleicos, contribuindo para a cascata de morte neuronal (Lafon-Cazal et al., 1993) (Figura 6).

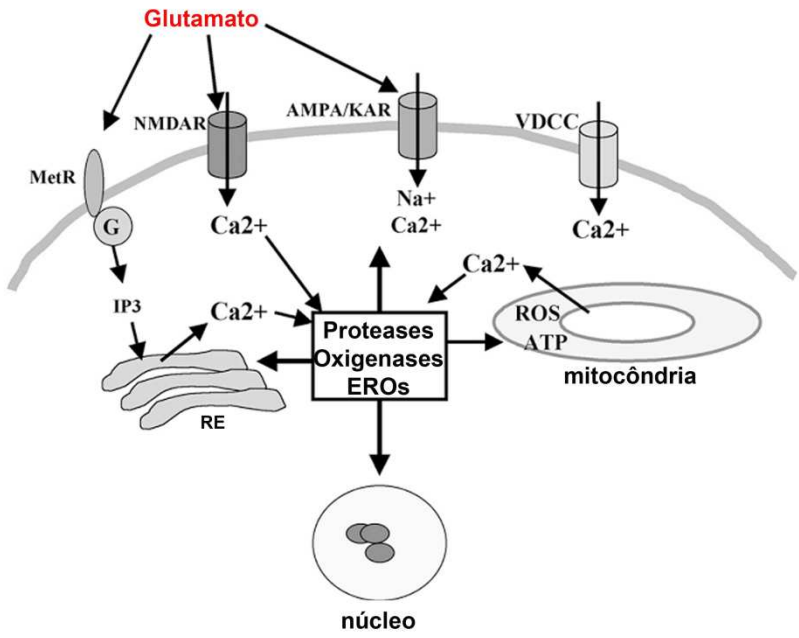

Figura 6. Mecanismos de excitotoxicidade. Ligação do glutamato aos receptores AMPA e kainato abre os canais de membrana resultando em influxo de Na^{+} e consequente despolarização da membrana, abrindo os canais de Ca^{2+} voltagem dependentes (VDCC). A ligação do glutamato ao receptores NMDA em condições de despolarização abre os canais NMDA, resultando em uma grande entrada de Ca^{2+} para o citosol. A ativação dos receptores metabotrópicos (MetR) induz a produção de IP_3 e ativação dos receptores IP_3 na membrana do RE, resultando em liberação de Ca^{2+} dos estoques internos. O aumento nos níveis intracelulares de Ca^{2+} em resposta a ativação dos receptores glutamatérgicos pode induzir a captação de Ca^{2+} pela mitocôndria que, se for excessivo, pode induzir a produção de espécies reativas de oxigênio (EROs) e inibir a produção de ATP. O Ca^{2+} também pode induzir a ativação de proteases e oxigenases, contribuindo para a morte celular excitotóxica (Adaptado de Mattson et al, 2002).

1.6. CITOESQUELETO, ÁCIDO QUINOLÍNICO E DOENÇA DE HUNTINGTON

Visto que tanto alterações do citoesqueleto quanto nas concentrações de QUIN são eventos iniciais em diversas doenças neurodegenerativas, o acompanhamento da evolução temporal das primeiras alterações que ocorrem logo após o insulto excitotóxico é de extrema importância na compreensão das alterações encontradas nos pacientes acometidos com doenças neurodegenerativas. Esses estudos podem ajudar a definir uma janela de oportunidade para uma possível intervenção terapêutica. Além disso, a análise dos insultos que ocorrem no cérebro em desenvolvimento pode ajudar a entender os diferentes fenótipos encontrados na doença de Huntington na fase adulta e na fase juvenil.

2. OBJETIVOS

2.1. OBJETIVO GERAL

Investigar as ações do QUIN sobre o cérebro de ratos jovens, com ênfase na modulação do citoesqueleto através da fosforilação e reorganização dos FI, bem como as vias de sinalização envolvidas nesses efeitos. Além disso, estudar os efeitos da injeção intraestriatal de QUIN sobre parâmetros morfológicos e comportamentais em ratos jovens, relacionando com as alterações no citoesqueleto neural, numa tentativa de elucidar algumas das alterações encontradas nos pacientes com a DHJ.

2.2. OBJETIVOS ESPECÍFICOS

2.2.1. Desenho experimental 1

Analisar os efeitos desencadeados pela injeção com QUIN sobre parâmetros morfológicos e comportamentais nas primeiras semanas após a injeção, comparando os efeitos com as alterações encontradas na DHJ, numa tentativa de padronizar um modelo com QUIN em ratos jovens para o estudo da doença.

Avaliar os efeitos da injeção intraestriatal de QUIN sobre o conteúdo e a fosforilação dos FI neuronais e gliais nas primeiras semanas após a injeção no estriado, córtex cerebral e hipocampo de ratos de 30 dias de idade.

Investigar a participação de cinases e fosfatases nos efeitos desencadeados pelo QUIN sobre o citoesqueleto neural, bem como mecanismos envolvendo o Ca^{2+} e o glutamato.

Relacionar os efeitos comportamentais e morfológicos encontrados nos animais injetados com QUIN com as alterações no citoesqueleto neural.

2.2.2. Desenho experimental 2

Avaliar os efeitos do QUIN sobre o citoequeleto neural, utilizando fatias de estriado, para investigar os mecanismos de ação desses efeitos, como a participação dos receptores glutamatérgicos, homeostase do Ca^{2+}, bem como a participação de cinases envolvidas nesses efeitos.

Analisar os efeitos do QUIN sobre sítios de fosforilação específicos das subunidades dos NF, como os sítios Ser55 e Ser57 da NFL e os sítios KSP *repeats* das subunidades NFM e NFH.

2.2.3. Desenho experimental 3

Analisar os efeitos do QUIN sobre o citoesqueleto de astrócitos e neurônios em cultura primária, investigando os mecanismos de ação envolvidos nesses efeitos.

Avaliar a ação do QUIN sobre a viabilidade celular e reorganização do citoesqueleto de actina e GFAP (em cultura de astrócitos primários) e de MTs (em cultura de neurônios primários).

Investigar possíveis mecanismos de proteção de astrócitos e neurônios nos efeitos desencadeados pelo QUIN em co-cultura neurônio-astrócito

3. Materiais e métodos

A seção materiais e métodos está inserida em cada um dos cinco capítulos da parte II dessa tese.

Os resultados estão apresentados na forma de artigos científicos.

Abaixo segue a descrição resumida de cada modelo utilizado para o estudo dos três desenhos experimentais.

3.1. Desenho experimental 1 – Modelo *in vivo*

O modelo *in vivo* foi utilizado para a padronização do modelo da DHJ em animais jovens, comparando os resultados obtidos com as alterações encontradas nos pacientes acometidos com a doença. Além disso, o modelo teve como objetivo o estudo da relação entre as alterações morfológicas em comportamentais encontradas nos animais, com alterações na homeostase do citoesqueleto neural. Para isso, utilizou-se ratos Wistar adolescentes (30 dias de idade). Os ratos foram anestesiados com uma solução de Equitesina (2.5 mL/kg i.p.) e colocados em um aparelho estereotáxico. Os ratos receberam uma injeção intraestriatal de QUIN (150 nmol/0.5 µL) ou de solução salina (ratos controle-Sham) durante 4 min. Os ratos foram sacrificados por decapitação 30 min, 1, 7, 14 e 21 dias após a injeção e o corpo estriado, córtex e hipocampo foram dissecados para posterior avaliação dos parâmetros investigados: captação de glutamato, captação de cálcio, fosforilação dos FI neurais, atividade de cinases e fosfatases e

análise imunohistoquímica. Os ratos também foram utilizados para análise de parâmetros comportamentais 1, 7, 14 e 21 dias após a injeção com QUIN ou solução salina (sham).

3.2. Desenho experimental 2 – Modelo *ex vivo*

O modelo ex vivo foi utilizado para o estudo mais aprofundado das vias de sinalização envolvidas nos efeitos do QUIN sobre o citoesqueleto neural. Neste modelo experimental utilizou-se ratos Wistar de 30 dias de idade. Os ratos foram sacrificados por decapitação, o corpo estriado foi dissecado e cortado em fatias de 400 µm em um chopper Mcllwain. As fatias foram pré-incubadas a 30 °C por 10 min em um tampão fisiológico (Krebs-Hepes-pH 7.4) na presença ou ausência de diferentes ferramentas farmacológicas para o estudo das vias de sinalização envolvidas nos efeitos do QUIN. Após a pré-incubação, o meio foi trocado por 100 µL do tampão fisiológico na presença ou ausência de QUIN por 20 min. Após 20 min, 100 µCi de [^{32}P]- ortofosfato de sódio foram adicionados ao meio de incubação por mais 30 min. Após as incubações, procedeu-se com a técnica para extração da fração enriquecida em FI, como descrito no capítulo três da parte II dessa tese.

3.3. Desenho experimental 3 – Modelo *in vitro*

O modelo *in vitro* foi desenvolvido com o intuito de relacionar as alterações no sistema fosforilante associado ao citoesqueleto neural com possíveis alterações morfológicas causadas pelo QUIN em células isoladas, além de avaliar a resposta de cada tipo celular ao insulto causado pelo metabólito, e a interação neurônio-astrócito nesses efeitos. Neste modelo experimental utilizou-se cultura primária de astrócitos e

neurônios estriatais para análise dos parâmetros estudados. As culturas de astrócitos primários foram preparadas utilizando o corpo estriado de ratos Wistar recém-nascidos. A cultura foi mantida por 15 dias in vitro (15 DIV) em meio DMEM suplementado com 10% de soro bovino fetal. Após 15 dias, os astrócitos foram incubados com QUIN em diferentes concentrações ou apenas com meio DMEM sem soro (controles) por 24 h. Após a incubação, procedeu-se as análises descritas no capítulo quatro e cinco da parte II dessa tese. As culturas neuronais primárias foram preparadas utilizando o corpo estriado de ratos Wistar embrionários (18 dias de gestação). A cultura foi mantida por 7 DIV em meio Neurobasal. Após 7 DIV, os neurônios foram incubados com diferentes concentrações de QUIN ou apenas com meio Neurobasal (controles) por 24 h. Após a incubação, procedeu-se as análises descritas no capítulo cinco da parte II dessa tese.

PARTE II

Capítulo 1

BIOCHEMICAL, HISTOPATOLOGICAL AND BEHAVIORAL ALTERATIONS CAUSED BY INTRASTRIATAL ADMINISTRATION OF QUINOLINIC ACID TO YOUNG RATS

Paula Pierozan, Carolina Gonçalves Fernandes, Márcio Ferreira Dutra, Pablo Pandolfo, Fernanda Ferreira, Bárbara Ortiz de Lima, Lisiane Porciúncula, Moacir Wajner, Regina Pessoa-Pureur

Artigo publicado no **FEBS journal**

the FEBS Journal

Biochemical, histopathological and behavioral alterations caused by intrastriatal administration of quinolic acid to young rats

Paula Pierozan[1], Carolina G. Fernandes[1], Márcio F. Dutra[1,2], Pablo Pandolfo[1,3], Fernanda Ferreira[1], Bárbara O. de Lima[1], Lisiane Porciúncula[1], Moacir Wajner[1] and Regina Pessoa-Pureur[1]

1 Departamento de Bioquímica, Instituto de Ciências Básicas da Saúde, UFRGS, Porto Alegre, RS, Brasil
2 Departamento de Biologia Celular, Embriologia e Genética, Centro Ciências Biológicas, Universidade Federal de Santa Catarina, Florianópolis, SC, Brasil
3 Departamento de Neurobiologia, Instituto de Biologia, Universidade Federal Fluminense, Niterói, RJ, Brasil

Keywords
astrogliosis; excitotoxicity; neurodegeneration; quinolinic acid; striatum

Correspondence
R. Pessoa-Pureur, Departamento de Bioquímica, Instituto de Ciências Básicas da Saúde, Universidade Federal do Rio Grande do Sul, Rua Ramiro Barcelos 2600 anexo, CEP 90035-003 Porto Alegre, RS, Brazil
Fax: +55 51 3308 5535
Tel: +55 51 3308 5565
E-mail: rpureur@ufrgs.br

(Received 13 November 2013, revised 3 February 2014, accepted 19 February 2014)

doi:10.1111/febs.12762

Quinolinic acid (QUIN) is a neuroactive metabolite of the kinurenine pathway, and is considered to be involved in aging and some neurodegenerative disorders, including Huntington's disease. QUIN was injected intrastriatally into adolescent rats, and biochemical and histopathological analyses in the striatum, cortex, and hippocampus, as well as behavioral tests, were carried out in the rats over a period of 21 days after drug injection. Decreased [^{3}H] glutamate uptake and increased $^{45}Ca^{2+}$ uptake were detected shortly after injection in the striatum and cerebral cortex. In the hippocampus, increased $^{45}Ca^{2+}$ uptake preceded the decreased [^{3}H]glutamate uptake, without histopathological alterations. Also, corticostriatal astrogliosis was observed 7 days later, progressing to neuronal death at day 14. QUIN-treated rats also showed cognitive deficits 24 h after injection, concurrently with striatal astrogliosis. Motor deficits appeared later, after corticostriatal neurodegeneration. We assume that glutamate excitotoxicity could represent, at least in part, a molecular mechanism associated with the cognitive and motor impairments, corticostriatal astrogliosis and neuronal death observed in the QUIN-treated rats. We propose that our findings could be relevant for understanding the pathophysiology of human neurodegenerative diseases affecting young people, such as the juvenile form of Huntington's disease, and for the design of potential therapeutic strategies to slow down the progression of the disease.

Introduction

Quinolinic acid (QUIN) is a neuroactive intermediate of the kinurenine pathway, which is the major route for the metabolism of the essential amino acid tryptophan. QUIN's excitatory properties are attributable to its direct, selective stimulation of *N*-methyl-D-aspartate (NMDA) receptors, as originally demonstrated with selective NMDA receptor antagonists [1]. This metabolite is present at nanomolar concentrations in human and rat brains, under normal conditions [2]. However, under pathological conditions, the kynurenine pathway is stimulated, leading to an increase in the level of QUIN, therefore augmenting the risk of excitotoxic events. QUIN is produced by microglia, and must exit those cells to be metabolized in a separate population of

Abbreviations
CNS, central nervous system; DAPI, 4′,6-diamidino-2-phenylindole; FJC, Fluoro-Jade C; GFAP, glial fibrillary acidic protein; HD, Huntington's disease; IF, intermediate filament; JHD, juvenile-onset Huntington's disease; NeuN, neuron-specific nuclear antigen; NMDA, *N*-methyl-D-aspartate; OF, open field; OR, object recognition; QUIN, quinolinic acid; YM, Y-maze.

cells [3]. There are substantially fewer cells containing the enzyme 3-hydroxyanthranilic acid-3,4-dioxygenase, which produces QUIN, than those containing QUIN phosphoribosyl transferase, which converts QUIN to NAD^+ [4]. Consequently, the production of QUIN occurs as a much higher rate within the brain that the conversion to NAD^+. As we have suggested previously [5], this has implications for the accumulation of QUIN in the brain under certain pathological conditions. As Foster *et al.* [6] concluded, the brain areas that preferentially accumulate QUIN in pathological conditions are the frontal cortex, striatum and hippocampus.

High QUIN levels are considered to be involved in aging and in the pathophysiology of some neurodegenerative diseases, including Huntington's disease (HD) [7]. In pathological conditions, this metabolite causes excessive excitation of NMDA receptors, resulting in increased cytoplasmic Ca^{2+} concentrations, and causes mitochondrial dysfunction, decreased ATP levels, cytochrome *c* release, and oxidative stress, further leading to selective loss of 4-aminobutyrate-producing and cholinergic neurons [8]. Indeed, despite the compelling evidence that aberrant neuronal signaling and energetic dysfunctions underlie the toxic actions triggered by QUIN, the production of reactive oxygen and nitrogen species caused by high concentrations of QUIN also have a major role in the development of the neurotoxic actions caused by this compound. [9].

Neurodegeneration is a chronic process that results in progressive loss of function, structure and number of neural cells, leading to generalized atrophy. Neurodegenerative processes affect the connectivity of neural networks, which is critical for information processing and cognitive power [10]. Indeed, insults to the brain or to the spinal cord trigger a specific and evolutionarily conserved glial defense response generally known as reactive gliosis. This response is manifested as a series of histopathological and functional changes, which, in astrocytes, are represented by reactive astrogliosis [11,12]. The hallmark of reactive gliosis in central nervous system (CNS) ischemia, trauma or neurodegeneration is characteristic hypertrophy of cellular processes of astrocytes, upregulation of glial fibrillary acidic protein (GFAP) and vimentin, and re-expression of nestin, all of which participate in the formation of the intermediate filament (IF) network. The IF network becomes very prominent, in particular in the main processes and the somata of astrocytes [13,14].

In several animal models of neurodegeneration, including those induced by QUIN, neuronal loss is mediated by excitotoxicity, i.e. neuronal damage resulting from excessive glutamate receptor activation [15]. It follows that microglia-derived QUIN might function as a trigger molecule in the neurodegenerative process [16]. Excitotoxic cell death is dependent on the increase in the intracellular concentration of Ca^{2+} after its influx through NMDA receptors. Ca^{2+}-activated enzymes, such as proteases, endonucleases, and phospholipases, contribute to the degradation of different cell components and neuronal death. In addition, excitotoxic stimulation is associated with extremely high Ca^{2+} influx and intramitochondrial Ca^{2+} overload. Altered mitochondrial activity and disrupted ATP production, impairing ATP-dependent Ca^{2+} loading and extrusion mechanisms, contribute to sustained excitotoxicity [17,18].

Interestingly, pharmacological lesioning of the striatum with excitotoxins, such as QUIN, results in neuropathological changes whose features and time progression clearly resemble those encountered in HD [19], including motor and behavioral deficits [20], further supporting the idea that QUIN-lesioned rats may represent a suitable model with which to study disease progression.

QUIN-induced behavioral and biochemical alterations in adult and aged rodents have been extensively described in recent years [21–23]. However, little information is available on the excitotoxic events elicited by QUIN in the brains of young rats. In this context, we previously reported that QUIN elicited NMDA-induced Ca^{2+}-mediated disruption of the cytoskeleton of neural cells and oxidative stress 30 min after its intrastriatal injection into adolescent rats [24].

In the present study, we searched for brain biochemical, histopathological and behavioral alterations elicited by a single intrastriatal injection of QUIN into adolescent rats. We assume that intrastriatal QUIN injection into young rats could mimic the early steps of the pathophysiological cascades involved in the deleterious events occurring in neurodegenerative diseases, such as juvenile-onset HD (JHD). Neurodegeneration and disturbance of glutamate metabolism are involved in JHD. As the behavioral changes depend on the brain region affected, we evaluated the time course of the biochemical changes, including [^{3}H]glutamate and $^{45}Ca^{2+}$ uptake, the histopathological findings in the striatum, cerebral cortex, and hippocampus, and the behavior and motor activity in response to QUIN.

Results

Biochemical findings

To assess glutamate-mediated excitotoxicity resulting from QUIN administration, [^{3}H]glutamate uptake and $^{45}Ca^{2+}$ uptake were measured in sham and

QUIN-injected rats at 30 min, 1, 7, 14 and 21 days after injection. The results showed that QUIN injection decreased [^{3}H]glutamate uptake in the striatum at 30 min and 14 days after injection (Fig. 1A). Furthermore, [^{3}H]glutamate uptake was decreased at 30 min, 1 and 2 weeks in the cerebral cortex (Fig. 1B) and at 1, 3 and 4 weeks after intrastriatal injection into the hippocampus (Fig. 1C). We also measured $^{45}Ca^{2+}$ uptake in the three brain regions from 30 min until week 4 after QUIN injection. The results showed increased $^{45}Ca^{2+}$ uptake in the striatum 30 min and 1 day after injection (Fig. 1D), with a return to sham values 7, 14 and 21 days later. In the cerebral cortex, $^{45}Ca^{2+}$ uptake was increased from 30 min until 7 days after QUIN injection (Fig. 1E), returning to sham levels at day 14 and increasing again at day 21. Otherwise, in the hippocampus, $^{45}Ca^{2+}$ uptake was persistently increased from 30 min after injection until day 21 (Fig. 1F).

Histopathological findings

To search for histopathological changes in QUIN-treated rats, we carried out histological analysis in striatal, cortical and hippocampal sections at day 1, day 7, day 14 and day 21 after QUIN injection. Tissue sections were processed for immunofluorescence with antibody against GFAP or neuron-specific nuclear antigen (NeuN), as well as for nuclear staining with 4′,6-diamidino-2-phenylindole (DAPI). Moreover, degenerating neurons were recognized with Fluoro-Jade C (FJC). Tissue sections were analyzed with confocal microscopy, as shown in Fig. 2. Twenty-four hour after QUIN injection, we observed an absence of FJC-labeled cells and unaltered NeuN immunostaining (showing in supporting information), and increased GFAP-immunostaining (showing in Fig. 2A) in the striatum as compared with sham-operated rats. In contrast, we did not detect any altered staining in the cerebral cortex between groups (Supporting information). Taken together, these results indicate reactive astrogliosis and an absence of neuronal death in the striatum 24 h after QUIN injection. Figure 2B shows increased GFAP immunostaining in the striatum and cerebral cortex 7 days after QUIN administration, indicating persistent astrogliosis in the striatum and a later response in the cerebral cortex relative to initial astrogliosis. Furthermore, we found unaltered NeuN immunostaining and FJC staining in the striatum and cortex, indicating an absence of neuronal loss in these brain regions (Supporting information). Figure 2C

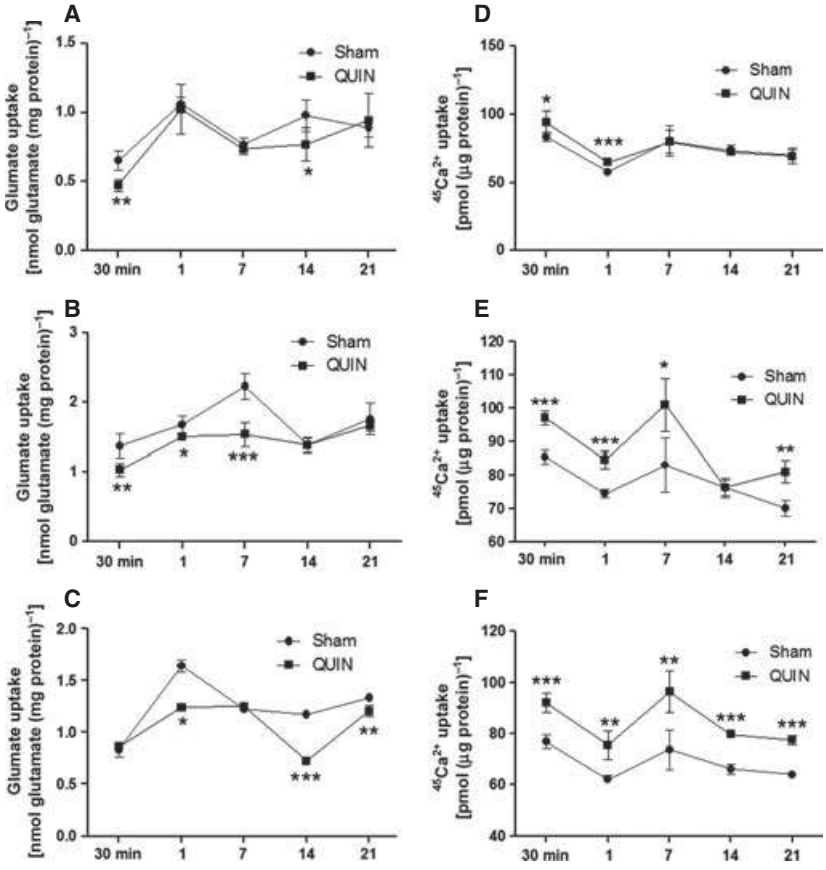

Fig. 1. Effect of QUIN on [^{3}H]glutamate and [$^{45}Ca^{2+}$] uptake in the three cerebral structures studied. (A–C) [^{3}H]Glutamate uptake in the striatum (A), cerebral cortex (B), and hippocampus (C). (D–F) [$^{45}Ca^{2+}$] uptake in the striatum (D), cerebral cortex (E), and hippocampus (F). Measurements were carried out 30 min, 1, 7, 14 and 21 days after injection. Data are reported as mean ± standard deviation for eight rats, and expressed as percentage of control. Statistically significant differences from sham rats, as determined with one-way ANOVA followed by the Tukey–Kramer test, are indicated: $*P \leq 0.05$; $**P \leq 0.01$; $***P \leq 0.001$.

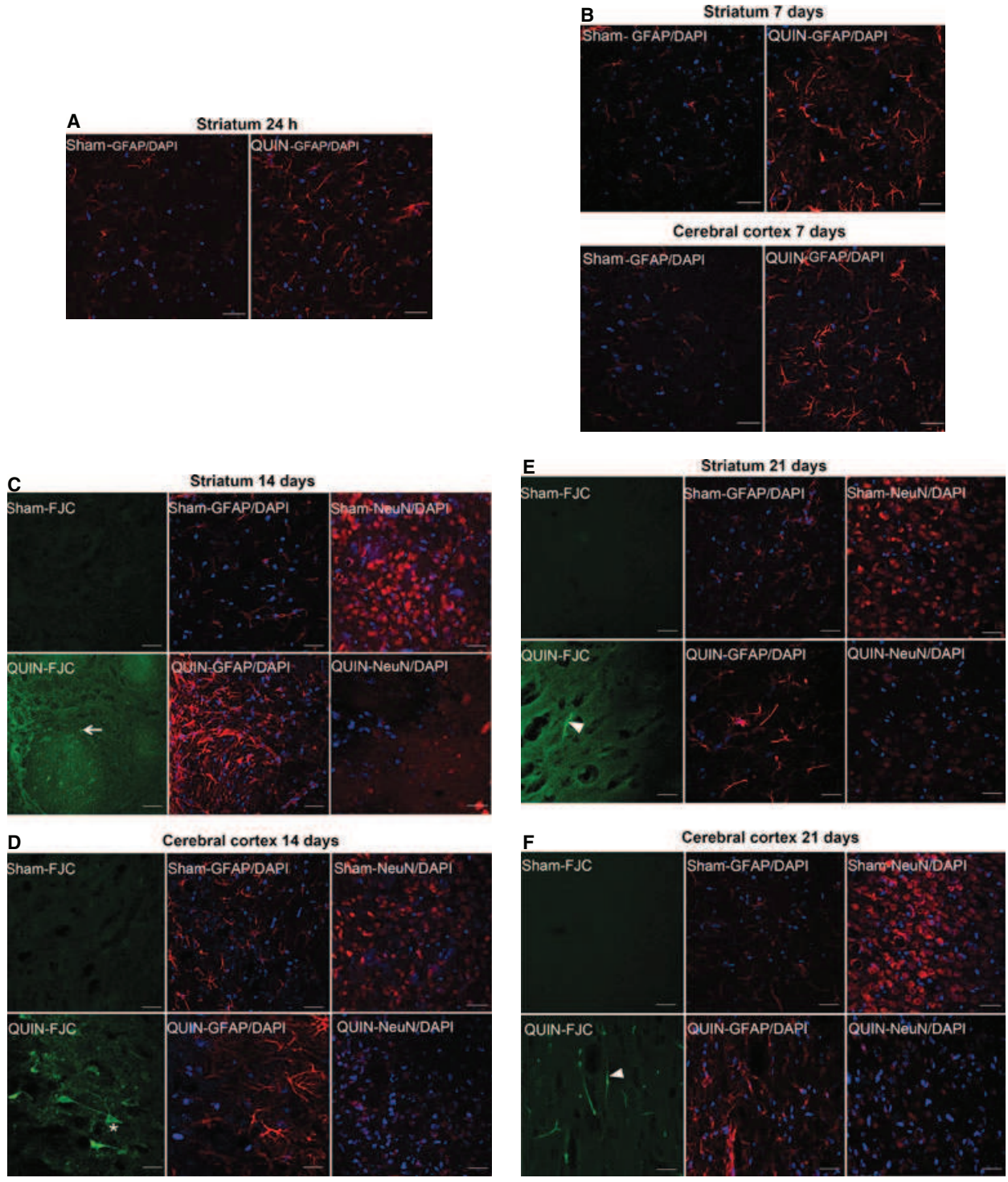

Fig. 2. QUIN-induced lesions assessed with FJC staining, and NeuN and GFAP immunohistochemistry. Rats were subjected to an intrastriatal injection of 150 nmol of QUIN in the right striatum, and the lesion was assessed 1, 7, 14 and 21 weeks postsurgery. Representative images are shown. (A) Astrogliosis in the striatum 24 h after injection. Note more ramified cells with wider projections. (B) Reactive astrogliosis in the striatum and cerebral cortex 7 days after injection. (C–F) Reactive astrogliosis and neuronal death are shown in the striatum (C) and cerebral cortex (D) 14 and 21 days after injection [(E) striatum; (F) cortex]. The staining shows dot-shaped structures (arrow) in (C) and fiber-like structures (arrowhead) in (E) and (F). The asterisk in (D) indicates a pyramidal neuron characteristic of layer V in the cerebral cortex. Representative images of eight rats. Scale bar: 30 μm (magnification: × 40).

shows persistent astrogliosis, decreased NeuN immunostaining and a large number of both linear and dot-shaped FJC-positive structures in the striatum at day 14 after injection. Figure 2D shows FJC-positive cell bodies with a neuronal profile, increased GFAP immunostaining, and decreased NeuN immunostaining, indicating astrogliosis and neuronal death in the cerebral cortex 14 days after QUIN injection. Figure 2E,F shows the remaining FJC-labeled FJC debris, diminished NeuN immunostaining and increased GFAP immunostaining in the striatum (Fig. 2E) and cortex (Fig. 2F) 21 days after lesion. No histological alterations were observed in the hippocampus of QUIN-treated rats at any time analyzed during the study (Supporting information). Taken together, these results show progressive injury in which astrogliosis preceded neuronal loss in the corticostriatal region over the first weeks after the QUIN-induced damage.

Behavioral evaluation

Behavioral evaluation was carried out for 4 weeks after intrastriatal QUIN injection. The behavioral tests were performed on four sequential days in each week. Locomotor functions were evaluated with an open field (OF) task at day 1, day 7, day 14 and day 21 in rats from the naïve, sham and QUIN groups. Habituation and anxiety were tested on day 2, day 8, day 15 and day 22 with an OF task. Spatial memory was tested on day 4, day 10, day 17 and day 24 with a Y-maze (YM) task in the same groups. Short-term memory was evaluated with an object recognition (OR) task on day 3, day 9, day 16, and day 23. The timeline of the experimental procedures used to evaluate the behavioral consequences of intrastriatal QUIN injection is shown in Fig. 3A.

The results for locomotor activity evaluated with the OF task at 1, 2, 3 and 4 weeks after QUIN injection are summarized in Fig. 3B. One-way ANOVA (control groups versus QUIN injection) revealed no significant differences between groups in the total distance traveled until week 3 after treatment. However, on week 4, rats that received QUIN showed significantly reduced locomotor activity as compared with the sham and naïve groups, indicating a deficit in locomotor activity. The sham-treated group did not

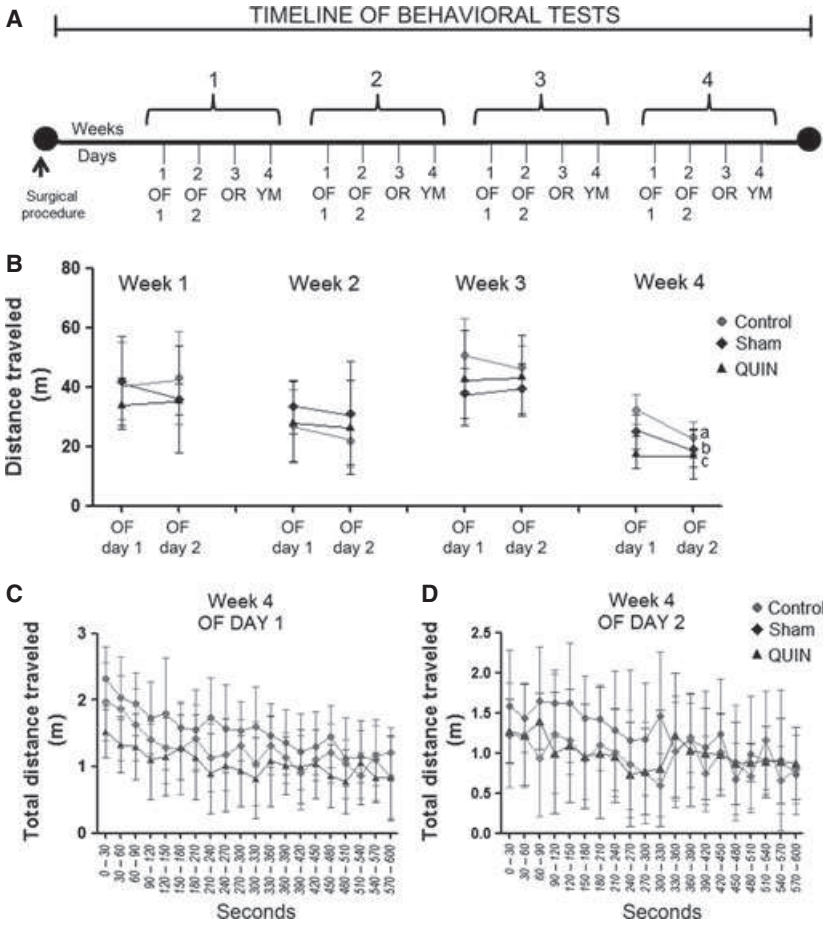

Fig. 3. (A) The timeline of the behavioral tests. (B) Effect of QUIN administration on locomotor activity and spatial memory in the OF task, measured as the distance traveled in meters. The rats were exposed for 10 min to the OF on day 1, and 24 h later they were exposed again to the OF on day 2. Values are expressed as mean ± standard deviation. $^{a}P < 0.05$ in the naïve group between OF day 1 and OF day 2. $^{b}P < 0.05$ within the sham group between OF day 1 and OF day 2. $^{c}P < 0.05$ for the difference between QUIN rats and control groups (ANOVA followed by the Tukey *post hoc* test).

show a significant difference from the naïve group in locomotor activity.

In addition, it is important to note that, in the OF task performed at week 4, the distance traveled by the sham and naïve rats on OF day 2 was significantly decreased as compared with that on OF day 1, whereas the distance traveled by the QUIN group was not altered, suggesting a locomotor deficit or lack of habituation. To further demonstrate the exploratory behavior of the different groups in week 4, we show a detailed analysis of OF day 1 and day 2 (Fig. 3C,D). On OF day 1, locomotor activity declined significantly only in the sham and naïve groups, indicating habituation to the OF (Fig. 3C). On OF day 2, naïve and sham rats started the test with less exploratory activity, which, in turn, remained constant over the time of the test. Otherwise, QUIN-treated rats showed the same exploratory activity as observed on OF day 1 (Fig. 3D). Taken together, the results further support lack of habituation in the QUIN group as compared with the sham and control groups at week 4.

Figure 4 shows the effect of intrastriatal administration of QUIN on the sample phase (Fig. 4A) and discrimination phase (Fig. 4B), respectively, in the OR task. Results for the sample phase revealed no significant difference between groups in the time spent in exploring the objects (Fig. 4A). Figure 4B shows the effect of the intrastriatal injection of QUIN on discrimination score. Statistical analysis revealed that QUIN decreased the discrimination score as compared with control groups at all times studied, indicating short-term memory impairment in QUIN-treated rats.

To further investigate the effects of QUIN injection on spatial memory, naïve, sham and QUIN rats were subjected to a YM task. There were no significant differences between the groups tested for all parameters analyzed (number of entries, total duration of visits in the novel arm, and time spent in the arms), suggesting no loss of spatial recognition memory (Table S1) as detectable with this specific test.

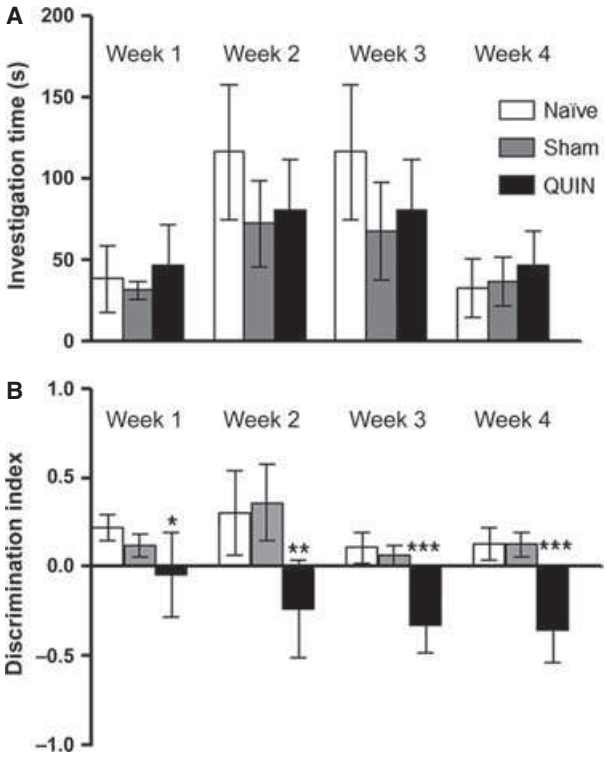

Fig. 4. Effects of the intrastriatal administration of QUIN on performance in the OR task. (A) The investigation time (s) was calculated as the sum of the time that the rats spent investigating C1 and C2. (B) The discrimination index was calculated as the time that the rats spent investigating [(T − C3)/(T + C3)]. Data are presented as mean ± standard deviation. $*P < 0.05$, $**P < 0.01$ and $***P < 0.001$ versus the naïve and sham groups (ANOVA followed by the Tukey *post hoc* test.

Discussion

Consistent with previous data in the literature, we found that intrastriatal injection of QUIN induced reactive gliosis and neuronal loss, as well as motor and behavioral alterations [25,26], in rats. The great vulnerability of the young brain to the excitotoxic effects of intrastriatally injected QUIN has been previously reported. In this context, Figueredo-Cardenas *et al.* [27] have described the influence of animal age, QUIN concentration and injection speed on the survival of striatal interneurons following QUIN injection. Also, Sun *et al.* [28] found greater damage to enkephalinergic striatal projection neurons in young rats than in adult rats, emphasizing the age-dependent decline in excitotoxic vulnerability to injected QUIN. However, the present study presents novel information about the time course of the effect of QUIN in young rats. We were interested in evaluating the impact that intrastriatal QUIN-induced lesioning could have away from the injection site, in other regions of the CNS. Therefore, we analyzed the progression of cellular damage in the striatum, cerebral cortex, and hippocampus, as well as the behavior and motor activity of these young rats for 4 weeks following QUIN injection. Unraveling the mechanisms that occur soon after intrastriatal QUIN injection and how these events progress from the striatum itself to other brain regions is important for understanding the biochemical and histopathological basis of neurodegeneration and behavioral changes in injured animals.

We found decreased [^{3}H]glutamate and increased $^{45}Ca^{2+}$ uptake, supporting glutamate excitotoxicity in

QUIN-injected rats. These phenomena could underlie, at least in part, the molecular mechanisms associated with cognitive and motor impairments, as well as the selective astrogliosis and neurodegeneration observed in the QUIN-treated rats. QUIN-treated rats showed decreased corticostriatal [^{3}H]glutamate uptake 30 min after lesion; uptake was restored to sham levels after 1 day in the striatum, but the decrease persisted for 2 weeks in the cerebral cortex. $^{45}Ca^{2+}$ uptake slightly increased in the striatum until day 1, returning to sham values thereafter. Moreover, decreased cortical [^{3}H]glutamate uptake and increased $^{45}Ca^{2+}$ uptake were observed until day 14. In the hippocampus, an important increase in $^{45}Ca^{2+}$ uptake persisted for 21 days after QUIN injection, whereas [^{3}H]glutamate uptake oscillated during the same period. Taken together, these results suggest a causal relationship between the activity of the glutamatergic system and intracellular Ca^{2+} levels in these brain structures, at least in the corticostriatal region, until day 7 after QUIN injection. It is feasible that voltage-dependent Ca^{2+} channels might mediate additional entry of Ca^{2+} from the extracellular space, supporting the increased $^{45}Ca^{2+}$ uptake, despite the oscillations observed in [^{3}H]glutamate uptake. It is also possible that the observed long durations of the QUIN responses are not attributable to the NMDA receptor properties, but to the slow release of glutamate from astrocytes elicited by the long-lasting intracellular Ca^{2+} increases. In this context, our experiments do not rule out the possibility that the astrocytes release glutamate or another factor that contributes to the excitotoxic cycle [29].

The spreading of the excitotoxic wave from the zone of lesion to other brain regions suggests spatiotemporal cell damage caused by QUIN for up to 4 weeks after lesion. It is therefore feasible that the early glutamate excitotoxicity in the striatal region may be involved in the persistent astrogliosis observed at 24 h after injection. Conversely, reactive astrocytes were detected only 7 days after injection in the cerebral cortex, which could suggest different temporally evoked molecular mechanisms underlying the glutamate-elicited cell damage in these brain regions.

We assessed astrogliosis in the striatrum, cerebral cortex and hippocampus by determining GFAP immunofluorescence and neuronal loss with double-labeling studies in brain sections, by combining FJC staining with immunofluorescence with the neuronal marker NeuN. An important finding of our work was that acute administration of QUIN provoked astrogliosis in the striatum soon after injection (24 h) that persisted throughout the period of the experiment (7, 14, and 21 days). Furthermore, a progressive neurodegenerative process in the striatum as determined by increased FJC staining, initiated between days 7 and 14, was verified by the histopathological abnormalities observed, such as shrunken cell bodies and swollen fibers [30]. In the cerebral cortex, astrogliosis as verified by increased GFAP immunoreactivity occurred at a later stage after QUIN administration (day 7), and was followed by the appearance of highly stained FJC-positive neurons in the pyramidal bodies at day 14. In addition, in the fourth week after QUIN administration, cortical degeneration progressed to the histological alterations observed earlier in the striatum.

It is important to note that QUIN administration did not result in acute neuronal loss, as would be expected with a potent excitotoxin [31]. As astrocytes were rapidly activated, especially in the striatum, and neuronal death occurred later in response to the excitotoxic damage provoked by QUIN injection, it is conceivable that astrocytes produced soluble factors that were toxic to neurons, as previously shown in other neurodegenerative pathologies [32]. It is emphasized that reactive astrogliosis is a prominent process leading to the formation of the glial scar that inhibits axonal regeneration after CNS injury. Upon becoming reactive, astrocytes undergo various molecular and morphological changes, including upregulation of the expression of GFAP, vimentin, and chondroitin sulfate proteoglycans, as well as of other molecules that are inhibitory to axon growth. Our present results showing late neuronal death in young rats are different from those obtained with QUIN injection in adult rats. In adult animals, QUIN causes massive neuronal damage near the site of QUIN injection in the striatum within aperiod of 30 min up to 2 days, followed by continuous and evolving neuronal damage in a progressive transitional zone in the periphery of the lesion over a period of at least 14 days after QUIN administration [33,34].

The hippocampus was less susceptible than the cerebral cortex and striatum to the excitotoxic injury causede by QUIN injection, as no histopathological alterations were detected in this structure until the fourth week after drug administration. This is consistent with previous observations that the hippocampus seems to be spared from injury in a genetic model of JHD [35] and in autopsied brains from the early stages of HD [36]. We should also consider that several factors, such as intrinsic neuronal properties, degree of myelination, state of receptor and ion channel maturation, and functional maturation of synaptic contacts, could contribute to region-dependent differences in the response to the insult, as well as to its long-term deleterious effects [37].

Concerning the behavioral consequences of cell damage induced by QUIN, we observed impairment of short-term memory in the OR task in rats shortly after QUIN administration that persisted throughout the experiment. Furthermore, lack of habituation and motor deficits were observed only at 21 days after QUIN injection. It is apparent from these findings and from the histopathoplogical studies that neuronal death in these brain regions is not required for the onset of cognitive deficits (OR), but it could underlie the motor disability observed, consistent with the hypothesis that motor changes result from loss of neurons in the striatum [38].

Lack of habituation was observed only in 50–55-day-old rats injected with QUIN; adolescent rats did not show this behavior. A possible explanation for these findings is that younger animals have a higher level of exploratory activity, and this may possibly mask a habituation deficit at this age [39]. Thus, the lack of habituation can be tentatively interpreted as being attributable to increased anxiety and exploratory activity. Accordingly, previous studies demonstrated that QUIN-injected rats showed motor alterations, such as perseveration to novel stimuli exposure and reduced fear/anxiety [40]. In this regard, behavioral alterations such as disinhibition, enhanced impulsivity and emotional disorders have been reported in the initial stages of JHD [41]. On the other hand, although QUIN-injected adult rats showed spatial learning deficits in the Morris water maze task and in the radial arm water maze [42,43], we did not find differences in the YM task at the evaluated periods following QUIN administration. Our findings are in accordance with other results obtained in R6/1 mice, used as a transgenic model for JHD, which also did not show any change in YM task performance [44]. The apparently conflicting results in young and adult animals could possibly be attributable to the differences in animal age between our present study and previous studies.

Overall, in the present study, we have provided new insights into the molecular mechanisms and behavioral aspects of QUIN toxicity in adolescent rats, showing early cognitive deficits followed by late motor impairment. Selective and progressive astrogliosis and neuronal loss was elicited from the striatum to cerebral cortex without affecting the hippocampus, despite the early Ca^{2+} influx observed in the three brain regions. Thus, we are tempted to propose that the deleterious effect of intrastriatal QUIN injection may not solely be a consequence of neuronal damage and loss as such, but could result from the fact that QUIN interferes with the highly regulated signaling mechanisms in the immature brain [37].

In this context, we have recently found [24] that acute intrastriatal administration of QUIN in 30-day-old rats affects the phosphorylating system associated with the cytoskeleton of neural striatal cells, causing IF hyperphosphorylation. As we have shown previously [45], this effect was mediated by Ca^{2+} influx through NMDA channels and by oxidative stress. Additionally, alterations in the homeostasis of the cytoskeleton of astrocytes and neurons were found in rat striatal slices treated with 100 μM QUIN. These events were associated with increased Ca^{2+} influx through NMDA receptors and L-type voltage-dependent Ca^{2+} channels in astrocytes. In neurons, QUIN actions involved metabotropic glutamate receptors and the Ca^{2+} from intracellular stores as well as Ca^{2+} influx through NMDA receptor and L-type voltage-dependent Ca^{2+} channels. In both cases, the increase in the intracellular Ca^{2+} levels set off a cascade of events, including activation of the second messenger-dependent protein kinases, which phosphorylate head domain sites on GFAP and neurofilament subunits, potentially leading to misregulation of IF assembly in both glia and neuronal cells [45].

Although QUIN is classically used as a model for HD, little information is available on QUIN toxicity in adolescent rodents *in vivo*. For this reason, it is important to develop more research to clarify the molecular mechanisms involved in the brain damage that mimics QUIN-associated neurodegenerative diseases at this age. To our knowledge, this is the first report describing biochemical, histopathological and behavioral alterations following QUIN administration over time in very young animals. In this context, it has been long recognized that early and severe cognitive deficits followed by later motor impairments characterize the onset of JHD in humans [46–48], as found in the present study. It is expected that our approach may serve as a model with which to better understand early-onset human neurodegeneration.

Experimental procedures

Animals

Adolescent (30-day-old) Wistar rats, obtained from the Central Animal House of the Department of Biochemistry, Federal University of Rio Grande do Sul, Porto Alegre, Brazil, were used in the studies. Rats were considered to be adolescent at postnatal days 24–45 [39]. The rats were maintained on a 12 : 12-h light/dark cycle in an air-conditioned constant-temperature (22 ± 1 °C) colony room, with food and water available *at libitum*. The experimental protocol followed the *Principles of Laboratory Animal Care* (NIH publication 85–23, revised 1985), and was approved by the Ethics

Committee for Animal Research of the Federal University of Rio Grande do Sul. All efforts were made to minimize the number of animals used and their suffering.

Radiochemicals and compounds

L-[^{3}H]Glutamate (52 Ci·mmol^{-1}) and [^{45}Ca]$CaCl_2$ (specific activity of 321 kBq·mg^{-1} Ca^{2+}) were purchased from PerkinElmer Life and Analytical Sciences (Boston, MA, USA). QUIN and GFAP Ig (clone 6F2), anti-rabbit Cy3 Ig and anti-mouse Cy3 Ig were obtained from Sigma (St Louis, MO, USA). Anti-NeuN Ig and FJC were obtained from Millipore. DPX was obtained from Dako (St Louis, MO, USA). All other chemicals were of analytical grade and were purchased from standard commercial suppliers.

Surgery

The rats were deeply anesthetized with Equitesin solution (2.5 mL·kg^{-1}, intraperitoneal), and placed in a stereotaxic apparatus. A small hole was drilled in the skull for microinjection, and 150 nmol (0.5 μL) of QUIN (pH adjusted to 7.4 with NaOH) or NaCl/P_i (sham-operated groups) was slowly injected over a period of 4 min into the right striatum via a needle connected by a polyethylene tube to a 10-μL Hamilton Syringe (Hamilton; 701 N) and an infusion pump (Insight, São Paulo, SP, Brazil). The needle was left in place for another 4 min before been gently removed, so that the total procedure lasted for 8 min. The coordinates for injection were as follows: 0.6 mm posterior to bregma, 2.6 mm lateral to the midline, and 4.5 mm ventral from dura [49]. The correct position of the needle was tested by injecting 0.5 μL of methylene blue (4% in saline solution) and carrying out histological analysis. The dose and method of QUIN administration were based on a previous study [50].

Experimental groups

Experimental groups (n = 8 rats per group) were as follows: naïve rats (untreated); sham rats (intrastriatal injection of 0.5 μL of vehicle); and treated rats (intrastriatal QUIN). Behavioral, biochemical and histopathological characteristics of these rats were then assessed at 1, 2, 3 and 4 weeks after surgery. [^{3}H]Glutamate and $^{45}Ca^{2+}$ uptake were assessed at 30 min, 1, 2, 3 and 4 weeks after surgery. All groups were independent.

Biochemical and histopathological assessment

[^{3}H]Glutamate uptake

Rats were decapitated, and brains were immediately removed and submerged in HBSS containing 137 mM NaCl, 0.63 mM Na_2HPO_4, 4.17 mM $NaHCO_3$, 5.36 mM KCl, 0.44 mM KH_2PO_4, 1.26 mM $CaCl_2$, 0.41 mM $MgSO_4$, and 1.11 mM glucose, adjusted to pH 7.2. The striatum, cerebral cortex and hippocampus were dissected, cut into 400-μm-thick slices with a McIlwain chopper, and washed with HBSS. [^{3}H]Glutamate uptake was performed according to Frizzo *et al.* [51]. Tissue slices were initially preincubated at 35 °C for 15 min. After preincubation, the medium was changed by adding 12.2 MBq·L^{-1} L[^{3}H]glutamate and 100 mM unlabeled glutamate in HBSS. The reaction was stopped after 7 min by washing with 0.5 mL of ice-cold HBSS, and this was followed by the addition of 0.5 M NaOH. Nonspecific uptake was determined by the use of *N*-methyl-D-glucamine. [^{3}H] Glutamate uptake was calculated as the difference between the uptake measured in a sodium-containing medium and the uptake measured in the absence of sodium. Incorporated radioactivity was determined with a Wallac scintillation spectrometer. All experiments were performed in triplicate, and the mean was used for the statistical calculations.

$^{45}Ca^{2+}$ uptake

Rats were killed by decapitation, and brains were removed and placed in Krebs Ringer/bicarbonate buffer (122 mM NaCl, 3 mM KCl, 1.2 mM $MgSO_4$, 1.3 mM $CaCl_2$, 0.4 mM KH_2PO_4, 25 mM $NaHCO_3$). The striatum, cerebral cortex and hippocampus were dissected, cut into 400-μm-thick slices with a McIlwain chopper, and washed with Krebs Ringer/bicarbonate buffer; the sections were then separated. Slices were preincubated for 15 min at 35 °C (pH 7.4). The medium was exchanged with fresh Krebs Ringer/bicarbonate buffer buffer, and the slices were preincubated with 0.2 μCi·mL^{-1} $^{45}Ca^{2+}$ for 1 h. Extracellular $^{45}Ca^{2+}$ was thoroughly washed off for 10 min with a wash solution containing 127.5 mM NaCl, 4.6 mM KCl, 1.2 mM $MgSO_4$, 10 mM Hepes, 11 mM glucose, and 10 mM $LaCl_3$ (pH 7.3). The presence of La^{3+} during the washing stages was found to be essential to prevent the release of the intracellular $^{45}Ca^{2+}$ [52]. After washing, tissue slices were digested and homogenized with 0.5 M NaOH, and 200-μL aliquots were placed in scintillation fluid and counted in an LKB rack β-liquid scintillation spectrometer (Wallac scintillation spectrometer), and 5-μL aliquots were used for protein quantification as described by Lowry *et al.* [53].

Immunofluorescence and FJC staining

After surgery (1, 7, 14 and 21 days), each rat was overdosed with sodium thiopental and perfused intracardially with 0.9% saline followed by 4% paraformaldehyde. The brain was removed, and postfixed overnight in 4% paraformaldehyde at 4 °C. The tissue was then rinsed in 0.1 M phosphate buffer, and transferred to the 15% and 30% sucrose solution in NaCl/P_i at 4 °C. After the brain had sunk (2–3 days), it was frozen by immersion in isopentane cooled with CO_2, and stored in a freezer (−80 °C) for later analyses. Serial coronal sections (30 μm) of the striatum, cerebral cortex and

hippocampus were obtained with a cryostat at −20 °C (Leica, St. Louis, MO, USA.). A set of eight sections, taken from the same region in all groups throughout the rostrocaudal axis of the dorsal striatum, frontal cortex, and dorsal hippocampus, were used for histochemical analysis. The sections of striatum were located around the tip of the cannula. The sections were incubated, according Heimfarth *et al.* [54], with polyclonal rabbit with GFAP Ig (clone 6F2) or mouse NeuN Ig (clone A60) or mouse anti-NeuN Ig (clone A60) for 48 h, and diluted 1 : 3000 and 1 : 1000, respectively, in $NaCl/P_i$ (0.3% Triton X-100) and 2% BSA. Negative controls were carried out with omission of the primary antibodies. After being washed repeatedly in $NaCl/P_i$, tissue sections were incubated with rabbit Ig or mouse Ig Cy3 (F(ab')2 fragment), both diluted 1 : 500 in $NaCl/P_i$, 0.3% Triton X-100 and 2% BSA for 1 h at room temperature. The sections were then washed numerous times in $NaCl/P_i$, and transfer to gelatinized slides. To visualize degenerative neurons, the slides were air-dried and subjected to FJC staining, with a method adapted from Ehara and Ueda [30]. Briefly, slides were rinsed for 5 min in distilled water, and then incubated in 0.06% potassium permanganate solution for 10 min. Following a 2-min water rinse, slides were incubated for 10 min in the FJC staining solution with 0.001% DAPI. The slides were washed, dried, coverslipped in acidic mount media (DPX), and examined under an epifluorescence microscope. The images were obtained with an Olympus IX-81 confocal FV-1000 microscope, and analyzed with OLYMPUS FLUOVIEW software (Shinjuku, Tokyo, Japan).

Protein determination

The protein concentration was determined with the method of Lowry *et al.* [53], using BSA as the standard.

Behavioral assessment

Habituation and locomotion

The motor activity and the habituation of rats were evaluated in the OF test. The OF was made of wood covered with impermeable wood, had a black floor measuring 60 cm^2, and was surrounded by 60-cm-high walls. In the habituation task, the rats were allowed to explore the OF for 10 min on two consecutive days. The distance traveled was registered on the first day as an index of general activity [55]. The rats were individually placed in the center of the OF, and behavioral parameters were recorded and subsequently elaborated with an automated activity-monitoring system (Any-maze; Stoelting, Wood Dale, IL, USA).

OR task

The OR task was conducted in the OF, as previously described by Ennaceur and Delacour [56], and adapted by Pamplona *et al.* [57]. It consisted of three distinct phases: habituation, sample, and discrimination. In the habituation phase, the rats were allowed to explore the OF for 10 min on two consecutive days. In the sample phase, two identical objects (C1 and C2; cubes) were placed in opposite corners of the OF, 20 cm distant from the walls and ~ 60 cm apart from each other, and the rats were allowed to explore them for 5 min. After the end of the sample phase, the rats were removed from the OF and kept in the home cage. After a delay period of 30 min, in the discrimination phase, an identical copy of the familiar object (C3) and a novel T-shaped object (T) were placed in the locations previously occupied by C1 and C2, and the rats were allowed to explore the objects for 5 min. All of the objects were constructed with plastic LEGO blocks. The locations of the objects were counterbalanced in each session. The time spent by the rats in exploring each object was monitored with a video system placed in an adjacent room. Exploration of an object was defined as directing the nose to the object at a distance of ≤ 2 cm and/or touching it with the nose. Analyses were performed on the following measures: the total time spent exploring the two objects in the sample phase (C1 + C2) and the discrimination index, which is defined by the difference in exploration time between the novel and the familiar objects, divided by the total time spent exploring these two objects in the discrimination phase [(T − C3)/(T + C3)].

YM task

The apparatus consisted of three arms (30 × 10 × 15 cm^3 and 120° apart) made of black wood, placed in a room with visual cues on the walls; YM testing consisted of two trials separated by an interval of 1 h [58,59]. In the first trial, the rat was placed in the end of one arm, and allowed access to that arm and another arm for 5 min. The third arm (the novel arm) was blocked with a guillotine door. The rat was then removed from the maze and returned to its home cage. For the second trial, the rat was placed back into the start arm of the maze, and given free access to all three arms for 5 min. The number of entries and the time spent in each arm were recorded. The percentage of entries and time spent in the novel arm were compared with random exploration of the three arms of the maze (i.e. 33%).

All behavioral experiments were conducted in a sound-attenuated room under low-intensity light, and were monitored by an experimenter who was unaware of the treatments. All apparatus was cleaned with a 10% ethanol solution, and then dried with a paper towel after each trial, in order to avoid odor impregnation.

Statistical analysis

Data were analyzed statistically with one-way or two-way ANOVA followed by the Tukey–Kramer multiple comparison test when the *F*-test was significant. All analyses

were performed with SPSS on an IBM-PC-compatible computer.

Acknowledgements

This work was supported by grants from the Conselho Nacional de Desenvolvimento Científico e Tecnológico (CNPq), Fundação de Amparo à Pesquisa do Estado do Rio Grande do Sul (FAPERGS), and Pro-Reitoria de Pesquisa de Pós Graduação of Universidade Federal do Rio Grande do Sul (Propesq-UFRGS).

References

1 Stone TW & Perkins MN (1981) Quinolinic acid: a potent endogenous excitant at amino acid receptors in CNS. *Eur J Pharmacol* **72**, 411–412.
2 Chen Y & Guillemin GJ (2009) Kynurenine pathway metabolites in humans: disease and healthy states. *Int J Tryptophan Res* **2**, 1–19.
3 Guillemin GJ, Smythe G, Takikawa O & Brew BJ (2005) Expression of indoleamine 2,3-dioxygenase and production of quinolinic acid by human microglia, astrocytes, and neurons. *Glia* **49**, 15–23.
4 Kohler C, Eriksson LG, Okuno E & Schwarcz R (1988) Localization of quinolinic acid metabolizing enzymes in the rat brain. Immunohistochemical studies using antibodies to 3-hydroxyanthranilic acid oxygenase and quinolinic acid phosphoribosyltransferase. *Neuroscience* **27**, 49–76.
5 Lugo-Huitron R, Ugalde Muniz P, Pineda B, Pedraza-Chaverri J, Rios C & Perez-de la Cruz V (2013) Quinolinic acid: an endogenous neurotoxin with multiple targets. *Oxid Med Cell Longev* **2013**, 104024.
6 Foster AC, Zinkand WC & Schwarcz R (1985) Quinolinic acid phosphoribosyltransferase in rat brain. *J Neurochem* **44**, 446–454.
7 Tan L & Yu JT (2012) The kynurenine pathway in neurodegenerative diseases: mechanistic and therapeutic considerations. *J Neurol Sci* **323**, 1–8.
8 Perez-De La Cruz V, Elinos-Calderon D, Robledo-Arratia Y, Medina-Campos ON, Pedraza-Chaverri J, Ali SF & Santamaria A (2009) Targeting oxidative/nitrergic stress ameliorates motor impairment, and attenuates synaptic mitochondrial dysfunction and lipid peroxidation in two models of Huntington's disease. *Behav Brain Res* **199**, 210–217.
9 Pérez-De La Cruz V, Carrillo-Mora P & Santamaría A (2012) Quinolinic acid, an endogenous molecule combining excitotoxicity, oxidative stress and other toxic mechanisms. *Int J Tryptophan Res* **5**, 1–8.
10 Knight RA & Verkhratsky A (2010) Neurodegenerative diseases: failures in brain connectivity? *Cell Death Differ* **17**, 1069–1070.
11 Li L, Lundkvist A, Andersson D, Wilhelmsson U, Nagai N, Pardo AC, Nodin C, Stahlberg A, Aprico K, Larsson K *et al.* (2008) Protective role of reactive astrocytes in brain ischemia. *J Cereb Blood Flow Metab* **28**, 468–481.
12 Pekny M & Nilsson M (2005) Astrocyte activation and reactive gliosis. *Glia* **50**, 427–434.
13 Bushong EA, Martone ME & Ellisman MH (2004) Maturation of astrocyte morphology and the establishment of astrocyte domains during postnatal hippocampal development. *Int J Dev Neurosci* **22**, 73–86.
14 Bushong EA, Martone ME, Jones YZ & Ellisman MH (2002) Protoplasmic astrocytes in CA1 stratum radiatum occupy separate anatomical domains. *J Neurosci* **22**, 183–192.
15 Schwarcz R & Meldrum B (1985) Excitatory aminoacid antagonists provide a therapeutic approach to neurological disorders. *Lancet* **2**, 140–143.
16 Schwarcz R & Pellicciari R (2002) Manipulation of brain kynurenines: glial targets, neuronal effects, and clinical opportunities. *J Pharmacol Exp Ther* **303**, 1–10.
17 Dugan LL & Kim-Han JS (2006) Hypoxic–ischemic brain injury and oxidative stress. Basic Neurochemistry: Molecular, Cellular and Medical Aspects, pp. 563–569. Elsevier Academic Press, New York, NY.
18 Sánchez AME, Mejía-Toiber J & Massieu L (2008) Excitotoxic neuronal death and the pathogenesis of Huntington's disease. *Arch Med Res* **39**, 265–276.
19 Beal MF, Ferrante RJ, Swartz KJ & Kowall NW (1991) Chronic quinolinic acid lesions in rats closely resemble Huntington's disease. *J Neurosci* **11**, 1649–1659.
20 Scattoni ML, Valanzano A, Popoli P, Pezzola A, Reggio R & Calamandrei G (2004) Progressive behavioural changes in the spatial open-field in the quinolinic acid rat model of Huntington's disease. *Behav Brain Res* **152**, 375–383.
21 Kalonia H, Mishra J & Kumar A (2012) Targeting neuro-inflammatory cytokines and oxidative stress by minocycline attenuates quinolinic-acid-induced Huntington's disease-like symptoms in rats. *Neurotox Res* **22**, 310–320.
22 Sadan O, Shemesh N, Barzilay R, Dadon-Nahum M, Blumenfeld-Katzir T, Assaf Y, Yeshurun M, Djaldetti R, Cohen Y, Melamed E *et al.* (2012) Mesenchymal stem cells induced to secrete neurotrophic factors attenuate quinolinic acid toxicity: a potential therapy for Huntington's disease. *Exp Neurol* **234**, 417–427.
23 Colle D, Hartwig JM, Soares FA & Farina M (2012) Probucol modulates oxidative stress and excitotoxicity in Huntington's disease models in vitro. *Brain Res Bull* **87**, 397–405.
24 Pierozan P, Zamoner A, Soska AK, Silvestrin RB, Loureiro SO, Heimfarth L, Mello e Souza T, Wajner M & Pessoa-Pureur R (2010) Acute intrastriatal

administration of quinolinic acid provokes hyperphosphorylation of cytoskeletal intermediate filament proteins in astrocytes and neurons of rats. *Exp Neurol* **224**, 188–196.
25 Guidetti P & Schwarcz R (1999) 3-Hydroxykynurenine potentiates quinolinate but not NMDA toxicity in the rat striatum. *Eur J Neurosci* **11**, 3857–3863.
26 Moresco RM & Fazio F (2005) Molecular imaging of individual behaviour. *Eur J Nucl Med Mol Imaging* **32**, 717–719.
27 Figueredo-Cardenas G, Chen Q & Reiner A (1997) Age-dependent differences in survival of striatal somatostatin-NPY-NADPH-diaphorase-containing interneurons versus striatal projection neurons after intrastriatal injection of quinolinic acid in rats. *Exp Neurol* **146**, 444–457.
28 Sun Z, Chen Q & Reiner A (2003) Enkephalinergic striatal projection neurons become less affected by quinolinic acid than substance P-containing striatal projection neurons as rats age. *Exp Neurol* **184**, 1034–1042.
29 Parpura V, Basarsky TA, Liu F, Jeftinija K, Jeftinija S & Haydon PG (1994) Glutamate-mediated astrocyte–neuron signalling. *Nature* **369**, 744–747.
30 Ehara A & Ueda S (2009) Application of Fluoro-Jade C in acute and chronic neurodegeneration models: utilities and staining differences. *Acta Histochem Cytochem* **42**, 171–179.
31 Guillemin GJ (2012) Quinolinic acid, the inescapable neurotoxin. *FEBS J* **279**, 1356–1365.
32 Olivera-Bravo S, Fernandez A, Sarlabos MN, Rosillo JC, Casanova G, Jimenez M & Barbeito L (2011) Neonatal astrocyte damage is sufficient to trigger progressive striatal degeneration in a rat model of glutaric acidemia-I. *PLoS One* **6**, e20831.
33 Brickell KL, Nicholson LF, Waldvogel HJ & Faull RL (1999) Chemical and anatomical changes in the striatum and substantia nigra following quinolinic acid lesions in the striatum of the rat: a detailed time course of the cellular and GABA(A) receptor changes. *J Chem Neuroanat* **17**, 75–97.
34 Beal MF, Kowall NW, Ellison DW, Mazurek MF, Swartz KJ & Martin JB (1986) Replication of the neurochemical characteristics of Huntington's disease by quinolinic acid. *Nature* **321**, 168–171.
35 Shelbourne P, Coote E, Dadak S & Cobb SR (2007) Normal electrical properties of hippocampal neurons modelling early Huntington disease pathogenesis. *Brain Res* **1139**, 226–234.
36 Kremer HP, Roos RA, Dingjan G, Marani E & Bots GT (1990) Atrophy of the hypothalamic lateral tuberal nucleus in Huntington's disease. *J Neuropathol Exp Neurol* **49**, 371–382.
37 Holopainen IE (2008) Seizures in the developing brain: cellular and molecular mechanisms of neuronal damage, neurogenesis and cellular reorganization. *Neurochem Int* **52**, 935–947.
38 Albin RL, Reiner A, Anderson KD, Penney JB & Young AB (1990) Striatal and nigral neuron subpopulations in rigid Huntington's disease: implications for the functional anatomy of chorea and rigidity-akinesia. *Ann Neurol* **27**, 357–365.
39 Spear LP (2000) The adolescent brain and age-related behavioral manifestations. *Neurosci Biobehav Rev* **24**, 417–463.
40 Thiel CM, Muller CP, Huston JP & Schwarting RK (1999) High versus low reactivity to a novel environment: behavioural, pharmacological and neurochemical assessments. *Neuroscience* **93**, 243–251.
41 Paulsen JS, Ready RE, Hamilton JM, Mega MS & Cummings JL (2001) Neuropsychiatric aspects of Huntington's disease. *J Neurol Neurosurg Psychiatry* **71**, 310–314.
42 Furtado JC & Mazurek MF (1996) Behavioral characterization of quinolinate-induced lesions of the medial striatum: relevance for Huntington's disease. *Exp Neurol* **138**, 158–168.
43 Haik KL, Shear DA, Schroeder U, Sabel BA & Dunbar GL (2000) Quinolinic acid released from polymeric brain implants causes behavioral and neuroanatomical alterations in a rodent model of Huntington's disease. *Exp Neurol* **163**, 430–439.
44 Ransome MI & Hannan AJ (2012) Behavioural state differentially engages septohippocampal cholinergic and GABAergic neurons in R6/1 Huntington's disease mice. *Neurobiol Learn Mem* **97**, 261–270.
45 Pierozan P, Zamoner A, Soska AK, de Lima BO, Reis KP, Zamboni F, Wajner M & Pessoa-Pureur R (2012) Signaling mechanisms downstream of quinolinic acid targeting the cytoskeleton of rat striatal neurons and astrocytes. *Exp Neurol* **233**, 391–399.
46 Squitieri F, Frati L, Ciarmiello A, Lastoria S & Quarrell O (2006) Juvenile Huntington's disease: does a dosage-effect pathogenic mechanism differ from the classical adult disease? *Mech Ageing Dev* **127**, 208–212.
47 Myers RH, Vonsattel JP, Stevens TJ, Cupples LA, Richardson EP, Martin JB & Bird ED (1988) Clinical and neuropathologic assessment of severity in Huntington's disease. *Neurology* **38**, 341–347.
48 Butters N, Sax D, Montgomery K & Tarlow S (1978) Comparison of the neuropsychological deficits associated with early and advanced Huntington's disease. *Arch Neurol* **35**, 585–589.
49 Paxinos G, Watson C, Pennisi M & Topple A (1985) Bregma, lambda and the interaural midpoint in stereotaxic surgery with rats of different sex, strain and weight. *J Neurosci Methods* **13**, 139–143.
50 Qin Y, Soghomonian JJ & Chesselet MF (1992) Effects of quinolinic acid on messenger RNAs encoding

somatostatin and glutamic acid decarboxylases in the striatum of adult rats. *Exp Neurol* **115**, 200–211.
51 Frizzo ME, Lara DR, Prokopiuk Ade S, Vargas CR, Salbego CG, Wajner M & Souza DO (2002) Guanosine enhances glutamate uptake in brain cortical slices at normal and excitotoxic conditions. *Cell Mol Neurobiol* **22**, 353–363.
52 Zamoner A, Royer C, Barreto KP, Pessoa-Pureur R & Silva FR (2007) Ionic involvement and kinase activity on the mechanism of nongenomic action of thyroid hormones on $^{45}Ca^{2+}$ uptake in cerebral cortex from young rats. *Neurosci Res* **57**, 98–103.
53 Lowry OH, Rosebrough NJ, Farr AL & Randall RJ (1951) Protein measurement with the Folin phenol reagent. *J Biol Chem* **193**, 265–275.
54 Heimfarth L, Loureiro SO, Dutra MF, Petenuzzo L, de Lima BO, Fernandes CG, da Rocha JB & Pessoa-Pureur R (2013) Disrupted cytoskeletal homeostasis, astrogliosis and apoptotic cell death in the cerebellum of preweaning rats injected with diphenyl ditelluride. *Neurotoxicology* **34**, 175–188.
55 Rodgers RJ (1997) Animal models of 'anxiety': where next? *Behav Pharmacol* **8**, 477–496; discussion 497–504.
56 Ennaceur A & Delacour J (1988) A new one-trial test for neurobiological studies of memory in rats. 1: behavioral data. *Behav Brain Res* **31**, 47–59.
57 Pamplona FA, Pandolfo P, Savoldi R, Prediger RD & Takahashi RN (2009) Environmental enrichment improves cognitive deficits in spontaneously hypertensive rats (SHR): relevance for attention deficit/hyperactivity disorder (ADHD). *Prog Neuropsychopharmacol Biol Psychiatry* **33**, 1153–1160.
58 Dellu F, Fauchey V, Le Moal M & Simon H (1997) Extension of a new two-trial memory task in the rat: influence of environmental context on recognition processes. *Neurobiol Learn Mem* **67**, 112–120.
59 Pandolfo P, Machado NJ, Kofalvi A, Takahashi RN & Cunha RA (2011) Caffeine regulates frontocorticostriatal dopamine transporter density and improves attention and cognitive deficits in an animal model of attention deficit hyperactivity disorder. *Eur Neuropsychopharmacol* **23**, 317–328.

Supporting information

Additional supporting information may be found in the online version of this article at the publisher's web site:

Table S1. Spatial memory in the Y-maze task 1, 2, 3 and 4 weeks after intrastriatal injection of QUIN.
Fig. S1. Striatum 24 h.
Fig. S2. Cerebral cortex 24 h.
Fig. S3. Striatum 7 days.
Fig. S4. Cerebral cortex 7 days.
Fig. S5. Striatum 7 days.
Fig. S6. Cerebral cortex 7 days.
Fig. S7. Striatum 21 days.
Fig. S8. Cerebral cortex 21 days.

Biochemical, histopathological and behavioral alterations caused by intrastriatal administration of quinolic acid to young rats

Paula Pierozan[a], Carolina Gonçalves Fernandes[a], Márcio Ferreira Dutra[a,b], Pablo Pandolfo[a,c], Fernanda Ferreira[a], Bárbara Ortiz de Lima[a], Lisiane Porciúncula[a], Moacir Wajner[a], Regina Pessoa-Pureur[a]

Supplementary information

TABLE S1: Spatial memory in Y-maze task after 1, 2, 3 and 4 weeks after intrastriatal injection with QUIN. Y-maze (YM) testing consisted of two trials separated by an interval of one hour [58, 59]. In the first trial, the animal was placed into the end of one arm and allowed access to that arm and another arm during 5 min. The third arm (the novel arm) was blocked by a guillotine door. The rat was then removed from the maze and returned to its home cage. For the second trial, the rat was placed back into the start arm of the maze and given free access to all three arms for 5 min. The number of entries and the time spent in each arm were recorded. The percentage of entries and time spent in the novel arm was compared to random exploration of the three arms of the maze (i.e., 33%).

	1st week			2nd week			3rd week			4th week		
	Control	Sham	Quin	Control	Sham	Quin	Control	Sham	Quin	Control	Sham	Quin
Number of visits in novel arm	9±3.7	12±3	8±4	9±3	9.5±4	8±2	9±5	9.4±4	9±3.3	9±3	9±2	8±4
Duration of visit in novel arm (%)	32±9	30±19	35±9	36±6	43±2	41±1	48±10	36±12	39±9	32±7	32±7	29±9
Time spent in novel arm (s)	79.63 ±22	66.3 ±43	61.86 ±38	80 ±17	98 ±16	96 ±22	78 ±40	81 ±30	79 ±33	75 ±15	74 ±15	62 ±20

Exploration [duration (%), number of visits and time spent (s) in the novel arm] of the Y-maze task. Percentage of exploration in novel arm with respect to these measured in the three arms. The measurements (mean ± S.D.) were recorded during the second trial.

Suppelementary Figure S1: Striatum 24 h. Quinolinic acid-induced lesions assessed with FJC staining NeuN and GFAP immunohistochemistry. Rats were subjected to an intrastriatal injection of 150 nmol of QUIN in right striatum. Astrogliosis in the striatum 24 h after injectin with absence of FJC-labeled cells and unaltered NeuN immunostaining. Note more ramified cells with wider projections. Representative images of 8 animals. Bar scale= 30 μm (magnification: 40x).

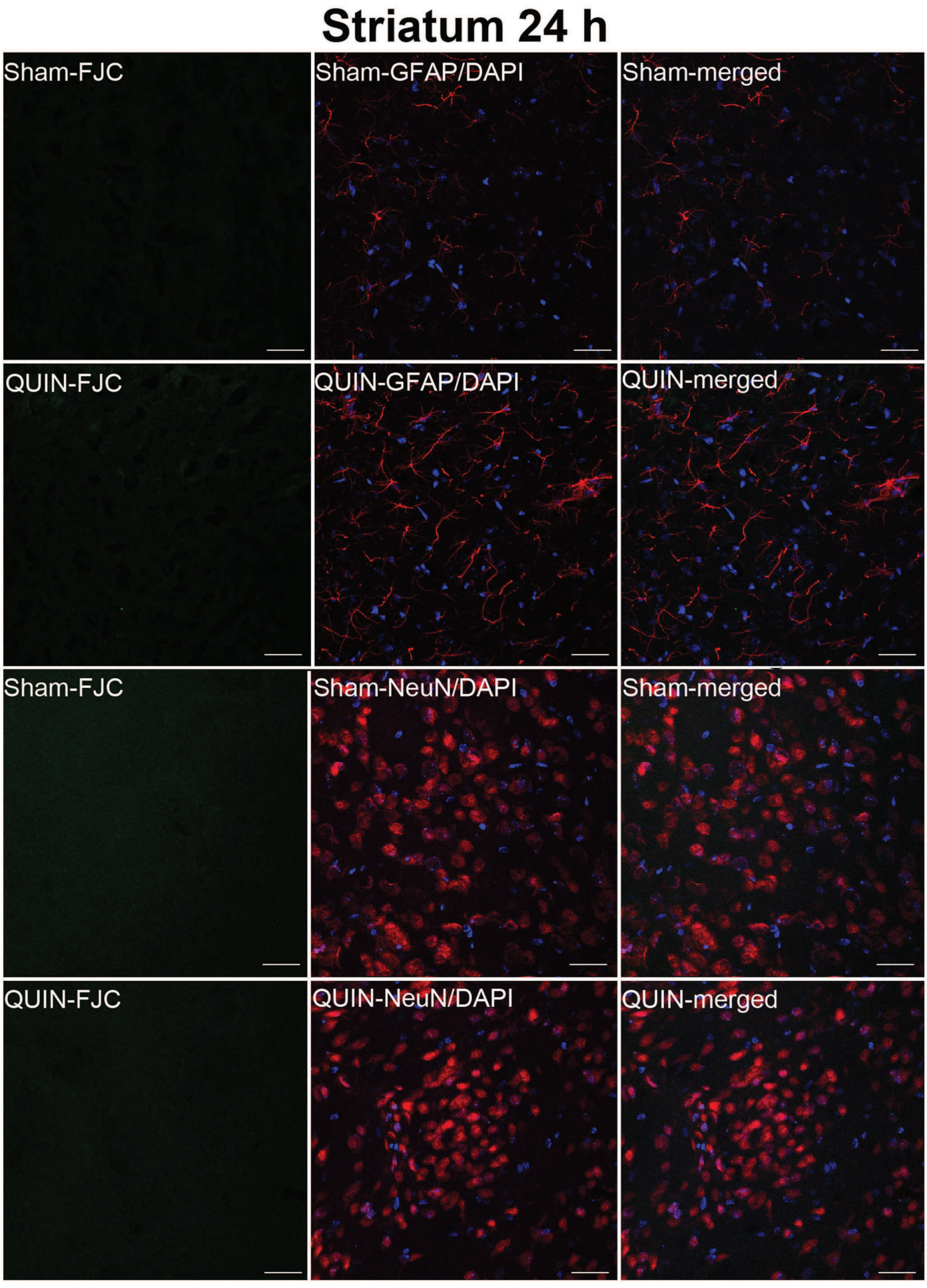

Suppelementary Figure S2: Cerebral cortex 24 h. Quinolinic acid-induced lesions assessed with FJC staining NeuN and GFAP immunohistochemistry. Rats were subjected to an intrastriatal injection of 150 nmol of QUIN in right striatum. Absence of FJC-labeled cells and unaltered NeuN and GFAP immunostaining. Representative images of 8 animals. Bar scale= 30 µm (magnification: 40x).

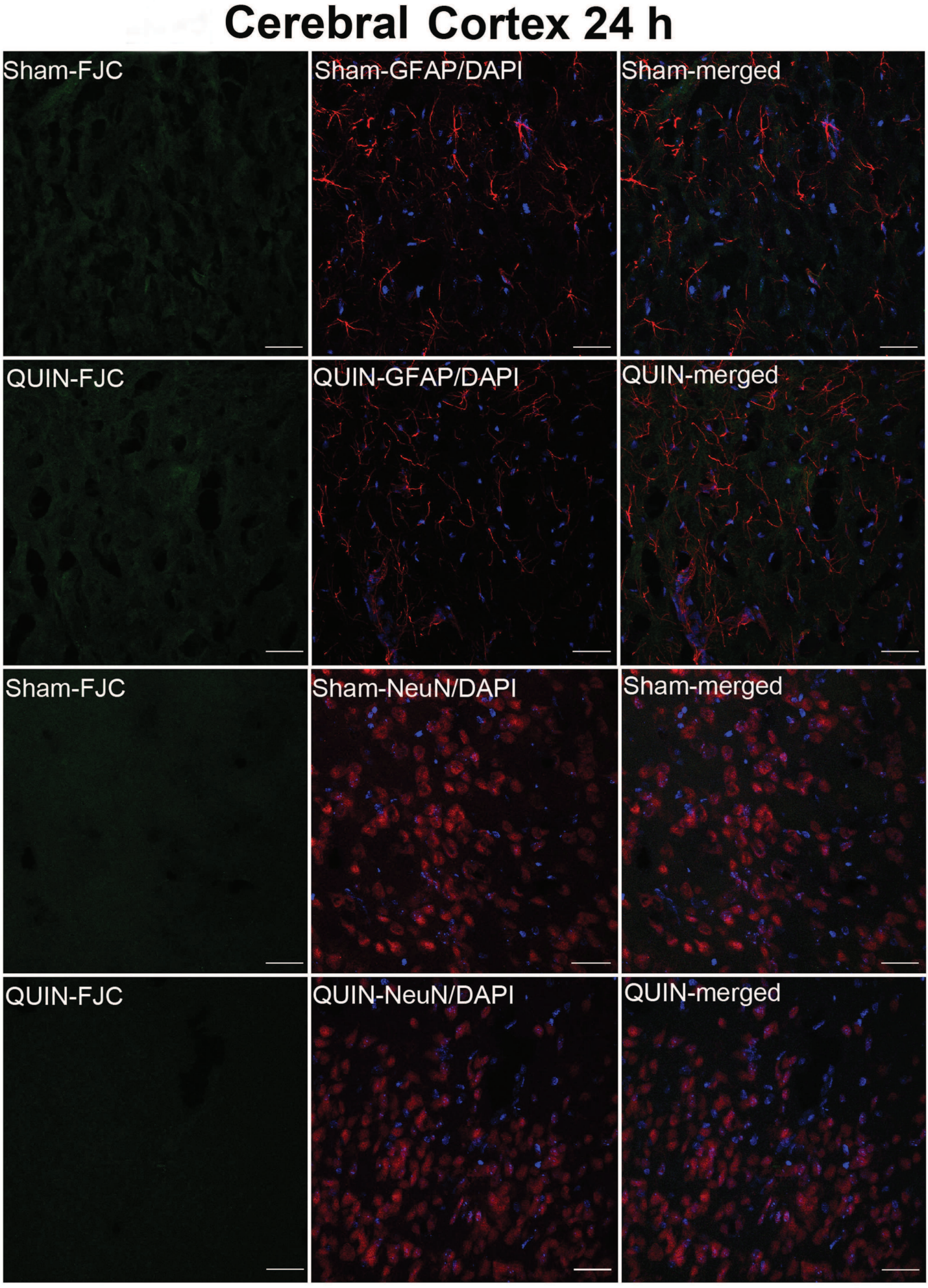

Suppelementary Figure S3: Striatum 7 days. Quinolinic acid-induced lesions assessed with FJC staining NeuN and GFAP immunohistochemistry. Rats were subjected to an intrastriatal injection of 150 nmol of QUIN in right striatum. Panel shows increased GFAP immunoreactivity in striatum 7 days after injection, indicating persistent astrogliosis with unaltered NeuN immunostaining and absence of FJC-labeled cells. Representative images of 8 animals. Bar scale= 30 µm (magnification: 40x).

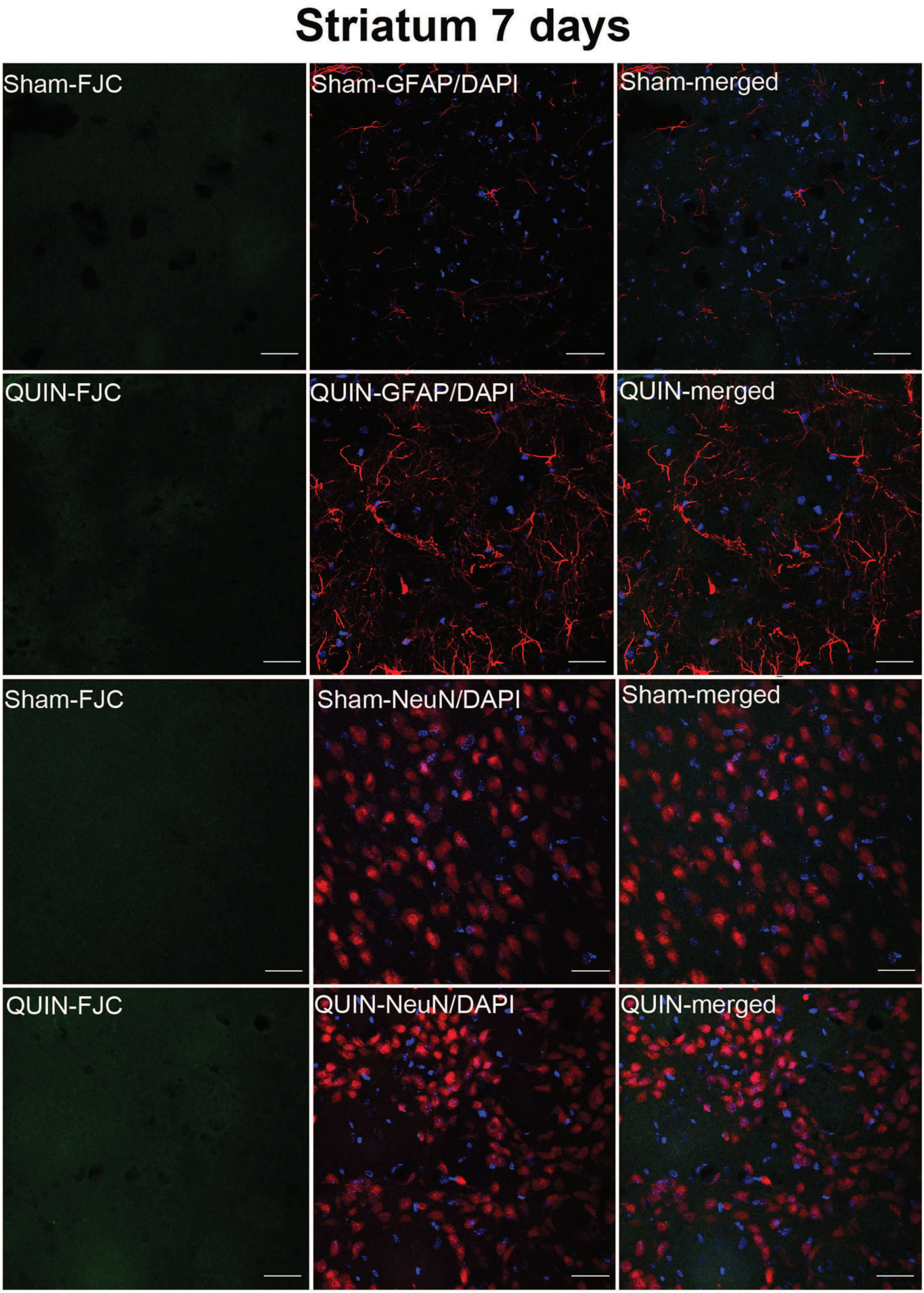

Suppelementary Figure S4: Cerebral cortex 7 days. Quinolinic acid-induced lesions assessed with FJC staining NeuN and GFAP immunohistochemistry. Rats were subjected to an intrastriatal injection of 150 nmol of QUIN in right striatum. Panel shows increased GFAP immunoreactivity in cerebral cortex 7 days after injection with unaltered NeuN immunostaining and absence of FJC-labeled cells. Representative images of 8 animals. Bar scale= 30 µm (magnification: 40x).

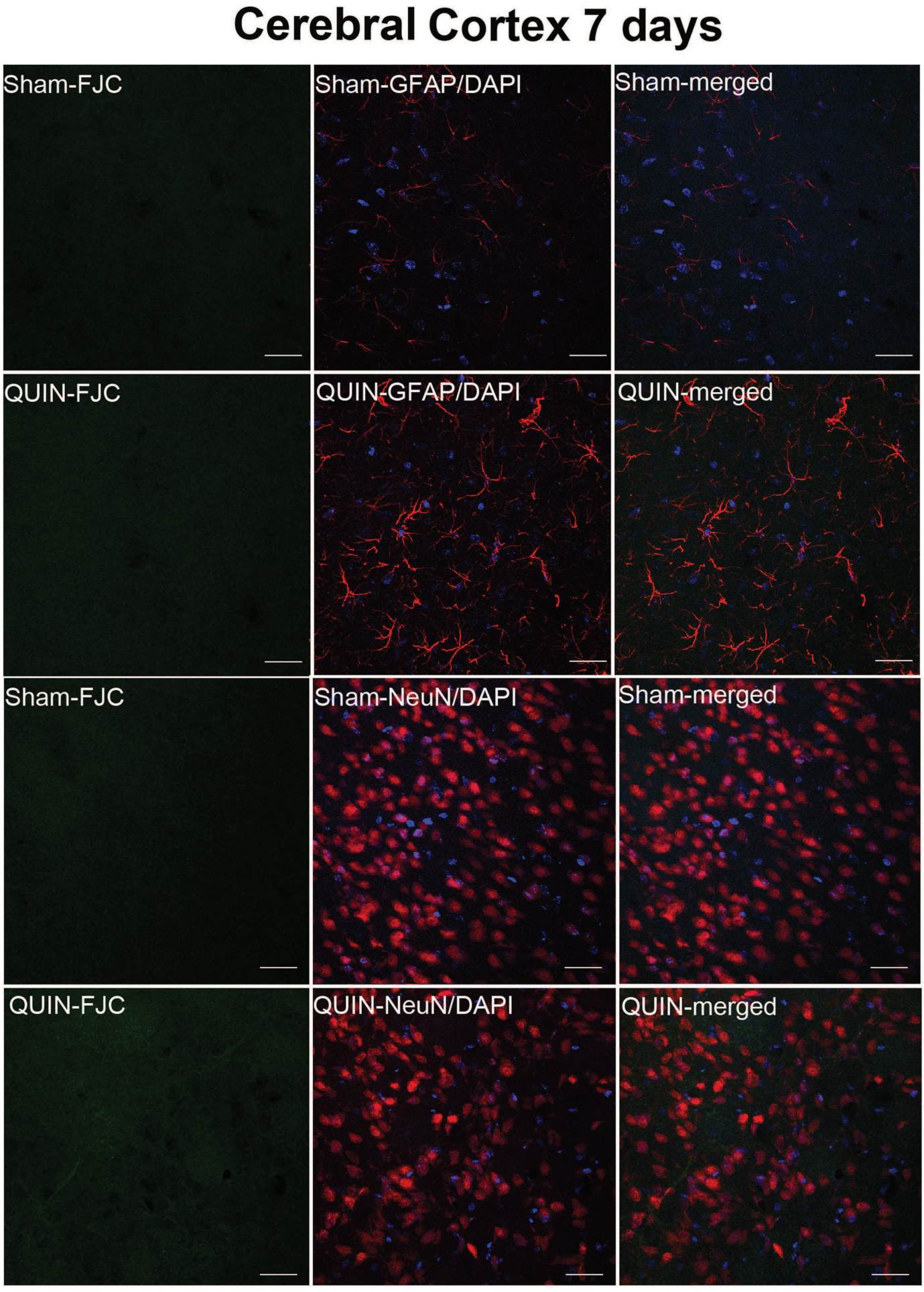

Suppelementary Figure S5: Striatum 14 days. Quinolinic acid-induced lesions assessed with FJC staining NeuN and GFAP immunohistochemistry. Rats were subjected to an intrastriatal injection of 150 nmol of QUIN in right striatum. Panel shows persistent astrogliosis, decreased NeuN immunostaining and a large number of both linear and dot-shaped FJC-structures in striatum 14 days after injection. Staining shows dot-shaped structure (arrow). Representative images of 8 animals. Bar scale= 30 µm (magnification: 40x).

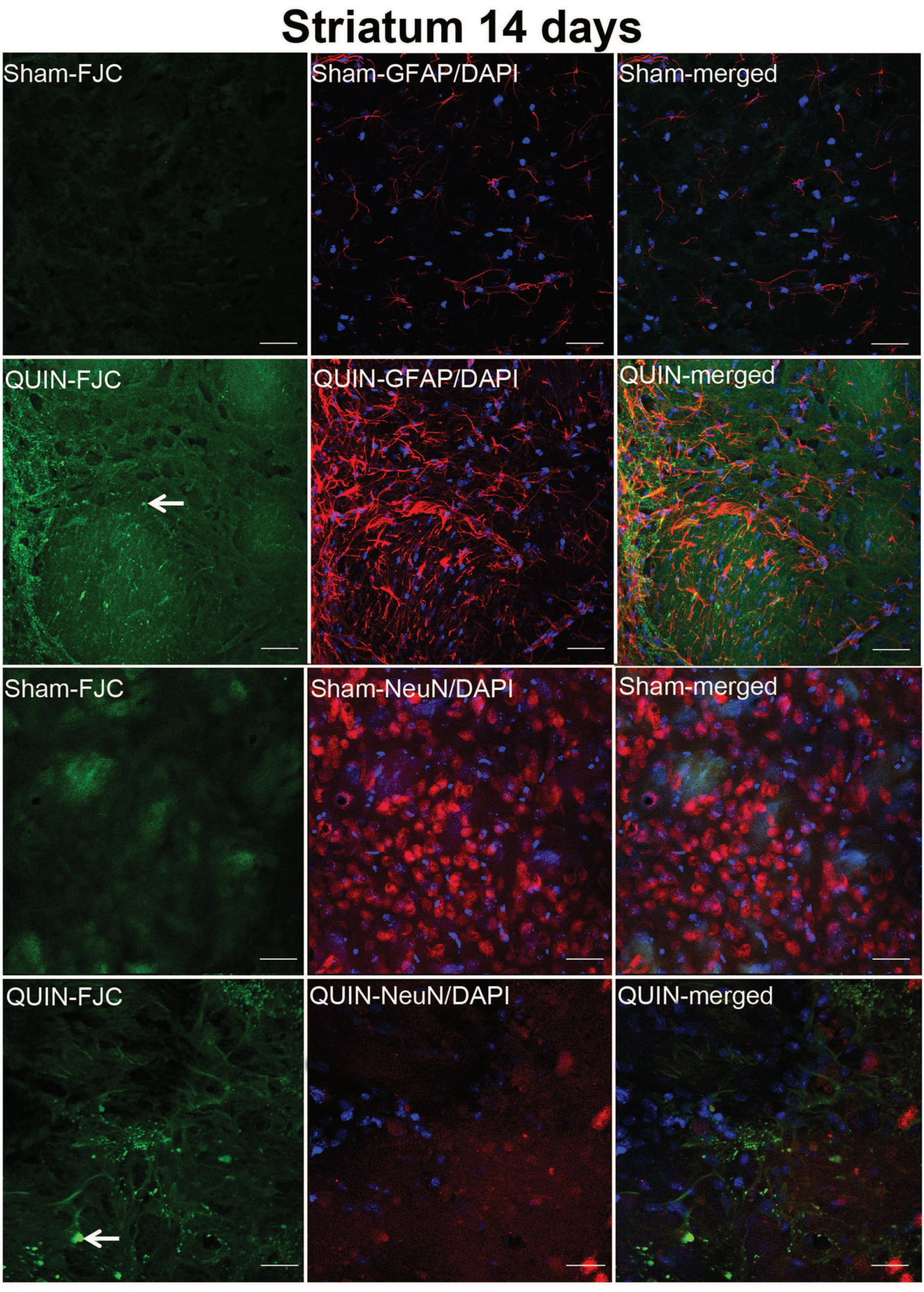

Suppelementary Figure S6: Cerebral cortex 14 days. Quinolinic acid-induced lesions assessed with FJC staining NeuN and GFAP immunohistochemistry. Rats were subjected to an intrastriatal injection of 150 nmol of QUIN in right striatum. Panel shows persistent astrogliosis, decreased NeuN immunostaining, FJC-positive cell bodies with neuronal profile 14 days after injection in cerebral cortex. Staining shows fiber-like structures (arrow head) and asterisk indicates a pyramidal neuron characteristic of layer V in cerebral cortex. Representative images of 8 animals. Bar scale= 30 µm (magnification: 40x).

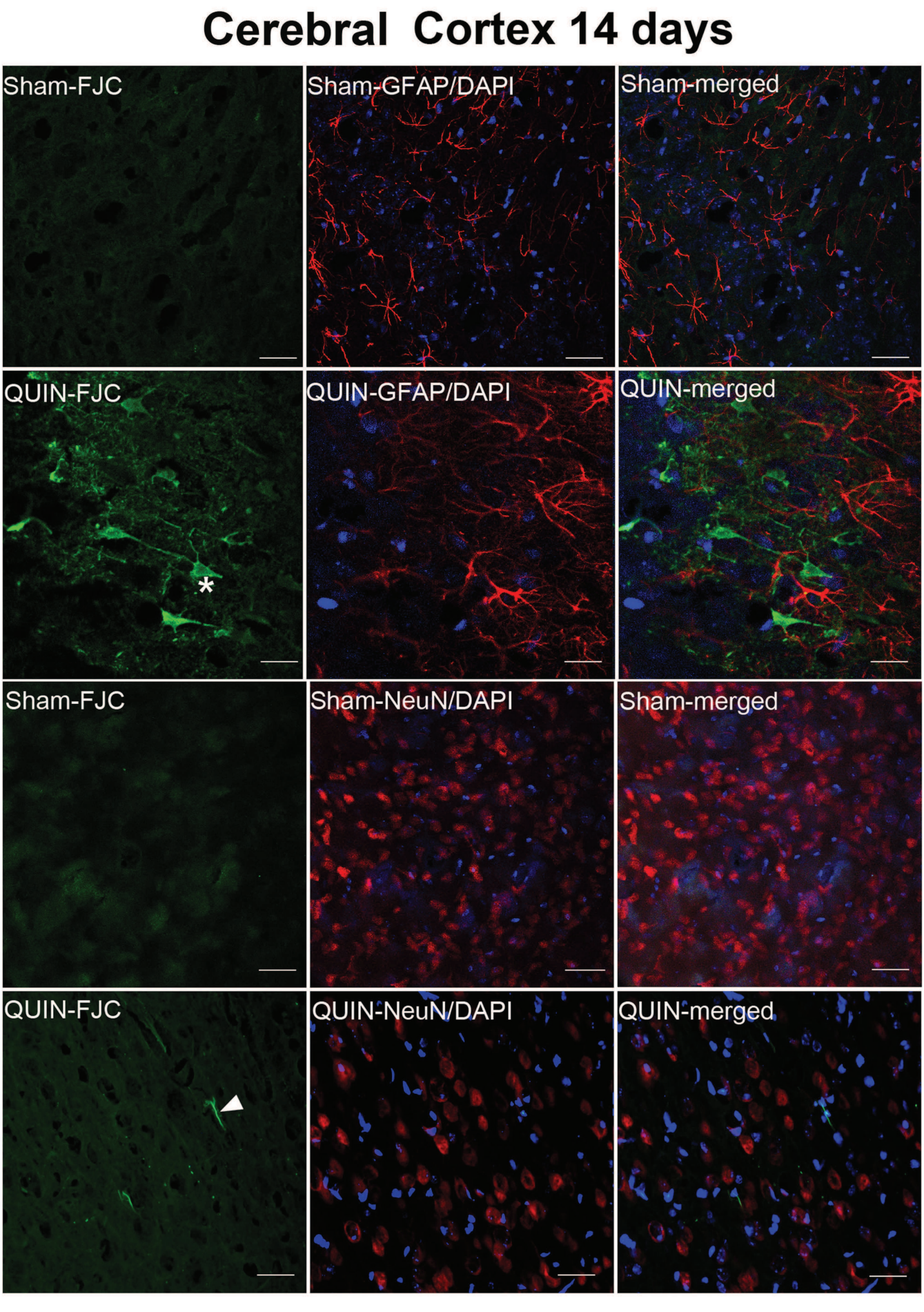

Suppelementary Figure S7: Striatum 21 days. Quinolinic acid-induced lesions assessed with FJC staining NeuN and GFAP immunohistochemistry. Rats were subjected to an intrastriatal injection of 150 nmol of QUIN in right striatum. Panel shows remained labeled FJC debris, diminished NeuN and increased GFAP immunofluorescence in striatum 21 days after injection. Staining shows fiber-like structures (arrow head) and dot-shaped structures (arrow). Representative images of 8 animals. Bar scale= 30 µm (magnification: 40x).

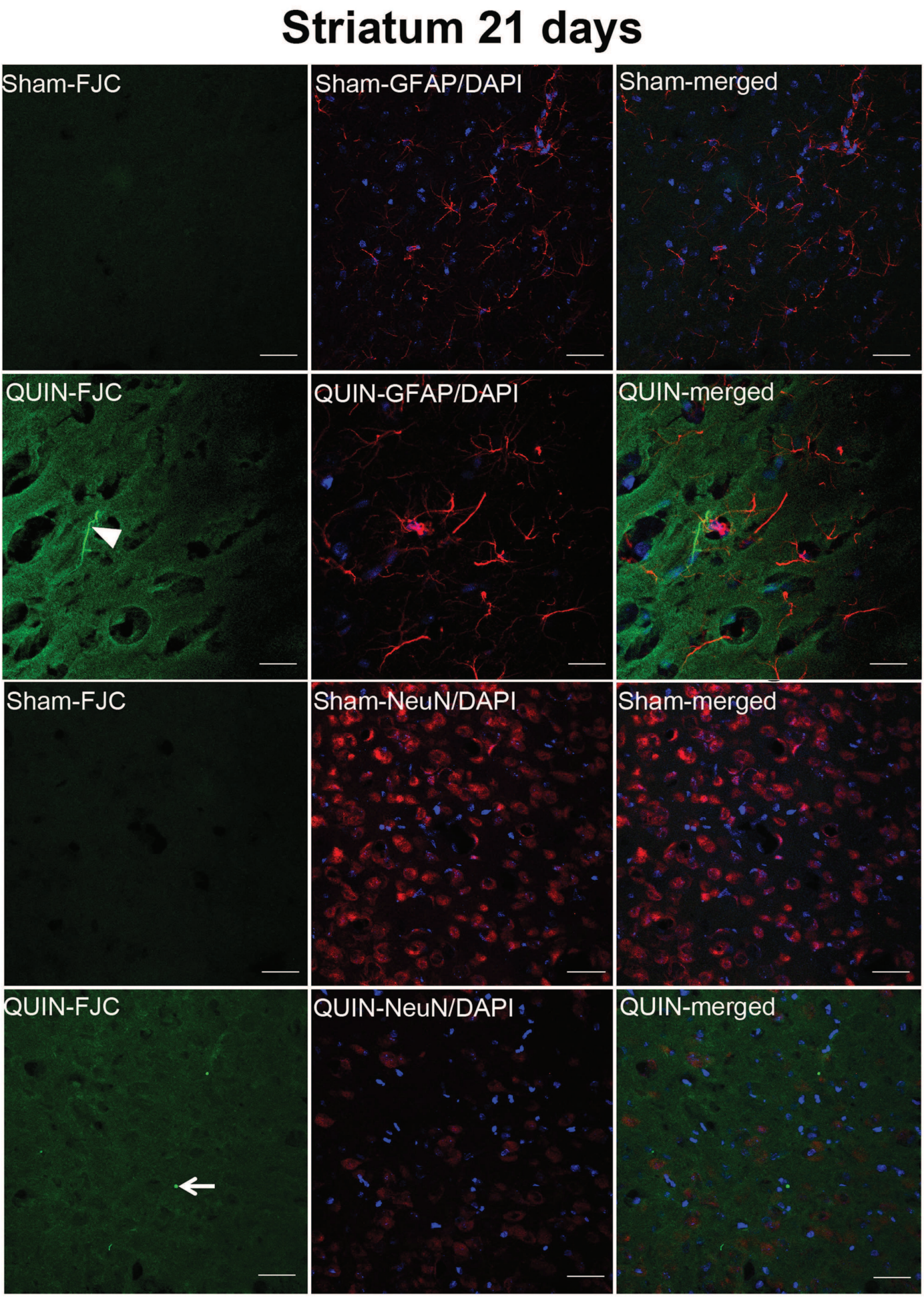

Suppelementary Figure S8: Cerebral cortex 21 days. Quinolinic acid-induced lesions assessed with FJC staining NeuN and GFAP immunohistochemistry. Rats were subjected to an intrastriatal injection of 150 nmol of QUIN in right striatum. Panel shows remained labeled FJC debris, diminished NeuN and increased GFAP immunofluorescence in cerebral cortex 21 days after injection. Staining shows fiber-like structures (arrow head) and dot-shaped structures (arrow). Representative images of 8 animals. Bar scale= 30 µm (magnification: 40x).

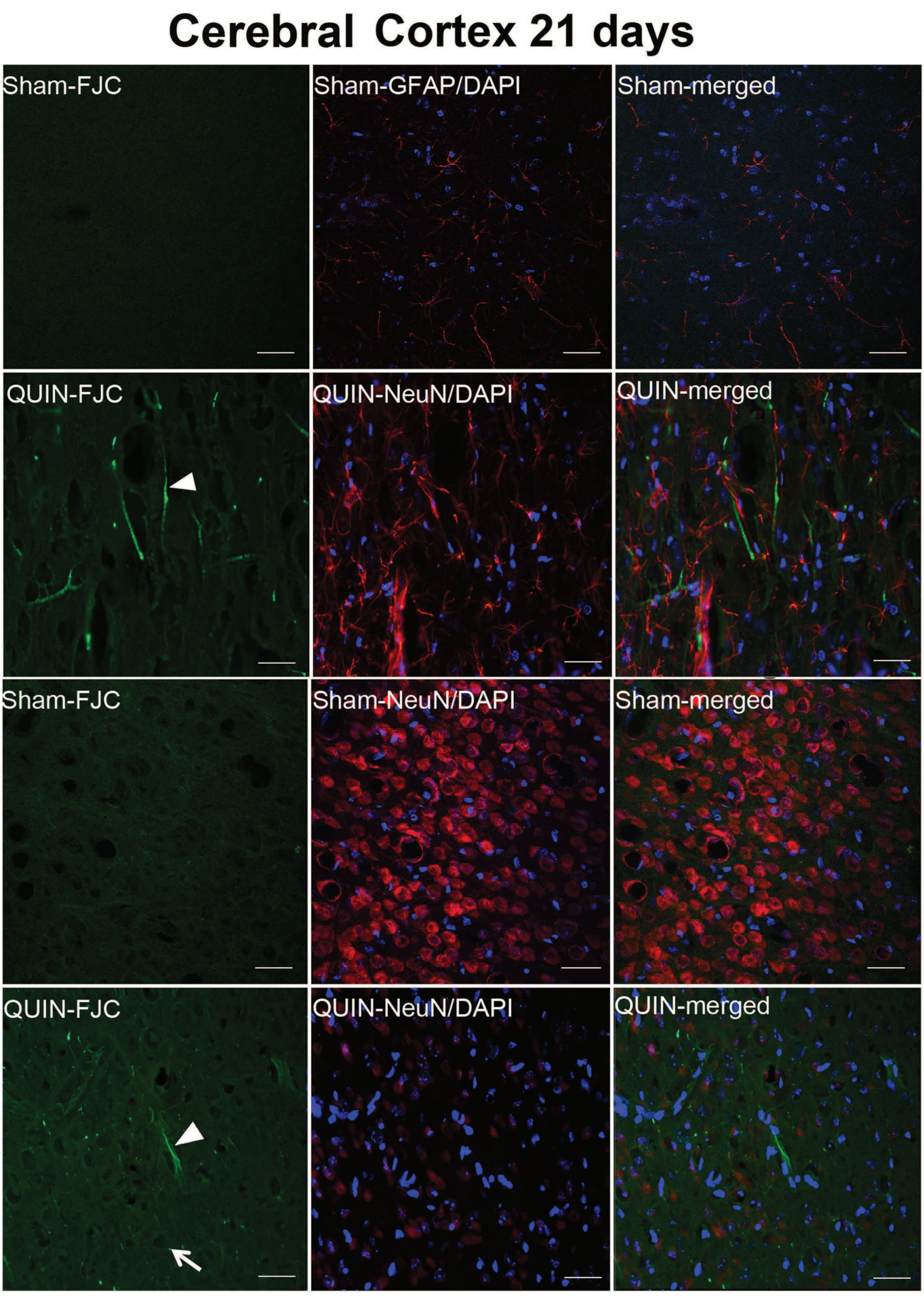

Capítulo 2

ACUTE INTRASTRIATAL INJECTION OF QUINOLINIC ACID PROVOKES LONG-LASTING MISREGULATION OF THE CYTOSKELETON IN THE STRIATUM, CEREBRAL CORTEX AND HIPPOCAMPUS OF YOUNG RATS

Paula Pierozan, Carolina Gonçalves Fernandes, Fernanda Ferreira and Regina Pessoa-Pureur

Artigo submetido ao **Brain Research**

BRAIN RESEARCH

'My EES Hub' available for consolidated users ... more
Discover the latest news for Elsevier authors
Maintenance outage on 11 May 2014 ... more

Username: rpureur@ufrgs.br
Switch To: Author

Version: EES 2014.3

Submissions Being Processed for Author Regina Pessoa-Pureur, Ph.D.

Page: 1 of 1 (1 total submissions)

Display 10 results per page.

Action	Manuscript Number	Title	Initial Date Submitted	Current Status
View Submission Send E-mail	BRES-D-14-00501	ACUTE INTRASTRIATAL INJECTION OF QUINOLINIC ACID PROVOKES LONG-LASTING MISREGULATION OF THE CYTOSKELETON IN THE STRIATUM, CEREBRAL CORTEX AND HIPPOCAMPUS OF YOUNG RATS	Apr 09, 2014	In reviewer Agreement

Page: 1 of 1 (1 total submissions)

Display 10 results per page.

<< Author Main Menu

11:40
07/05/2014

Elsevier Editorial System(tm) for Brain Research
Manuscript Draft

Manuscript Number: BRES-D-14-00501

Title: ACUTE INTRASTRIATAL INJECTION OF QUINOLINIC ACID PROVOKES LONG-LASTING MISREGULATION OF THE CYTOSKELETON IN THE STRIATUM, CEREBRAL CORTEX AND HIPPOCAMPUS OF YOUNG RATS

Article Type: Research Report

Section/Category: Cell Biology, Signaling and Synaptic Transmission

Keywords: quinolinic acid; cytoskeleton; intermediate filament phosphorylation; cell signaling; neurotoxicity

Corresponding Author: Regina Pessoa-Pureur, Ph.D.

Corresponding Author's Institution: Ciencias Basicas da Saude

First Author: Paula Pierozan

Order of Authors: Paula Pierozan; Carolina G Fernandes; Fernanda Ferreira; Regina Pessoa-Pureur, Ph.D.

Manuscript Region of Origin: BRAZIL

Abstract: Quinolinic acid (QUIN) is a neuroactive metabolite of the kinurenine pathway, considered to be involved in aging and some neurodegenerative disorders, including Huntington's disease. In the present work we have studied the long-lasting effect of acute intrastriatal injection of QUIN (150 nmol/0.5μL) in 30 day-old rats on the phosphorylating system associated with the astrocytic and neuronal intermediate filament (IF) proteins: glial fibrillary acidic protein (GFAP), and neurofilament (NF) subunits (NFL, NFM and NFH) respectively, until 21 days after injection. The acute administration of QUIN altered the homeostasis of IF phosphorylation in a selective manner, progressing from striatum to cerebral cortex and hippocampus. Twenty four h after QUIN injection, the IFs were hyperphosphorylated in the striatum. This effect progressed to cerebral cortex causing hypophosphorylation at day 14 and appeared in the hippocampus as hyperphosphorylation at day 21 after QUIN infusion. PKA and PKCaMII have been activated in striatum and hippocampus, since Ser55 and Ser57 in NFL head domain were hyperphosphorylated. However, MAPKs (Erk1/2, JNK and p38MAPK) were hyperphosphorylated/activated only in the hippocampus, suggesting different signaling mechanisms in these two brain structures during the first weeks after QUIN infusion. Also, protein phosphatase 1 (PP1) and 2B (PP2B)-mediated hypophosphorylation of the IF proteins in the cerebral cortex 14 after QUIN injection reinforce the selective signaling mechanisms in different brain structures. Increased GFAP immunocontent in the striatum and cerebral cortex 24 h and 14 days after QUIN injection respectively, suggests reactive astrocytes in these brain regions. We propose that disruption of cytoskeletal homeostasis in neural cells takes part of the long-lasting molecular mechanisms of QUIN toxicity in adolescent rats, showing selective and progressive misregulation of the signaling mechanisms targeting the IF proteins in the striatum, cerebral cortex and hippocampus with important implications for brain function.

Editorial Office

Brain Research

Dear Editor,

I am sending you our manuscript entitled: "**Acute intrastriatal injection of quinolinic acid provokes long-lasting misregulation of the cytoskeleton in the striatum, cerebral cortex and hippocampus of young rats**", to your consideration for publication in **Brain Research.**

I look forward to hearing from you soon.

Yours sincerely,

Dr. Regina Pessoa Pureur

- Quinolinic acid (QUIN) disrupts the corticostriatal and hippocampal cytoskeleton
- Disrupted cytoskeleton supports *in vivo* QUIN induced brain damage
- Hyperphosphorylated cytoskeleton is observed in the first weeks after QUIN injection
- Ca^{2+} mechanisms underlie misregulated phosphorylation/dephosphorylation pathways

*Suggested Reviewers
Click here to download Suggested Reviewers: referees suggested.docx

Dr Pant H.C.

National Institute of Neurological Disorders
and Stroke, National Institutes of Health, 49 Convent
Dr., MSC 4479, Bldg. 49, Rm. 2A28, Bethesda, MD 20892,
USA.

E-mail: panth@ninds.nih.gov

Dr Stone T.W.

Institute of Neuroscience and Psychology, West Medical
Building, University of Glasgow, Glasgow G12 8QQ, UK
Corresponding author. Tel: +44-(0)141-330-4481; fax: +44-(0)141-
330-5481.
E-mail address: Trevor.Stone@glasgow.ac.uk

Dr Tasca C.I.

Centro de Biologia Molecular e Estrutural, Departamento de Bioquímica, CCB, UFSC,
Trindade, 88040-900 Florianópolis, SC, Brazil. Tel.: +55 483721 6426; fax: +55 48
37211 9672.

E-mail address: tasca@ccb.ufsc.br

ACUTE INTRASTRIATAL INJECTION OF QUINOLINIC ACID PROVOKES LONG-LASTING MISREGULATION OF THE CYTOSKELETON IN THE STRIATUM, CEREBRAL CORTEX AND HIPPOCAMPUS OF YOUNG RATS

Authors: Paula Pierozan, Carolina Gonçalves Fernandes, Fernanda Ferreira and Regina Pessoa-Pureur

Departamento de Bioquímica, Instituto de Ciências Básicas da Saúde, UFRGS, Porto Alegre, RS, Brasil,

CORRESPONDENCE ADDRESS: Dr. Regina Pessoa-Pureur, Universidade Federal do Rio Grande do Sul, Instituto de Ciências Básicas da Saúde, Departamento de Bioquímica, Rua Ramiro Barcelos 2600 anexo, CEP 90035-003 Porto Alegre - RS, BRASIL, Fax: 5551 3308 5535, Tel: 5551 3308 5565; E-mail: rpureur@ufrgs.br

Running title: Quinolinic acid and cytoskeletal homeostasis

Abstract

Quinolinic acid (QUIN) is a neuroactive metabolite of the kinurenine pathway, considered to be involved in aging and some neurodegenerative disorders, including Huntington's disease. In the present work we have studied the long-lasting effect of acute intrastriatal injection of QUIN (150 nmol/0.5μL) in 30 day-old rats on the phosphorylating system associated with the astrocytic and neuronal intermediate filament (IF) proteins: glial fibrillary acidic protein (GFAP), and neurofilament (NF) subunits (NFL, NFM and NFH) respectively, until 21 days after injection. The acute administration of QUIN altered the homeostasis of IF phosphorylation in a selective manner, progressing from striatum to cerebral cortex and hippocampus. Twenty four h after QUIN injection, the IFs were hyperphosphorylated in the striatum. This effect progressed to cerebral cortex causing hypophosphorylation at day 14 and appeared in the hippocampus as hyperphosphorylation at day 21 after QUIN infusion. PKA and PKCaMII have been activated in striatum and hippocampus, since Ser55 and Ser57 in NFL head domain were hyperphosphorylated. However, MAPKs (Erk1/2, JNK and p38MAPK) were hyperphosphorylated/activated only in the hippocampus, suggesting different signaling mechanisms in these two brain structures during the first weeks after QUIN infusion. Also, protein phosphatase 1 (PP1) and 2B (PP2B)-mediated hypophosphorylation of the IF proteins in the cerebral cortex 14 after QUIN injection reinforce the selective signaling mechanisms in different brain structures. Increased GFAP immunocontent in the striatum and cerebral cortex 24 h and 14 days after QUIN injection respectively, suggests reactive astrocytes in these brain regions. We propose that disruption of cytoskeletal homeostasis in neural cells takes part of the long-lasting molecular mechanisms of QUIN toxicity in adolescent rats, showing selective and

progressive misregulation of the signaling mechanisms targeting the IF proteins in the striatum, cerebral cortex and hippocampus with important implications for brain function.

Keywords: quinolinic acid; cytoskeleton; intermediate filament phosphorylation; cell signaling; neurotoxicity

1. Introduction

Intrastriatal injection of quinolinic acid (QUIN), an endogenous metabolite of tryptophan pathway and N-methyl-D-aspartate (NMDA) receptor agonist, has been reported to cause an increase in Ca^{2+} influx, a decrease in ATP production, and excitotoxic cell death producing a pattern of striatal cell loss that mimics the depletion of projections of striatal neurons observed in Huntington Disease (HD) (Beal et al., 1986). It was also shown that QUIN induces lipid peroxidation and mitochondrial dysfunction in the brain in a concentration-dependent manner (Perez-De La Cruz et al., 2005).

Huntington Disease is a hereditary neurodegenerative disorder characterized by an extensive neurodegeneration in striatum and cerebral cortex, which results in motor, cognitive and neuropsychiatric disorders (Martin and Gusella, 1986). The juvenile-onset or Juvenil Huntington's disease (JHD) and adult-onset forms of HD appear to differ in their pattern of striatal projection neuron loss and in the onset of symptoms (Albin et al., 1990). The mechanisms underlying the selective neurodegeneration in HD are still unknown, but is has been proposed that NMDA receptor-mediated excitotoxic processes may be involved.

The cytoskeleton, consisting of microtubules, intermediate filaments (IFs) and actin filaments is indispensable for any eukaryotic cell. The IF proteins constitute an important network of cytoskeletal proteins of vertebrate cells expressed in a tissue-and development-specific manner.

Neurons express specific IF named neurofilaments (NFs) which consist of three subunits divided according to their molecular mass: NF heavy-chain (NFH), NF middle

chain (NFM) and NF light chain (NFL). Neurofilaments are important elements of the axonal cytoskeleton where they are longitudinally oriented and crosslinked to other structures constituting the most important supporting network for adult axons. Although a considerable body of evidence supports that the most essential function of NFs is maintaining the axonal diameter and thereby the conduction velocity (Friede and Samorajski, 1970; Zhu et al., 1997), recent evidence points the axonal cytoskeleton as a highly dynamic and responsive structure, able to alter their homeostasis in response to a variety of physiological and pathological signals. (Zamoner and Pessoa-Pureur, 2011a; Zanatta et al., 2012).

Glial fibrillary acidic protein (GFAP) is the main IF protein expressed in mature astrocytes, where it is thought to help maintaining mechanical strength, as well as the shape of cells. However, recent evidence has shown that GFAP plays a role in a variety of additional astrocyte functions, such as cell motility/migration, cell proliferation, glutamate homeostasis, neurite outgrowth and injury/protection (Middeldorp and Hol, 2011). Also, after injury of CNS, astrocytes become reactive and respond in a typical manner, termed reactive gliosis (Eng et al., 2000) which is characterized by astrocyte proliferation, increased production of GFAP or by decreased GFAP turnover, causing increased protein content.

Intermediate filament proteins are known to be phosphorylated on their head and tail domains and the dynamics of their phosphorylation/dephosphorylation plays a major role in regulating the structural organization and function of IFs in a cell-and tissue-specific manner (Grant and Pant, 2000; Inagaki et al., 1990; Nixon and Sihag, 1991; Omary et al., 2006). Amino-terminal phosphorylation is mainly involved in regulating the assembly/disassembly equilibrium of GFAP, NFL and NFM subunits of

NFs (Sihag et al., 2007). *In vivo* and *ex vivo* studies from our group and from others have demonstrated that the phosphate groups on the amino-terminal head domain of GFAP, vimentin and NFL are added by second messenger-dependent protein kinases, such as cAMP-dependent protein kinase (PKA), Ca^{2+}/calmodulin-dependent protein kinase II (PKCaMII) and protein kinase C (PKC) (Pierozan et al., 2010; Pierozan et al., 2012; Sihag et al., 2007). GFAP phosphorylation is possibly a key factor in astrocyte, since cell uses phosphorylation/dephosphorylation levels to regulate the dynamic of the polymerization/depolymerization of these proteins promoting cell survival and physiological roles.

Also, the assembly of NFs into a heteropolymer is dependent on the head domains of NFL and NFM and more specifically on the phosphorylation level of these domains. In this context, some of the major sites of *in vivo* and *in vitro* phosphorylation by QUIN on NFL and NFM subunits were identified to be Ser-55 (PKA) and Ser-57 (PKCaMII) (Pierozan et al., 2012).

On the other hand, phosphorylation sites in the tail domain of NFM and NFH were found to be Ser residues located in Lys-Ser-Pro (KSP) repeat regions of the tail domain of these subunits. The KSP repeats are phosphorylated by the proline-directed kinases Cdk5, the mitogen-activated protein kinases (MAPK) such as Erk1/2, JNK, p38MAPK, as well as glycogen synthase kinase 3 (GSK3) (Giasson and Mushynski, 1996; Guidato et al., 1996a; Guidato et al., 1996b; Veeranna et al., 1998).

We have recently found that intrastriatally QUIN-injected adolescent rats showed progressive biochemical and histopathological alterations in the striatum, cerebral cortex and hippocampus, as well as behavioral deficits over a period of 21 days after drug injection, mimicking JHD (Pierozan et al., 2014). However, little is known about

the role of the cytoskeleton in the cell damage induced by QUIN over the first weeks after the intrastriatal injection. In line with this, we have recently described that QUIN is able to induce hyperphosphorylation of neuronal and glial IF proteins in QUIN-exposed striatal slices of young rats and this effect was mediated by glutamate receptors and $_{i}Ca^{2+}$ levels (Pierozan et al., 2012). It is important to note that the disrupted homeostasis of the cytoskeleton of striatal neural cells was demonstrated to be an early event observed 30 min after intrastriatal QUIN injection in young rats (Pierozan et al., 2010). The evidence of a link between misregulation of cell signaling mechanisms, disruption of IF phosphorylation and cell damage in response to QUIN point to a critical role of the signaling pathways regulating the IF phosphorylation in the early events of QUIN-induced toxicity and lead us to search for the role of the cytoskeleton in the progress of brain injury.

Therefore, in the present report we investigated the long-lasting QUIN actions targeting the phosphorylating system associated with the IF-enriched cytoskeleton in the striatum, cerebral cortex and hippocampus of young rats, identifying activated kinases and phosphatases over 21 days after QUIN injection. We hypothesize that disruption of cytoskeletal homeostasis could be implicated in the neural damage and behavioral changes induced by acutely injected QUIN during the first weeks after the insult.

2. Results

Initially we studied the effects of intrastriatally injected QUIN on the endogenous phosphorylating system associated with IF-enriched cytosleletal fraction of striatum, cerebral cortex and hippocampus of 30 day-old rats over 21 days after the insult. As

depicted in Figure 1A, we found hyperphosphorylated IF proteins from striatal astrocytes (GFAP) and neurons (NFL, NFM and NFH) 24 h after injection, restoring control values afterwards. In cerebral cortex, the phosphorylation level of these proteins remained similar to those of control rats 24 h after QUIN injection, progressing to hypophosphorylation 14 days after injection and restoring again control levels at day 21 (Figure 1B). In the hippocampus, hyperphosphorylation of these cytoskeletal proteins was observed only 21 days after injection (Figure 1C).

Concomitantly with altered incorporation of ^{32}P-orthophosphate into GFAP we detected increased immunocontent of this protein in the homogenate of striatum and cerebral cortex 24 h and 14 days after QUIN injection, respectively (Figure 2A and B). Nonetheless, in the hippocampus we did not observe altered GFAP immunocontent concomitant with hyperphosphorylation at day 21 (Figure 2C). Increased GFAP levels in striatum and cerebral cortex could be associated with the astrocytic response to the QUIN insult and is compatible with reactive gliosis (Liberto et al., 2004).

In order to search for the protein kinases and phosphatases activated by QUIN in these brain structures we used Western blot analysis with specific monoclonal antibodies. We first assayed the MAPKs (Erk1/2, JNK and p38MAPK) and we found that MAPKs were not phosphorylated/activated in the striatum 24 h after QUIN injection (Figure 3A), however they were phosphorylated/activated in the hippocampus 21 days after QUIN injection (Figure 3C). These results suggest that in QUIN-injected rats, hyperphosphorylation of IF proteins in the striatum is independent of MAPK activation while in the hippocampus these kinases are probably involved. Otherwise, protein phosphatase 1 (PP1) and 2B (PP2B) were activated in the cerebral cortex at day 14 after QUIN injection, while the level of PP2A was similar to that of control animals

(Figure 3B). Therefore we could presume that hypophosphorylation of IF proteins in the cerebral cortex 14 days after QUIN injection was mediated by PP1 and PP2B.

According with these results, Western blot analysis using anti-KSP repeat antibody demonstrated hyperphosphorylation of the KSP repeats located in the long tail domains of NFM and NFH (Holmgren et al 2012), both in striatum (24 h after QUIN injection) and hippocampus (21 days after QUIN injection), while in the cerebral cortex the KSP repeats were hypophosphorylated 14 days after QUIN injection (Figure 4). In addition, pNFL Ser55 and pNFLSer57 appeared hyperphosphorylated in striatum and hippocampus and hypophosphorylated in cerebral cortex (Figure 4). The phosphorylation of NFL subunit in Ser55 and Ser57 phosphorylation sites is consistent with PKA and PKCaM activation, respectively (Pierozan et al., 2010; Pierozan et al., 2012). Interestingly, these results are in line with altered ^{32}P incorporation into NFM and NFH in the different brain structures, shown in Figure 1.

3. Discussion

In this study we analyzed the progress of cytoskeletal disruption during the first weeks after the excitotoxic insult caused by intrastriatally injected QUIN (150 nmol/0.5μL) in 30 day-old rats. We have focused on the effect of QUIN on the phosphorylating system associated with cytoskeletal IF proteins from striatum, cerebral cortex and hippocampus until 21 days after injection since the dynamics of IFs is mostly regulated by phosphorylation.

We are demonstrating the long-lasting involvement of the cytoskeleton in the injury caused by acutely injected QUIN in the first weeks after the insult. Also, the

present results show different susceptibilities of the phosphorylating system depending on the brain region and on the progress of the lesion. Activation of PKA and PKCaMII was evident in the striatum 24 h after infusion and in the hippocampus 21 days afterwards. Considering that the phosphorylating sites on Ser-55 and Ser-57 on NFL are targeted by PKA and PKCaMII, respectively (Pierozan et al., 2012), it is feasible that these kinases mediated the hyperphosphorylation of Ser-55 and Ser57 on NFL subunit in these brain regions in response to QUIN injection. The phosphorylation of these subunits is important for the polymerization of NF itself, and hyperphosphorylation of these subunits may cause a blockage in the association of NF (Sihag and Nixon, 1990). Thus, we propose that QUIN could interfere with the homeostasis of IFs in axons *in vivo*.

Interestingly, KSP repeats on NFM and NFH tail domains in the striatum are not hyperphosphorylated 30 min after QUIN injection (Pierozan et al., 2010), suggesting that kinases known to phosphorylate these sites, such as MAPKs and cdk5 (Sihag et al., 2007) are not involved in the early events of QUIN toxicity in this brain structure. Our present findings show that 24 h after QUIN injection MAPKs remain inactivated in the striatum, however the KSP repeats on NFM and NFH subunits presented statistically increased hyperphosphorylation compared with controls. We could, therefore, propose that the tail domains of these NF subunits are phosphorylated by Cdk5. This is consistent with previous *ex-vivo* results showing the activation of cdk5 by group I mGLURs, particularly mGLUR1 and mGLUR5 in striatal slices exposed to QUIN (Pierozan et al., 2012). This is also supported by the role of mGLUR5, which is described to be upstream of several kinases, including Cdk5 (Wang et al., 2004).

Moreover, we cannot exclude the possibility of cdk5-induced inactivation of the MAPK pathway (Li et al., 2002; Sharma et al., 2002) in the striatum.

Activation of Erk1/2, JNK and p38MAPK in the hippocampus 21 days after QUIN injection suggests a long-lasting response of signaling mechanisms away from the site of lesion. Hyperphosphorylation of KPS repeats in neuronal IFs is considered an important event promoting the aggregation between NF and causing the formation of agglomerates into the axons (Holmgren et al., 2012) Moreover, the phosphorylation level at the KSP repeats determines association of NFs with the motor proteins kinesin and dynein. Hyperphosphorylation interferes with their binding with kinesin decreasing the rate of the axonal transport (Holmgren et al 2012). Therefore, extensively phosphorylated NFH and MAPK activation observed in the hippocampus of QUIN-injected animals could interfere with NF axonal transport and explain, at least in part, the neural dysfunction and behavioral deficits associated with acutely injected QUIN in rat brain (Pierozan *et al,* 2014).

The most frequent Ser–Thr phosphatases involved in the modulation of the phosphorylating level of IF cytoskeletal proteins are PP1, PP2A and PP2B (Heimfarth et al., 2012). We have found QUIN-induced activation of PP1 and PP2B without affecting PP2A activity in the cerebral cortex 14 after injection. PP2B is implicated in the regulation of neuronal cytoskeleton in response to extracellular signals that increase intracellular Ca^{2+} (Kayyali et al., 1997; Letourneau, 1996). Otherwise, the involvement of PP1 could be regulated by the 32-kDa dopamine- and adenosine 30,50-monophosphate-regulated phosphoprotein (DARPP-32), an important endogenous regulator of PP1 activity, whose biochemical effects are dependent on the phosphorylating level of specific sites. When pThr34DARPP-32 is dephosphorylated by

PP2B, it is itself inhibited, promoting the release of PP1 activity (Hakansson et al., 2004; Heimfarth et al., 2012). Therefore, we could propose a stimulatory effect of PP2B on PP1, reinforcing hypophosphorylation of IF proteins in the cerebral cortex in response to QUIN. The dephosphorylation of NF is involved in its degradation in nerve terminals (Cohen 1987) and his premature proteolysis (Goldstein 1987; Pant, HC 1988).

Interestingly, altered phosphorylation levels of IF proteins were accompanied by increased immunoreactivity of GFAP in the striatum and cerebral cortex but not in the hippocampus. These findings are in line with previous immunohistochemical analysis showing corticostriatal reactive astrogliosis initiated 24 h after QUIN injection and absence of astrogliosis in the hippocampus until 21 days after the insult (Pierozan *et al,* 2014).

Concerning the susceptibility of hippocampus to acutely injected QUIN, it is interesting to note that misregulation of hippocampal cytoskeleton and activation of MAPK pathway are later responses to the insult. Since p38MAPK is activated in cell death processes, and ERK1/2 contributes to the process of astrogliosis (Che 2001; Ito 2009) we could presume that disruption of the cytoskeleton and MAPK activation are initial steps of a later neuronal death and reactive gliosis in the hippocampus, since we have not detected any histopathological alterations in this brain structure until the fourth week after QUIN injection (Pierozan *et al,* 2014).

Taking into account our previous *in vivo* and *in vitro* findings, we could propose that QUIN effects on the cytoskeleton, that we are showing in the present report, could be initiated by the activation of NMDA receptors, voltage-dependent Ca^{2+} channels type L (L-VDCC) and metabotropic glutamate receptors 1 and 5 (nGLUR1 and mGLUR5), and the signal is transduced downstream of Ca^{2+} mobilization through different

kinase/phosphatase pathways, regulating the dynamics of the cytoskeleton (Pierozan et al., 2010; Pierozan et al., 2012).

In agreement with the excitotoxicity provoked by QUIN (Pierozan et al., 2012) our present findings support the relevance of Ca^{2+} overload on the misregulation of the phosphorylating system associated with the cytoskeleton in the long-lasting response to QUIN in striatum, cerebral cortex and hippocampus. In the striatum and hippocampus, increased cytosolic Ca^{2+} levels lead to astrocyte and neuronal IF hyperphosphorylation directly activating PKCaMII and indirectly activating PKA, as a consequence of the neural isoforms of adenylyl cyclase activated by Ca^{2+} (Steiner et al., 2006). Therefore, the phosphorylation of GFAP and NFL could be a critical mechanism in the misregulation of filament assembly (Gill et al., 1990; Heins et al., 1993). Similarly, hypophosphorylation of IF proteins in the cerebral cortex could be downstream of Ca^{2+} increase, since PP2B is directly activated by high Ca^{2+} levels, while PP1 activity can be modulated by complex mechanisms downstream of PP2B. Also, Ca^{2+} influx activates MAPK pathway in neuronal cells (Li et al., 2002) which could underlie the hyperphosphorylation of IF proteins in the hippocampus.

Alterations in IF phosphorylation, both hyper and hypophosphorylation have been shown in animal models of neurometabolic diseases (Loureiro et al., 2010; Pessoa-Pureur and Wajner, 2007; Pierozan et al., 2010; Pierozan et al., 2012; Zamoner et al., 2008; Zamoner and Pessoa-Pureur, 2011b) and are ascribed to be directly or indirectly involved with human disease (Omary et al., 2006). Taking into account our present findings and immunohistochemical results (Pierozan *et al,* 2014) showing astrogliosis in the striatum and cerebral cortex 24 h and 14 days after QUIN injection, respectively, we could propose a link between misregulation of cell signaling mechanisms, disruption

of IF phosphorylation and cell damage as part of QUIN toxicity in these brain structures.

4. Conclusion

In the present report we provide evidence that disruption of cytoskeletal homeostasis takes part of the molecular mechanisms of QUIN toxicity in adolescent rats showing selective and progressive misregulation of the signaling mechanisms targeting the IF proteins in the striatum, cerebral cortex and hippocampus. It is feasible that Ca^{2+} influx previously observed by us could be upstream of these effects in the three brain regions. Thus, we are tempted to propose that the long-lasting deleterious effect of intrastriatal QUIN injection could be due to the fact that QUIN interferes with the highly regulated signaling mechanisms targeting the cytoskeleton in the immature brain and these mechanisms could contribute, at least in part, to the brain injury observed in the juvenile form of HD.

5. Experimental Procedures

5.1. Radiochemical and compounds

Radiolabeled sodium orthophosphate ($^{[32]}Na_2PO_4$) was purchased from CNEN, São Paulo, Brazil. Quinolinic acid (QUIN), benzamidine, leupeptin, antipain, pepstatin, chymostatin, acrylamide, bis-acrylamide, anti-NFL (N5264), anti-NFM (N2787), anti-NFH (N0142), anti-GFAP (G3893), anti calcineurin(α-subunit), anti-Protein Phosphatase 2A (c-subunit) and anti-Protein Phosphatase 1α monoclonal antibodies were obtained from Sigma (St. Louis, MO, USA). Anti-p44/42 MAP kinase (anti-ERK1/2), antiphospho-p44/42 MAP kinase (anti-phospho-ERK1/2), anti-p38 MAPK,

anti-phospho p38 MAPK, anti-SAPK/JNK, anti-phospho-SAPK/JNK, anti-KSP repeat (#MAB1592) and anti-β-actin antibodies were from Cell signaling Technology, Inc. (Danvers, MA, USA). Anti-pNFL(Ser55) and anti-pNFL(Ser57) were from Santa Cruz Biotechnology (Santa Cruz, CA, USA). The chemiluminescence ECL kit peroxidase and the conjugated anti-rabbit and anti-mouse IgG were obtained from Amersham (Oakville, Ontario, Canada). All other chemicals were of analytical grade.

5.2. Animals

Adolescent (thirty-day-old) Wistar rats obtained from Central Animal House of the Department of Biochemistry, Federal University of Rio Grande do Sul, Porto Alegre, Brazil, were used in the studies. The animals were maintained on a 12:12 light/dark cycle in an air-contidioned constant temperature (22°C±1°C) colony room, with food and water at libitum. The experimental protocol followed the "Principles of Laboratory Animal Care" (NIH publication 85-23, revised 1985) and was approved by the Ethics Committee for Animal Research of the Federal University of Rio Grande do Sul (number 18266). All efforts were made to minimize the number of animals used and their suffering.

5.3. Quinolinic acid injection

The animals were anesthetized with equitesin solution (2.5 ml/Kg i.p.) The skull was exposed and the head was positioned in stereotaxic apparatus. A 10 μL Hamilton syringe (Hamilton, 701 N) with a stainless needle was used to inject 150 nmol/0.5 μL of QUIN (pH 7.4 adjusted with NaOH) (QUIN-injected) or saline-phosphate buffer (SHAM) over 4 min into the right striatum with an infusion pump (Insight, Brazil). Control animals were not operated. The needle was left in place for another 4 min

before removed, so that the total procedure lasted 8 min. The coordinates for injection were as follows: 0.6 mm posterior to the bregma, 2.6 mm lateral to the midline and 4.5 ventral from dura (Paxinos et al., 1985). The correct position of the needle was tested by 0.5 μL of methylene blue injection (4% in saline solution) and carrying out histological analysis. The dose and method of QUIN administration were based in previous work (Pierozan et al., 2010). Postoperatively, rats were kept in a warm cage until they recovered from anesthesia.

5.4. Preparation of slices

Animals were sacrificed by decapitation without anesthesia 24 h, 7, 14 and 21 days after surgery, and the striatum, cerebral cortex and hippocampus were dissected onto Petri dishes placed on ice and cut into 400 μm thick slices with a Mcllwain chopper.

5.5. Preincubation

Tissues slices were preincubated at 30°C for 20 min in a Krebs-Hepes medium containing 124 mM NaCl, 4 mM KCl, 1.2 mM $MgSO_4$, 25 mM Na-HEPES (pH 7.4), 12 mM glucose and 1 mM $CaCl_2$, and the following proteases inhibitors: 1 mM benzamidine, 0.1 μM leupeptin, 0.7 μM antipain, 0.7 μM pepstatin and 0.7 μM chymostatin.

5.6. Incubation

After preincubation, the medium was changed and incubation was carried out at 30 °C with 100 ml of the basic medium containing 100 μCi $^{[32]}Na_2PO_4$, as previously described by Funchal et al (Funchal et al., 2003). The labeling reaction was allowed to proceed for 30 min at 30°C and stopped with 1 ml of cold stop buffer (150 mM NaF, 5

mM EDTA, 5 mM EGTA, 50 mM Tris-HCl, pH 6.5) and the protease inhibitors described above. Slices were then washed twice with stop buffer to remove the excess of radioactivity.

5.7. Preparation of the high-salt Triton-insoluble cytoskeletal fraction from tissue slices.

The IF-enriched cytoskeletal fractions were obtained from slices of striatum, cerebral cortex and hippocampus (Funchal et al., 2003). Briefly, after the labeling reaction, slices were homogenized in 400 µL of ice-cold high-salt buffer containing 5 mM KH_2PO_4 (pH 7.1), 600 mM KCl, 10 mM $MgCl_2$, 2 mM EGTA, 1 mM EDTA, 1% Triton X-100 and the proteases inhibitors described above. The homogenate was centrifuged at 15.800 x g for 10 min at 4°C in an Eppendorf centrifuge, the supernatant was discarded and the pellet was homogenized with the same volume of the high-salt medium. The resuspended homogenate was centrifuged as described and the supernatant was discarded. The Triton-insoluble IF-enriched pellet, containing the IFs, was dissolved in 1% SDS and protein concentration was determined.

5.8. Total tissue homogenate

Tissues slices from striatum, cerebral cortex and hippocampus were homogenized in 100 µL of a lysis solution containing 2 mM EDTA, 50 mM Tris-HCl, pH 6.8, 4% (v/v) SDS. For electrophoresis analysis, samples were dissolved in 25% (v/v) of solution containing 40% glycerol, 5% mercaptoethanol, 50 mM Tris-HCl, pH 6.8 and boiled for 3 min.

5.9. Protein determination

The protein concentration was determined by the method of Lowry (Lowry et al., 1951) using serum bovine albumin as the standard.

5.10. Polyacrylamide gel electrophoresis (SDS-PAGE)

The cytoskeletal fraction and the total tissue homogenate were prepared as described above. For electrophoretical analysis, samples were dissolved in 25% (v/v) of a solution containing 40% glycerol, 5% mercaptoethanol, 50 mM Tris-HCl, pH 6.8 and boiled for 3 min. Equal protein concentrations were loaded onto 7% or 10% polyacrylamide gels and analyzed by SDS-PAGE according to the discontinuous system of Laemmly (Laemmli, 1970). In the in vitro ^{32}P incorporation experiments, the gels containing the IF-enriched cytoskeletal fractions were exposed to X-ray films (T-mat G/RA) at -70°C with intensifying screens, and finally the autoradiograms were obtained and quantified by scanning the films with a Hawlett-Packard Scanjet 6100 scanner and determining optical densities with an Optiquant version 02.00 software (Packard Instruments Company). Optical density values were obtained for the band corresponding to each protein. Protein loading was controlled by Coomassie blue R staining or actin immunoblotting. All bands being measured were within the linear range of the film.

5.11.Western blot analysis

The homogenates (30 μg) were analyzed by SDS-PAGE and transferred to nitrocellulose membranes (Trans-blot SD semi-dry transfer cell, BioRad) for 1 h at 15 V in transfer buffer (48 mM Trizma, 39 mM glycine, 20% methanol and 0.25% SDS). The nitrocellulose membranes were washed for 10 min in Tris buffered saline (TBS; 0.5 M NaCl, 20 mM Trizma, pH 7.5), followed by 2 h incubation in blocking solution (TBS

plus 5% defatted dried milk or albumin bovine). After incubation, the blot was washed twice for 5 min with TBS plus 0.05% Tween-20 (T-TBS), and then incubated overnight at 4°C in blocking solution containing one of the following monoclonal antibodies: anti-NFH (clone N52) diluted 1:1000; anti-NF-150 (clone NN-18) diluted 1:500; anti-NF-68 (clone NR-4) diluted 1:1000; anti-GFAP (clone G-A-5) diluted 1:500; anti-pNFLSer55 or anti-pNFLSer57 diluted 1:800; anti-KSP repeats diluted 1:1000. In experiments designated to study the MAPK cascade anti-ERK1/2, anti-phosphoERK1/2; anti-p38 MAPK; anti-phospho-p38 MAPK; anti-SAP/JNK or anti-phospho-SAPK/JNK, were used diluted 1:1000. The following anti-protein phosphatase antibodies: anti-calcineurin (PP2B) (α-subunit), anti-protein phosphatase 1α (PP1) and anti-protein phosphatase 2A (PP2A) (c-subunit) were diluted 1:1000. The blot was then washed for 5 min with T-TBS and incubated for 2 h in TBS containing peroxidase conjugated rabbit anti-mouse IgG diluted 1:2000, or anti-rabbit IgG 1:2000. In addition, we used the following controls in the antibody experiments: primary antibody only, secondary antibody only and negative controls (lacking the sample containing the antigen of interest). These controls (not shown) stated the specificity and sensibility of the antibodies. The blot was washed twice again for 5 min with T-TBS and twice for 5 min with TBS. The blot was then developed using a chemiluminescence ECL kit and quantified as described above.

5.12.Statistical analysis

Data were analyzed statistically by one-way analysis of variance (ANOVA) followed by the Tukey-kramer post hoc comparision when the F-test was significant and by t test. All analyses were performed using the SPSS software program on an IBM-PC compatible computer.

Acknowledgements

This work was supported by grants of the Conselho Nacional de Desenvolvimento Científico e Tecnológico (CNPq), Fundação de Amparo à Pesquisa do Estado do Rio Grande do Sul (FAPERGS) and Pro-Reitoria de Pesquisa de Pós Graduação - Universidade Federal do Rio Grande do Sul (Propesq-UFRGS).

References

Albin, R.L., Young, A.B., Penney, J.B., Handelin, B., Balfour, R., Anderson, K.D., Markel, D.S., Tourtellotte, W.W., Reiner, A., 1990. Abnormalities of striatal projection neurons and N-methyl-D-aspartate receptors in presymptomatic Huntington's disease. N Engl J Med. 322**,** 1293-8.

Beal, M.F., Kowall, N.W., Ellison, D.W., Mazurek, M.F., Swartz, K.J., Martin, J.B., 1986. Replication of the neurochemical characteristics of Huntington's disease by quinolinic acid. Nature. 321**,** 168-71.

Eng, L.F., Ghirnikar, R.S., Lee, Y.L., 2000. Glial fibrillary acidic protein: GFAP-thirty-one years (1969-2000). Neurochem Res. 25**,** 1439-51.

Friede, R.L., Samorajski, T., 1970. Axon caliber related to neurofilaments and microtubules in sciatic nerve fibers of rats and mice. Anat Rec. 167**,** 379-87.

Funchal, C., de Almeida, L.M., Oliveira Loureiro, S., Vivian, L., de Lima Pelaez, P., Dall Bello Pessutto, F., Rosa, A.M., Wajner, M., Pessoa Pureur, R., 2003. In vitro phosphorylation of cytoskeletal proteins from cerebral cortex of rats. Brain Res Brain Res Protoc. 11**,** 111-8.

Giasson, B.I., Mushynski, W.E., 1996. Aberrant stress-induced phosphorylation of perikaryal neurofilaments. J Biol Chem. 271**,** 30404-9.

Gill, S.R., Wong, P.C., Monteiro, M.J., Cleveland, D.W., 1990. Assembly properties of dominant and recessive mutations in the small mouse neurofilament (NF-L) subunit. J Cell Biol. 111**,** 2005-19.

Grant, P., Pant, H.C., 2000. Neurofilament protein synthesis and phosphorylation. J Neurocytol. 29**,** 843-72.

Guidato, S., Bajaj, N.P., Miller, C.C., 1996a. Cellular phosphorylation of neurofilament heavy-chain by cyclin-dependent kinase-5 masks the epitope for monoclonal antibody N52. Neurosci Lett. 217**,** 157-60.

Guidato, S., Tsai, L.H., Woodgett, J., Miller, C.C., 1996b. Differential cellular phosphorylation of neurofilament heavy side-arms by glycogen synthase kinase-3 and cyclin-dependent kinase-5. J Neurochem. 66**,** 1698-706.

Hakansson, K., Lindskog, M., Pozzi, L., Usiello, A., Fisone, G., 2004. DARPP-32 and modulation of cAMP signaling: involvement in motor control and levodopa-induced dyskinesia. Parkinsonism Relat Disord. 10**,** 281-6.

Heimfarth, L., Loureiro, S.O., Reis, K.P., de Lima, B.O., Zamboni, F., Lacerda, S., Soska, A.K., Wild, L., da Rocha, J.B., Pessoa-Pureur, R., 2012. Diphenyl ditelluride induces hypophosphorylation of intermediate filaments through modulation of DARPP-32-dependent pathways in cerebral cortex of young rats. Arch Toxicol. 86**,** 217-30.

Heins, S., Wong, P.C., Muller, S., Goldie, K., Cleveland, D.W., Aebi, U., 1993. The rod domain of NF-L determines neurofilament architecture, whereas the end domains specify filament assembly and network formation. J Cell Biol. 123**,** 1517-33.

Holmgren, A., Bouhy, D., Timmerman, V., 2012. Neurofilament phosphorylation and their proline-directed kinases in health and disease. J Peripher Nerv Syst. 17**,** 365-76.

Inagaki, M., Gonda, Y., Nishizawa, K., Kitamura, S., Sato, C., Ando, S., Tanabe, K., Kikuchi, K., Tsuiki, S., Nishi, Y., 1990. Phosphorylation sites linked to glial filament disassembly in vitro locate in a non-alpha-helical head domain. J Biol Chem. 265**,** 4722-9.

Kayyali, U.S., Zhang, W., Yee, A.G., Seidman, J.G., Potter, H., 1997. Cytoskeletal changes in the brains of mice lacking calcineurin A alpha. J Neurochem. 68**,** 1668-78.

Laemmli, U.K., 1970. Cleavage of structural proteins during the assembly of the head of bacteriophage T4. Nature. 227**,** 680-5.

Letourneau, P.C., 1996. The cytoskeleton in nerve growth cone motility and axonal pathfinding. Perspect Dev Neurobiol. 4**,** 111-23.

Li, B.S., Zhang, L., Takahashi, S., Ma, W., Jaffe, H., Kulkarni, A.B., Pant, H.C., 2002. Cyclin-dependent kinase 5 prevents neuronal apoptosis by negative regulation of c-Jun N-terminal kinase 3. EMBO J. 21**,** 324-33.

Liberto, C.M., Albrecht, P.J., Herx, L.M., Yong, V.W., Levison, S.W., 2004. Pro-regenerative properties of cytokine-activated astrocytes. J Neurochem. 89**,** 1092-100.

Loureiro, S.O., Romao, L., Alves, T., Fonseca, A., Heimfarth, L., Moura Neto, V., Wyse, A.T., Pessoa-Pureur, R., 2010. Homocysteine induces cytoskeletal remodeling and production of reactive oxygen species in cultured cortical astrocytes. Brain Res. 1355**,** 151-64.

Lowry, O.H., Rosebrough, N.J., Farr, A.L., Randall, R.J., 1951. Protein measurement with the Folin phenol reagent. J Biol Chem. 193**,** 265-75.

Martin, J.B., Gusella, J.F., 1986. Huntington's disease. Pathogenesis and management. N Engl J Med. 315**,** 1267-76.

Middeldorp, J., Hol, E.M., 2011. GFAP in health and disease. Prog Neurobiol. 93**,** 421-43.

Nixon, R.A., Sihag, R.K., 1991. Neurofilament phosphorylation: a new look at regulation and function. Trends Neurosci. 14**,** 501-6.

Omary, M.B., Ku, N.O., Tao, G.Z., Toivola, D.M., Liao, J., 2006. "Heads and tails" of intermediate filament phosphorylation: multiple sites and functional insights. Trends Biochem Sci. 31**,** 383-94.

Paxinos, G., Watson, C., Pennisi, M., Topple, A., 1985. Bregma, lambda and the interaural midpoint in stereotaxic surgery with rats of different sex, strain and weight. J Neurosci Methods. 13**,** 139-43.

Perez-De La Cruz, V., Gonzalez-Cortes, C., Galvan-Arzate, S., Medina-Campos, O.N., Perez-Severiano, F., Ali, S.F., Pedraza-Chaverri, J., Santamaria, A., 2005. Excitotoxic brain damage involves early peroxynitrite formation in a model of Huntington's disease in

rats: protective role of iron porphyrinate 5,10,15,20-tetrakis (4-sulfonatophenyl)porphyrinate iron (III). Neuroscience. 135**,** 463-74.

Pessoa-Pureur, R., Wajner, M., 2007. Cytoskeleton as a potential target in the neuropathology of maple syrup urine disease: insight from animal studies. J Inherit Metab Dis. 30**,** 664-72.

Pierozan, P., Zamoner, A., Soska, A.K., Silvestrin, R.B., Loureiro, S.O., Heimfarth, L., Mello e Souza, T., Wajner, M., Pessoa-Pureur, R., 2010. Acute intrastriatal administration of quinolinic acid provokes hyperphosphorylation of cytoskeletal intermediate filament proteins in astrocytes and neurons of rats. Exp Neurol. 224**,** 188-96.

Pierozan, P., Zamoner, A., Soska, A.K., de Lima, B.O., Reis, K.P., Zamboni, F., Wajner, M., Pessoa-Pureur, R., 2012. Signaling mechanisms downstream of quinolinic acid targeting the cytoskeleton of rat striatal neurons and astrocytes. Exp Neurol. 233**,** 391-9.

Pierozan, P., Fernandes, C.G., Dutra, M.F., Pandolfo, P., Ferreira, F., de Lima, B.O., Porciuncula, L., Wajner, M., Pessoa-Pureur, R., 2014. Biochemical, histopathological and behavioral alterations caused by intrastriatal administration of quinolic acid to young rats. FEBS J.

Sharma, P., Veeranna, Sharma, M., Amin, N.D., Sihag, R.K., Grant, P., Ahn, N., Kulkarni, A.B., Pant, H.C., 2002. Phosphorylation of MEK1 by cdk5/p35 down-regulates the mitogen-activated protein kinase pathway. J Biol Chem. 277**,** 528-34.

Sihag, R.K., Inagaki, M., Yamaguchi, T., Shea, T.B., Pant, H.C., 2007. Role of phosphorylation on the structural dynamics and function of types III and IV intermediate filaments. Exp Cell Res. 313**,** 2098-109.

Steiner, D., Saya, D., Schallmach, E., Simonds, W.F., Vogel, Z., 2006. Adenylyl cyclase type-VIII activity is regulated by G(betagamma) subunits. Cell Signal. 18**,** 62-8.

Veeranna, Amin, N.D., Ahn, N.G., Jaffe, H., Winters, C.A., Grant, P., Pant, H.C., 1998. Mitogen-activated protein kinases (Erk1,2) phosphorylate Lys-Ser-Pro (KSP) repeats in neurofilament proteins NF-H and NF-M. J Neurosci. 18**,** 4008-21.

Wang, Q., Walsh, D.M., Rowan, M.J., Selkoe, D.J., Anwyl, R., 2004. Block of long-term potentiation by naturally secreted and synthetic amyloid beta-peptide in hippocampal slices is mediated via activation of the kinases c-Jun N-terminal kinase, cyclin-dependent kinase 5, and p38 mitogen-activated protein kinase as well as metabotropic glutamate receptor type 5. J Neurosci. 24**,** 3370-8.

Zamoner, A., Pierozan, P., Vidal, L.F., Lacerda, B.A., Dos Santos, N.G., Vanzin, C.S., Pessoa-Pureur, R., 2008. Vimentin phosphorylation as a target of cell signaling mechanisms induced by 1alpha,25-dihydroxyvitamin D3 in immature rat testes. Steroids. 73**,** 1400-8.

Zamoner, A., Pessoa-Pureur, R., 2011a. Nongenomic actions of thyroid hormones: every why has a wherefore. Immunology, Endocrine & Metabolic Agents in Medical Chemistry. 11(3)**,** 165-178.

Zamoner, A., Pessoa-Pureur, R., 2011b. Nongenomic actions of thyroid hormones: every why has a wherefore. Immunology, Endocrine & Metabolic Agents in Medical Chemistry. 11(3):**,** 165-178, .

Zanatta, L., Goulart, P.B., Goncalves, R., Pierozan, P., Winkelmann-Duarte, E.C., Woehl, V.M., Pessoa-Pureur, R., Silva, F.R., Zamoner, A., 2012. 1alpha,25-dihydroxyvitamin D(3) mechanism of action: modulation of L-type calcium channels leading to calcium uptake and intermediate filament phosphorylation in cerebral cortex of young rats. Biochim Biophys Acta. 1823**,** 1708-19.

Zhu, Q., Couillard-Despres, S., Julien, J.P., 1997. Delayed maturation of regenerating myelinated axons in mice lacking neurofilaments. Exp Neurol. 148**,** 299-316.

Figure legends

Figure 1. Electrophoretic pattern (SDS-PAGE) and autoradiogram of the phosphorylated IFs in the striatum (A), cerebral cortex (B) and hippocampus (C) of 30 day-old-rats. Animals were intrastriatally injected with 150 nmol QUIN and sacrificed 24 h, 7, 14 and 21 days afterwards. The labeling reaction with ^{32}P orthophosphate was proceed as described in Materials and Methods and the radioactivity incorporated into the high molecular weight neurofilament subunit (NFH), middle molecular weight neurofilament subunit (NFM), low molecular weight subunit (NFL) and glial fibrillary acidic protein (GFAP) associated with the cytoskeletal fraction was measured. Data are reported as means ± S.D. expressed as percentage of controls. Statistically significant differences from controls, as determined by one-way ANOVA followed by Tukey-kramer multiple comparision test are indicated: ***$p<0.001$. Coomassie blue stained representative gels of control (C), sham (S) and QUIN-treated (Q) animals with corresponding autoradiographs are presented. Western blot analysis of the cytoskeletal fraction with anti-NFH, anti-NFM, anti-NFL and anti-GFAP antibodies was used to identify the IF proteins. Equal amounts of the cytoskeletal fraction (50 μg) were run in 7.5 % SDS-PAGE. MW: molecular weight standard proteins. WB: Western blot.

Figure 2. Effect of QUIN on the immunocontent of IF subunits in the striatum (A), cerebral cortex (B) and hippocampus (C) of young rats 24 h, 14 and 21 days after

injection, respectively. Western blot analysis of sham (S) or QUIN-treated animals (QUIN) was carried out with anti-NFH, anti-NF-150, anti-NF-68 and anti-GFAP antibodies. Representative Western blots are shown. Western blot of β-actin was used as loading control. Statistically significant differences from controls, as determined by one-way ANOVA followed by Tukey-kramer multiple comparision test are indicated: ***$p<0.001$ and **$p>0.01$.

Figure 3. Effect of QUIN injection on the activity of cytoskeletal associated kinases and phosphatases. Western blot analysis using the specific antibodies: anti-ERK1/2, anti-phosphoERK1/2, anti-p38 MAPK, anti-phospho-p38 MAPK, anti-SAP/JNK, anti-phospho-SAPK/JNK, anti-calcineurin (PP2B) (α-subunit), anti-protein phosphatase 1α (PP1) and anti-protein phosphatase 2A (PP2A) (c-subunit) were used. Enzyme activities ERK1/2 (A and G), JNK (B and H), p38 MAPK (C and I), were measured in Sham or QUIN-injected animals 24 h (A, B and C) and 21 days (G, H and I) after injection. Calcineurin (PP2B) (α-subunit) (D), PP1α (E) and PP2A (c-subunit) (F) were measured 14 days after injection. Representative Western blots of the proteins studied are shown. Western blot of β-actin was used as loading control. Data are reported as means ± S.D. and expressed as percent of control. Statistically significant differences from controls as determined by one way ANOVA followed by Tukey-kramer test are indicated: ***$p<0.001$.

Figure 4. Effect of QUIN injection on the phosphoNFH/NFM KSP repeats, phosphoNFL(Ser55) and phosphoNFL(Ser57) in the striatum (A), cerebral cortex (B) and hippocampus (C) 24 h, 14 and 21 days after injection, respectively. Representative Western blots of the proteins studied are shown. Western blot of β-actin was used as loading control. Data are reported as means ± S.D. and expressed as percent of control.

Statistically significant differences from controls, as determined by t-test are indicated: ***$p<0.001$; **$p<0.01$ and *$p<0.05$.

Figure 1
Click here to download high resolution image

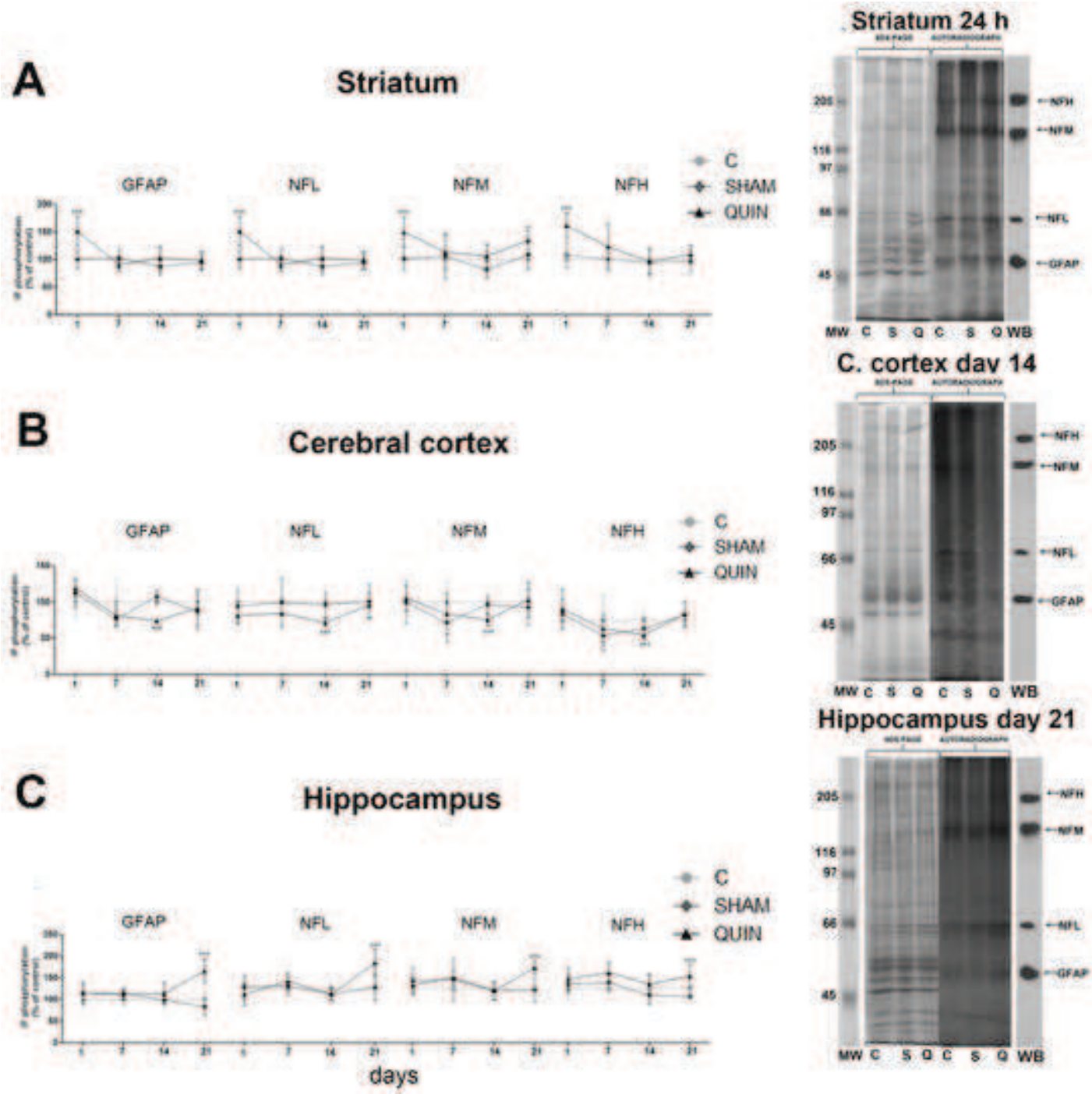

Figure 2
Click here to download high resolution image

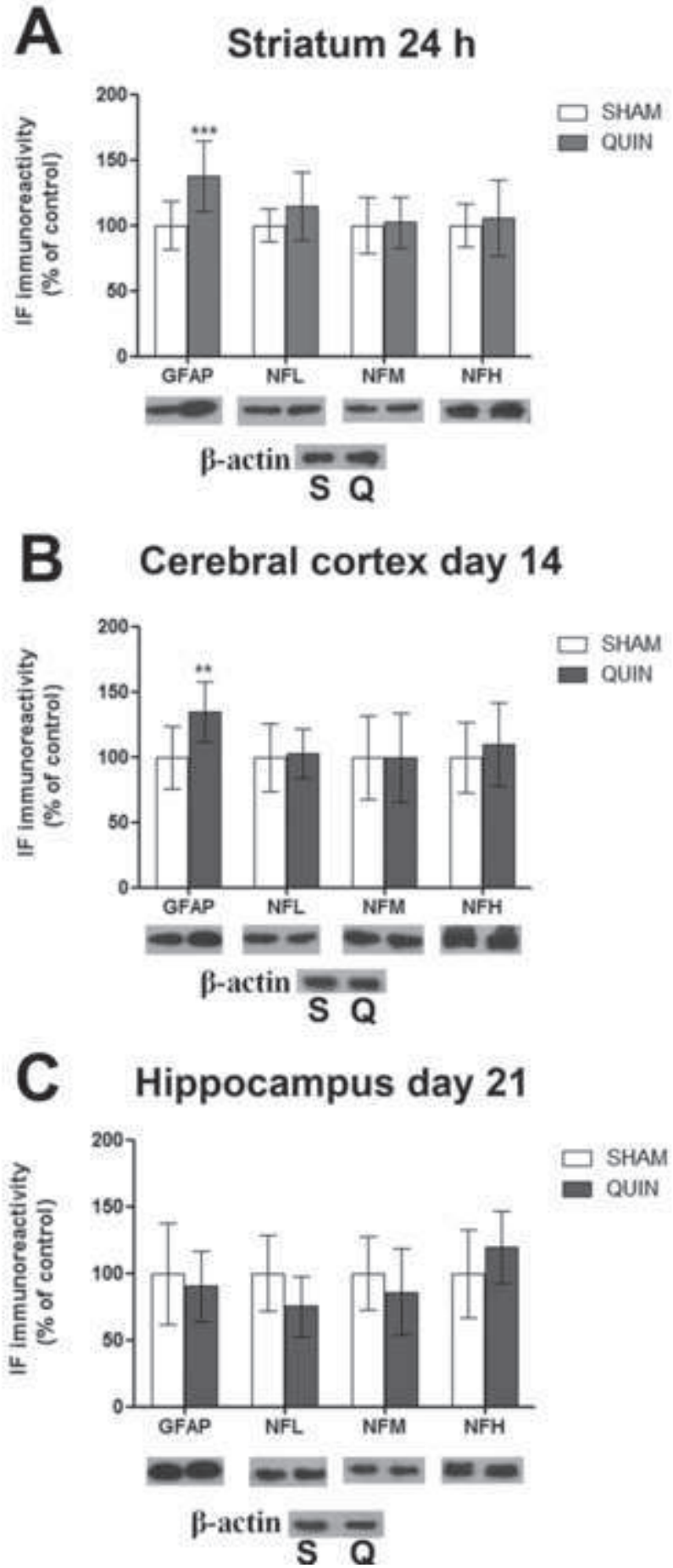

Figure 3

Click here to download high resolution image

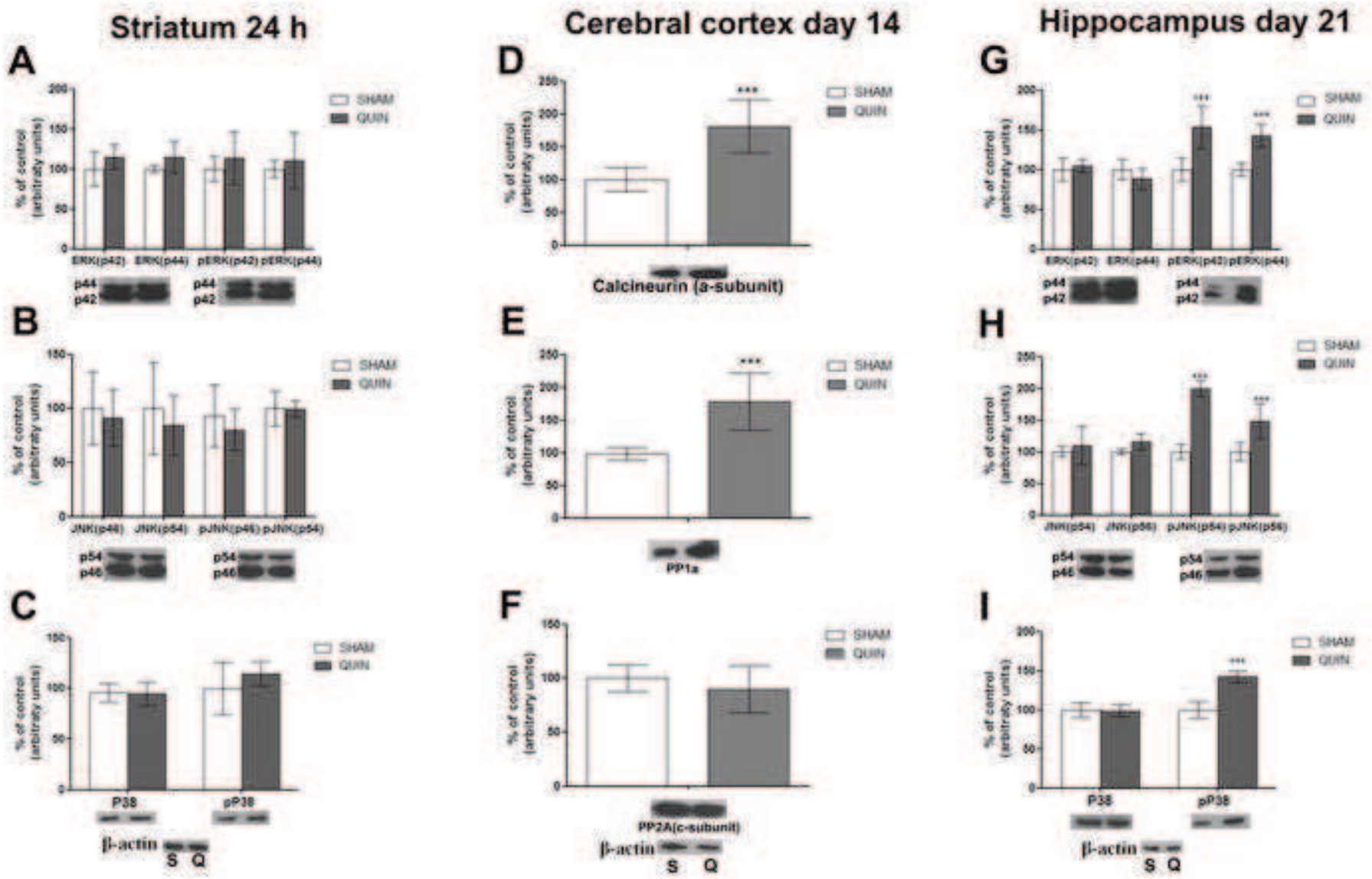

Figure 4

Click here to download high resolution image

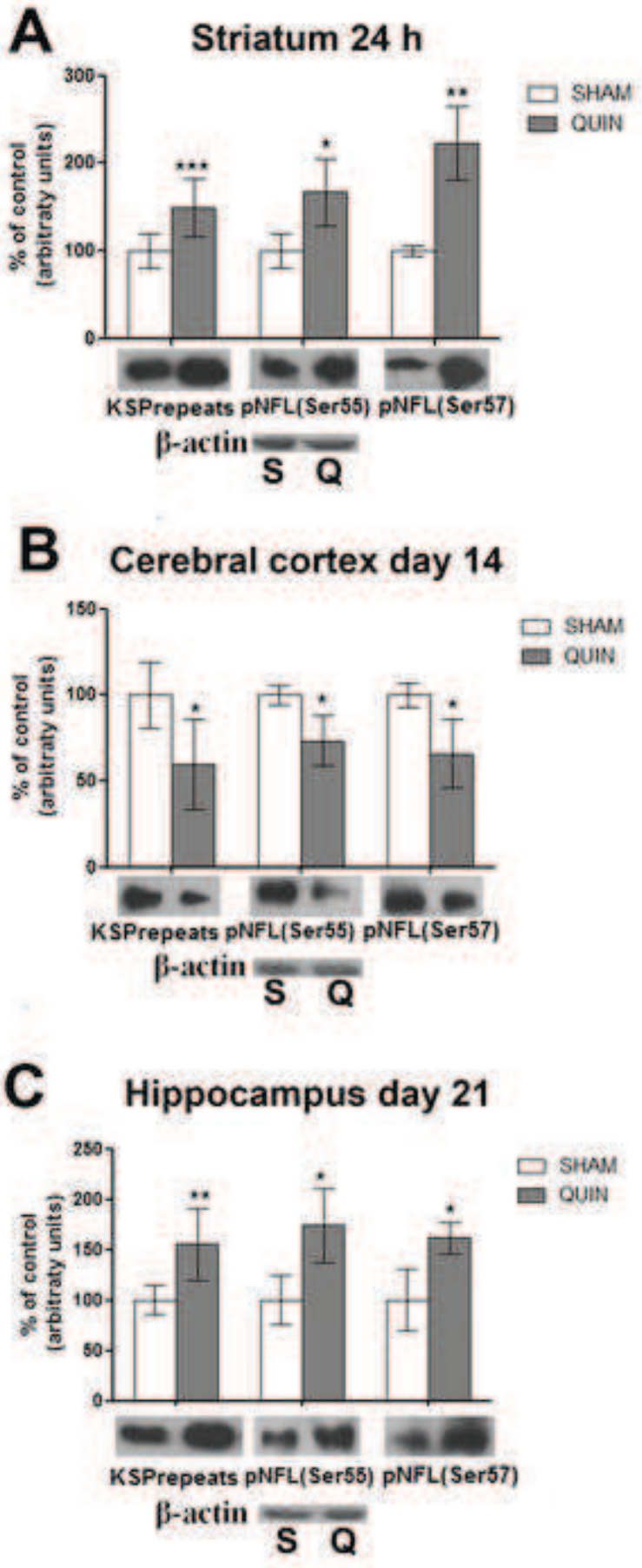

Capítulo 3

SIGNALING MECHANISMS DOWNSTREAM OF QUINOLINIC ACID TARGETING THE CYTOSKELETON OF RAT STRIATAL NEURONS AND ASTROCYTES

Paula Pierozan, Ariane Zamoner, Ângela Krombauer Soska, Bárbara Ortiz de Lima, Karina Pires Reis, Fernanda Zamboni, Moacir Wajner, Regina Pessoa-Pureur

Artigo publicado na **Experimental Neurology**

Experimental Neurology 233 (2012) 391–399

Contents lists available at SciVerse ScienceDirect

Experimental Neurology

journal homepage: www.elsevier.com/locate/yexnr

Regular Article

Signaling mechanisms downstream of quinolinic acid targeting the cytoskeleton of rat striatal neurons and astrocytes

Paula Pierozan, Ariane Zamoner, Ângela Krombauer Soska, Bárbara Ortiz de Lima, Karina Pires Reis, Fernanda Zamboni, Moacir Wajner, Regina Pessoa-Pureur *

Departamento de Bioquímica, Instituto de Ciências Básicas da Saúde, UFRGS, Porto Alegre, RS, Brazil

ARTICLE INFO

Article history:
Received 5 October 2011
Revised 31 October 2011
Accepted 7 November 2011
Available online 13 November 2011

Keywords:
Quinolinic acid
Hyperphosphorylation
Intermediate filaments
Cell signaling
Calcium
Glutamate receptors
Cyclin-dependent kinase 5

ABSTRACT

The studies of signaling mechanisms involved in the disruption of the cytoskeleton homeostasis were performed in a model of quinolinic acid (QUIN) neurotoxicity *in vitro*. This investigation focused on the phosphorylation level of intermediate filament (IF) subunits of astrocytes (glial fibrillary acidic protein — GFAP) and neurons (low, medium and high molecular weight neurofilament subunits — NFL, NFM and NFH, respectively). The activity of the phosphorylating system associated with the IFs was investigated in striatal slices of rat exposed to QUIN or treated simultaneously with QUIN plus glutamate receptor antagonists, calcium channel blockers or kinase inhibitors. Results showed that in astrocytes, the action of 100 μM QUIN was mainly due to increased Ca^{2+} influx through NMDA and L-type voltage-dependent Ca^{2+} channels (L-VDCC). In neuronal cells QUIN acted through metabotropic glutamate receptor (mGluR) activation and influx of Ca^{2+} through NMDA receptors and L-VDCC, as well as Ca^{2+} release from intracellular stores. These mechanisms then set off a cascade of events including activation of PKA, PKCaMII and PKC, which phosphorylate head domain sites on GFAP and NFL. Also, Cdk5 was activated downstream of mGluR5, phosphorylating the KSP repeats on NFM and NFH. mGluR1 was upstream of phospholipase C (PLC) which, in turn, produced diacylglycerol (DAG) and inositol 3,4,5 triphosphate (IP3). DAG is important to activate PKC and phosphorylate NFL, while IP_3 contributed to Ca^{2+} release from internal stores promoting hyperphosphorylation of KSP repeats on the tail domain of NFM and NFH. The present study supports the concept of glutamate and Ca^{2+} contribution in excitotoxic neuronal damage provoked by QUIN associated to dysfunction of the cytoskeleton homeostasis and highlights the differential signaling mechanisms elicited in striatal astrocytes and neurons.

Introduction

Quinolinic acid (QUIN) is an intermediate of the kynurenine pathway, a central route in tryptophan (TRP) metabolism in most mammalian tissues. The kynurenine pathway has been demonstrated to be involved in many diseases and disorders, including Alzheimer's disease, amyotrophic lateral sclerosis, Huntington's disease, AIDS dementia complex, malaria, cancer, depression and schizophrenia (Chen and Guillemin, 2009).

QUIN is a co-agonist of the NMDA receptor subgroup containing the NR2A and NR2B subunits (de Carvalho et al., 1996), with low receptor affinity. It is known that QA can cause excitotoxicity through a direct activation of NMDA receptors (Stone and Perkins, 1981) due to inhibition of release and uptake of endogenous glutamate (Connick and Stone, 1988; Tavares et al., 2002). In this context, it is generally accepted that excitotoxic cell death elicited by QUIN involves bioenergetic failure resulting from Ca^{2+} overload and the generation of reactive oxygen species (ROS) by mitochondria (Behan et al., 1999; Rios and Santamaria, 1991).

QUIN at high concentrations is an excitotoxin that produces a pattern of cell death that mimics the selective neuronal vulnerability seen in Huntington's disease patients with loss of striatal neurons (Beal et al., 1986; Estrada Sanchez et al., 2008). Intrastriatal QUIN injection has been used as a model of neurotoxicity loading striatal degeneration, behavioral, biochemical and cellular alterations (Kalonia et al., 2011a) and oxidative damage (Kalonia et al., 2011b).

The neuronal cytoskeleton comprises a protein network formed mainly by microtubules (MT) and neurofilaments (NF), the IFs of neurons. NF, known as type IV IF, are composed of three different polypeptides whose approximate molecular weights are 200, 160, and 68 kDa, and are commonly referred to as heavy (NFH), medium (NFM), and light (NFL) NF subunits (Ackerley et al., 2003). Type III IF proteins includes vimentin, desmin, glial fibrillary acidic protein (GFAP) and peripherin. GFAP is the IF of mature astrocytes (Eng et al., 2000), peripherin is found in neural cells of the peripheral nervous system, and vimentin is the IF of cells of mesenchymal origin (Albert et al., 2008). Otherwise, desmin constitutes the IF of muscle cells (Albert et al., 2008). IFs play an important structural or tension-bearing role in

* Corresponding author at: Universidade Federal do Rio Grande do Sul, Instituto de Ciências Básicas da Saúde, Departamento de Bioquímica, Rua Ramiro Barcelos 2600 anexo, CEP 90035-003 Porto Alegre, RS, Brazil. Fax: +55 51 3308 5535.
E-mail address: rpureur@ufrgs.br (R. Pessoa-Pureur).

0014-4886/$ – see front matter © 2011 Elsevier Inc. All rights reserved.
doi:10.1016/j.expneurol.2011.11.005

the cell. Evidence is now emerging that IFs also act as an important framework for the modulation and control of essential cell processes, in particular, signal transduction events (Kim and Coulombe, 2007; Paramio and Jorcano, 2002).

Protein phosphorylation is the most widespread type of posttranslational modification used in signal transduction (Ubersax and Ferrell, 2007) affecting basic cellular processes, including regulation of the structural organization of the cytoskeleton (Fuchs and Weber, 1994; Sihag et al., 2007). Accordingly, phosphorylation of types III and IV (NF triplet proteins and α-internexin) IFs is known to regulate their organization and function (Sihag et al., 2007). IF proteins are known to be phosphorylated on their head and tail domains. Type III filaments are phosphorylated on head domain sites by second messenger-dependent protein kinases and it is described that phosphorylation plays a major role in regulating the assembly/disassembly of these filaments (Sihag et al., 2007). Similarly, the three subunits of NFs are highly phosphorylated (Shea and Chan, 2008). The major sites of phosphorylation of NFL and NFM subunits were identified as Ser-55, which is phosphorylated by protein kinase A (PKA), Ser-57 phosphorylated by Ca^{2+}/calmodulin-dependent protein kinase II (PKCaMII), Ser-51 for protein kinase C (PKC) (Gill et al., 1990; Heins et al., 1993), and Ser-23 for PKA and protein kinase C (PKC), respectively (Daile et al., 1975; Kemp et al., 1975). Nonetheless, PKCaMII is able to phosphorylate head domain sites on NFL subunit *in vitro* (Songyang et al., 1994). On the other hand, most of the phosphorylation sites on NFM and NFH are located on multiple lysine-serine-proline (KSP) repeat motifs abundant in the carboxyl-terminal tail domain of these NF subunits (Geisler et al., 1987; Lee et al., 1988; Xu et al., 1992). It is now evident that proline-directed kinases, such as cyclin-dependent kinase 5 (Cdk5) and mitogen-dependent protein kinase (MAPK) are the main kinases that phosphorylate Ser residues on the KSP repeats (Jaffe et al., 1998; Sun et al., 1996; Veeranna et al., 1998). The C-terminal regions of NFH and NFM protrude laterally from the filament backbone when phosphorylated (Sihag et al., 2007) and a considerable body of evidence, supports the notion that phosphorylation of C-terminal side arms, in particular those of NFH, regulates NF axonal transport (Shea and Chan, 2008). This is in concern with the evidence that carboxyl-terminal phosphorylation of NFH progressively restricts association of NFs with the anterograde motor kinesin, providing one mechanism by which the NF axonal transport is slowed (Yabe et al., 2000). In fact, perykarial accumulations/aggregations of aberrantly phosphorylated NFs are a pathological feature of several human neurodegenerative diseases, such as Alzheimer's disease, motor neuron diseases and Parkinson's disease (Grant and Pant, 2000; Lariviere and Julien, 2004; Nixon, 1993; Nixon and Sihag, 1991; Sasaki et al., 2006).

In this context, we have recently described that acute intrastriatal administration of QUIN targets the phosphorylating system associated with the cytoskeleton of neural striatal cells, causing IF hyperphosphorylation 30 min after injection (Pierozan et al., 2010). These findings suggested the participation of QUIN-elicited transduction pathways targeting the cytoskeleton. Therefore, misregulation of the phosphorylating system associated with IF proteins could represent an early step in the pathophysiological cascade of deleterious events exerted by QUIN in rat striatum. However, the cell signaling cascades in QUIN-induced IF hyperphosphorylation are incompletely understood. To extend the scope of our previous findings, the purpose of the present study was to elucidate the signaling mechanisms provoking hyperphosphorylation of IF proteins focusing in the differential pathways attaining neuronal and glial cells in striatal slices exposed to QUIN.

Materials and methods

Radiochemical and compounds

[^{32}P]Na_2HPO_4 was purchased from Comissão Nacional de Energia Nuclear (CNEN), São Paulo, Brazil. Quinolinic acid, 1,2-bis (2-aminophenoxy) ethane-*N*-*N*-*N*′-*N*′-tetraacetic acid tetrakis (acetoxymethyl ester) (BAPTA-AM), D-2-amino-5-phosphonopentanoic acid (DP-AP5), ethylene glycol tetraacetic acid (EGTA), verapamil hydrochloride, dantrolene, phaclophen, bicuculine, staurosporine, benzamidine, leupeptin, antipain, pepstatin, chymostatin, acrylamide, bisacrilamide, SP600125, and roscovitine were obtained from Sigma (St. Louis, MO, USA). KN-93, PD98056 and H89 were obtained from Calbiochem (La Jolla CA, USA). Anti-pNFL(Ser55), anti-pNFL(Ser57) and p38 inhibitor were from Santa Cruz Biotechnology (Santa Cruz, CA, USA). 6-Cyano-7-nitroquinoxaline-2,3-dione (CNQX), (S)-α-methyl-4-carboxyphenylglycine (MCPG), 2-methyl-6-(phenylethynyl)pyridine hydrochloride (MPEP) and (S)-4-carboxy-3-hydroxyphenylglycine (4C3HPG) were obtained from Tocris Bioscience (Ellisville, Missouri, USA). Pictrotoxin was obtained from TCI America (Portland, OR, USA). The antibody NFH (anti-KSP repeats) was from Chemicon (Temecula, CA, USA). The chemiluminescence ECL kit peroxidase and the conjugated anti-rabbit IgG were obtained from Amersham (Oakville, Ontario, Canada). All other chemicals were of analytical grade.

Animals

Thirty-day-old Wistar rats obtained from Central Animal House of the Departament of Biochemistry Federal University of Rio Grande do Sul, Porto Alegre, Brazil, were used in the experiments. The animals were maintained on a 12:12 h light/dark cycle in an air-conditioned constant temperature (22 °C ± 1 °C) colony room, with food and water at libitum. The experimental protocol followed the "Principles of Laboratory Animal Care" (NHI publication 85-23, revised 1985) and was approved by the Ethics Committee for Animal Research of the Federal University of Rio Grande do Sul.

Preincubation

Rats were sacrificed by decapitation, the striatum was dissected onto Petri dishes placed on ice and cut into 400 μm thick slices with a McIlwain chopper. Tissue slices were initially preincubated at 30 °C for 10 min in a Krebs-Hepes medium containing 124 mM NaCl, 4 mM KCl, 1.2 mM,$MgSO_4$, 25 mM Na–Hepes (pH 7.4), 12 mM glucose, 1 mM $CaCl_2$, and the following protease inhibitors: 1 mM benzamidine, 0.1 μM leupeptin, 0.7 μM antipain, 0.7 μM pepstatin and 0.7 μM chymostatin in the presence or absence of 100 mM DL-AP5, 50 μM BAPTA-AM, 1 mM EGTA, 30 μM verapamil, 50 μM dantrolene, 10 μM KN93, 1 μM staurosporine, 30 μM PD98059 and 10 μM U73122 (Loureiro et al., 2008), 50 μM CNQX, 100 μM MCPG (Loureiro et al., 2005), 10 μM H89 (Cortes et al., 2010), 30 μM SP600125 (Katayama et al., 2009), 10 μM p38 MAPK inhibitor VIII (Rigon et al., 2008), 10 μM roscovitine (Tomizawa et al., 2002), 20 μM bicuculine and 100 μM picrotoxin (Adermark et al., 2010), 10 μM phaclofen (Seto et al., 2002), 30 μM MPEP hydrochloride (Domenici et al., 2004) and 30 μM (S)-4-carboxy-3-hydroxyphenylglycine (Orlando et al., 2001), when indicated.

Incubation

After preincubation, the medium was changed by 100 ml of the basic medium with or without 100 μM QUIN and/or the inhibitors cited above, and incubation was carried out for 20 min at 30 °C. After this, 100 μCi of [^{32}P]-orthophosphate was added to the incubation medium and the labeling reaction was allowed to proceed for 30 min at 30 °C. Reaction was stopped with 1 ml of cold stop buffer (150 mM NaF, 5 mM, EDTA, 5 mM EGTA, 50 mM Tris–HCl, pH 6.5, and the protease inhibitors described above). Slices were then washed twice with stop buffer to remove excess radioactivity.

Preparation of the high salt-triton-insoluble cytoskeletal fraction from tissue slices

After treatment, preparations of IF-enriched cytoskeletal fractions were obtained from striatum of rats as previously described by us (Funchal et al., 2003). Briefly, after the labeling reaction, slices were homogenized in 400 ml of ice-cold high salt buffer containing 5 mM KH_2PO_4, (pH 7.1), 600 mM KCl, 10 mM $MgCl_2$, 2 mM EGTA, 1 mM EDTA, 1% Triton X-100 and the protease inhibitors described above. The homogenate was centrifuged at 15,800×*g* for 10 min at 4 °C, in an Eppendorf centrifuge, the supernatant discarded and the pellet homogenized with the same volume of the high salt medium. The resuspended homogenate was centrifuged as described and the supernatant was discarded. The Triton-insoluble IF-enriched pellet, containing NF subunits and GFAP, was dissolved in 1% SDS.

Total tissue homogenate

Tissue slices from striatum were homogenized in 100 ml of a lysis solution containing 2 mM EDTA, 50 mM Tris–HCl, pH 6.8, 4% (v\v) SDS. For electrophoresis analysis, samples were dissolved in 25% (v\v) of solution containing 40% glycerol, 5% mercaptoethanol, 50 mM Tris–HCl, pH 6.8 and boiled for 3 min.

Cell integrity

Measurement of cell integrity was determined by lactate dehydrogenase (LDH) activity using a colorimetric commercial kit (from Doles, Brazil), (Whitaker and McKay, 1969). Total LDH activity was determined after adding a final concentration of 10% Triton X-100 and disrupting the slices by homogenization with a Tissue Tearor (Biospec). Results were expressed as percentage relative to 100% LDH activity.

Cell viability

Mitochondrial dehydrogenase activity to reduce MTT (3-(4,5-dimethylthiazol-2-yl)-2,5-diphenyltetrazolium bromide) was used to determine cell survival (Liu et al., 1997). The tetrazolium ring of MTT is cleaved by various dehydrogenase enzymes in active mitochondria and then precipitated as a blue formazan product. Striatal slices were incubated with MTT (0.5 mg/mL) in KRB buffer, pH 7.4 (122 mM Na-gluconate, 5 mM K-gluconate, 2 mM HEPES, 25 mM $NaHCO_3$, 1 mM $MgSO_4$, 1.2 mM NaH_2PO_4, 0.9 mM Ca-gluconate, 1 mM L-glutamine, 5 mM glucose; KRB buffer) for 20 min at 37 °C. The medium was then aspirated, the precipitated formazan was solubilized with dimethyl sulfoxide, and viable cells were quantified spectrophotometrically at a wavelength of 550 nm.

Polyacrylamide gel electrophoresis (SDS-PAGE)

The cytoskeletal fraction and total tissue homogenate were prepared as described above. For electrophoresis analysis, samples were dissolved 25% (v/v) in a solution containing 40% glycerol, 5% mercaptoethanol, 50 mM Tris–HCl, pH 6.8 and boiled for 3 min. Samples containing equal protein content (50 μg) were loaded onto 7% or 10% polyacrylamide gels and analyzed by SDS-PAGE according to the discontinuous system of Laemmli (Laemmli, 1970). In the *in vitro* ^{32}P incorporation experiments, the gels containing the IF-enriched cytoskeletal fraction were exposed to X-ray films (T-mat G/RA) at −70 °C with intensifying screens and finally the autoradiograph was obtained. Cytoskeletal proteins were quantified by scanning the films with a Hewlett-Packard Scanjet 6100C scanner and determining optical densities with an Optiquant version 02.00 software (Packard Instrument Company). Optical density values were obtained for the band corresponding to each protein. Protein loading was controlled by Comassie blue R staining or actin immunoblotting. All bands being measured were within the linear range of the film.

Western blot analysis

Cytoskeletal fractions (50 μg) were analyzed by SDS-PAGE and transferred to nitrocellulose membranes (Trans-blot SD semi-dry transfer cell, BioRad) for 1 h at 15 V in transfer buffer: 48 mM Trizma, 39 mM glycine, 20% methanol and 0.25% SDS. The nitrocellulose membranes were washed for 10 min in Tris buffered saline (TBS; 0.5 M NaCl, 20 mM Trizma and pH 7.5), followed by 2 h incubation in blocking solution (TBS plus 5% defatted dried milk). After incubation, the blots were washed twice for 5 min with TBS plus 0.05% Tween-20 (T-TBS), and then incubated overnight at 4 °C in blocking solution containing the following monoclonal antibodies: anti-p-NFL(Ser55) diluted 1:800, anti-p-NFL(Ser57) diluted 1:800, anti-NFH/NFM KSP repeats diluted 1:100 and anti-β-actin diluted 1:1000. The blot was then washed twice for 5 min with T-TBS and incubated for 2 h in TBS containing peroxidase conjugated rabbit anti-mouse IgG or anti-rabbit IgG diluted 1:2000. In addition, we used the following negative controls: antibody negative control (lacking the sample containing the antigen of interest) and sample negative control (lacking the first antibody). These controls (not shown) stated the specificity and sensibility of the antibodies. The blot was washed twice again for 5 min with T-TBS and twice for 5 min with TBS. The blot was then developed using a chemiluminescence ECL kit and quantified as described above.

Protein determination

The protein concentration was determined by the method of Lowry (Lowry et al., 1951) using serum bovine albumin as the standard.

Statistical analysis

Data were analyzed statistically by one-way analysis of variance (ANOVA) followed by the Tukey-Kramer post hoc comparison when the F-test was significant. A $p<0.05$ was considered significant. All analyses were performed using the SPSS software program on an IBM-PC compatible computer.

Results

We initially evaluated the cell integrity of mitochondrial damage in our experimental model, measuring LDH extracellular activity and MTT which indicates overall mitochondrial dehydrogenase activity, respectively. Our results showed that the *in vitro* treatment with 100 μM QUIN preserved cell integrity and viability in striatal slices of 30 day-old rats (results not shown). Thereafter, we studied the effect of QUIN on the phosphorylation of IF-enriched cytoskeletal fraction of striatal slices. Results showed that after 50 min exposition to 100 μM QUIN the phosphorylation level of NF subunits (NFL, NFM and NFH) and GFAP was increased (Fig. 1), suggesting that the cytoskeleton of both neurons and astrocytes of striatal slices is an important *in vitro* target of QUIN at a concentration described to be neurotoxic (Perez-De La Cruz et al., 2010).

Action of QUIN on the second messenger-dependent and -independent kinases targeting the IF proteins in astrocytes and neurons of striatal slices

Since it is described that the second messenger-dependent protein kinases are able to phosphorylate sites at GFAP and NFL head domains (Hisanaga et al., 1990; Sihag and Nixon, 1989; Sihag et al., 2007), we focused on the role of PKA, PKCaMII and PKC mediating the action of QUIN on the phosphorylation level of these IF subunits. Results showed that H89 (PKA inhibitor) and KN93 (PKCaMII inhibitor)

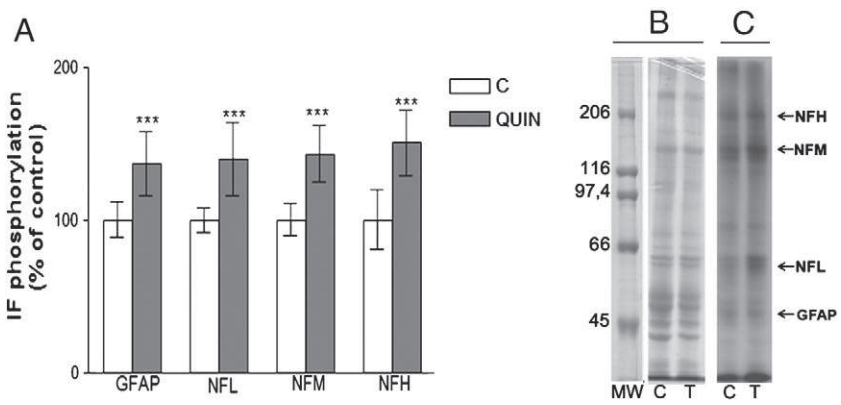

Fig. 1. Effect of QUIN on the phosphorylation of intermediate filament subunits in the cytoskeletal fraction from slices of striatum of 30-day-old rats. A) Slices were incubated with 100 μM of QUIN in the presence of ^{32}P-orthophosphate. The cytoskeletal fraction was extracted and the radioactivity incorporated into NFL, NFM, NFH and GFAP was measured as described in Materials and methods. Data are reported as mean ± S.D. of 18 animals in each group and expressed as percent of controls. Statistically significant differences from controls, as determined by one-way ANOVA followed by Tukey–Kramer multiple comparison test are indicated: ***p<0.001compared with control and ###p<0.001 compared with QUIN group. B) Coomassie blue stained molecular weight standards and representative stained gel of a control and a treated sample; C) corresponding autoradiograph. Equal amounts of the cytoskeletal fraction (50 μg) from control (C) and treated (T) samples were run in 7.5% polyacrylamide gel electrophoresis. MW: molecular weight standard proteins.

prevented hyperphosphorylation of GFAP and NFL without affecting the QUIN-induced NFM and NFH hyperphosphorylation. Conversely, staurosporine, a specific PKC inhibitor, was ineffective in preventing GFAP hyperphosphorylation and only partially prevented this effect on NFL (Fig. 2A).

In order to identify the kinases targeting the phosphorylating sites on NFM and NFH subunits, we used specific MAP kinases and Cdk5 inhibitors. Results showed that PD98059, a MAPKK (MEK) inhibitor and p38 MAPK inhibitor VIII were not able to prevent the QUIN-induced NFM and NFH hyperphosphorylation, while SP600125, a JNK inhibitor

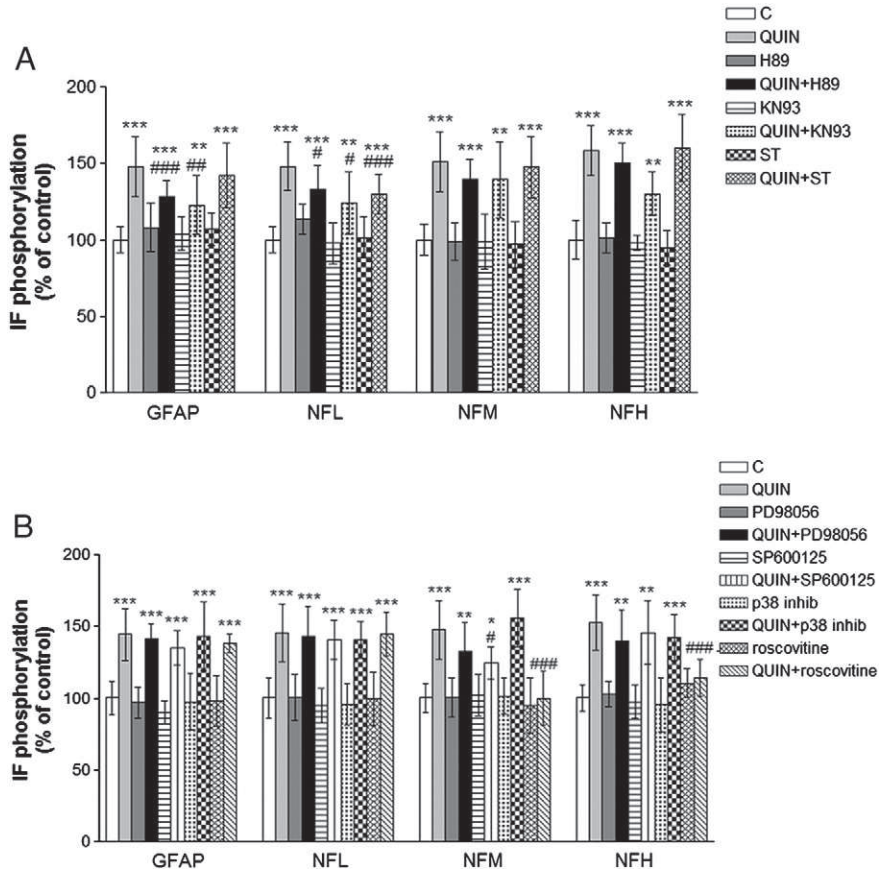

Fig. 2. Involvement of protein kinases on QUIN-induced IF *in vitro* hyperphosphorylation in striatum of 30 day-old rats. (A) Participation of second messenger dependent protein kinases PKA, PKCaMII and PKC was tested by using the specific inhibitors 10 μM H89, 10 μM KN93 and 1 μM staurosporina, respectively. (B) Participation of MEK/ERK, JNK, p38MAPK and Cdk5 was tested using the specific inhibitors 30 μM PD9859, 30 μM SP600125, 10 μM p38 MAPK inhibitor and 10 μM roscovitine, respectively. Slices were preincubated in the presence or absence of inhibitors for 10 min followed by incubation with 100 μM QUIN for 20 min. After, slices were incubated with ^{32}P-orthophosphate with or without 100 μM QUIN and/or inhibitors, as described in Materials and methods. The cytoskeletal fraction was extracted and the radioactivity incorporated into NFL, NFM, NFH and GFAP was measured. Data are reported as means ± S.D. of 18 animals in each group and expressed as % of control. Statistically significant differences from controls, as determined by one-way ANOVA followed by Tukey–Kramer multiple comparison test are indicated: ***p<0.001; **p<0.01; *p<0.05 compared with control group; ###p<0.001; ##P<0.01 and #p<0.05 compared with QA group.

(DeFuria and Shea, 2007), partially prevented NFM hyperphosphorylation. Furthermore, roscovitine, a Cdk5 inhibitor (Zhou et al., 2010) totally prevented NFM and NFH hyperphosphorylation (Fig. 2B).

QUIN-induced signaling pathways targeting specific phosphorylating sites on NF subunits in striatal slices

In an attempt to identify the phosphorylating sites targeted by QUIN on NFL head domain, we assayed the immunoreactivity of NFLSer55 and NFLSer57 for PKA and PKCaMII, described to be regulatory sites for the NF assembly (Grant and Pant, 2000). Western blot assays showed that the immunoreactivity with anti-phosphoSer55 and anti-phosphoSer57 antibodies was increased in the cytoskeletal fraction of striatal slices exposed to QUIN. Moreover, phosphorylation of NFLSer55 was prevented by H89 and phosphorylation of NFLSer57 was prevented by KN93, PKA and PKCaMII inhibitors, respectively (Fig. 3A). Moreover, the KSP repeats, located in the NFH tail domain were the targets for the action of QUIN, as demonstrated by Western blot assay with anti-phosphoKSP repeat antibody. Interestingly, QA-induced phosphorylation of KSP repeats was totally prevented by MPEP (mGluR5 antagonist) and roscovitine, suggesting that QUIN would be upstream of mGluR5, which in turn, would activate cdk5 provoking hyperphosphorylation of the KSP repeat sites in the NFH tail domain (Fig. 3B).

Participation of neurotransmitters in the action of QUIN in striatal slices: Testing the roles of glutamatergic and GABAergic systems

Since QUIN is considered a NMDA glutamate agonist (Schwarcz and Pellicciari, 2002; Stone, 1993), we assayed the participation of glutamate receptors in the action of QUIN on the phosphorylating system associated with the IFs of the striatal neural cells. Tissue slices were coincubated with QUIN and DL-AP5, a competitive NMDA ionotropic antagonist, CNQX, a nonNMDA ionotropic antagonist and MCPG, a metabotropic glutamate antagonist. As shown in Fig. 4, hyperphosphorylation induced by QUIN was totally prevented in the IF subunits by the NMDA antagonist, while CNQX attenuated the effect of QUIN on NFL. In addition, the metabotropic glutamate antagonist MCPG attenuated the action of QUIN on NFM. To further identify the types of mGluR involved in such action, we tested 4-C3-HPG and MPEP, specific mGluR1 and mGluR5 antagonists, respectively. Results showed that mGluR1 inhibition totally prevented the QUIN-induced hyperphosphorylation of NFL head domain sites. In addition, mGluR5 inhibition prevented the hyperphosphorylation of KSP repeats on NFM and NFH and partially in the head domain sites on NFL. Taken together, these findings suggest the participation of mGluRs in the action caused by QUIN on the dynamic phosphorylation of NF subunits.

We also, tested the involvement of the GABAergic system on the action of QUIN *in vitro* on the striatal tissue, since we have previously demonstrated that this neurotransmitter system was involved in the dynamics of the phosphorylating system associated with the IF proteins in brain slices (Funchal et al., 2004). Moreover, Rekik et al. (2011) reported increased $GABA_{B1}$ or $GABA_{B2}$ immunoreactivity in the lesioned striatum after QUIN injection. In line with this, Fujiyama et al. (2002) described upregulation of $GABA_A$ receptors in the substantia nigra of rats that have received intrastriatal QUIN injection. However, results obtained in the present study with the specific antagonists for $GABA_A$ (bicuculine and pictrotoxin) and $GABA_B$ (phaclofen) receptors, respectively, indicated that IF hyperphosphorylation induced by QUIN was not mediated by the GABAergic system in striatal slices (results not shown).

Roles of Ca^{2+} mediating the actions of QUIN on the phosphorylating system associated with the cytoskeleton

Taking into account the relevance of Ca^{2+} in the intracellular events that result in the regulation of cell function, particularly in what concerns to the cytoskeletal phosphorylation system (Funchal et al., 2004, 2005a,b; Loureiro et al., 2008; Stull, 2001), we examined the involvement of Ca^{2+} in the QUIN-mediated increase of the *in vitro* ^{32}P incorporation into IF in rat striatum. To test the involvement of Ca^{2+} influx through voltage-dependent Ca^{2+} channels (VDCC), we used the specific L-VDCC blocker verapamil. Results showed that co-incubation of the tissue slices with QUIN and verapamil totally prevented the effect of QUIN on the phosphorylating system, suggesting that Ca^{2+} influx via L-VDCC was involved in the ability of QUIN to alter the phosphorylating/dephosphorylating equilibrium of IF proteins recovered in the cytoskeletal fraction. To further investigate the role of intra and extracellular Ca^{2+} levels in this process we performed experiments using EGTA, as an extracellular Ca^{2+} chelator and BAPTA-AM the membrane-permeable form of BAPTA, an intracellular Ca^{2+} chelator (Tymianski et al., 1994). In the experiments designed to verify the involvement of the Ca^{2+} release from the intracellular stores we used dantrolene, an inhibitor of ryanodine Ca^{2+} channels of the endoplasmic reticulum. Taken together, the results showed that the action of QUIN was dependent on the cytosolic Ca^{2+} levels and on the Ca^{2+} influx from external medium in both neuronal and glial cells. In addition, dantrolene at a concentration described to irreversibly inhibit ryanodine channel opening (Serysheva and Hamilton, 1998), prevented the IF

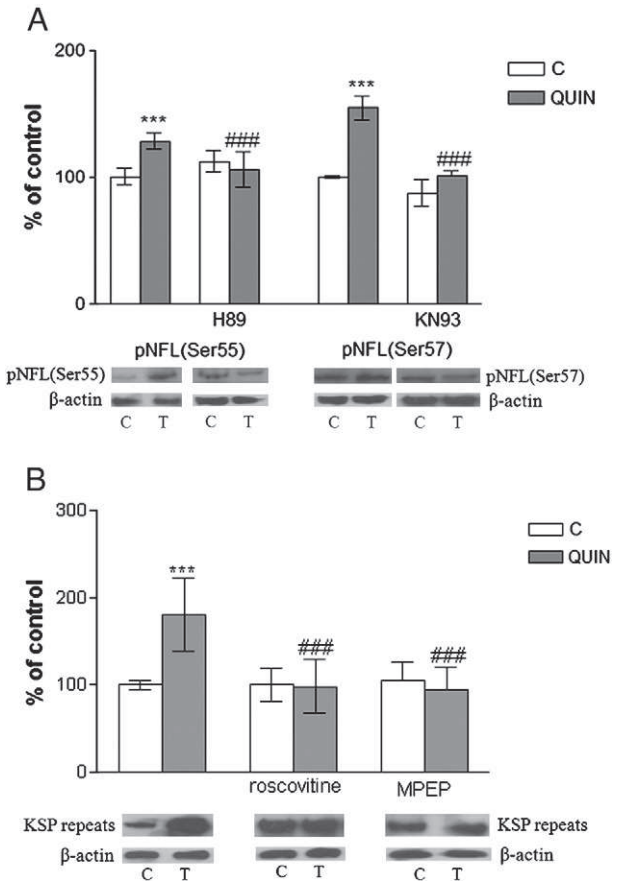

Fig. 3. Effect of QA and different inhibitors on QA-hyperphosphorylation of specific sites of NF. (A) Effect on QUIN-hyperphosphorylation of NFL(Ser55) and NFL(Ser57) of striatum of rats. H89 (10 μM), KN93 (10 μM), 4-C3-HPG (30 μM) are incubated in slices before QUIN, as described in Material and Methods. The cytoskeletal fraction was extracted and the immunocontent of phosphoNFL(Ser55) and phosphoNFL(Ser57) was measured. (B) Effect of QUIN on immunocontent of phosphoNFH(KSP repeats) in slices of striatum of rats. Roscovitine (10 μM) and MPEP (30 μM) are incubated in slices before QUIN, as described in Materials and methods. The cytoskeletal fraction was extracted and the immunocontent of phosphoNFH(KSP repeats) was measured. Densitometric data are shown. Representative immunoblots are represented. Results are expressed as mean ± S.D. Statistical analysis: one-way ANOVA followed by Tukey–Kramer test is indicated: ***$p<0.001$ compared with control group and ###$p<0.001$ compared with QUIN group.

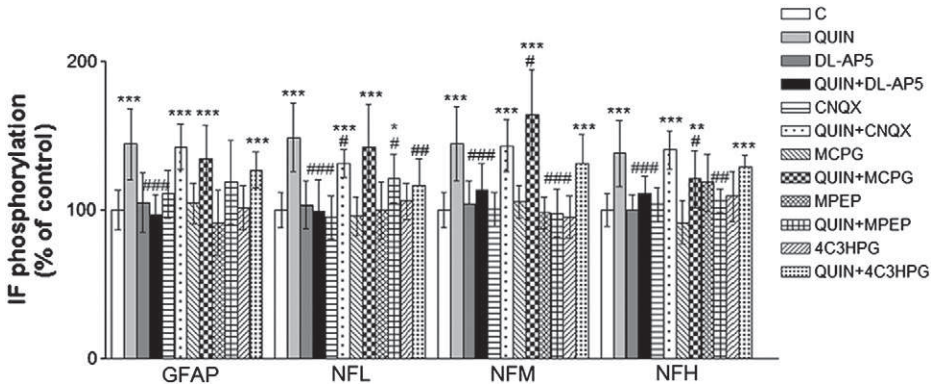

Fig. 4. Involvement of glutamate receptors on QUIN-induced IF hyperphosphorylation in striatum of 30-day-old rats. Slices were preincubated for 20 min in the presence of 100 μM DL-AP5, 50 μM CNQX, 100 μM MCPG, 30 μM MPEP, 30 μM 4C3HPG and incubated with 100 μM of QUIN for 30 min. After, the slices were incubated with ^{32}P-orthophosphate with or without the blockers and/or 100 μM QUIN. The cytoskeletal fraction was extracted and the radioactivity incorporated into NFL, NFM, NFH and GFAP was measured. Data are reported as means ± S.D. of 18 animals in each group and expressed as percent of control. Statistically significant differences as determined by one-way ANOVA followed by Tukey–Kramer multiple comparison test are indicated: ***p<0.001; **p<0.01 and *p<0.05 compared with control; ###p<0.001; ##p<0.01 and #p<0.05 compared with QUIN group.

hyperphosphorylation induced by QUIN (Fig. 5), in neurons, but not in astrocytes, which is consistent with the presence of these channels in excitable cell types, such as muscle and neurons (Bennett et al., 1996).

Finally, to characterize the role of phospholipase C in the QUIN-activated signaling pathways targeting the IF-associated phosphorylating system, we used U73122, a specific PLC inhibitor. Results showed a partial involvement of PLC in the phosphorylation level of NFL, compatible with a role of diacylglycerol (DAG) in the activation of PKC and phosphorylation of head-domain phosphorylating sites on NFL (Fig. 2).

Discussion

We have recently demonstrated that intrastriatal QUIN injection provoked the disruption of the homeostasis of the phosphorylating system associated with the cytoskeleton in neurons and in astrocytes of 30-day-old rats and that this effect was mediated by Ca^{2+} influx through NMDA channels and by oxidative stress. We then proposed that alterations of the phosphorylation system associated with the IF proteins could represent an early event on the cascade of neurodegeneration mediated by QUIN *in vivo* (Pierozan et al., 2010). Taking into account these findings and the relevance of the cytoskeleton in the physiology and pathophysiology of neural cells, we were interested to assess the molecular mechanisms underlying the actions of QUIN on the phosphorylating system associated with the cytoskeleton in the striatal astrocytes and neurons. Therefore, in the present report we used an *in vitro* model in which striatal slices of 30-day-old rats were exposed to 100 μM QUIN for 50 min demonstrating that QUIN, at a concentration described to induce excitotoxic effects in striatal slices (Perez-De La Cruz et al., 2010), is upstream of complex signaling pathways provoking hyperphosphorylation of GFAP, the IF protein from mature astrocytes, as well as of NFL, NFM and NFH, constituents of neuronal IFs.

It was found that QUIN disrupted the homeostasis of the cytoskeleton of astrocytes and neurons by cell specific mechanisms. In astrocytes, the action of QUIN was mediated by increased Ca^{2+} influx through NMDA and L-VDCC channels. High Ca^{2+} levels in the cytosol induced hyperphosphorylation of GFAP, by the second messenger-dependent protein kinases PKA and PKCaMII. These findings are in agreement with the previous evidence showing that the neural isoforms of adenylyl cyclase are activated by Ca^{2+}, supporting the PKA activation by high Ca^{2+} levels (Steiner et al., 2006). It is of note that PKCaMII is a Ca^{2+}/calmodulin protein kinase implicated in the phosphorylation of sites in the head domain of type III IF proteins, including GFAP (Leal et al., 1997; Omary et al., 2006).In this context, phosphorylation of the head domain of homopolymeric filaments like vimentin, desmin and GFAP is known to be important for filament assembly and plays a special role in dividing cells. Therefore, abnormal phosphorylation of the head domain sites of these type III IF proteins could lead to nonphysiological disassembly of IFs contributing to disruption of cell homeostasis (Gill et al., 1990; Heins et al., 1993).

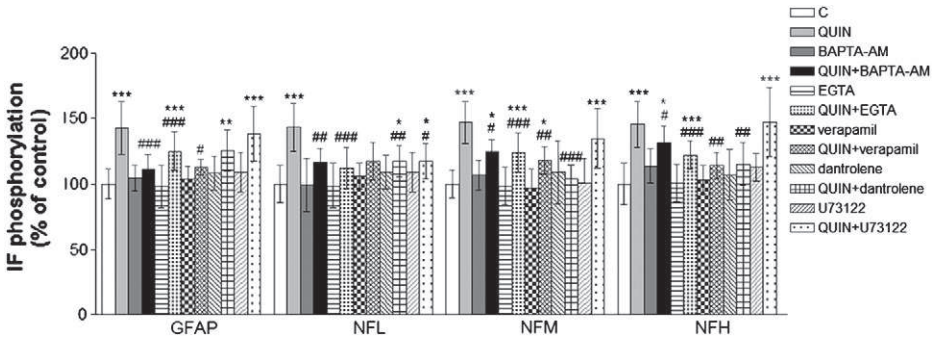

Fig. 5. Involvement of intra and extracellular Ca^{2+} and phospholipase C on QUIN-induced IF *in vitro* phosphorylation. Slices were preincubated for 20 min in the presence of 50 μM BAPTA-AM, 1 mM EGTA, 30 μM verapamil, 30 μM dantrolene and 10 μM U73122 and incubated with 100 μM of QUIN for 30 min. After, the slices were incubated with ^{32}P-orthophosphate with or without the blockers and/or 100 μM QUIN. The cytoskeletal fraction was extracted and the radioactivity incorporated into NFL, NFM, NFH and GFAP was measured. Data are reported as means ± S.D. of 18 animals in each group and expressed as percent of control. Statistically significant differences as determined by one-way ANOVA followed by Tukey–Kramer multiple comparison test are indicated: ***p<0.001; **p<0.01; *p<0.05 compared with control; ###p<0.001; ##p<0.01 and #p<0.05 compared with QUIN group.

In neurons QUIN elicited more complex actions involving metabotropic glutamate receptors and the release of Ca^{2+} from intracellular stores besides Ca^{2+} influx through NMDA and L-VDCC membrane channels. These events resulted in the hyperphosphorylation of both head-domain sites on NFL and tail-domain sites on NFM and NFH proteins.

It was observed that in QUIN-induced hyperphosphorylation of NFL head domain sites was mediated by PKC, PKA and PKCaMII. NFL hyperphosphorylation was partially prevented by the mGluR1 antagonist and by inhibiting PLC activity. These findings indicate that QUIN is upstream of mGluR1/PLC pathway implicated in the hydrolysis of phosphatidyl inositol 4,5-biphosphate ($PI(4,5)P_2$) in neurons, producing inositol 1,4,5-triphosphate (IP3) and diacylglycerol (DAG) which, in turn, is able to activate PKC. Moreover, the use of site- and phosphorylation state-specific antibodies, as well as protein kinase inhibitors, pointed to PKA phosphorylating NFL subunit on Ser55 and PKCaMII phosphorylating NFL on Ser57. Differently from homopolymeric filaments, phosphorylation of the head domain sites on NFL was not involved in filament disassembly. NFs are present in the postmitotic neurons, and once formed, do not undergo depolymerization (Sihag et al., 2007). Thus, the roles of head domain phosphorylation of rat NFL and NFM are thought to be related to the obligate heteropolymeric NF filament formation (Ching and Liem, 1999), suggesting, therefore, that QUIN neurotoxicity in striatal slices includes destabilization of the IF network of neuronal cells. In this context, we have previously demonstrated that hyperphosphorylation of NFL on Ser55 is on the basis of neuronal dysfunction related to congenital hypothyroidism (Zamoner et al., 2008a).

Moreover, the KSP repeats located on NFM and NFH carboxyl-terminal tail domains were hyperphosphorylated by cdk5, while JNK/MAPK only partially contributed to NFM hyperphosphorylation in response to the QUIN insult. In this context, it has been described that Cdk5 phosphorylates cytoskeletal proteins, including the NFs and the microtubule associated protein Tau (Ackerley et al., 2003; Bu et al., 2002; Pant et al., 1997; Shea et al., 2004; Zhou et al., 2010). Cdk5 is a member of the Cdk family, whose activity is predominantly detected in post-mitotic neurons (Hisanaga and Saito, 2003). Two related proteins, p35 and p39, activate Cdk5 upon direct binding. During neurotoxic stress, intracellular rise in Ca^{2+} activates calpain, which cleaves p35 to generate p25. The long half-life of Cdk5/p25 results in a hyperactive aberrant Cdk5 that hyperphosphorylates Tau, NF and other cytoskeletal proteins (Hisanaga and Saito, 2003). It is known that carboxyl-terminal phosphorylation of NFH progressively restricts the association of neurofilaments with kinesin, the axonal anterograde motor protein, and stimulates its interaction with dynein, the axonal retrograde motor protein (Motil et al., 2006). This event could represent one of the mechanisms by which carboxyl-terminal phosphorylation would slow neurofilament axonal transport. These hyperphosphorylated cytoskeletal proteins set the groundwork to forming neurofibrillary tangles and aggregates of phosphorylated proteins, that are hallmarks of neurodegenerative diseases like Alzheimer's disease, Parkinson's disease and Amyotropic Lateral Sclerosis (Kanungo et al., 2008).

Proline-directed Cdk5 and MAP kinases are among the main proline-directed kinases phosphorylating Ser residues on KSP tail domain on the NFM and NFH (Jaffe et al., 1998; Sun et al., 1996; Veeranna et al., 1998) in response to signal transduction cascades triggered by a variety of signals (Dashiell et al., 2002; DeFuria and Shea, 2007; Li et al., 1999a, 2000), including Ca^{2+} influx (Li et al., 1999b). It is important to note that our results showing that QUIN induced NFM and NFH hyperphosphorylation was mediated by cdk5 while Erk and p38MAPK were not involved in this effect, and JNK partially phosphorylated NFM subunit. These findings could be correlated with cdk5-induced inactivation of the MAPK pathway (Li et al., 2002; Sharma et al., 2002).

In the neuronal cells the glutamate receptors were also important mediators of the neurotoxicity of QUIN in striatal slices. We observed that hyperphosphorylation of NFL, NFM and NFH was dependent on NMDA as well as group I metabotropic glutamate receptors (mGluR1 and mGluR5), but not on AMPA and kainate receptors. However, we cannot exclude the possibility that QUIN-induced increase of IF phosphorylation through mGLUR could be due to and indirect effect of QUIN causing glutamate release. In this context, although Connick and Stone (1988) have described that high concentrations (2 mM and higher) of QUIN were able to release glutamate *in vivo*, this metabolite failed to induce glutamate release in concentrations as high as 5 mM *in vitro*. Therefore it is improbable that glutamate release could be provoked by QUIN (100 μM) in our experimental conditions.

Activation of group I mGluRs by QUIN is consistent with a central role of these receptors in the striatum, whereas activation of mGlu1 and mGlu5 receptors exerts distinct actions, depending on the neuronal subtype involved (Bonsi et al., 2008). Consistently with our results, the mGluR1/5 signal transduction is complex and involves multiple partners leading to activation of a wide variety of signaling pathways. It is noted that mGluRs coupled to $G\alpha(q/)_{11}$ proteins activated phospholipase Cβ1 resulting in DAG and IP3 formation is followed by PKC activation. In addition, mGluR activation can lead to modulation of a number of ion channels, such as different types of Ca^{2+} and K^+ channels

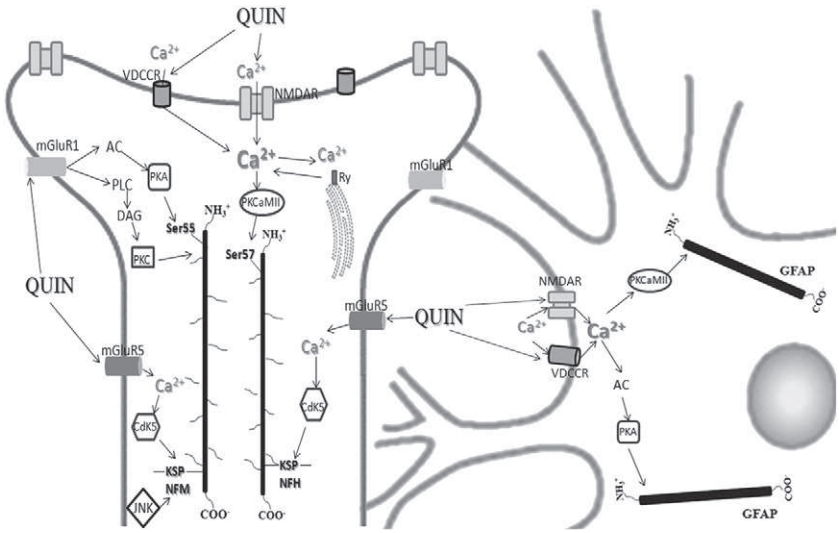

Fig. 6. Proposed mechanism by which QUIN activates IF phosphorylation in neural cells of striatum of rats. The effects of QUIN are initiated by mGluR activation and excessive influx of Ca^{2+} through NMDA receptors and L-VDCC, together with Ca^{2+} release from intracellular stores leads to an overload of Ca^{2+} within the cell, which set off a cascade of events including activation of PKA, PKCaMII and PKC, which phosphorylate head domain sites on GFAP and NFL subunits. Cdk5 is activated downstream of mGluR5 phosphorylating the KSP repeats of NFM and NFH, and mGluR1 is upstream of PLC which produces DAG which, in turn, activate PKC and phosphorylate NFL.

(Ribeiro et al., 2010). Also, mGluR5 is reported to be upstream of several kinases, including cdk5 (Wang et al., 2004). Otherwise, activation of NMDA receptors is implicated in the increased cytoplasmic Ca^{2+} concentrations, which in turn, can trigger a range of downstream neurotoxic cascades, including the activation and overstimulation of protein kinases (Szydlowska and Tymianski, 2010).

Regarding to the relevance of Ca^{2+} overload on the modulation of the phosphorylating system associated with the cytoskeleton (Heimfarth et al., 2010; Loureiro et al., 2005, 2010; Zamoner et al., 2008b), the blockade of L-VDCC and the intra and extracellular Ca^{2+} chelation totally prevented the effect of QUIN on IF phosphorylation. Interestingly, dantrolene-induced inhibition of Ca^{2+} release from the endoplasmic reticulum through ryanodine receptors prevented this effect in neurons but was ineffective in astrocyte IFs, reinforcing the cell type specific signaling mechanisms. On the basis of our results QUIN increased cytosolic Ca^{2+} in neural cells downstream of Ca^{2+} influx through NMDA, L-VDCC and Ca^{2+} release from intracellular stores. These findings show the role of Ca^{2+} in the actions of QUIN on the cytoskeleton.

Taking into account our experimental results we could reach to the proposal depicted in Fig. 6, that the *in vitro* action of QUIN on the endogenous phosphorylating system targeting the cytoskeleton of striatal cells is a complex intracellular process initiated by mGluR activation and excessive influx of Ca^{2+} through NMDA receptors and L-VDCC. These events, together with Ca^{2+} release from intracellular stores lead to an overload of Ca^{2+} within the cell. Elevated Ca^{2+} levels then set off a cascade of events including activation of the second messenger-dependent protein kinases PKA, PKCaMII and PKC, which phosphorylate head domain sites on GFAP and NFL subunits and potentially misregulating IF assembly in both glial and neuronal cells. It was also found that Cdk5 is activated downstream of mGluR5, phosphorylating the KSP repeats on NFM and NFH. Also, mGluR1 is upstream of PLC which, in turn, produces DAG and IP3. Our results are also in accordance to the evidence that DAG is important to activate PKC and phosphorylate NFL, while IP3 contributes to Ca^{2+} release from internal stores promoting hyperphosphorylation of KSP repeats on the tail domain of NFM and NFH. Besides the action on the phosphorylation sites on IF subunits, Cdk5 is probably able to inhibit MAPK pathway. Taking together, these signaling pathways eventually contribute to the fate of the affected astrocytes and neurons exposed to QUIN.

Acknowledgments

This work was supported by grants of the Conselho Nacional de Desenvolvimento Científico e Tecnológico (CNPq), Fundação de Amparo à Pesquisa do Estado do Rio Grande do Sul (FAPERGS) and Pro-Reitoria de Pesquisa de Pós Graduação of the Universidade Federal do Rio Grande do Sul (Propesq-UFRGS).

References

Ackerley, S., Thornhill, P., Grierson, A.J., Brownlees, J., Anderton, B.H., Leigh, P.N., Shaw, C.E., Miller, C.C., 2003. Neurofilament heavy chain side arm phosphorylation regulates axonal transport of neurofilaments. J. Cell Biol. 161 (3), 489–495.

Adermark, L., Clarke, R.B., Soderpalm, B., Ericson, M., 2010. Ethanol-induced modulation of synaptic output from the dorsolateral striatum in rat is regulated by cholinergic interneurons. Neurochem. Int. 58 (6), 693–699.

Albert, B., Johnson, A., Lewis, J., Raff, M., Roberts, K., Walter, P., 2008. Molecular Biology of the Cell Published by Garland Science. Taylor and Francis Group, New York USA Fifth Edition.

Beal, M.F., Kowall, N.W., Ellison, D.W., Mazurek, M.F., Swartz, K.J., Martin, J.B., 1986. Replication of the neurochemical characteristics of Huntington's disease by quinolinic acid. Nature 321 (6066), 168–171.

Behan, W.M., McDonald, M., Darlington, L.G., Stone, T.W., 1999. Oxidative stress as a mechanism for quinolinic acid-induced hippocampal damage: protection by melatonin and deprenyl. Br. J. Pharmacol. 128 (8), 1754–1760.

Bennett, D.L., Cheek, T.R., Berridge, M.J., De Smedt, H., Parys, J.B., Missiaen, L., Bootman, M.D., 1996. Expression and function of ryanodine receptors in nonexcitable cells. J. Biol. Chem. 271 (11), 6356–6362.

Bonsi, P., Platania, P., Martella, G., Madeo, G., Vita, D., Tassone, A., Bernardi, G., Pisani, A., 2008. Distinct roles of group I mGlu receptors in striatal function. Neuropharmacology 55 (4), 392–395.

Bu, B., Li, J., Davies, P., Vincent, I., 2002. Deregulation of cdk5, hyperphosphorylation, and cytoskeletal pathology in the Niemann–Pick type C murine model. J. Neurosci. 22 (15), 6515–6525.

Chen, Y., Guillemin, G.J., 2009. Kynurenine Pathway Metabolites in Humans: Disease and Healthy States. Int J of Trypt Res 2 (1), 1–19.

Ching, G.Y., Liem, R.K., 1999. Analysis of the roles of the head domains of type IV rat neuronal intermediate filament proteins in filament assembly using domain-swapped chimeric proteins. J. Cell Sci. 112 (Pt 13), 2233–2240.

Connick, J.H., Stone, T.W., 1988. Quinolinic acid effects on amino acid release from the rat cerebral cortex in vitro and in vivo. Br. J. Pharmacol. 93 (4), 868–876.

Cortes, H., Paz, F., Erlij, D., Aceves, J., Floran, B., 2010. GABA(B) receptors modulate depolarization-stimulated [(3)H]glutamate release in slices of the pars reticulata of the rat substantia nigra. Eur. J. Pharmacol. 649 (1–3), 161–167.

Daile, P., Carnegie, P.R., Young, J.D., 1975. Synthetic substrate for cyclic AMP-dependent protein kinase. Nature 257 (5525), 416–418.

Dashiell, S.M., Tanner, S.L., Pant, H.C., Quarles, R.H., 2002. Myelin-associated glycoprotein modulates expression and phosphorylation of neuronal cytoskeletal elements and their associated kinases. J. Neurochem. 81 (6), 1263–1272.

de Carvalho, L.P., Bochet, P., Rossier, J., 1996. The endogenous agonist quinolinic acid and the non endogenous homoquinolinic acid discriminate between NMDAR2 receptor subunits. Neurochem. Int. 28 (4), 445–452.

DeFuria, J., Shea, T.B., 2007. Arsenic inhibits neurofilament transport and induces perikaryal accumulation of phosphorylated neurofilaments: roles of JNK and GSK-3beta. Brain Res. 1181, 74–82.

Domenici, M.R., Pepponi, R., Martire, A., Tebano, M.T., Potenza, R.L., Popoli, P., 2004. Permissive role of adenosine A2A receptors on metabotropic glutamate receptor 5 (mGluR5)-mediated effects in the striatum. J. Neurochem. 90 (5), 1276–1279.

Eng, L.F., Ghirnikar, R.S., Lee, Y.L., 2000. Glial fibrillary acidic protein: GFAP-thirty-one years (1969–2000). Neurochem. Res. 25 (9–10), 1439–1451.

Estrada Sanchez, A.M., Mejia-Toiber, J., Massieu, L., 2008. Excitotoxic neuronal death and the pathogenesis of Huntington's disease. Arch. Med. Res. 39 (3), 265–276.

Fuchs, E., Weber, K., 1994. Intermediate filaments: structure, dynamics, function, and disease. Annu. Rev. Biochem. 63, 345–382.

Fujiyama, F., Stephenson, F.A., Bolam, J.P., 2002. Synaptic localization of GABA(A) receptor subunits in the substantia nigra of the rat: effects of quinolinic acid lesions of the striatum. Eur J Neurosci 15 (12), 1961–1975.

Funchal, C., Dall Bello Pessutto, F., de Almeida, L.M., de Lima, Pelaez P., Loureiro, S.O., Vivian, L., Wajner, M., Pessoa-Pureur, R., 2004. Alpha-keto-beta-methylvaleric acid increases the in vitro phosphorylation of intermediate filaments in cerebral cortex of young rats through the gabaergic system. J. Neurol. Sci. 217 (1), 17–24.

Funchal, C., de Almeida, L.M., Oliveira Loureiro, S., Vivian, L., de Lima, Pelaez P., Dall Bello Pessutto, F., Rosa, A.M., Wajner, M., Pessoa, Pureur R., 2003. In vitro phosphorylation of cytoskeletal proteins from cerebral cortex of rats. Brain Res. Brain Res. Protoc. 11 (2), 111–118.

Funchal, C., Zamoner, A., dos Santos, A.Q., Loureiro, S.O., Wajner, M., Pessoa-Pureur, R., 2005a. Alpha-ketoisocaproic acid increases phosphorylation of intermediate filament proteins from rat cerebral cortex by mechanisms involving Ca^{2+} and cAMP. Neurochem. Res. 30 (9), 1139–1146.

Funchal, C., Zamoner, A., dos Santos, A.Q., Moretto, M.B., Rocha, J.B., Wajner, M., Pessoa-Pureur, R., 2005b. Evidence that intracellular Ca^{2+} mediates the effect of alpha-ketoisocaproic acid on the phosphorylating system of cytoskeletal proteins from cerebral cortex of immature rats. J. Neurol. Sci. 238 (1–2), 75–82.

Geisler, N., Vandekerckhove, J., Weber, K., 1987. Location and sequence characterization of the major phosphorylation sites of the high molecular mass neurofilament proteins M and H. FEBS Lett. 221 (2), 403–407.

Gill, S.R., Wong, P.C., Monteiro, M.J., Cleveland, D.W., 1990. Assembly properties of dominant and recessive mutations in the small mouse neurofilament (NF-L) subunit. J. Cell Biol. 111 (5 Pt 1), 2005–2019.

Grant, P., Pant, H.C., 2000. Neurofilament protein synthesis and phosphorylation. J. Neurocytol. 29 (11–12), 843–872.

Heimfarth, L., Loureiro, S.O., Reis, K.P., de Lima, B.O., Zamboni, F., Lacerda, S., Soska, A.K., Wild, L., da Rocha, J.B., Pessoa-Pureur, R., 2010. Diphenyl ditelluride induces hypophosphorylation of intermediate filaments through modulation of DARPP-32-dependent pathways in cerebral cortex of young rats. Arch. Toxicol.

Heins, S., Wong, P.C., Muller, S., Goldie, K., Cleveland, D.W., Aebi, U., 1993. The rod domain of NF-L determines neurofilament architecture, whereas the end domains specify filament assembly and network formation. J. Cell Biol. 123 (6 Pt 1), 1517–1533.

Hisanaga, S., Gonda, Y., Inagaki, M., Ikai, A., Hirokawa, N., 1990. Effects of phosphorylation of the neurofilament L protein on filamentous structures. Cell Regul. 1 (2), 237–248.

Hisanaga, S., Saito, T., 2003. The regulation of cyclin-dependent kinase 5 activity through the metabolism of p35 or p39 Cdk5 activator. Neurosignals 12 (4–5), 221–229.

Jaffe, H., Veeranna, Shetty K.T., Pant, H.C., 1998. Characterization of the phosphorylation sites of human high molecular weight neurofilament protein by electrospray ionization tandem mass spectrometry and database searching. Biochemistry 37 (11), 3931–3940.

Kalonia, H., Kumar, P., Kumar, A., 2011a. Comparative neuroprotective profile of statins in quinolinic acid induced neurotoxicity in rats. Behav. Brain Res. 216 (1), 220–228.

Kalonia, H., Kumar, P., Kumar, A., 2011b. Pioglitazone ameliorates behavioral, biochemical and cellular alterations in quinolinic acid induced neurotoxicity: possible role of peroxisome proliferator activated receptor-Upsilon (PPARUpsilon) in Huntington's disease. Pharmacol. Biochem. Behav. 96 (2), 115–124.

Kanungo, J., Zheng, Y.L., Amin, N.D., Pant, H.C., 2008. The Notch signaling inhibitor DAPT down-regulates cdk5 activity and modulates the distribution of neuronal cytoskeletal proteins. J. Neurochem. 106 (5), 2236–2248.
Katayama, T., Tanaka, H., Yoshida, T., Uehara, T., Minami, M., 2009. Neuronal injury induces cytokine-induced neutrophil chemoattractant-1 (CINC-1) production in astrocytes. J. Pharmacol. Sci. 109 (1), 88–93.
Kemp, B.E., Bylund, D.B., Huang, T.S., Krebs, E.G., 1975. Substrate specificity of the cyclic AMP-dependent protein kinase. Proc. Natl. Acad. Sci. U. S. A. 72 (9), 3448–3452.
Kim, S., Coulombe, P.A., 2007. Intermediate filament scaffolds fulfill mechanical, organizational, and signaling functions in the cytoplasm. Genes Dev. 21 (13), 1581–1597.
Laemmli, U.K., 1970. Cleavage of structural proteins during the assembly of the head of bacteriophage T4. Nature 227 (5259), 680–685.
Lariviere, R.C., Julien, J.P., 2004. Functions of intermediate filaments in neuronal development and disease. J. Neurobiol. 58 (1), 131–148.
Leal, R.B., Goncalves, C.A., Rodnight, R., 1997. Calcium-dependent phosphorylation of glial fibrillary acidic protein (GFAP) in the rat hippocampus: a comparison of the kinase/phosphatase balance in immature and mature slices using tryptic phosphopeptide mapping. Brain Res. Dev. Brain Res. 104 (1–2), 1–10.
Lee, V.M., Otvos Jr., L., Carden, M.J., Hollosi, M., Dietzschold, B., Lazzarini, R.A., 1988. Identification of the major multiphosphorylation site in mammalian neurofilaments. Proc. Natl. Acad. Sci. U. S. A. 85 (6), 1998–2002.
Li, B.S., Veeranna, Grant P., Pant, H.C., 1999a. Calcium influx and membrane depolarization induce phosphorylation of neurofilament (NF-M) KSP repeats in PC12 cells. Brain Res. Mol. Brain Res. 70 (1), 84–91.
Li, B.S., Veeranna, J.G., Grant, P., Pant, H.C., 1999b. Activation of mitogen-activated protein kinases (Erk1 and Erk2) cascade results in phosphorylation of NF-M tail domains in transfected NIH 3T3 cells. Eur J Biochem 262, 211–217.
Li, B.S., Zhang, L., Gu, J., Amin, N.D., Pant, H.C., 2000. Integrin alpha(1) beta(1)-mediated activation of cyclin-dependent kinase 5 activity is involved in neurite outgrowth and human neurofilament protein H Lys-Ser-Pro tail domain phosphorylation. J. Neurosci. 20, 6055–6062.
Li, B.S., Zhang, L., Takahashi, S., Ma, W., Jaffe, H., Kulkarni, A.B., Pant, H.C., 2002. Cyclin-dependent kinase 5 prevents neuronal apoptosis by negative regulation of c-Jun N-terminal kinase 3. EMBO J. 21 (3), 324–333.
Liu, Y., Peterson, D.A., Kimura, H., Schubert, D., 1997. Mechanism of cellular 3-(4,5-dimethylthiazol-2-yl)-2,5-diphenyltetrazolium bromide (MTT) reduction. J. Neurochem. 69 (2), 581–593.
Loureiro, S.O., de Lima, Pelaez P., Heimfarth, L., Souza, D.O., Wajner, M., Pessoa-Pureur, R., 2005. Propionic and methylmalonic acids increase cAMP levels in slices of cerebral cortex of young rats via adrenergic and glutamatergic mechanisms. Biochim. Biophys. Acta 1740 (3), 460–466.
Loureiro, S.O., Heimfarth, L., Pelaez Pde, L., Lacerda, B.A., Vidal, L.F., Soska, A., Santos, N.G., Andrade, C., Tagliari, B., Scherer, E.B., Guma, F.T., Wyse, A.T., Pessoa-Pureur, R., 2010. Hyperhomocysteinemia selectively alters expression and stoichiometry of intermediate filament and induces glutamate- and calcium-mediated mechanisms in rat brain during development. Int. J. Dev. Neurosci. 28 (1), 21–30.
Loureiro, S.O., Heimfarth, L., Pelaez Pde, L., Vanzin, C.S., Viana, L., Wyse, A.T., Pessoa-Pureur, R., 2008. Homocysteine activates calcium-mediated cell signaling mechanisms targeting the cytoskeleton in rat hippocampus. Int. J. Dev. Neurosci. 26 (5), 447–455.
Lowry, O.H., Rosebrough, N.J., Farr, A.L., Randall, R.J., 1951. Protein measurement with the Folin phenol reagent. J. Biol. Chem. 193 (1), 265–275.
Motil, J., Chan, W.K., Dubey, M., Chaudhury, P., Pimenta, A., Chylinski, T.M., Ortiz, D.T., Shea, T.B., 2006. Dynein mediates retrograde neurofilament transport within axons and anterograde delivery of NFs from perikarya into axons: regulation by multiple phosphorylation events. Cell Motil. Cytoskeleton 63, 266–286.
Nixon, R.A., 1993. The regulation of neurofilament protein dynamics by phosphorylation: clues to neurofibrillary pathobiology. Brain Pathol. 3 (1), 29–38.
Nixon, R.A., Sihag, R.K., 1991. Neurofilament phosphorylation: a new look at regulation and function. Trends Neurosci. 14 (11), 501–506.
Omary, M.B., Ku, N.O., Tao, G.Z., Toivola, D.M., Liao, J., 2006. "Heads and tails" of intermediate filament phosphorylation: multiple sites and functional insights. Trends Biochem. Sci. 31 (7), 383–394.
Orlando, L.R., Alsdorf, S.A., Penney Jr., J.B., Young, A.B., 2001. The role of group I and group II metabotropic glutamate receptors in modulation of striatal NMDA and quinolinic acid toxicity. Exp. Neurol. 167 (1), 196–204.
Pant, A.C., Veeranna, Pant H.C., Amin, N., 1997. Phosphorylation of human high molecular weight neurofilament protein (hNF-H) by neuronal cyclin-dependent kinase 5 (cdk5). Brain Res. 765 (2), 259–266.
Paramio, J.M., Jorcano, J.L., 2002. Beyond structure: do intermediate filaments modulate cell signalling? Bioessays 24 (9), 836–844.
Perez-De La Cruz, V., Elinos-Calderon, D., Carrillo-Mora, P., Silva-Adaya, D., Konigsberg, M., Moran, J., Ali, S.F., Chanez-Cardenas, M.E., Perez-De La Cruz, G., Santamaria, A., 2010. Time-course correlation of early toxic events in three models of striatal damage: modulation by proteases inhibition. Neurochem. Int. 56 (6–7), 834–842.
Pierozan, P., Zamoner, A., Soska, A.K., Silvestrin, R.B., Loureiro, S.O., Heimfarth, L., Mello e Souza, T., Wajner, M., Pessoa-Pureur, R., 2010. Acute intrastriatal administration of quinolinic acid provokes hyperphosphorylation of cytoskeletal intermediate filament proteins in astrocytes and neurons of rats. Exp. Neurol. 224 (1), 188–196.
Rekik, L., Daguin-Nerriere, V., Petit, J.Y., Brachet, P., 2011. gamma-Aminobutyric acid type B receptor changes in the rat striatum and substantia nigra following intrastriatal quinolinic acid lesions. J Neurosci Res 89 (4), 524–535.
Ribeiro, F.M., Paquet, M., Cregan, S.P., Ferguson, S.S., 2010. Group I metabotropic glutamate receptor signalling and its implication in neurological disease. CNS Neurol. Disord. Drug Targets 9 (5), 574–595.
Rigon, A.P., Cordova, F.M., Oliveira, C.S., Posser, T., Costa, A.P., Silva, I.G., Santos, D.A., Rossi, F.M., Rocha, J.B., Leal, R.B., 2008. Neurotoxicity of cadmium on immature hippocampus and a neuroprotective role for p38 MAPK. Neurotoxicology 29 (4), 727–734.
Rios, C., Santamaria, A., 1991. Quinolinic acid is a potent lipid peroxidant in rat brain homogenates. Neurochem. Res. 16 (10), 1139–1143.
Sasaki, T., Gotow, T., Shiozaki, M., Sakaue, F., Saito, T., Julien, J.P., Uchiyama, Y., Hisanaga, S., 2006. Aggregate formation and phosphorylation of neurofilament-L Pro22 Charcot–Marie–Tooth disease mutants. Hum. Mol. Genet. 15 (6), 943–952.
Schwarcz, R., Pellicciari, R., 2002. Manipulation of brain kynurenines: glial targets, neuronal effects, and clinical opportunities. J. Pharmacol. Exp. Ther. 303 (1), 1–10.
Serysheva, I.I., Hamilton, S.L., 1998. Ryanodine binding sites on the sarcoplasmic reticulum Ca2C release channel. In: Sitsapesan, R., Willaims, A.J. (Eds.), Structure and Function of Ryanodine Receptors, pp. 95–104.
Seto, D., Zheng, W.H., McNicoll, A., Collier, B., Quirion, R., Kar, S., 2002. Insulin-like growth factor-I inhibits endogenous acetylcholine release from the rat hippocampal formation: possible involvement of GABA in mediating the effects. Neuroscience 115 (2), 603–612.
Sharma, P., Veeranna, Sharma M., Amin, N.D., Sihag, R.K., Grant, P., Ahn, N., Kulkarni, A.B., Pant, H.C., 2002. Phosphorylation of MEK1 by cdk5/p35 down-regulates the mitogen-activated protein kinase pathway. J. Biol. Chem. 277 (1), 528–534.
Shea, T.B., Chan, W.K., 2008. Regulation of neurofilament dynamics by phosphorylation. Eur. J. Neurosci. 27 (8), 1893–1901.
Shea, T.B., Zheng, Y.L., Ortiz, D., Pant, H.C., 2004. Cyclin-dependent kinase 5 increases perikaryal neurofilament phosphorylation and inhibits neurofilament axonal transport in response to oxidative stress. J. Neurosci. Res. 76 (6), 795–800.
Sihag, R.K., Inagaki, M., Yamaguchi, T., Shea, T.B., Pant, H.C., 2007. Role of phosphorylation on the structural dynamics and function of types III and IV intermediate filaments. Exp. Cell Res. 313 (10), 2098–2109.
Sihag, R.K., Nixon, R.A., 1989. In vivo phosphorylation of distinct domains of the 70-kilodalton neurofilament subunit involves different protein kinases. J. Biol. Chem. 264 (1), 457–464.
Songyang, Z., Blechner, S., Hoagland, N., Hoekstra, M.F., Piwnica-Worms, H., Cantley, L.C., 1994. Use of an oriented peptide library to determine the optimal substrates of protein kinases. Curr. Biol. 4 (11), 973–982.
Steiner, D., Saya, D., Schallmach, E., Simonds, W.F., Vogel, Z., 2006. Adenylyl cyclase type-VIII activity is regulated by G(betagamma) subunits. Cell. Signal. 18 (1), 62–68.
Stone, T.W., 1993. Neuropharmacology of quinolinic and kynurenic acids. Pharmacol. Rev. 45 (3), 309–379.
Stone, T.W., Perkins, M.N., 1981. Quinolinic acid: a potent endogenous excitant at amino acid receptors in CNS. Eur. J. Pharmacol. 72 (4), 411–412.
Stull, J.T., 2001. Ca^{2+}-dependent cell signaling through calmodulin-activated protein phosphatase and protein kinases minireview series. J. Biol. Chem. 276 (4), 2311–2312.
Sun, D., Leung, C.L., Liem, R.K., 1996. Phosphorylation of the high molecular weight neurofilament protein (NF-H) by Cdk5 and p35. J. Biol. Chem. 271 (24), 14245–14251.
Szydlowska, K., Tymianski, M., 2010. Calcium, ischemia and excitotoxicity. Cell Calcium 47 (2), 122–129.
Tavares, R.G., Tasca, C.I., Santos, C.E., Alves, L.B., Porciuncula, L.O., Emanuelli, T., Souza, D.O., 2002. Quinolinic acid stimulates synaptosomal glutamate release and inhibits glutamate uptake into astrocytes. Neurochem. Int. 40 (7), 621–627.
Tomizawa, K., Ohta, J., Matsushita, M., Moriwaki, A., Li, S.T., Takei, K., Matsui, H., 2002. Cdk5/p35 regulates neurotransmitter release through phosphorylation and down-regulation of P/Q-type voltage-dependent calcium channel activity. J. Neurosci. 22 (7), 2590–2597.
Tymianski, M., Spigelman, I., Zhang, L., Carlen, P.L., Tator, C.H., Charlton, M.P., Wallace, M.C., 1994. Mechanism of action and persistence of neuroprotection by cell-permeant Ca^{2+} chelators. J. Cereb. Blood Flow Metab. 14 (6), 911–923.
Ubersax, J.A., Ferrell Jr., J.E., 2007. Mechanisms of specificity in protein phosphorylation. Nat. Rev. Mol. Cell Biol. 8 (7), 530–541.
Veeranna, Amin N.D., Ahn, N.G., Jaffe, H., Winters, C.A., Grant, P., Pant, H.C., 1998. Mitogen-activated protein kinases (Erk1,2) phosphorylate Lys-Ser-Pro (KSP) repeats in neurofilament proteins NF-H and NF-M. J. Neurosci. 18 (11), 4008–4021.
Wang, Q., Walsh, D.M., Rowan, M.J., Selkoe, D.J., Anwyl, R., 2004. Block of long-term potentiation by naturally secreted and synthetic amyloid beta-peptide in hippocampal slices is mediated via activation of the kinases c-Jun N-terminal kinase, cyclin-dependent kinase 5, and p38 mitogen-activated protein kinase as well as metabotropic glutamate receptor type 5. J. Neurosci. 24 (13), 3370–3378.
Whitaker, A.N., McKay, D.G., 1969. Studies of catecholamine shock. I. Disseminated intravascular coagulation. Am J Pathol 56 (2), 153–176.
Xu, Z.S., Liu, W.S., Willard, M.B., 1992. Identification of six phosphorylation sites in the COOH-terminal tail region of the rat neurofilament protein M. J. Biol. Chem. 267 (7), 4467–4471.
Yabe, J.T., Jung, C., Chan, W.K., Shea, T.B., 2000. Phospho-dependent association of neurofilament proteins with kinesin in situ. Cell Motil. Cytoskeleton 45 (4), 249–262.
Zamoner, A., Heimfarth, L., Oliveira Loureiro, S., Royer, C., Mena Barreto Silva, F.R., Pessoa-Pureur, R., 2008a. Nongenomic actions of thyroxine modulate intermediate filament phosphorylation in cerebral cortex of rats. Neuroscience 156 (3), 640–652.
Zamoner, A., Heimfarth, L., Pessoa-Pureur, R., 2008b. Congenital hypothyroidism is associated with intermediate filament misregulation, glutamate transporters down-regulation and MAPK activation in developing rat brain. Neurotoxicology 29, 1092–1099.
Zhou, J., Wang, H., Feng, Y., Chen, J., 2010. Increased expression of cdk5/p25 in N2a cells leads to hyperphosphorylation and impaired axonal transport of neurofilament proteins. Life Sci. 86 (13–14), 532–537.

Capítulo 4

THE PHOSPHORYLATION STATUS AND CYTOSKELETAL REMODELING OF STRIATAL ASTROCYTES TREATED WITH QUINOLINIC ACID

Paula Pierozan; Fernanda Ferreira; Bárbara O de Lima; Carolina G Fernanda; Priscila T Monteforte; Natália C Medaglia; Cláudia Bincoletto; Soraya S Smaili; Regina Pessoa-Pureur

Artigo publicado na **Experimental Cell Research**

EXPERIMENTAL CELL RESEARCH ▮ (▮▮▮▮) ▮▮▮–▮▮▮

Available online at www.sciencedirect.com

ScienceDirect

journal homepage: www.elsevier.com/locate/yexcr

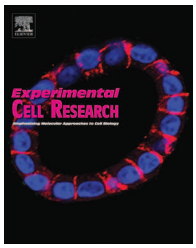

Research Article

The phosphorylation status and cytoskeletal remodeling of striatal astrocytes treated with quinolinic acid

Paula Pierozan[a], *Fernanda Ferreira*[a], *Bárbara Ortiz de Lima*[a], *Carolina Gonçalves Fernandes*[a], *Priscila Totarelli Monteforte*[b], *Natalia de Castro Medaglia*[b], *Claudia Bincoletto*[b], *Soraya Soubhi Smaili*[b], *Regina Pessoa-Pureur*[a,*]

[a]*Departamento de Bioquímica, Instituto de Ciências Básicas da Saúde, Universidade Federal do Rio Grande do Sul, Porto Alegre, RS 90035-003, Brazil*

[b]*Departamento de Farmacologia, Universidade Federal de São Paulo (UNIFESP/EPM), São Paulo, SP, Brazil*

ARTICLE INFORMATION

Article Chronology:
Received 18 September 2013
Received in revised form
10 January 2014
Accepted 19 February 2014

Keywords:
Quinolinic acid
Cytoskeleton remodelling
Astrocyte, cell signaling
GFAP phosphorylation

ABSTRACT

Quinolinic acid (QUIN) is a glutamate agonist which markedly enhances the vulnerability of neural cells to excitotoxicity. QUIN is produced from the amino acid tryptophan through the kynurenine pathway (KP). Dysregulation of this pathway is associated with neurodegenerative conditions. In this study we treated striatal astrocytes in culture with QUIN and assayed the endogenous phosphorylating system associated with glial fibrillary acidic protein (GFAP) and vimentin as well as cytoskeletal remodeling. After 24 h incubation with 100 μM QUIN, cells were exposed to ^{32}P-orthophosphate and/or protein kinase A (PKA), protein kinase dependent of Ca^{2+}/calmodulin II (PKCaMII) or protein kinase C (PKC) inhibitors, H89 (20 μM), KN93 (10 μM) and staurosporin (10 nM), respectively. Results showed that hyperphosphorylation was abrogated by PKA and PKC inhibitors but not by the PKCaMII inhibitor. The specific antagonists to ionotropic NMDA and non-NMDA (50 μM DL-AP5 and CNQX, respectively) glutamate receptors as well as to metabotropic glutamate receptor (mGLUR; 50 μM MCPG), mGLUR1 (100 μM MPEP) and mGLUR5 (10 μM 4C3HPG) prevented the hyperphosphorylation provoked by QUIN. Also, intra and extracellular Ca^{2+} quelators (1 mM EGTA; 10 μM BAPTA-AM, respectively) prevented QUIN-mediated effect, while Ca^{2+} influx through voltage-dependent Ca^{2+} channel type L (L-VDCC) (blocker: 10 μM verapamil) is not implicated in this effect. Morphological analysis showed dramatically altered actin cytoskeleton with concomitant change of morphology to fusiform and/or flattened cells with retracted cytoplasm and disruption of the GFAP meshwork, supporting misregulation of actin cytoskeleton. Both hyperphosphorylation and cytoskeletal remodeling were reversed 24 h after QUIN removal. Astrocytes are highly plastic cells and the vulnerability of astrocyte cytoskeleton may have important implications for understanding the neurotoxicity of QUIN in neurodegenerative disorders.

*Correspondence to: Universidade Federal do Rio Grande do Sul, Instituto de Ciências Básicas da Saúde, Departamento de Bioquímica, Rua Ramiro Barcelos 2600 anexo, CEP 90035-003 Porto Alegre - RS, BRASIL. Fax: +5551 3308 5535.
E-mail address: rpureur@ufrgs.br (R. Pessoa-Pureur).

http://dx.doi.org/10.1016/j.yexcr.2014.02.024
0014-4827 © 2014 Published by Elsevier Inc.

Introduction

Kynurenine pathway (KP) catabolises the essential amino acid L-tryptophan to nicotinamide adenine dinucleotide. KP also leads to the production of several neuroactive metabolites, of which the NMDA receptor agonist, quinolinic acid (QUIN) is likely to be more important in terms of biological activity [1]. Dysregulation of this pathway is associated with neurodegenerative conditions, such as Huntington's disease [2], Alzheimer's disease (AD) [3,4] and other neurological disorders, as well as with psychiatric diseases such as depression and schizophrenia [5].

QUIN is produced and released by infiltrating macrophages and activated microglia, the very cells that are prominent during neuroinflammation. QUIN acts as an agonist of the *N*-methyl-D-aspartate (NMDA) receptor and as such is considered to be a brain endogenous excitotoxin [6]. The primary mechanism exerted by QUIN in the central nervous system (CNS) has been largely related with the overactivation of NMDA receptors and increased cytosolic Ca^{2+} concentrations, followed by mitochondrial dysfunction, cytochrome *c* release, ATP exhaustion, free radical formation and oxidative damage [6,7].

In this context, Rahman et al. [8] described a NMDA-mediated role of QUIN in the AD pathology through promotion of tau phosphorylation, since QUIN in pathophysiological concentrations is co-localized with hyperphosphorylated tau within cortical neurons in AD brain. Accordingly, we have previously described QUIN-elicited hyperphosphorylation of glial fibrillary acidic protein (GFAP) in astrocytes and neurofilaments (NF) in neurons, achieved by rat intrastriatal QUIN injection. NMDA-mediated Ca^{2+} events and oxidative stress were able to be related to the altered hyperphosphorylation of these cytoskeletal proteins and could represent an early step in the pathophysiological cascade of deleterious events exerted by QUIN in rat striatum [9]. Moreover, studies of signaling mechanisms involved in the disruption of the cytoskeletal homeostasis were performed in striatal slices acutely exposed to an excitotoxic concentration of QUIN (100 μM). In astrocytes, the action of QUIN was mainly due to increased Ca^{2+} influx through NMDA and L-type voltage-dependent Ca^{2+} channels (L-VDCC). In neurons, QUIN acted through metabotropic glutamate receptor (mGluR) activation and influx of Ca^{2+} through NMDA receptors and L-VDCC, as well as Ca^{2+} release from intracellular stores. These mechanisms set off a cascade of events including activation of cAMP-dependent protein kinase (PKA), Ca^{2+}/calmodulin-dependent protein kinase (PKCaMII) and protein kinase C (PKC), which phosphorylate head domain sites on GFAP in astrocytes [10].

GFAP is the main intermediate filament (IF) protein expressed in mature astrocytes, where it is thought to help maintaining mechanical strength, and the shape of cells. However, recent evidence has shown that GFAP plays a role in a variety of additional astrocyte functions, such as cell motility/migration, cell proliferation, glutamate homeostasis, neurite outgrowth and injury/protection [11].

Because of their multiple roles into the cell, cytoskeletal protein components are among the main targets modified in response to extracellular signals that ultimately determine cell morphology and physiological role [12]. Consequently, it is not surprising that IFs are likely to be targeted in several genetically determined protein misfolding/aggregation diseases [13–15] as well as by a variety of pathogens [16] and toxins [17–20].

IF proteins are known to be phosphorylated on their head and tail domains and the dynamics of their phosphorylation/dephosphorylation plays a major role in regulating the structural organization and function of IFs in a cell- and tissue-specific manner [21]. Amino-terminal phosphorylation plays a major role in regulating the assembly/disassembly equilibrium of type III IFs (GFAP, vimentin) as well as of low and medium molecular weight NF proteins (NF-L and NF-M, respectively) [22]. In vivo and ex vivo studies from our group and from others demonstrated that the phosphate groups on the amino-terminal head domain on GFAP, vimentin and NF-L are added by the second messenger-dependent protein kinases PKA, PKCaMII and PKC [9,10,22–24]. Phosphorylation of Ser-8, Thr-7, Ser-13 and Ser-38 in the N-terminal region (head domain) of GFAP [25,26] causes disassembly of the IFs and conversely, dephosphorylation (by protein phosphatases) restores their ability to polymerize [27]. GFAP phosphorylation is possibly a key factor in astrocytes, since cell uses phosphorylation/dephosphorylation levels to regulate the dynamic of the polymerization/depolymerization of these proteins promoting cell survival and physiological roles.

Astrocytes are involved in a wide range of CNS pathologies, including trauma, [28] ischaemia [29], and neurodegeneration [30]. Alterations of the functionality of glial cells, including changes in morphology and proliferative activity, are a common feature of pathologies [31], and during brain inflammation associated with HD, astrocytes are activated leading to their cellular hypertrophy and/or proliferation [28]. Also, astrocytes in culture have been long time considered a useful model for evaluating neurotoxic-induced injury [32]. In addition, we have previously described that the cells change both their morphology and phosphorylation status of GFAP and/or vimentin, in response to metabolites or toxins [18,33].

Therefore, considering the pivotal role of cytoskeletal remodeling and the relevance of astrocyte plasticity in several pathologies that affect CNS, the aim of the present work was to study the effects of QUIN in concentrations previously described as neurotoxic to astrocytes and neurons in acute slices [9,10], on the cytoskeleton of primary astrocytes. We searched for the implications of glutamate mechanisms and Ca^{2+} levels on GFAP and vimentin phosphorylation and their link with actin cytoskeletal remodeling.

Material and methods

Phalloidin-fluorescein, anti-GFAP (clone GA-5), monoclonal anti-vimentin (clone Vim 13.2), anti-mouse IgG (whole molecule), anti-mouse IgG (whole molecule)–FITC, F(ab0)2 fragment-Cy3, quinolinic acid (QUIN), benzamidine, leupeptin, antipain, pepstatin, chymostatin, acrylamide, bis-acrylamide and material for cell culture were obtained from Sigma (St. Louis, MO, USA). Polyclonal anti-GFAP was from DAKO. 40, 60-diamidino-2-phenylindole (DAPI) was from Calbiochem (La Jolla, CA, USA). β-actin was from Cell Signaling (Boston, MA, USA). [^{32}P]-orthophosphate was purchased from CNEN, São Paulo, Brazil. Fetal bovine serum (FBS), Dulbecco's Modified Eagle's Medium (DMEM), fungizone and penicillin/streptomicin were purchased from Gibco BRL (Carslbad, CA, USA). All other chemicals were of analytical grade.

Animals

Pregnant Wistar rats (200–250 g) were obtained from our breeding stock. Rats were maintained on a 12-h light/12-h dark cycle in a constant temperature (22 °C) colony room, with food and water at libitum and animals were observed on gestational day 22.

Please cite this article as: P. Pierozan, et al., The phosphorylation status and cytoskeletal remodeling of striatal astrocytes treated with quinolinic acid, Exp Cell Res (2014), http://dx.doi.org/10.1016/j.yexcr.2014.02.024

As soon as delivery finished, mothers and pups were sacrificed by decapitation without anesthesia. The experimental protocol followed the "Principles of Laboratory Animal Care" (NHI publication 85-23, revised 1985) and was approved by the Ethics Committee for Animal Research of the Federal University of Rio Grande do Sul (number 18266). All efforts were made to minimize the number of animal used and their suffering.

Primary astrocyte cultures

Astrocyte primary cultures were prepared from the striatum of newborn (0–1 day old; P0) Wistar rats, as described previously [33]. Briefly, rats were decapitated and striatum was carefully removed. Mechanically dissociated cells were plated in Dulbecco's Modified Eagle's medium (DMEM)/10% FBS (pH 7.4) supplemented with glucose (33 mM), glutamine (2 mM), and sodium bicarbonate (3 mM) into a 15.6 and 34.8 mm diameter well (6 and 24-well plate) (Corning Inc., New York, New York), previously coated with polyornithine (1.5 mg/mL, Sigma, St. Louis, MO). These cells were grown in a humid incubator (37 °C, 5% CO_2), with the media replaced every 3 days. After astrocytes reached semi-confluence, the culture medium was removed by suction and the cells were incubated until 24 h at 37 °C in an atmosphere of 5% CO_2 in DMEM without FBS in the absence (controls) or presence of different QUIN concentrations (300 nM – 1 mM). Cultures of striatal astrocytes containing more than 95% GFAP positive cells were used for all the experiments. Morphological studies were performed using cells fixed for immunocytochemistry.

Cell viability

Cells were seeded at a density of 2×10^4 cells/well in 96-well plates. They were treated with 300 nM – 1 mM QUIN for 24 h with 3 replicates of each treatment. Cell viability was measured by the 3-(4,5 dimethyl-2-yl)-2, 5-diphenyl-2 H-tetrazolium bromide (MTT) and lactate dehydrogenase (LDH) assays, as described below.

MTT assay

Astrocyte viability was determined by MTT assay, which is based on the conversion of the tetrazolium salt to the colored product, formazan. In brief, 0.5 mg/mL of MTT was added into each well of the 96-well plates (containing 100 mL medium and cells) 4 h before the end of incubation with QUIN. The supernatant was then separated, and 100 μL dimethylsulfoxide (DMSO) was added to each well followed by incubation and shaking for 10 min. The formazan product generated during the incubation was solubilized in DMSO and measured at 490 and 630 nm. Only viable cells are able to reduce MTT.

LDH assay

The viability of astrocytes was assessed by measuring the release of the cytosolic enzyme lactate dehydrogenase into the medium. A LDH measurement was carried out in 250 μL aliquots using the LDH kit (Doles reagents).

In vitro phosphorylation

Astrocytes were incubated for 24 h in the presence or absence of QUIN, then the medium was changed and incubation for 1 h was carried out at 30 °C with 1000 μL of a medium containing (in mM): 124 NaCl; 4 KCl; 1.2 $MgSO_4$, 25 Na-HEPES (pH 7.4); 12 glucose; 1 $CaCl_2$ and the following protease inhibitors: 1 mM benzamidine, 0.1 μM leupeptin, 0.7 μM antipain, 0.7 μM pepstatin, 0.7 μM chymostatin, and 10 μCi of [^{32}P]- orthophosphate with or without addition of the QUIN (10, 100 and 500 μM). In the experiments designed to study signaling mechanisms, cells were pre-incubated for 30 min in the presence or absence of 50 μM DL-AP5, MCPG and CNQX [33], 100 μM 4C3HPG [34], 10 μM MPEP [35], 10 μM verapamil [36],10 μM BAPTA-AM [37], 1 mM EGTA [38], 20 μM H89 [39], 10 nM staurosporin [40], 10 μM KN93 [41], 10 μm SP600125 [42], 10 μM PD98056, 3 μM p38 inhibitor [43] and 10 μM roscovitine [44]. In the experiments designed to study the reversibility of QUIN effects, the metabolite was removed after 24 h of treatment and cells were observed 48 h afterwards. The labeling reaction was normally allowed to proceed for 1 h at 30 °C and stopped with 1 mL of cold stop buffer (150 mM NaF, 5 mM EDTA, 5 mM EGTA, Tris–HCl, 50 mM, pH 6.5, and the protease inhibitors described above). Cells were then washed twice by decantation with stop buffer to remove excess radioactivity. After, preparations of IF-enriched high-salt Triton-insoluble cytoskeletal fraction were obtained from striatal primary astrocytes, as described by Funchal et al. [45]. Briefly, cells were homogenized in 200 μL of ice-cold high salt buffer containing 5 mM KH_2PO_4 (pH 7.1), 600 mM KCl, 10 mM $MgCl_2$, 2 mM EGTA, 1% Triton X-100, and the protease inhibitors described above. The homogenate was centrifuged at 15,800 × *g* for 10 min at 4 °C in an Eppendorf centrifuge and the supernatant discarded. The Triton-insoluble IF-enriched pellet, containing GFAP and vimentin, was dissolved in 1% SDS and protein concentration was determined by the method of Lowry et al. [46].

Polyacrylamide gel electrophoresis (SDS-PAGE)

The cytoskeletal fraction from striatal astrocytes was prepared as described above. Equal protein concentrations were loaded onto 7.5% polyacrylamide gels and analyzed by SDS-PAGE according to the discontinuous system of Laemmli [47]. After drying, gels were exposed to X-ray films (X-Omat XK1) at -70 °C with intensifying screens and finally the autoradiograph was obtained. Proteins were quantified by scanning the films with a Hewlett-Packard Scanjet 6100C scanner and determining optical densities with an Optiquant version 02.00 software (Packard Instrument Company). Density values were obtained for the studied proteins.

Ca^{2+} measurements

For Ca^{2+} measurements, cells adhered to poly-lysine coated coverslips were incubated with 5 μM acetoxymethyl ester of Fura-2 (Fura-2AM) in a buffer containing: 130 mM NaCl; 5.36 mM KCl; 0.8 mM $MgCl_2$; 1.5 mM $CaCl_2$; 1.0 mM Na_2HPO_4; 2.5 mM $NaHCO_3$; 25 mM glucose, and 20 mM Hepes, pH 7.3 for 30 min at room temperature. After loading, cover slips were washed, mounted in a Leiden chamber and positioned at the microscope and cells were maintained to a temperature of 37 °C. Cytoplasmic Ca^{2+} measurements were evaluated by fluorescence

Please cite this article as: P. Pierozan, et al., The phosphorylation status and cytoskeletal remodeling of striatal astrocytes treated with quinolinic acid, Exp Cell Res (2014), http://dx.doi.org/10.1016/j.yexcr.2014.02.024

microscopy (Nikon TE300; Nikon, Osaka, Japan) coupled to a CCD camera (Quantix 512-Roper Scientific Inc., Princeton Instruments, Princeton, NJ). Images were acquired in BioIP software (Anderson Eng, Delaware, USA). Basal Ca^{2+} levels were considered to be the first 20 images, and then exposed to QUIN (100 μM) for 30 min. Fura-2 fluorescence (emission = 510 nm) was monitored following alternate excitation at 340 and 380 nm. Results were expressed as ratio (340/380) values, normalized from the basal fluorescence and data were normalized by the $(F-F_0)/F_0 \times 100$ formula, in which F_0 represents the basal Ca^{2+} level. Calibrations were performed using digitonin (100 μM) to obtain maximum fluorescence (R_{max}) of the system. For experiments using the antagonists, cells were incubated with DL-AP5 (50 μM), CNQX (50 μM) and BAPTA-AM (10 μM) 30 min after FURA 2/AM and QUIN incubation.

Western blot analysis

After treatment, astrocytes were disrupted by lysis solution containing 2 mM EDTA, 50 mM Tris–HCl, pH 6.8, 4% SDS. For electrophoretic analysis, samples were dissolved in 25% (v/v) of a solution containing 40% glycerol, 5% mercaptoethanol, 50 mM Tris–HCl, pH 6.8, and boiled for 3 min. Total protein homogenate was analyzed by 10% SDS-PAGE (50 mg of total protein/lane) and transferred (Trans-blot SD semidry transfer cell, BioRad) to nitrocellulose membranes for 1 h at 15 V in transfer buffer (48 mM Trizma, 39 mM glycine, 20% methanol, and 0.25% SDS). The blot was then washed for 20 min in TBS (500 mM NaCl, 20 mM Trizma, pH 7.5), followed by 2 h incubation in blocking solution (TBS plus 5% defatted dry milk). After incubation, the blot was washed twice for 5 min with blocking solution plus 0.05% Tween-20 (T-TBS) and then incubated overnight at 4 °C in blocking solution containing one of the following monoclonal antibodies: anti-GFAP (clone G-A-5) diluted 1:1000, anti-β-actin diluted 1:500, anti-vimentin diluted 1:1000. The blot was then washed twice for 5 min with T-TBS and incubated for 2 h in a solution containing peroxidase-conjugated rabbit anti-mouse IgG diluted 1:2000 or peroxidase-conjugated anti-rabbit IgG diluted 1:2000. The blot was washed again twice with T-TBS for 5 min and twice with TBS for 5 min. The blot was developed using a chemiluminescence ECL kit.

Immunocytochemistry

Immunocytochemistry was performed as described previously [33]. Briefly, cultured cells plated on glass coverslips were fixed with 4% paraformaldehyde for 30 min and permeabilized with 0.1% Triton X-100 in phosphate-buffered saline (PBS) for 5 min at room temperature. After blocking, cells were incubated overnight with polyclonal anti-GFAP (1:500) and phaloidin-fluorescein (1:100) at room temperature, followed by PBS washes and incubation with specific secondary antibody conjugated with Cy3 (1:1000) for 1 h. In all immunostaining-negative controls, reactions were performed by omitting the primary antibody. No reactivity was observed when the primary antibody was excluded. The nucleus was stained with DAPI (0.25 μg/mL). Cells were viewed with a Nikon inverted microscope and images transferred to a computer with a digital camera (Sound Vision Inc, USA).

Morphometric analysis

Astrocytes stained for actin cytoskeleton and nucleus were measured using the labeling for phalloidin-fluorescein and DAPI, respectively. Measurement of cytoplasm and nucleus were obtained using the Image J Software (NIH, Bethesda, MD). Cytoplasmic area (total area–nuclear area) and cytoplasm/nucleus ratio of the cells were used as a criterion of morphological alteration.

Statistical analysis

Data from the experiments were analyzed statistically by one-way analysis of variance (ANOVA) followed by the Tukey test when the *F*-test was significant. Values of $p < 0.05$ were considered to be significant. All analyses were carried out in an IBM compatible PC using the Statistical Package for Social Sciences (SPSS) software.

Results

Initially, astrocyte viability was tested to certify that 24 h exposure to QUIN was not able to induce significantly important cell death. For this, LDH and MTT assays were carried out in the presence of QUIN from 300 nM to 1 mM, and results showed absence of significantly increased release of the cytosolic enzyme LDH in the medium or decreased production of reduced MTT in all the concentrations tested (Fig. 1). These results indicate that QUIN exposure for 24 h failed to induce necrotic cell death or mitochondrial damage in cultured striatal astrocytes.

We therefore assayed the ability of QUIN in misregulating the endogenous phosphorylating system associated with the IF proteins in the cytoskeletal fraction of striatal astrocytes. The in vitro incorporation of ^{32}P orthophosphate into the cytoskeletal proteins GFAP and vimentin was measured and results showed that 24 h incubation

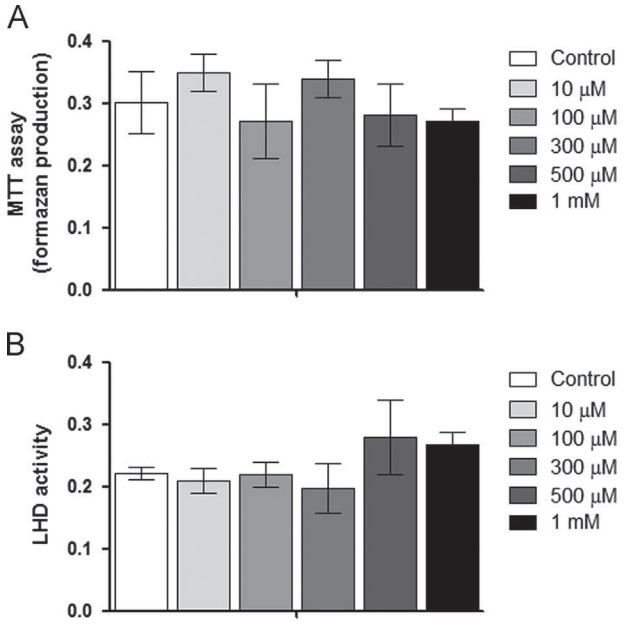

Fig. 1 – Effect of quinolinic acid (QUIN) on the viability of striatal astrocytes in culture. Cells were treated with QUIN at different concentrations (10 μM–1 M) for 24 h. (A) Viability assay performed by the colorimetric MTT method. (B) The viability was assessed by measuring the released cytosolic enzyme lactate dehydrogenase (LDH) into the medium. Three independent experiments were performed in triplicate. Data were statistically analyzed by one-way ANOVA.

Please cite this article as: P. Pierozan, et al., The phosphorylation status and cytoskeletal remodeling of striatal astrocytes treated with quinolinic acid, Exp Cell Res (2014), http://dx.doi.org/10.1016/j.yexcr.2014.02.024

with 10 μM QUIN failed to alter the IF phosphorylation level, while 100 and 500 μM QUIN induced hyperphosphorylation of these cytoskeletal proteins (Fig. 2A and B). GFAP and vimentin are known to be good substrates for second messenger-dependent protein kinases [10,48], therefore we used specific kinase inhibitors to assess the serine/threonine kinases involved in the QUIN-mediated hyperphosphorylation of these proteins. After 24 h incubation with 100 μM QUIN, cells were exposed to ^{32}P-orthophosphate and/or protein kinase A (PKA), protein kinase dependent of Ca^{2+}/calmodulin II (PKCaMII) or protein kinase C (PKC) inhibitors H89 (20 μM), KN93 (10 μM) and staurosporina (10 nM), respectively. Results showed that hyperphosphorylation was abrogated by PKA and PKC inhibitors but not by the PKCaMII inhibitor (Fig. 3).

To search for the role of glutamate receptors on QUIN-induced IF hyperphosphorylation we used ionotropic NMDA and non-NMDA (50 μM DL-AP5 and CNQX, respectively), as well as metabotropic (50 μM MCPG) glutamate antagonists. Metabotropic glutamate receptor 1(mGLUR1; 100 μM MPEP) and mGLUR5 (10 μM 4C3HPG) specific antagonists were also tested. Results showed that the ionotropic NMDA and non-NMDA glutamate receptors as well as metabotropic glutamate receptors prevented the hyperphosphorylation provoked by QUIN. Moreover, the mGLUR1 and mGLUR5 are partially involved in this effect, as depicted in Fig. 4A.

Using intra and extracellular Ca^{2+} quelators (1 mM EGTA; 10 μM BAPTA-AM, respectively) and a voltage-dependent Ca^{2+} channel type L (L-VDCC) blocker (10 μM verapamil), we showed that intra and extracellular Ca^{2+} buffering prevented QUIN-mediated effect, moreover Ca^{2+} influx through L-VDCC is not implicated in QUIN action (Fig. 4B).

To further demonstrate the role of Ca^{2+} in the QUIN actions, we evaluated the cytosolic Ca^{2+} levels in different experimental conditions in astrocytes loaded with Fura-2AM. Results showed that QUIN (100 μM) exposure induced significantly increased cytosolic Ca^{2+} levels, represented by an elevation in fluorescence ratio (340/380) in cells (Fig. 5A). By using DL-AP5 and CNQX we evaluate the participation of NMDA and AMPA/Kainate receptors, respectively, in QUIN-induced Ca^{2+} levels alterations. Results showed that the presence of the glutamatergic antagonists prevented QUIN-induced cytosolic Ca^{2+} increase. Also, BAPTA-AM was capable to prevent the increased cytosolic Ca^{2+} levels induced by QUIN (Fig. 5A). Fig. 5B demonstrates the profile of cytosolic Ca^{2+} alterations caused by QUIN, which evoked a gradual increase in the Ca^{2+} concentrations.

Interestingly, we showed that QUIN-mediated GFAP and vimentin hyperphosphorylation is a reversible mechanism, since when the metabolite is removed from the incubation medium after 24 h of treatment, hyperphosphorylation observed 48 h afterwards is totally reversed, recovering control values (Fig. 6).

Next, we evaluated the effect of QUIN on the morphology of striatal astrocytes in culture, as depicted in Fig. 7. To analyze the organization of actin filaments cells were incubated for 24 h with 10, 100 or 500 μM QUIN and actin/phalloidin-FITC was analyzed by fluorescent microscopy afterwards. Results showed that untreated

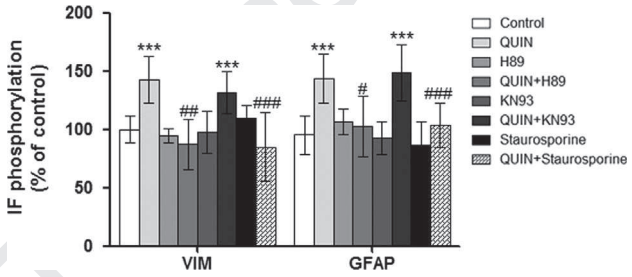

Fig. 3 – Involvement of protein kinases on QUIN-induced IF in vitro hyperphosphorylation. Cells were exposed to 100 μM QUIN and the participation of second messenger-dependent protein kinases PKA, PKCaMII and PKC was tested by using the specific inhibitors H89 (20 μM), KN93(10 μM) and staurosporine (10 nM), respectively. Data are reported as means ± S.D. of four different experiments and expressed as % of control. Statistically significant differences from controls, as determined by one-way ANOVA followed by Tukey–Kramer multiple comparison test are indicated: ***$p<0.001$ compared with control group; ###$p<0.001$, ##$p<0.01$ and #$p<0.05$ compared with QUIN group.

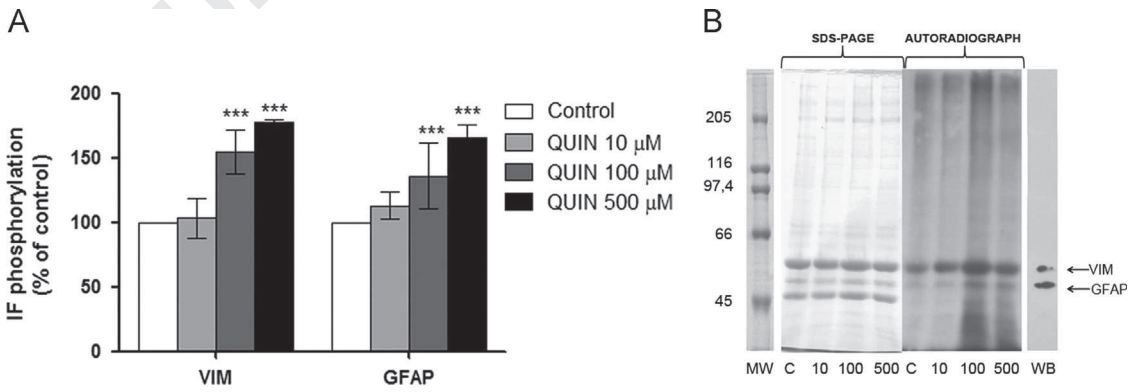

Fig. 2 – Effect of QUIN on the phosphorylation of GFAP and vimentin in the cytoskeletal fraction from striatal astrocytes in culture. (A) Data are reported as mean ± S.D. of four different experiments and expressed as percent of controls. Statistically significant differences from controls, as determined by one-way ANOVA followed by Tukey–Kramer multiple comparison test are indicated: ***$p<0.001$compared with control. (B) Coomassie blue stained molecular weight standards and representative stained gel of a control and treated samples with corresponding autoradiograph. Equal amounts of the cytoskeletal fraction (50 μg) from control (C) and treated samples were run in 7.5% polyacrylamide gel electrophoresis (SDS-PAGE). MW: molecular weight standard proteins. Representative Western blot (WB) with anti-vimentin and anti-GFAP antibodies.

Please cite this article as: P. Pierozan, et al., The phosphorylation status and cytoskeletal remodeling of striatal astrocytes treated with quinolinic acid, Exp Cell Res (2014), http://dx.doi.org/10.1016/j.yexcr.2014.02.024

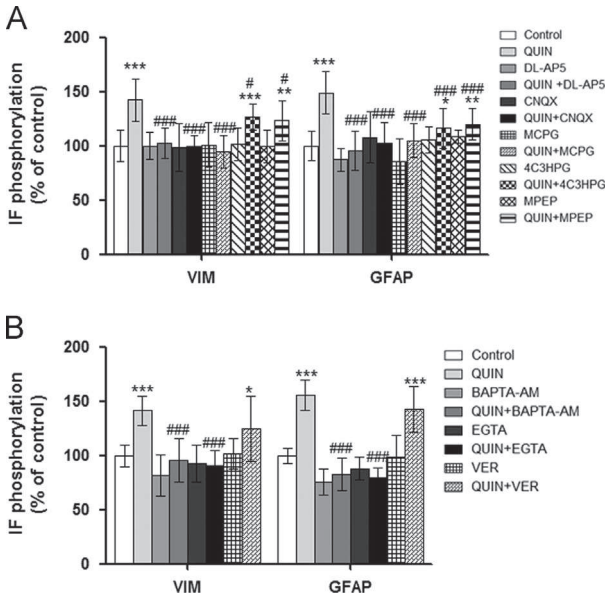

Fig. 4 – Involvement of glutamate receptors, intra and extracellular Ca^{2+} on QUIN-induced IF hyperphosphorylation in striatal astrocytes in culture. Cells were exposed to 100 μM QUIN and/or the glutamate receptor blockers (A): DL-AP5 (50 μM), CNQX (50 μM) and MCPG (50 μM), MPEP (100 μM) and 4C3HPG (10 μM). (B) Intra and extracellular Ca^{2+} were buffered with BAPTA-AM (50 μM) and EGTA (1 mM) respectively; L-VDCC blocker verapamil (30 μM). Data are reported as means ± S.D. of four different experiments and expressed as percent of control. Statistically significant differences as determined by one-way ANOVA followed by Tukey–Kramer multiple comparision test are indicated: $^{***}p<0.001$; $^{**}p<0.01$, $^{*}p<0.05$ compared with control. $\#\#\#p<0.001$ and $\#p<0.05$ compared with QUIN group.

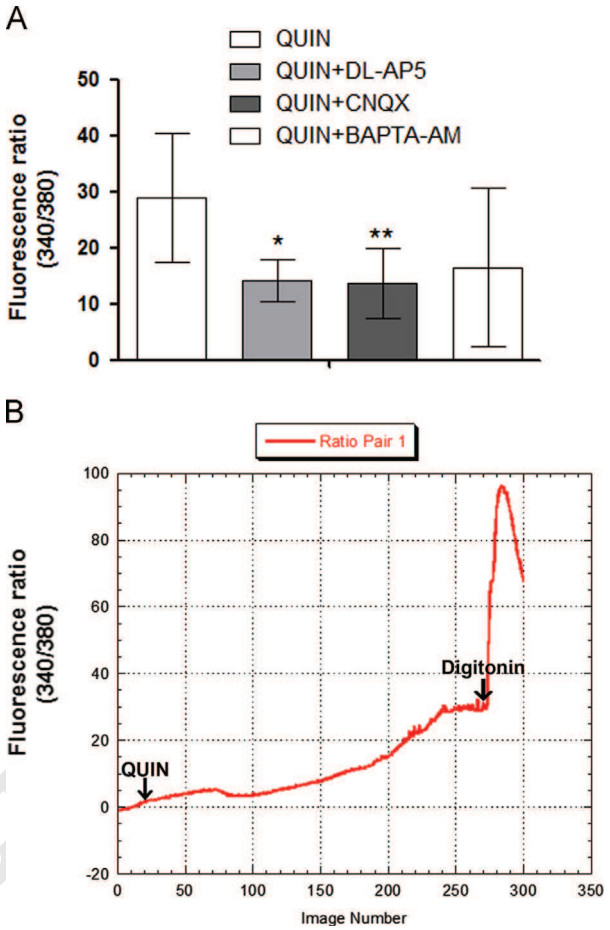

Fig. 5 – Ca^{2+} influx promoted by QUIN in rat striatal astrocytes. Astrocytes were loaded with Fura-2AM (5 μM) and stimulated with QUIN (100 μM) in the absence or presence of DL-AP5 (50 μM), CNQX (50 μM) AND BAPTA-AM (10 μM). (A) Histogram represents the cytosolic Ca^{2+} peaks obtained after the addition of QUIN in the presence or absence of glutamate antagonists or BAPTA-AM. Experiments were individually calibrated with the addition of digitonin (100 μM) at the end of the experiments and data are expressed as a percentage of the baseline normalized fluorescence. Data presented as mean ± S.D. of three independent experiments measuring 20–25 individual cells/experiment. (B) Representative trace of the effect evoked by QUIN. Statistically significant differences, determined by one-way ANOVA followed by Tukey–Kramer multiple comparison test are indicated: $^{**}p<0.01$, $^{*}p<0.05$.

cells presented a flat polygonal morphology and that actin filaments were largely distributed into well-organized actin stress fibers, a predominant characteristic of cultured astrocytes. Few stellate cells were observed in our control cultures. After 24 h exposure, the QUIN-treated cells presented a dramatic morphological alteration evidenced by a dose-dependent reorganization of actin stress fibers (Fig. 7A). Disruption of actin meshwork seems to be associated with cell spreading, as determined by cytoplasm/nucleus ratio, reflected by the appearance of fusiform and/or flattened cells with retracted cytoplasm (Fig. 7B and C). Immunocytochemical analysis using Cy3-labeled anti-GFAP antibody showed a typical IF array extending across the cytoplasm in control cells and this IF network was also progressively disrupted in the presence of the increasing QUIN concentrations (Fig. 7A). Immunoblotting assay with anti-GFAP, anti-vimentin and anti-actin monoclonal antibodies showed that 24 h exposure to 100 μM QUIN was not able to alter the level of these proteins into the astrocytes (Fig. 7D), suggesting the disruption of the cytoskeleton on the basis of the plastic alteration induced by QUIN treatment.

This was further supported by reversion experiments, in which QUIN was removed from the incubation medium after 24 h. Interestingly,48 h after QUIN removing, both actin and GFAP meshworks restored their control organization and cells restored the flattened and circular morphology (Fig. 7A).

Discussion

We have previously demonstrated QUIN-induced hyperphosphorylation of IF proteins in astrocytes and neurons of intrastriatally injected rats [9] and in acute striatal slices [10]. In the present study we incubated striatal astrocytes in culture with the same QUIN concentration that was able to cause hyperphosphorylation in striatal slices (100 μM) and we searched for the link between hyperphosphorylation of IF proteins, cytoskeletal remodeling and signaling mechanisms downstream of QUIN exposure. We found that QUIN affected the endogenous phosphorylation system associated with the IF enriched cytoskeletal fraction in these

Please cite this article as: P. Pierozan, et al., The phosphorylation status and cytoskeletal remodeling of striatal astrocytes treated with quinolinic acid, Exp Cell Res (2014), http://dx.doi.org/10.1016/j.yexcr.2014.02.024

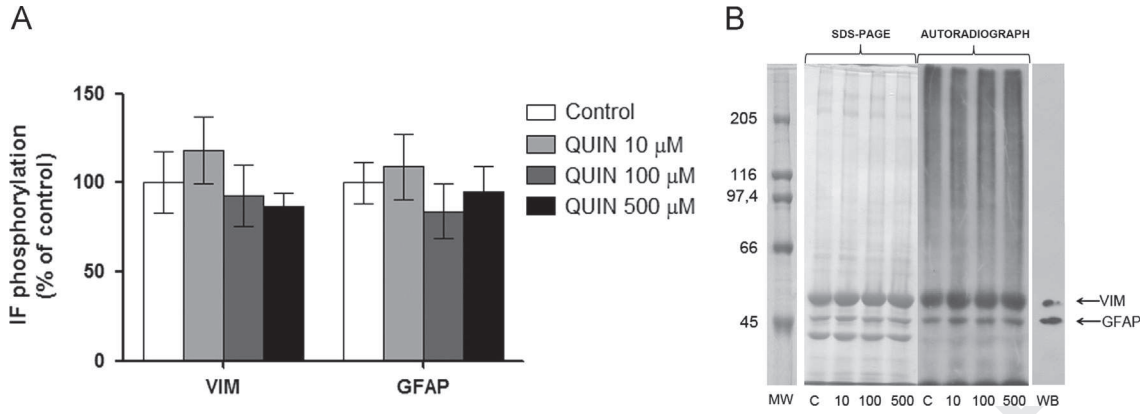

Fig. 6 – Phosphorylation level of GFAP and vimentin 24 h after QUIN removal from astrocyte cultures. In experiments designed to study reversion of QUIN effects, cells were treated for 24 h with 100 μM QUIN, the metabolite was removed and ^{32}P incorporation was measured 24 h afterwards. Data are reported as means ± S.D. of four different experiments and expressed as percent of control. Statistically significant differences as determined by one-way ANOVA.

cultured cells. Concomitant with hyperphosphorylation of GFAP/vimentin, we evidenced an altered organization of actin and GFAP networks in cells treated with QUIN for 24 h. Also, 24 h after removing QUIN from the primary astrocytes, the phosphorylation level of IF proteins restored control levels, indicating the reversibility of the effect. Moreover, reorganization of actin and GFAP filaments was totally reversed to a similar picture of the control conditions and cells restored their original morphology if QUIN was removed. Therefore, we could propose that, in QUIN-treated striatal astrocytes, disruption of the phosphorylation status of GFAP/vimentin was able to mediate reorganization of the cytoskeletal meshwork altering cell plasticity. This effect is downstream of glutamate signaling and high Ca^{2+} levels, activating PKA and PKC, which, together with actin remodeling, are responsible for disrupting the astrocyte cytoskeleton. Thus, it is possible that in QUIN treated astrocytes, glutamate signaling mediated the reorganization of actin cytoskeleton concomitant with GFAP/vimentin network in response to activation of phosphorylating signals.

It is important to note that QUIN-treated astrocytes failed to death and to present mitochondrial damage. This is in line with the role of cytoskeletal flexibility in the survival of cells exposed to a deleterious signal. Previous evidence supports that increased turnover of filamentous actin can promote cell longevity, whereas decreased turnover seems to trigger cell death through an apoptosis-like pathway [49]. These findings are in agreement with the previously reported effects of homocysteine on cortical astrocytes in culture which was able to induce GFAP/vimentin hyperphosphorylation and cytoskeletal remodeling without cell death [33]. Interestingly, our results on QUIN toxicity in striatal astrocytes from newborn rats are conflicting with previous studies using foetal human astrocytes. In this context, QUIN in concentrations of 50 nM is able to provoke apoptotic death of foetal human astrocytes in culture [50]. Also, Braidy et al. [51] showed increased LDH activity in human foetal astrocytes in culture exposed to 1–1000 μM QUIN for 24 h. The mechanism for QUIN toxicity in human astrocytes was ascribed to involve NMDA receptor activation and NO• production [52]. Although, further studies will be necessary to clarify our present findings, it must be also considered the role of mGLUR1 and 5 in the toxicity of QUIN in rat astrocytes. This is supported by the evidence that activation of mGLUR1 and 5 protects cortical astrocytes from ischemia-induced impairment [53].

QUIN is known as a classic NMDA agonist [5,54] and chemical preconditioning models using NMDA pre-treatment, have been demonstrated to lead to neuroprotection against seizures and damage to neuronal tissue induced by QUIN [55]. The existence of functional NMDA receptor expression in cultured astrocytes was first demonstrated by Lee et al. [56] who demonstrated that human foetal astrocytes were responsive to excitotoxic concentrations of glutamate and QUIN. The role of Ca^{2+} influx through NMDA receptors we observed in QUIN-treated astrocytes is, at least in part, compatible with the excitotoxic effect of QUIN and with the high Ca^{2+} levels required for the action of QUIN on the IF proteins, as demonstrated by buffering intra and extracellular Ca^{2+}. The close connection between QUIN action and cytosolic Ca^{2+} levels was demonstrated by loading astrocytes with Fura-2AM, proposing that the increase in cytosolic Ca^{2+} through NMDA receptors is an early and critical event upstream of signaling mechanisms targeting the cytoskeleton.

Interestingly, despite of the relevance of high Ca^{2+} levels to the action of QUIN on the cytoskeleton, GFAP/vimentin hyperphosphorylation was not mediated by CaMKII in primary astrocytes, differently from the ex-vivo system. These findings claim to the relevance of the interplay between astrocytes and neurons, since in acute slices Ca^{2+} influx induced by 100 μM QUIN was mediated by both NMDA and L-VDCC, activating CaMKII in astrocytes [10].

Otherwise, PKA-mediated GFAP/vimentin hyperphosphorylation in cultured astrocytes could be downstream of Ca^{2+}-dependent mechanisms, since the neural isoforms of adenylyl cyclase are activated by Ca^{2+}, supporting the PKA activation by high Ca^{2+} levels [57]. Moreover, glutamate neurotransmission has been long time recognized as an essential component of many forms of neuronal plasticity and PKA-mediated mechanisms have been implicated in those actions [58]. PKA catalytic and regulatory (RIIβ) subunits are members of the NMDA receptor complex [59]. This linkage facilitates phosphorylation-dependent modulation of NMDA receptor activity in agreement with findings that activation of PKA enhances NMDA receptor currents [60]. It is also possible that PKA is mediating QUIN-induced effects on GFAP/vimentin

Please cite this article as: P. Pierozan, et al., The phosphorylation status and cytoskeletal remodeling of striatal astrocytes treated with quinolinic acid, Exp Cell Res (2014), http://dx.doi.org/10.1016/j.yexcr.2014.02.024

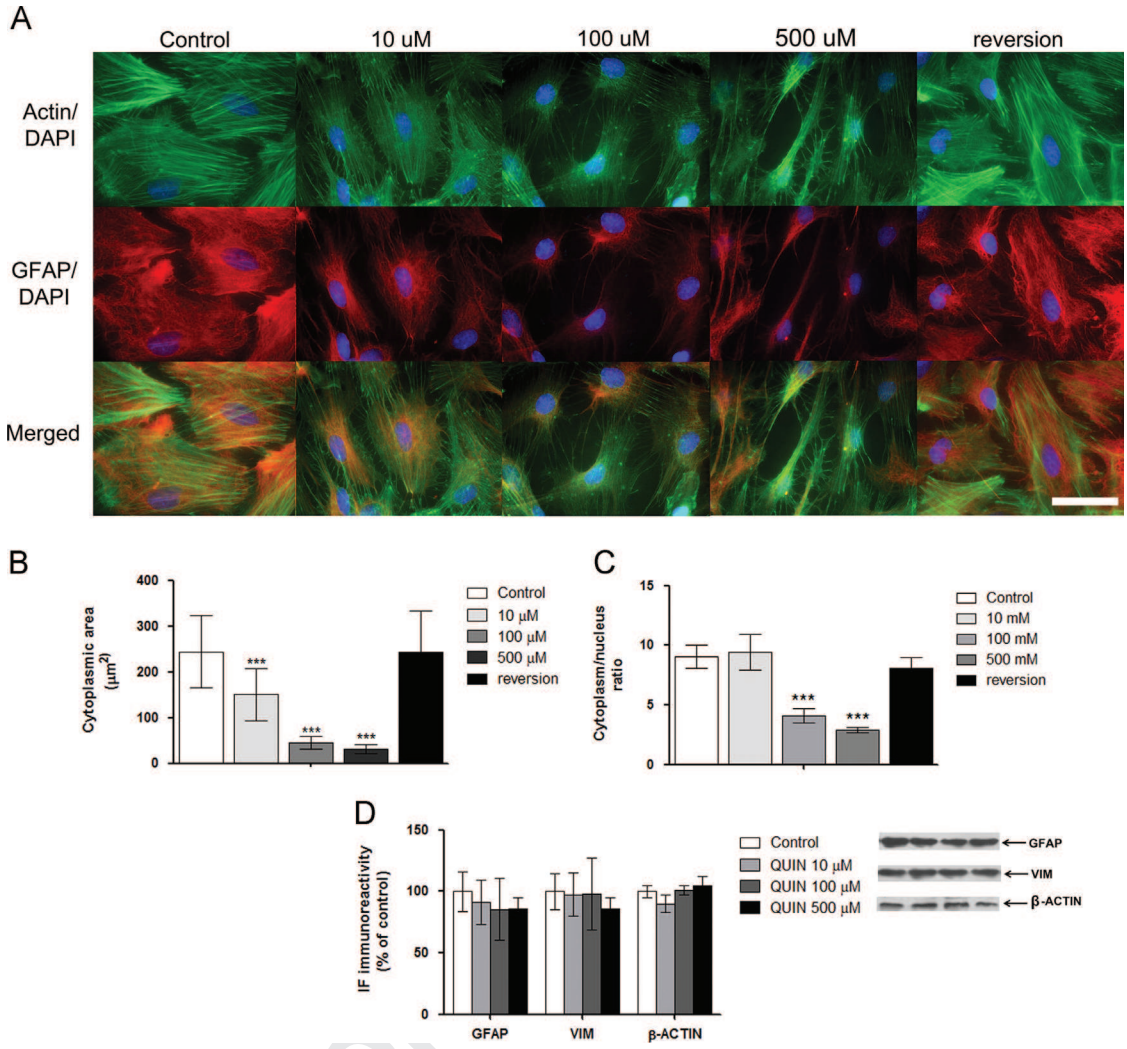

Fig. 7 – Actin and GFAP co-staining of striatal astrocytes exposed to QUIN. Cells were cultured to semi-confluence in DMEM/F12 10% fetal bovine serum (FBS). The medium was then changed to DMEM/F12 0% FBS in the presence or absence of 10, 100 and 500 μM QUIN for 24 h. (A) Representative images of QUIN-treated cells stained with phalloidin-fluorescein, anti-GFAP antibody and DAPI. GFAP disruption concomitant with actin reorganization was shown in the presence of increasing concentrations of QUIN. Representative images of QUIN treated cells co-stained for actin and GFAP, observed 24 h after QUIN removal, showing the reversion of the QUIN effect. Scale bar = 50 μm. (B) and (C) Morphometric analysis from control and treated astrocytes with the Image J Software: (B) cytoplasm area; (C) the cells were analyzed using the ratio between the size of cytoplasm and nucleus. (D) Western blot analysis of actin, vimentin and GFAP content in cell extract. All lanes received equivalent amount (30 μg) of total protein. Immunoblotting was carried out with monoclonal anti-β-actin, anti-vimentin and antiGFAP antibodies diluted 1:500. Data are reported as means ± S.D. of four different experiments expressed as percentage of controls.

hyperphosphorylation through cAMP, since certain forms of adenylyl cyclases in the brain are regulated by Ca^{2+} [61]. Therefore an increase in cellular Ca^{2+} levels resulting from increased entry of Ca^{2+} into the cell via NMDA receptor channels in response to QUIN would be expected to activate these enzymes.

Metabotropic glutamate receptors can also be coupled to the activation of phospholipase C (PLC) via Gaq/11 resulting in the cleavage of phosphatidylinositol-4,5-bisphosphate with the ensuing formation of the intracellular second messengers, inositol-1,4,5-trisphosphate (IP3), and diacylglycerol (DAG), which are known to activate PKC [62]. Otherwise, mGLUR1 and mGLUR5 are able to activate AMPA receptors through PKA-mediated phosphorylation of their GluA1 subunit [63], and this could be on the basis of the participation of AMPA glutamate receptors in the action of QUIN on the cytoskeleton of astrocytes. Moreover, activation of AMPA receptors could increase Ca^{2+} influx through NMDA receptors, since a strong depolarization induced by AMPA receptors expels the Mg^{2+} block and activates NMDA receptors [64]. This could explain our results showing that CNQX prevented increased cytosolic Ca^{2+} levels induced by QUIN.

A schematic representation of the molecular mechanisms proposed to lead to QUIN-elicited cytoskeletal hyperphosphorylation in striatal astrocytes is depicted in Fig. 8.

Moreover, it is possible that QUIN-induced signaling mechanisms provoking aberrant IF phosphorylation could also underlie the disrupted homeostasis of the actin cytoskeleton in the

Please cite this article as: P. Pierozan, et al., The phosphorylation status and cytoskeletal remodeling of striatal astrocytes treated with quinolinic acid, Exp Cell Res (2014), http://dx.doi.org/10.1016/j.yexcr.2014.02.024

cultures astrocytes. This is supported by the evidence that actin reorganization is controlled by associated proteins downstream of signaling phosphorylation cascades. In this context, fluctuations in intracellular Ca^{2+} [65] as well as cAMP/PKA [66–68] have the capacity to modulate actin cytoskeleton through inactivation of LIM kinase, the main kinase phosphorylating/inactivating the actin-binding protein cofilin.

Typically astrocytes respond to an injury undergoing hypertrophy, upregulating nestin, vimentin, and GFAP, and activating cell proliferation [69,70]. Although QUIN failed to induce overexpression of vimentin and GFAP within 24 h exposure, we could presume that altogether these responses represent an initial step in a program of reactive astrogliosis, provided that it is increasingly clear that the modalities and dynamics of the astrocyte response to damage are dependent on the degree of neurological damage [71].

The actions of QUIN on the cytoskeleton could represent a damage to the astrocyte, since GFAP/vimentin hyperphosphorylation inhibits filament assembly, induces disassembly [72,73] and disrupts the cytoskeletal array with consequences on cell plasticity and function. In line with this, QUIN is implicated in the reorganization of the filament meshwork and altered cell morphology since we observed total reversion of hyperphosphorylation, cytoskeletal remodeling and cell plasticity after QUIN removal.

Taking into account that the rearrangement of the cytoskeleton in response to an insult could modulate integrin signaling, reorganizing the extracellular matrix and favoring neuronal proliferation [74], we can presume a role for astrocytes in determining the vulnerability of neurons to the deleterious QUIN stimulus, however further experiments will be necessary to clarify these findings.

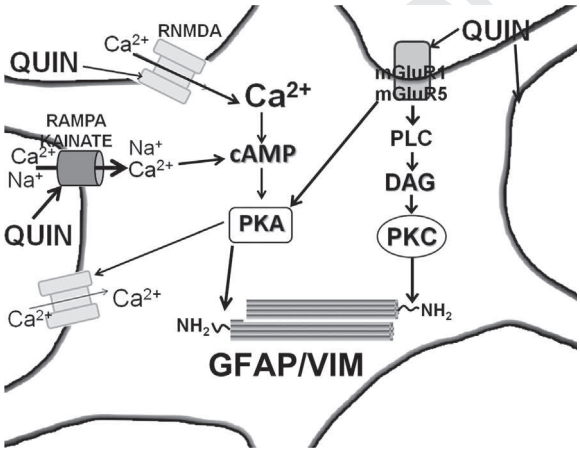

Fig. 8 – Proposed mechanism by which QUIN activates IF phosphorylation in cultured striatum astrocytes. The effects of QUIN are initiated by NMDA, AMPA/kainite and mGluR activation. Ca^{2+} influx through NMDA receptors leads to an overload of Ca^{2+} within the cell, which set off a cascade of events including activation of PKA and PKC, which phosphorylate head domain sites on GFAP and vimentin. mGluR1and 5 are upstream of PLC and DAG which activate PKC. Also, mGLUR1 and 5 could further activate PKA, which, in turn phosphorylate and activate AMPA and NMDA receptors, contributing to the enhanced Ca^{2+} influx.

Conclusion

Taken together, our present findings indicate that 100 μM QUIN elicits signaling mechanisms downstream of glutamate receptors and Ca^{2+} levels, which activate PKA and PKC, causing hyperphosphorylation of head domain sites on GFAP and vimentin of striatal astrocytes. Otherwise, we can propose that misregulation of the phosphorylation system associated with IF in QUIN-treated astrocytes could be also implicated in remodeling the actin cytoskeleton since actin reorganization is controlled by associated proteins downstream of signaling phosphorylation cascades. Therefore, we could hypothesize that disruption of the cytoskeleton could be one of the mechanisms implicated in the toxicity of QUIN in astrocytes. Astrocytes are known to be highly plastic cells and their dynamic morphological changes could affect the intercellular communication with surrounding synapses which could be important mechanisms underlying brain lesions [75]. Considering that astrocytes are polyvalent cells that are implicated in almost all processes that occur in the CNS, the vulnerability of astrocyte cytoskeleton may have important implications for understanding the effects of QUIN in the neurotoxicity linked to neurodegenerative disorders [76]. Therefore, further studies will be necessary to clarify the implications of the aberrant cytoskeletal organization in the striatal astrocytes exposed to QUIN on the vulnerability of neurons to the insult.

Acknowledgments

This work was supported by grants of the Conselho Nacional de Desenvolvimento Científico e Tecnológico (CNPq), Fundação de Amparo à Pesquisa do Estado do Rio Grande do Sul (FAPERGS) and Pro-Reitoria de Pesquisa de Pós Graduação of the Universidade Federal do Rio Grande do Sul (Propesq-UFRGS).

REFERENCES

[1] M.P. Heyes, Quinolinic acid and inflammation, Ann. N. Y. Acad. Sci. 679 (1993) 211–216.
[2] P. Guidetti, R.E. Luthi-Carter, S.J. Augood, R. Schwarcz, Neostriatal and cortical quinolinate levels are increased in early grade Huntington's disease, Neurobiol. Dis. 17 (2004) 455–461.
[3] H. Baran, K. Jellinger, L. Deecke, Kynurenine metabolism in Alzheimer's disease, J. Neural Transm. 106 (1999) 165–181.
[4] B. Widner, F. Leblhuber, J. Walli, G.P. Tilz, U. Demel, D. Fuchs, Tryptophan degradation and immune activation in Alzheimer's disease, J. Neural Transm. 107 (2000) 343–353.
[5] T.W. Stone, Neuropharmacology of quinolinic and kynurenic acids, Pharmacol. Rev. 45 (1993) 309–379.
[6] G.J. Guillemin, Quinolinic acid, the inescapable neurotoxin, FEBS J. 279 (2012) 1356–1365.
[7] V. Perez-De La Cruz, P. Carrillo-Mora, A. Santamaria, Quinolinic acid, an endogenous molecule combining excitotoxicity, oxidative stress and other toxic mechanisms, Int. J. Tryptophan Res. 5 (2012) 1–8.
[8] A. Rahman, K. Ting, K.M. Cullen, N. Braidy, B.J. Brew, G.J. Guillemin, The excitotoxin quinolinic acid induces tau phosphorylation in human neurons, PLoS One 4 (2009) e6344.
[9] P. Pierozan, A. Zamoner, A.K. Soska, R.B. Silvestrin, S.O. Loureiro, L. Heimfarth, T. Mello e Souza, M. Wajner, R. Pessoa-Pureur, Acute intrastriatal administration of quinolinic acid provokes hyperphosphorylation of cytoskeletal intermediate filament

proteins in astrocytes and neurons of rats, Exp. Neurol. 224 (2010) 188–196.
[10] P. Pierozan, A. Zamoner, A.K. Soska, B.O. de Lima, K.P. Reis, F. Zamboni, M. Wajner, R. Pessoa-Pureur, Signaling mechanisms downstream of quinolinic acid targeting the cytoskeleton of rat striatal neurons and astrocytes, Exp. Neurol. 233 (2012) 391–399.
[11] J. Middeldorp, E.M. Hol, GFAP in health and disease, Prog. Neurobiol. 93 (2011) 421–443.
[12] A. Zamoner, R. Pessoa-Pureur, Nongenomic Actions of Thyroid Hormones: Every Why has a Wherefore, IEMA-MC (2011) 165–178.
[13] E. Arbustini, M. Pasotti, A. Pilotto, C. Pellegrini, M. Grasso, S. Previtali, A. Repetto, O. Bellini, G. Azan, M. Scaffino, C. Campana, G. Piccolo, M. Vigano, L. Tavazzi, Desmin accumulation restrictive cardiomyopathy and atrioventricular block associated with desmin gene defects, Eur. J. Heart Fail 8 (2006) 477–483.
[14] G.M. Fabrizi, T. Cavallaro, C. Angiari, L. Bertolasi, I. Cabrini, M. Ferrarini, N. Rizzuto, Giant axon and neurofilament accumulation in Charcot-Marie-Tooth disease type 2E, Neurology 62 (2004) 1429–1431.
[15] D.A. Figlewicz, A. Krizus, M.G. Martinoli, V. Meininger, M. Dib, G.A. Rouleau, J.P. Julien, Variants of the heavy neurofilament subunit are associated with the development of amyotrophic lateral sclerosis, Hum. Mol. Genet. 3 (1994) 1757–1761.
[16] L. Hertel, Herpesviruses and intermediate filaments: close encounters with the third type, Viruses 3 (2011) 1015–1040.
[17] L. Heimfarth, S.O. Loureiro, M.F. Dutra, C. Andrade, L. Pettenuzzo, F.T. Guma, C.A. Goncalves, J.B. da Rocha, R. Pessoa-Pureur, In vivo treatment with diphenyl ditelluride induces neurodegeneration in striatum of young rats: implications of MAPK and Akt pathways, Toxicol. Appl. Pharmacol. 264 (2012) 143–152.
[18] L. Heimfarth, S.O. Loureiro, M.F. Dutra, L. Petenuzzo, B.O. de Lima, C.G. Fernandes, J.B. da Rocha, R. Pessoa-Pureur, Disrupted cytoskeletal homeostasis, astrogliosis and apoptotic cell death in the cerebellum of preweaning rats injected with diphenyl ditelluride, Neurotoxicology 34 (2013) 175–188.
[19] L. Heimfarth, S.O. Loureiro, K.P. Reis, B.O. de Lima, F. Zamboni, T. Gandolfi, R. Narvaes, J.B. da Rocha, R. Pessoa-Pureur, Cross-talk among intracellular signaling pathways mediates the diphenyl ditelluride actions on the hippocampal cytoskeleton of young rats, Chem. Res. Toxicol. 24 (2011) 1754–1764.
[20] L. Heimfarth, S.O. Loureiro, K.P. Reis, B.O. de Lima, F. Zamboni, S. Lacerda, A.K. Soska, L. Wild, J.B. da Rocha, R. Pessoa-Pureur, Diphenyl ditelluride induces hypophosphorylation of intermediate filaments through modulation of DARPP-32-dependent pathways in cerebral cortex of young rats, Arch. Toxicol. 86 (2012) 217–230.
[21] P. Grant, H.C. Pant, Neurofilament protein synthesis and phosphorylation, J. Neurocytol. 29 (2000) 843–872.
[22] R.K. Sihag, M. Inagaki, T. Yamaguchi, T.B. Shea, H.C. Pant, Role of phosphorylation on the structural dynamics and function of types III and IV intermediate filaments, Exp. Cell Res. 313 (2007) 2098–2109.
[23] A. Zamoner, C. Funchal, L. Heimfarth, F.R. Silva, R. Pessoa-Pureur, Short-term effects of thyroid hormones on cytoskeletal proteins are mediated by GABAergic mechanisms in slices of cerebral cortex from young rats, Cell. Mol. Neurobiol. 26 (2006) 209–224.
[24] L. Zanatta, P.B. Goulart, R. Goncalves, P. Pierozan, E.C. Winkelmann-Duarte, V.M. Woehl, R. Pessoa-Pureur, F.R. Silva, A. Zamoner, 1Alpha,25-dihydroxyvitamin D(3) mechanism of action: modulation of L-type calcium channels leading to calcium uptake and intermediate filament phosphorylation in cerebral cortex of young rats, Biochim. Biophys. Acta 1823 (2012) 1708–1719.
[25] K. Nishizawa, T. Yano, M. Shibata, S. Ando, S. Saga, T. Takahashi, M. Inagaki, Specific localization of phosphointermediate filament protein in the constricted area of dividing cells, J. Biol. Chem. 266 (1991) 3074–3079.
[26] Y. Matsuoka, K. Nishizawa, T. Yano, M. Shibata, S. Ando, T. Takahashi, M. Inagaki, Two different protein kinases act on a different time schedule as glial filament kinases during mitosis, EMBO J. 11 (1992) 2895–2902.
[27] M. Inagaki, Y. Gonda, K. Nishizawa, S. Kitamura, C. Sato, S. Ando, K. Tanabe, K. Kikuchi, S. Tsuiki, Y. Nishi, Phosphorylation sites linked to glial filament disassembly in vitro locate in a non-alpha-helical head domain, J. Biol. Chem. 265 (1990) 4722–4729.
[28] M. Eddleston, L. Mucke, Molecular profile of reactive astrocytes—implications for their role in neurologic disease, Neuroscience 54 (1993) 15–36.
[29] H. Nawashiro, M. Brenner, S. Fukui, K. Shima, J.M. Hallenbeck, High susceptibility to cerebral ischemia in GFAP-null mice, J. Cereb. Blood Flow Metab. 20 (2000) 1040–1044.
[30] S.K. Madathil, S.W. Carlson, J.M. Brelsfoard, P. Ye, A.J. D'Ercole, K.E. Saatman, Astrocyte-specific overexpression of insulin-like growth factor-1 protects hippocampal neurons and reduces behavioral deficits following traumatic brain injury in mice, PLoS One 8 (2013) e67204.
[31] R.C. Frederickson, Astroglia in Alzheimer's disease, Neurobiol. Aging 13 (1992) 239–253.
[32] M. Aschner, H.K. Kimelberg, The use of astrocytes in culture as model systems for evaluating neurotoxic-induced-injury, Neurotoxicology 12 (1991) 505–517.
[33] S.O. Loureiro, L. Romao, T. Alves, A. Fonseca, L. Heimfarth, V. Moura Neto, A.T. Wyse, R. Pessoa-Pureur, Homocysteine induces cytoskeletal remodeling and production of reactive oxygen species in cultured cortical astrocytes, Brain Res. 1355 (2010) 151–164.
[34] V. Bruno, G. Battaglia, G. Casabona, A. Copani, F. Caciagli, F. Nicoletti, Neuroprotection by glial metabotropic glutamate receptors is mediated by transforming growth factor-beta, J. Neurosci. 18 (1998) 9594–9600.
[35] N. Takagi, S. Besshoh, T. Marunouchi, S. Takeo, K. Tanonaka, Metabotropic glutamate receptor 5 activation enhances tyrosine phosphorylation of the *N*-methyl-D-aspartate (NMDA) receptor and NMDA-induced cell death in hippocampal cultured neurons, Biol. Pharm. Bull. 35 (2012) 2224–2229.
[36] M. Tang, M. Wang, T. Xing, J. Zeng, H. Wang, D.Y. Ruan, Mechanisms of unmodified CdSe quantum dot-induced elevation of cytoplasmic calcium levels in primary cultures of rat hippocampal neurons, Biomaterials 29 (2008) 4383–4391.
[37] Y. Yuan, C.Y. Jiang, H. Xu, Y. Sun, F.F. Hu, J.C. Bian, X.Z. Liu, J.H. Gu, Z.P. Liu, Cadmium-induced apoptosis in primary rat cerebral cortical neurons culture is mediated by a calcium signaling pathway, PLoS One 8 (2013) e64330.
[38] S. Kurusu, K. Matsui, T. Watanabe, T. Tsunou, M. Kawaminami, The cytotoxic effect of bromoenol lactone, a calcium-independent phospholipase A2 inhibitor, on rat cortical neurons in culture, Cell. Mol. Neurobiol. 28 (2008) 1109–1118.
[39] O. Masmoudi, P. Gandolfo, T. Tokay, J. Leprince, A. Ravni, H. Vaudry, M.C. Tonon, Somatostatin down-regulates the expression and release of endozepines from cultured rat astrocytes via distinct receptor subtypes, J. Neurochem. 94 (2005) 561–571.
[40] Y.H. Chong, M.J. Lee, Effect of HIV-1 gp41 peptides on secretion of beta-amyloid precursor protein in human astroglial cell line, T98G, J. Mol. Neurosci. 12 (1999) 147–156.
[41] C.Q. Kao, P.B. Goforth, E.F. Ellis, L.S. Satin, Potentiation of GABA(A) currents after mechanical injury of cortical neurons, J. Neurotrauma 21 (2004) 259–270.
[42] Y. Dong, H.D. Liu, R. Zhao, C.Z. Yang, X.Q. Chen, X.H. Wang, L.T. Lau, J. Chen, A.C. Yu, Ischemia activates JNK/c-Jun/AP-1 pathway to up-regulate 14-3-3gamma in astrocyte, J. Neurochem. 109 (Suppl. 1) (2009) 182–188.

Please cite this article as: P. Pierozan, et al., The phosphorylation status and cytoskeletal remodeling of striatal astrocytes treated with quinolinic acid, Exp Cell Res (2014), http://dx.doi.org/10.1016/j.yexcr.2014.02.024

[43] Y.K. Cha, Y.H. Kim, Y.H. Ahn, J.Y. Koh, Epidermal growth factor induces oxidative neuronal injury in cortical culture, J. Neurochem. 75 (2000) 298–303.
[44] H. Maldonado, E. Ramirez, E. Utreras, M.E. Pando, A.M. Kettlun, M. Chiong, A.B. Kulkarni, L. Collados, J. Puente, L. Cartier, M.A. Valenzuela, Inhibition of cyclin-dependent kinase 5 but not of glycogen synthase kinase 3-beta prevents neurite retraction and tau hyperphosphorylation caused by secretable products of human T-cell leukemia virus type I-infected lymphocytes, J. Neurosci. Res. 89 (2011) 1489–1498.
[45] C. Funchal, L.M. de Almeida, S. Oliveira Loureiro, L. Vivian, P. de Lima Pelaez, F. Dall Bello Pessutto, A.M. Rosa, M. Wajner, R. Pessoa Pureur, In vitro phosphorylation of cytoskeletal proteins from cerebral cortex of rats, Brain Res. Brain Res. Protoc. 11 (2003) 111–118.
[46] O.H. Lowry, N.J. Rosebrough, A.L. Farr, R.J. Randall, Protein measurement with the Folin phenol reagent, J. Biol. Chem. 193 (1951) 265–275.
[47] U.K. Laemmli, Cleavage of structural proteins during the assembly of the head of bacteriophage T4, Nature 227 (1970) 680–685.
[48] M.B. Omary, N.O. Ku, G.Z. Tao, D.M. Toivola, J. Liao, Heads and tails of intermediate filament phosphorylation: multiple sites and functional insights, Trends Biochem. Sci. 31 (2006) 383–394.
[49] C.W. Gourlay, K.R. Ayscough, The actin cytoskeleton: a key regulator of apoptosis and ageing?, Nat. Rev. Mol. Cell Biol. 6 (2005) 583–589.
[50] G.J. Guillemin, L. Wang, B.J. Brew, Quinolinic acid selectively induces apoptosis of human astrocytes: potential role in AIDS dementia complex, J. Neuroinflammation 2 (2005) 16.
[51] N. Braidy, R. Grant, S. Adams, B.J. Brew, G.J. Guillemin, Mechanism for quinolinic acid cytotoxicity in human astrocytes and neurons, Neurotox. Res. 16 (2009) 77–86.
[52] N. Braidy, R. Grant, B.J. Brew, S. Adams, T. Jayasena, G.J. Guillemin, Effects of Kynurenine pathway metabolites on intracellular NAD synthesis and cell death in human primary astrocytes and neurons, Int. J. Tryptophan Res. 2 (2009) 61–69.
[53] B. Liu, Q. Dong, S. Zhang, D. Su, Z. Yang, M. Lv, mGluR1,5 activation protects cortical astrocytes and GABAergic neurons from ischemia-induced impairment, Neurosci. Res. 75 (2013) 160–166.
[54] R. Schwarcz, R. Pellicciari, Manipulation of brain kynurenines: glial targets, neuronal effects, and clinical opportunities, J. Pharmacol. Exp. Ther. 303 (2002) 1–10.
[55] P.C. Severino, A. Muller Gdo, S. Vandresen-Filho, C.I. Tasca, Cell signaling in NMDA preconditioning and neuroprotection in convulsions induced by quinolinic acid, Life Sci. 89 (2011) 570–576.
[56] M.C. Lee, K.K. Ting, S. Adams, B.J. Brew, R. Chung, G.J. Guillemin, Characterisation of the expression of NMDA receptors in human astrocytes, PLoS One 5 (2010) e14123.
[57] D. Steiner, D. Saya, E. Schallmach, W.F. Simonds, Z. Vogel, Adenylyl cyclase type-VIII activity is regulated by G(betagamma) subunits, Cell Signal 18 (2006) 62–68.
[58] P.C. Kind, P.E. Neumann, Plasticity: downstream of glutamate, Trends Neurosci. 24 (2001) 553–555.
[59] H. Husi, M.A. Ward, J.S. Choudhary, W.P. Blackstock, S.G. Grant, Proteomic analysis of NMDA receptor-adhesion protein signaling complexes, Nat. Neurosci. 3 (2000) 661–669.
[60] R.S. Westphal, S.J. Tavalin, J.W. Lin, N.M. Alto, I.D. Fraser, L.K. Langeberg, M. Sheng, J.D. Scott, Regulation of NMDA receptors by an associated phosphatase-kinase signaling complex, Science 285 (1999) 93–96.
[61] D.M. Cooper, N. Mons, J.W. Karpen, Adenylyl cyclases and the interaction between calcium and cAMP signalling, Nature 374 (1995) 421–424.
[62] H. Wang, M. Zhuo, Group I metabotropic glutamate receptor-mediated gene transcription and implications for synaptic plasticity and diseases, Front Pharmacol. 3 (2012) 189.
[63] M.T. Dell'anno, S. Pallottino, G. Fisone, mGlu5R promotes glutamate AMPA receptor phosphorylation via activation of PKA/DARPP-32 signaling in striatopallidal medium spiny neurons, Neuropharmacology 66 (2013) 179–186.
[64] R. Malinow, R.C. Malenka, AMPA receptor trafficking and synaptic plasticity, Annu. Rev. Neurosci. 25 (2002) 103–126.
[65] M. Van Troys, L. Huyck, S. Leyman, S. Dhaese, J. Vandekerkhove, C. Ampe, Ins and outs of ADF/cofilin activity and regulation, Eur. J. Cell Biol. 87 (2008) 649–667.
[66] K.S. Nadella, M. Saji, N.K. Jacob, E. Pavel, M.D. Ringel, L.S. Kirschner, Regulation of actin function by protein kinase A-mediated phosphorylation of Limk1, EMBO Rep. 10 (2009) 599–605.
[67] Z.M. Goeckeler, R.B. Wysolmerski, Myosin phosphatase and cofilin mediate cAMP/cAMP-dependent protein kinase-induced decline in endothelial cell isometric tension and myosin II regulatory light chain phosphorylation, J. Biol. Chem. 280 (2005) 33083–33095.
[68] P.J. Meberg, S. Ono, L.S. Minamide, M. Takahashi, J.R. Bamburg, Actin depolymerizing factor and cofilin phosphorylation dynamics: response to signals that regulate neurite extension, Cell Motil. Cytoskeleton 39 (1998) 172–190.
[69] J.L. Ridet, S.K. Malhotra, A. Privat, F.H. Gage, Reactive astrocytes: cellular and molecular cues to biological function, Trends Neurosci. 20 (1997) 570–577.
[70] J. Silver, J.H. Miller, Regeneration beyond the glial scar, Nat. Rev. Neurosci. 5 (2004) 146–156.
[71] A. Buffo, C. Rolando, S. Ceruti, Astrocytes in the damaged brain: molecular and cellular insights into their reactive response and healing potential, Biochem. Pharmacol. 79 (2010) 77–89.
[72] S. Hisanaga, Y. Gonda, M. Inagaki, A. Ikai, N. Hirokawa, Effects of phosphorylation of the neurofilament L protein on filamentous structures, Cell Regul. 1 (1990) 237–248.
[73] S. Hisanaga, Y. Matsuoka, K. Nishizawa, T. Saito, M. Inagaki, N. Hirokawa, Phosphorylation of native and reassembled neurofilaments composed of NF-L, NF-M, and NF-H by the catalytic subunit of cAMP-dependent protein kinase, Mol. Biol. Cell. 5 (1994) 161–172.
[74] H. Hayashi, R.B. Campenot, D.E. Vance, J.E. Vance, Protection of neurons from apoptosis by apolipoprotein E-containing lipoproteins does not require lipoprotein uptake and involves activation of phospholipase Cgamma1 and inhibition of calcineurin, J. Biol. Chem. 284 (2009) 29605–29613.
[75] A. Volterra, J. Meldolesi, Astrocytes, from brain glue to communication elements: the revolution continues, Nat. Rev. Neurosci. 6 (2005) 626–640.
[76] K. Yamanaka, S.J. Chun, S. Boillee, N. Fujimori-Tonou, H. Yamashita, D.H. Gutmann, R. Takahashi, H. Misawa, D.W. Cleveland, Astrocytes as determinants of disease progression in inherited amyotrophic lateral sclerosis, Nat. Neurosci. 11 (2008) 251–253.

Please cite this article as: P. Pierozan, et al., The phosphorylation status and cytoskeletal remodeling of striatal astrocytes treated with quinolinic acid, Exp Cell Res (2014), http://dx.doi.org/10.1016/j.yexcr.2014.02.024

Capítulo 5

QUINOLINIC ACID INDUCES DISRUPTED CYTOSKELETAL HOMEOSTASIS IN STRIATAL NEURONS. PROTECTIVE ROLE OF ASTROCYTE-NEURON INTERACTION

Paula Pierozan, Fernanda Ferreira, Bárbara Ortiz de Lima and Regina Pessoa-Pureur

Artigo submetido ao **Neuroscience**

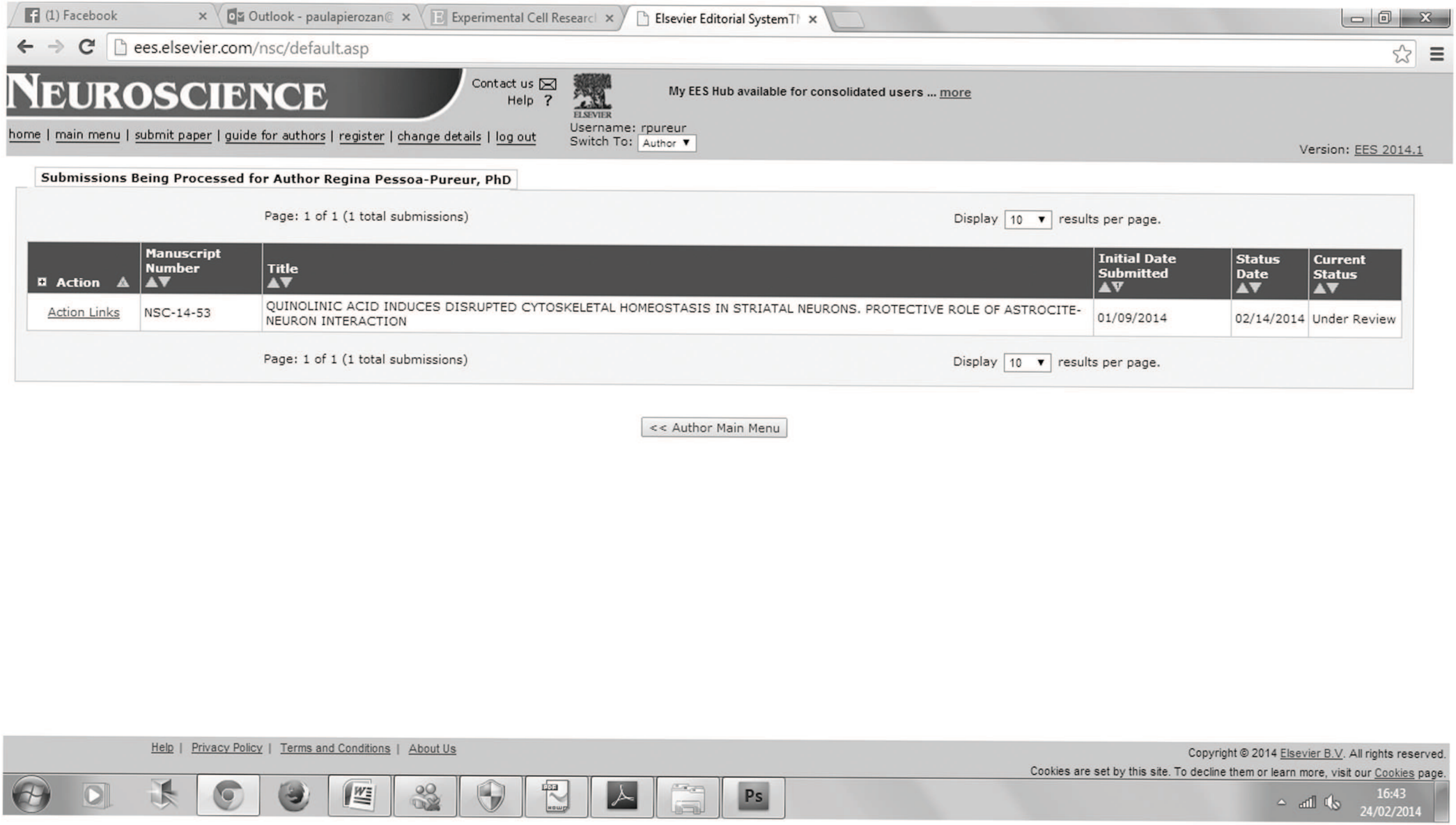
(1) Facebook
Outlook - paulapierozan@
Experimental Cell Researcl
Elsevier Editorial SystemTM
ees.elsevier.com/nsc/default.asp
NEUROSCIENCE
Contact us
Help ?
My EES Hub available for consolidated users ... more
home | main menu | submit paper | guide for authors | register | change details | log out
Username: rpureur
Switch To: Author
Version: EES 2014.1
Submissions Being Processed for Author Regina Pessoa-Pureur, PhD
Page: 1 of 1 (1 total submissions)
Display 10 results per page.
Action
Manuscript Number
Title
Initial Date Submitted
Status Date
Current Status
Action Links
NSC-14-53
QUINOLINIC ACID INDUCES DISRUPTED CYTOSKELETAL HOMEOSTASIS IN STRIATAL NEURONS. PROTECTIVE ROLE OF ASTROCITE-NEURON INTERACTION
01/09/2014
02/14/2014
Under Review
Page: 1 of 1 (1 total submissions)
Display 10 results per page.
<< Author Main Menu
Help | Privacy Policy | Terms and Conditions | About Us
Copyright © 2014 Elsevier B.V. All rights reserved.
Cookies are set by this site. To decline them or learn more, visit our Cookies page.
16:43
24/02/2014

Title: QUINOLINIC ACID INDUCES DISRUPTED CYTOSKELETAL HOMEOSTASIS IN STRIATAL NEURONS. PROTECTIVE ROLE OF ASTROCYTE-NEURON INTERACTION

Authors: Paula Pierozan, Fernanda Ferreira, Bárbara Ortiz de Lima and Regina Pessoa-Pureur

Departamento de Bioquímica, Instituto de Ciências Básicas da Saúde, Universidade Federal do Rio Grande do Sul, Porto Alegre, RS, Brazil

CORRESPONDENCE ADDRESS: Dr. Regina Pessoa-Pureur Universidade Federal do Rio Grande do Sul, Instituto de Ciências Básicas da Saúde, Departamento de Bioquímica, Rua Ramiro Barcelos 2600 anexo, CEP 90035-003 Porto Alegre - RS, BRASIL, Fax: 5551 3308 5535, Tel: 5551 3308 5565; E-mail: rpureur@ufrgs.br

Running Title: Quinolinic acid and astrocyte-neuron interaction

Abstract

Quinolinic acid (QUIN) is an endogenous metabolite of the kynurenine pathway involved in several neurological disorders. Among the several mechanisms involved in QUIN-mediated toxicity, disruption of the cytoskeleton has been demonstrated in striatally injected rats and in striatal slices. In the present work we searched for the actions of QUIN in striatal neurons in culture. Neurons exposed to 10 µM QUIN presented hyperphosphorylated neurofilament subunits (NFL, NFM and NFH). Hyperphosphorylation was abrogated in the presence of protein kinase A (PKA) and protein kinase C (PKC) inhibitors, H89 (20 µM) and staurosporina (10 nM), respectively, as well as by the specific antagonists to N-methyl-D-aspartate (NMDA) (50 µM DL-AP5) and metabotropic glutamate receptor 1 (mGLUR1), (100 µM MPEP). Also, intra and extracellular Ca^{2+} quelators (10µM BAPTA-AM and 1 mM EGTA, respectively), and Ca^{2+} influx through L-type voltage-dependent Ca^{2+} channel (L-VDCC) (10 µM verapamil) are implicated in QUIN-mediated effect. Cells immunostained for the neuronal markers β-tubulin III and MAP2 showed altered neurite/neuron ratio and neurite outgrowth. NF hyperphosphorylation and morphological alterations were totally prevented by conditioned medium from QUIN-treated astrocytes. Also, co-cultured astrocytes and neurons interacted with one another reciprocally protecting themselves against QUIN injury. Co-cultured cells preserved their cytoskeletal organization and cell morphology together with unaltered activity of the phosphorylating system associated with the cytoskeleton. Altogether, we described cytoskeletal disruption as one of the most relevant actions of QUIN toxicity in striatal neurons in culture and soluble factors secreted by astrocytes, as well as neuron-astrocyte interaction playing a role in neuroprotection.

Keywords: quinolinic acid; neuronal cytoskeleton; astrocyte conditioned medium; astrocyte-neuron interaction; neurite outgrowth; neurofilament

Introduction

Degradation of the essential amino acid tryptophan along the kynurenine pathway (KP) yields several neuroactive intermediates in astrocytes and microglial cells. Among them, the excitotoxic N-methyl-D-aspartate (NMDA) receptor agonist quinolinic acid (QUIN) is perhaps the most important in terms of biological activity (Schwarcz and Pellicciari, 2002).

QUIN is normally present in low nanomolar concentrations in human brain. However, substantial increase in QUIN levels to micromolar concentrations are found in cerebral insults or infection, and have been most clearly implicated in the AIDS-dementia complex (Stone et al., 2001), Huntington´s disease (McLin et al., 2006), Alzheimer's disease (Stone et al., 2001) and psychiatric disorders (Myint, 2012). In addition, it has been described that intracerebral injection of QUIN results in the development of axon-sparing lesions, characteristic of Huntington's disease (HD) (Schwarcz et al., 1983). The pattern of toxicity which results from increased QUIN levels is considerably complex with many mechanisms potentially involved. It has been assumed that QUIN exerts excessive excitation of NMDA receptors, increased Ca^{2+} influx, mitochondrial dysfunction, decreased ATP levels, cytochrome *c* release, selective loss of GABAergic and cholinergic neurons, and oxidative stress (Perez-De La Cruz et al., 2012).

Human neurons do not produce QUIN but they can take it up. Neuronal uptake of QUIN is likely to be part of a scavenging process in which activated microglia and/or infiltrating macrophages release high concentrations of QUIN (Guillemin et al., 2005, Guillemin et al., 2007). Chronic exposure of human neurons to QUIN causes significant

structural changes including dendritic beading, microtubular disruption and decrease in organelles (Whetsell and Schwarcz, 1989).

Previous evidence from our group (Pierozan et al., 2010, 2012) and from others (Kerr et al., 1998, Braidy et al., 2009, Rahman et al., 2009) showed that disruption of the cytoskeleton of neural cell is one of the main targets of the action of QUIN both *in vivo* and *in vitro*. The signaling mechanisms underlying the actions of intrastriatally injected QUIN, on the cytoskeleton of neural cells represent an early event, in which excitotoxicity and oxidative damage are possibly involved (Pierozan et al., 2010). In addition, in rat striatal slices, QUIN act through activation of metabotropic glutamate receptor (mGluR) and Ca^{2+} influx through NMDA receptors and L-type voltage-dependent Ca^{2+} channels (L-VDCC), as well as Ca^{2+} release from intracellular stores. These findings were associated with hyperphosphorylation of cytoskeletal proteins and disruption of cytoskeletal homeostasis in response to QUIN (Pierozan et al., 2012).

Neurofilaments (NF) are members of the intermediate filament (IF) family expressed in neurons. They consist of three subunits divided according to their molecular mass: NF heavy chain (NFH); NF middle chain (NFM) and NF light chain (NFL). NF proteins play an important structural role in neurons and together with microtubules, microtubule-associated proteins and other associated proteins, they sustain axonal and dendritic branching patterns and also promote axonal growth or thickening (Kesavapany et al., 2006). The IF network of mature astrocytes includes glial fibrillary acidic protein (GFAP) as a major component, together with vimentin and nestin. GFAP and vimentin have an important function for signal transduction and structural properties of astrocytes and form the cellular cytoskeleton together with microtubules and actin microfilaments (Thomsen et al., 2013).

Intermediate filament (IF) proteins are unique among the cytoskeletal proteins, in that phosphorylation takes a central role in their regulation. IF phosphorylation is due, in large part, to the abundance of potential Ser/Thr-phosphorylation sites targeted by specific protein kinases and to the location of these sites in accessible carboxyl and amino terminal domains (Omary et al., 2006). Most phosphorylation sites in NFM and NFH are found in their lysine-serine-proline (KSP) repeat regions, which can be specifically phosphorylated by proline-directed kinases. The tail domains of the NFM and NFH contain consensus sequences of Cdk5 and the mitogen activated protein kinase (MAPK) family. The KSP sites in NFM and NFH are extensively phosphorylated in axons but not in dendrites or cell bodies, under normal conditions. Nevertheless, all kinases and NF subunits are present all over the cell (Holmgren et al., 2012).

IFs such as GFAP, vimentin and NFL are phosphorylated by the second messenger-dependent protein kinases dependent on cAMP (PKA), dependent on Ca^{2+} and diacylglicerol (PKC) and dependent on Ca^{2+}/calmodulin (PKCaM). Phosphorylation occurs in the N-terminal head domain and prevents NFL assembly and induces the disassembly of NFL filaments *in vitro* (Kesavapany et al., 2006).

Although phosphorylation has a relevant physiological roles in the homeostasis of the cytoskeleton, aberrantly phosphorylated cytoskeletal proteins have been long time considered a hallmark of brain cell dysfunction associated with mitochondrial damage, oxidative stress, excitotoxicity and neural cell death in several neurodegenerative diseases (Pessoa-Pureur and Wajner, 2007) and in response to hormones (Zamoner and Pessoa-Pureur, 2011).

Even though we have previously found that the endogenous phosphorylating system associated with IF proteins was misregulated in response to QUIN both in intrastriatally injected rats and in acute slices (Pierozan et al., 2010, 2012), it is important to note that *in vivo* or *ex-vivo*, the extensive cell–cell interactions between different cell types of brain limits the study of selective cellular responses and vulnerability to QUIN-induced insult. Thus, primary astrocyte and/or neuron cultures represent useful tools to test whether the distinctive response of each brain cell type to QUIN reflects an inherent property of the cells. The current study used primary cultured and co-cultured striatal astrocytes and neurons to test cell–cell interactions and responses of these cell types to *in vitro* QUIN exposure and to clarify their role in the susceptibility of the cytoskeleton to the excitotoxic effects of QUIN and the contributions of astrocyte-neuron interactions in the protection against this effect.

Material and Methods

Materials

Phalloidin-fluorescein isothiocynate, anti-GFAP (clone GA-5), anti-β-III tubulin, anti-mouse IgG (whole molecule), anti-mouse IgG (whole molecule)-FITC, F(ab0)2 fragment-Cy3, anti-NFL, anti-NFM, anti-NFH, quinolinic acid (QUIN), peroxidase conjugated anti-mouse IgG, benzamidine, leupeptin, antipain, pepstatin, chymostatin, acrylamide, bis-acrylamide and material for cell culture were obtained from Sigma (St. Louis, MO, USA). Polyclonal anti-GFAP was from DAKO. 40, 60-diamidino-2-phenylindole (DAPI) was from Calbiochem (La Jolla, CA, USA). ECL detection kit was from Millipore (Millipore, Billerica, MA, USA). Anti β-actin and anti-MAP2

antibodies were from Cell Signaling (Boston, MA, USA). [^{32}P]orthophosphate was purchased from CNEN, São Paulo, Brazil. Fetal bovine serum (FBS), Dulbecco's Modified Eagle's Medium: Nutrient Mixture F-12 (DMEM/F12), Neurobasal medium, B-27 supplement, fungizone and penicillin/streptomycin were purchased from Gibco BRL (Carlsbad, CA, USA). Apoptosis detection kit I#556547 was obtained from BD Pharmigen. All other chemicals were of analytical grade.

Animals

Pregnant Wistar rats (200–250 g) were obtained from our breeding stock. Rats were maintained on a 12-h light/12-h dark cycle in a constant temperature (22 °C) colony room, with food and water at libitum and animals were observed on gestational day 22. As soon as delivery finished, mothers and pups were sacrificed by decapitation without anesthesia, and pups were used for astrocyte culture. For neuron culture, mothers were sacrificed on gestational day 18 by decapitation and the embryos were used for neuronal cultures. The experimental protocol followed the "Principles of Laboratory Animal Care" (NHI publication 85-23, revised 1985) and was approved by the Ethics Committee for Animal Research of the Federal University of Rio Grande do Sul (number 18266). All efforts were made to minimize the number of animal used and their suffering.

Astrocyte and neuron primary culture and co-culture

Astrocyte primary cultures were prepared from the striatum of newborn (0-1 day old; P0) Wistar rats, as described previously (Loureiro et al., 2010). Briefly, for primary astrocyte cultures, rats were decapitated and brain striatum was removed. Mechanically

dissociated cells were plated in Dulbecco's Modified Eagle's medium (DMEM/F12)/10% FBS (pH 7.4) supplemented with glucose (33 mM), glutamine (2 mM), and sodium bicarbonate (3 mM) into a 15.6 and 34.8 mm diameter well (6 and 24-well plate) (Corning Inc., New York, New York), previously coated with polyornithine (1.5 mg/mL, Sigma, St. Louis, MO). These cells were grown in a humid incubator (37°C, 5% CO_2), with the media replaced every 3 days. After astrocytes reached semi-confluence (15 days in vitro-DIV), the culture medium was removed by suction and the cells were incubated until 24 h at 37°C in an atmosphere of 5% CO_2 in DMEM/F12 without FBS in the absence (controls) or presence of different QUIN concentrations (10-100µM) during 24 h. Morphological studies were performed using cells fixed for immunocytochemistry.

Primary neuronal cell cultures were prepared from 18 day embryonic (E18) Wistar rats striatum, as previously described (Moura Neto et al., 1983). Briefly, single-cell suspensions were obtained by dissociating cells of striatum in DMEM/F12 medium supplemented with 33 mM glucose, 2 mM glutamine, and 3 mM sodium bicarbonate. Approximately 5 x 10^4 neuronal cells were plated on polyornitine-treated coverslips placed on a 24-well plate, or 1.5 x 10^6 neuronal cells for 6-well plate. The neuronal cultures were kept in Neurobasal medium supplemented with 2 mM glutamine and B27 for up to 24 h. After this time, the culture medium was removed by suction and the cells were incubated for 7 days in a humid incubator (37 °C, 5% CO_2). After this time, when culture has 7-8 DIV, the culture medium was removed and the cells were incubated until 24 h in Neurobasal medium in the absence (controls) or presence of different QUIN concentrations (10-100 µM). The controls were treated with the same QUIN vehicle (but without the drug). Morphological studies were performed using cells fixed

for immunocytochemistry. In the co-culture assays, striatal neurons were plated onto nontreated astrocyte monolayers.

Co-cultures were kept for 7 days at 37°C in a humidified 5% CO_2 air atmosphere. After this time, co-cultures were treated with QUIN for 24 h. In experiments designed to evaluate the role of the conditioned medium of astrocytes on neuron survival, neurite outgrowth and NFs phosphorylation, the astrocytes were pretreated with QUIN for 24h in serum-free DMEM/F12 medium, and after 24 h the medium was collected. The neuronal cultures were kept in Neurobasal medium supplemented with glutamine (2 mM) for 7 days followed by treatment with the astrocyte conditioned medium for 24 h.

Apoptotic detection assay

Apoptotic detection assay was carried out by surface labeling with the Ca^{2+} dependent phosphatydylserine-binding protein annexin V. After incubation with QUIN (10-500 µM) for 24 h, cells were recovered from the culture plates by 0.25% trypsin-EDTA treatment, centrifuged (1000 x g, 5 min) and washed once with PBS. Cells were labeled by incubation with Annexin V-FITC and propidium iodide (PI) in a binding buffer (Apoptosis detection Kit I # 556547, BD Pharmingen) for 15 min at room temperature in the dark, according to the manufacturer's instruction. Stained cells were acquired (10,000 for gated astrocytes) on a FACS Calibur flow cytometer. Analysis was performed using FlowJo Software.

***In vitro* phosphorylation**

Neurons in culture were incubated for 24 h in the presence or absence of QUIN, then the medium was changed and incubation for 1 h was carried out at 30°C with 1000 µL of a medium containing (in mM): 124 NaCl; 4 KCl; 1.2 $MgSO_4$, 25 Na-HEPES (pH

7.4); 12 glucose; 1 $CaCl_2$ and the following protease inhibitors: 1 mM benzamidine, 0.1 µM leupeptin, 0.7 µM antipain, 0.7 µM pepstatin, 07 µM chymostatin, and 10 µCi of [^{32}P] sodium orthophosphate with or without addition of QUIN (1, 10, 25 and 100 µM). In the experiments designed to study signaling mechanisms, cells were pre-incubated for 30 min in the presence or absence of 50 µM DL-AP5 and CNQX (Loureiro et al., 2010), 100 µM 4C3HPG (Copani et al., 1998), 10 µM MPEP (Takagi et al., 2012), 10 µM verapamil (Tang et al., 2008), 10 µM BAPTA-AM (Yuan et al., 2013), 1 mM EGTA (Kurusu et al., 2008), 20 µM H89 (Masmoudi et al., 2005), 10 nM Staurosporine (Chong and Lee, 1999), 10 µM KN93 (Kao et al., 2004), 10 µm SP600125 (Dong et al., 2009), 10 µM PD98056, 3 µM p38 inhibitor (Cha et al., 2000) and 10 µM roscovitine (Maldonado et al., 2011). The labeling reaction was normally allowed to proceed for 1h at 30°C and stopped with 1 mL of cold stop buffer (150 mM NaF, 5 mM EDTA, 5 mM EGTA, Tris–HCl, 50 mM, pH 6.5, and the protease inhibitors described above). Cells were then washed twice by decantation with stop buffer to remove excess radioactivity. After, preparations of IF-enriched high-salt Triton-insoluble cytoskeletal fraction were obtained from striatal primary neurons, as described by Funchal et al. (Funchal et al., 2003). Briefly, cells were homogenized in 200 µL of ice-cold high salt buffer containing 5 mM KH_2PO_4 (pH 7.1), 600 mM KCl, 10 mM $MgCl_2$, 2 mM EGTA, 1% Triton X-100, and the protease inhibitors described above. The homogenate was centrifuged at 15,800 x g for 10 min at 4°C in an Eppendorf centrifuge and the supernatant was discarded. The Triton-insoluble IF-enriched pellet, containing NF-L, NF-M and NF-H, was dissolved in 1% SDS and protein concentration was determined by the method of Lowry et al (Lowry et al., 1951).

Polyacrylamide gel electrophoresis (SDS-PAGE)

The cytoskeletal fraction from striatal neurons was prepared as described above. Equal protein concentrations were loaded onto 7.5% polyacrylamide gels and analyzed by SDS-PAGE according to the discontinuous system of Laemmli (Laemmli, 1970). After drying, the gels were exposed to X-ray films (X-Omat XK1) at -70°C with intensifying screens and finally the autoradiograph was obtained. Proteins were quantified by scanning the films with a Hewlett-Packard Scanjet 6100C scanner and determining optical densities with an Optiquant version 02.00 software (Packard Instrument Company). Density values were obtained for the studied proteins.

Western blot analysis

After treatment, neurons were disrupted by lysis solution containing 2 mM EDTA, 50 mM Tris–HCl, pH 6.8, 4% SDS. For electrophoretic analysis, samples were dissolved in 25% (v/v) of a solution containing 40% glycerol, 5% mercaptoethanol, 50 mM Tris–HCl, pH 6.8, and boiled for 3 min. Total protein homogenate was analyzed by 10% SDS-PAGE (30 μg of total protein/lane) and transferred (Trans-blot SD semidry transfer cell, BioRad) to nitrocellulose membranes for 1 h at 15 V in transfer buffer (48 mM Trizma, 39 mM glycine, 20% methanol, and 0.25% SDS). The blot was then washed for 20 min in TBS (500 mM NaCl, 20 mM Trizma, pH 7.5), followed by 2 h incubation in blocking solution (TBS plus 5% defatted dry milk). After incubation, the blot was washed twice for 5 min with blocking solution plus 0.05% Tween-20 (T-TBS) and then incubated overnight at 4°C in blocking solution containing one of the following monoclonal antibodies: anti-NFL, anti-NFM and anti-NFH diluted 1:500, anti-β-actin diluted 1:500. The blot was then washed twice for 5 min with T-TBS and incubated for 2 h in a solution containing peroxidase-conjugated rabbit anti-mouse IgG diluted 1:2000 or peroxidase-conjugated anti-rabbit IgG diluted 1:2000. The blot was

washed again twice with T-TBS for 5 min and twice with TBS for 5 min. The blot was developed using a chemiluminescence ECL kit.

Immunocytochemistry

Immunocytochemistry was performed as described previously (Loureiro et al., 2010). Briefly, cultured cells plated on glass coverslips were fixed with 4% paraformaldehyde for 30 min and permeabilized with 0.1% Triton X-100 in phosphate-buffered saline (PBS) for 5 min at room temperature. After blocking, neurons were incubated overnight with antibody anti-β-III tubulin (1:200) and anti-MAP2 protein (1:200), and co-cultures were incubated with anti-β-III tubulin (1:200) and anti-GFAP (1:500) at room temperature, followed by PBS washes and incubation with specific secondary antibody conjugated with Cy3 (sheep anti-rabbit; 1:1000) or with fluorescein isothiocynate (FITC) (sheep anti-mouse; 1:400) for 1h. In all immunostaining-negative controls, reactions were performed by omitting the primary antibody. No reactivity was observed when the primary antibody was excluded. The nucleus was stained with DAPI (0.25 µg/mL). Cells were viewed with a Nikon inverted microscope and images transferred to a computer with a digital camera (Sound Vision Inc, USA).

Morphometric analysis

Neurons stained with anti-β-III tubulin and anti-MAP2 antibodies were captured by a system coupled to a Nikon inverted fluorescent microscope (Nikon Eclipse T E300). The neurites/neuron ration and neurite length were analyzed by using the Image J Software as previously described (Baranes et al., 2012). Figure ?a demonstrates a schematic neuron and the morphometric parameters we measure: the number of originating neurites from the soma and the neurite length. The number of processes

originating from the soma are measured manually and all neurites emerged from neuronal soma were considered. To measure the processes length we use an ImageJ plugin (US National Institutes of Health, Bethesda, MD, USA) which enables semi automatic tracing of neurites and lengths measurements. Neurite length was analyzed either considering only the major process per neurons. At least, four independent experiments were performed in triplicate, encompassing ten fields randomly chosen in each group**.** The data were stored and morphometric analyses were carried out using the GraphPad Prism 5.

Astrocytes stained for actin cytoskeleton and nucleus were measured using the labeling for phalloidin-fluorescein and DAPI respectively. Figure ?b demonstrates a schematic astrocyte and the morphometric parameters we measure: the cytoplasmic and nucleus area and the cytoplasmic/nucleus ratio. Measurements of cytoplasm and nucleus were obtained using the Image J Software (NIH, Bethesda, MD) and cytoplasm/nucleus ratio of the cells was used as a criterion of morphologic alteration. To measure the cytoplasmic and nucleus area we use an ImageJ plugin (US National Institutes of Health, Bethesda, MD, USA) which enables semi automatic tracing of the area of interest. At least, four independent experiments were performed in triplicate, encompassing ten fields randomly chosen in each group**.** The data were stored and morphometric analyses were carried out using the GraphPad Prism 5.

Statistical analysis

Data from the experiments were analyzed statistically by one-way analysis of variance (ANOVA) followed by the Tukey test when the F-test was significant. Values of $p < 0.05$ were considered to be significant. All analyses were carried out in an IBM compatible PC using the Statistical Package for Social Sciences (SPSS) software.

Results

Initially we searched for the effect of QUIN on the viability of 7-8 DIV striatal neurons in primary culture. Cells were incubated with 10 to 500 µM QUIN for 24 h and tested for apoptosis and necrosis using Annexin V-FITC and propidium iodide (PI) assay. We have found significant apoptotic and necrotic cell death in neurons treated with 500 µM QUIN, however survival of cells treated with 10-100 µM QUIN was similar to control ones (Figure 1). On the basis of these results, we tested the effect of 10, 25 and 100 µM QUIN on the endogenous phosphorylating system associated to the cytoskeleton of the primary neurons during 24 h of treatment (Figure 2). We have found increased ^{32}P-orthophosphate incorporation into NFL, NFM and NFH without altered protein levels in all the QUIN concentrations studied (Figure 2A, B, C and D). Therefore, we have chosen to use 10 µM QUIN during 24 h, to search for the molecular mechanisms underlying the actions of QUIN on the neuronal cytoskeleton.

The contribution of different protein kinases known to target the NF proteins in striatal slices incubated with QUIN (Pierozan et al., 2012) was investigated and is shown in Figure 3. Interestingly, 10 µM QUIN-induced hyperphosphorylation of NFs in cultured neurons was unaffected in the presence of KN93 (10 µM), inhibitor of protein kinase dependent of Ca^{2+}/calmodulin (PKCaMII). However, H89 (10 µM), inhibitor of cAMP-dependent protein kinase (PKA), partially prevented NFL and NFM hyperphosphorylation without affecting ^{32}P-orthophosphate incorporation into NFH. Moreover, staurosporine (10 nM), a protein kinase C (PKC) inhibitor, totally prevented NFM and NFH, but only partially prevented NFL hyperphosphorylation (Figure 3A). On the other hand, the MAPK inhibitors, namely SP600125 (10 µM) for JNK; PD

98056 (10 μM) for Erk1/2; p38 inhibitor (30 μM) for p38MAPK, and roscovitine (10 μM) for Cdk5, totally prevented NFL, NFM and NFH hyperphosphorylation (Figure 3B). Altogether, these findings suggest a role for PKA, PKC, MAPK and Cdk5 in the QUIN action on the homeostasis of the phosphorylating system targeting the neuronal cytoskeleton in culture.

Since QUIN is considered a glutamate agonist (Stone, 1993, Schwarcz and Pellicciari, 2002), we assayed the participation of glutamate receptors in the action of QUIN on the phosphorylating system associated with the NFs of striatal neurons. Cells were co-incubated with 10 μM QUIN and 50 μM DL-AP5, a competitive NMDA ionotropic antagonist or 50 μM CNQX, a non-NMDA ionotropic antagonist. As shown in Figure 4A, hyperphosphorylation of NF subunits was totally prevented by the NMDA antagonist, while CNQX failed to prevent this effect. In addition, we tested (100 μM) 4-C3-HPG and (10 μM) MPEP, specific metabotropic glutamate receptor type 1 (mGluR1) and mGluR5 antagonists, respectively. Results showed that mGluR1 inhibition totally prevented QUIN-induced hyperphosphorylation of NFL, NFM and NFH. Conversely, mGluR5 inhibition was unable to impair hyperphosphorylation of the NF subunits. These findings suggest the participation of NMDA and mGluR1 in the action of QUIN on the hyperphosphorylation of NF subunits in cultured neurons treated with 10 μM QUIN.

Taking into account the relevance of Ca^{2+} in maintaining cytoskeletal homeostasis, particularly in what concerns to the cytoskeletal phosphorylation system in striatal slices exposed to QUIN (Pierozan et al., 2012), we examined the involvement of Ca^{2+} in the QUIN-mediated hyperphosphorylation of NF subunits in cultured striatal neurons. The role of Ca^{2+} influx through voltage-dependent Ca^{2+} channels (VDCC), was

tested using the specific L-VDCC blocker nifedipine (10 µM) (Figure 4B). Results showed that NFM and NFH hyperphosphorylation was totally prevented, while NFL hyperphosphorylation was partially prevented in the presence of the L-VDCC blocker. To investigate the role of intra and extracellular Ca^{2+} levels in this process we performed experiments using EGTA (1 mM), an extracellular Ca^{2+} chelator and BAPTA-AM (10 µM) the membrane-permeable form of BAPTA, an intracellular Ca^{2+} chelator (Tymianski et al., 1994). We found that quelation of extracellular Ca^{2+} partially prevented NF hyperphosphorylation, while intracellular Ca^{2+} buffering totally prevented this effect of QUIN (Figure 4B).

Since outgrowth of neuronal processes is dependent on dynamic changes in cytoskeleton properties (da Silva and Dotti, 2002, Dent and Gertler, 2003), we evaluated the consequences of NF hyperphosphorylation on some morphological parameters of neurites from QUIN-treated neurons. For this, we carried out immunocytochemical analysis using FITC-labeled anti-β-III tubulin and Cy3-labelled anti-MAP2 antibodies, in the presence of the same concentrations of QUIN able to provoke hyperphosphorylation. Results showed that control neurons presented complex neurite meshworks containing long processes (Figure 5A) however, neurons treated with 10 µM QUIN presented a slightly but not significantly reduced neurite/neuron ratio. However, in the presence of 25 and 100 µM QUIN neurite outgrowth progressed to a significantly reduced neurite/neuron ratio (Figure 5A and B). In addition, neurite lengths were decreased in all QUIN concentrations tested (Figure 5A and C). These findings suggest the compromised cytoskeletal framework of neurites in the presence of QUIN.

Next, we searched for the role of the conditioned medium secreted by astrocytes on the response of neurons to QUIN. Therefore, in some experiments, the conditioned medium of astrocyte monolayers treated with 10, 25 and 100 μM QUIN or of control cells was added on primary cultured neurons for 24 h. Thereafter, plates were fixed and immunostained for the neuronal markers β-tubulin III and MAP2. Results showed unaltered cytoskeletal parameters evaluated as neurite/neuron ration (Figure 6A and C) and number of neurites/neuron (Figure 6A and B) compared with neurons exposed to control conditioned medium (Figure 6A). Moreover, the NF subunits in neurons that received the conditioned medium from QUIN-treated astrocytes failed to present hyperphosphorylation (Figure 7). Taken together, these findings claim to the presence of protective factors secreted by stimulated astrocytes and protecting neurons against the QUIN-induced cell death and disruption of the cytoskeleton.

In order to evaluate the role of astrocyte/neuron interaction on QUIN effects, after primary astrocyte became confluent, neurons were plated onto astrocytic monolayer, co-culture was proceed and QUIN was added 7 days afterwards. Co-cultures proceeded for 24 hours and some plates were assayed for IF phosphorylation and others were fixed, immunostained for the astrocyte marker GFAP and for the neuronal marker β-tubulin III. Co-staining with the astrocyte and neuron marker showed that in QUIN treated co-cultures GFAP presented a typical IF array extending across the cytoplasm and this distribution was not altered compared with astrocytes from control co-cultures. It is important to note that we have previously described that primary astrocytes treated with QUIN presented cytoskeletal disruption and hyperphosphorylated IF proteins (unpublished results), evidencing the susceptibility of astrocyte cytoskeleton to QUIN. The morphometric analysis showed that the neurite/neuron ratio (Figure 8A and C) and

the neurite length (Figure 8A and B) were not altered in QUIN treated co-cultures, compared with control ones. Also, the cytoplasmic area (Figure 8A and D) and the cytoplasmic/nuclear area ratio (Figure 8 A and E) of astrocytes were not altered in QUIN treated co-cultures. These findings support a reciprocal protective role on the cytoskeleton, associated with the interaction between astrocytes and neurons. In line with this, the phosphorylation level of IF proteins in both cell types was similar to control ones (Figure 9).

Discussion

In the present report we describe that QUIN is toxic to striatal neurons in culture, inducing apoptotic death only in high concentrations, in agreement with previous evidence (Kim and Choi, 1987, Tavares et al., 2002, Kumar, 2008). In smaller concentrations QUIN disrupted the homeostasis of the cytoskeleton through hyperphosphorylation of NF subunits and altered morphometric parameters, such as neurite/neuron ratio and neurite length without inducing death. We also found a protective role of astrocyte-conditioned medium on the disrupted neuronal cytoskeleton and morphometric alterations, suggesting that QUIN-induced trophic factors secreted by astrocytes are able to modulate signaling mechanisms targeting the neuronal cytoskeleton. More interestingly, co-cultured astrocytes and neurons tightly and actively interacted with one another reciprocally protecting themselves against QUIN injury. Co-cultured astrocytes and neurons preserved their cytoskeletal organization and cell morphology together with unaltered activity of the phosphorylating system associated with the cytoskeleton. Such a mutual protection reinforces the concept of collaboration between neuron and astrocyte ability in processing signaling mechanisms. We also

evidenced that the neuronal cytoskeleton is more susceptible than astrocytic cytoskeleton to QUIN injury, since we found that ten-fold more concentrated QUIN is necessary to disrupt the cytoskeleton from astrocytes (100 µM) (unpublished results) than from neurons (10 µM).

Neurofilaments present in the axonal cytoskeleton are extensively phosphorylated and their phosphorylation level is pivotal for their properties and functions. Aberrantly phosphorylated NF subunits often result from a misregulated kinase or phosphatase activity, which could link stress-induced NF phosphorylation to disease (Shea and Chan, 2008, Holmgren et al., 2012). We have found that the NF subunits NFL, NFM and NFH of striatal neurons in culture are aberrantly phosphorylated in response to 10 µM QUIN exposure. PKA and PKC, as well as MAPKs and Cdk5 appeared as the main protein kinases phosphorylating head and tail domain sites of these proteins, respectively. The major sites of phosphorylation on NFL and NFM subunits are known to be Ser-55 for PKA and Ser-23 for PKA and PKC (Sihag and Nixon, 1991, Sihag et al., 1999, Pierozan et al., 2012). It has been demonstrated that phosphorylation of NFL subunit by PKA or PKC prevents their association and disassociates filaments formed from NFL (Hisanaga et al., 1990) interfering, therefore, with the axonal framework. In addition, we found that QUIN stimulus has also activated the MAPKs Erk 1/2, JNK and p38MAPK as well as Cdk5. These protein kinases are among the main kinases found to phosphorylate the Lysine-Serine-Proline (KSP) repeats in the C-terminal domain of NFM and NFH in response to stress (Giasson and Mushynski, 1997, Ackerley et al., 2004, Shea et al., 2004, Rudrabhatla et al., 2008), including QUIN actions in striatal slices (Pierozan et al., 2012). Although activation of MAPKs and Cdk5 causes an increase in NFH phosphorylation and neurite outgrowth (Sharma et al., 2002),

aberrantly phosphorylated NFH gives rise to disruption of the cytoskeleton related with neurodegeneration (Zhou et al., 2010). In support of this, several lines of evidence suggest that aberrant phosphorylation of C-terminal sites of NFs by proline-directed kinases affects their transport along axons (Perrot and Eyer, 2009) by interfering with their binding to the fast motor proteins kinesin and dynein (Uchida et al., 2009, Holmgren et al., 2012).

The morphological alterations we have found in QUIN-treated neurons, appear to arise due to QUIN-induced misregulation of signaling mechanisms related with disruption of NF homeostasis. However, we cannot exclude some kind of impairment in neurite sprouting, which in turn drive the formation of actin-based protrusions and neurite outgrowth (Gallo, 2011). In agreement with this hypothesis, Lopez-Picon and co-workers (Lopez-Picon et al., 2004), found hyperphosphorylated NFs implicated in maintaining normal microfilament organization and mossy fiber sprouting in a model of kainic acid-induced status epilepticus. Moreover, disruption of the cytoskeletal homeostasis of QUIN-treated neurons could represent, at least in part, an excitotoxic dendritic injury (Greenwood and Connolly, 2007), since dendrites have been proposed to be the initial sites of excitotoxic injury (Bindokas and Miller, 1995), resulting in either rapid necrosis or delayed apoptosis of the neuron depending of the severity of the insult (Bonfoco et al., 1995).

Interestingly, we have found that inhibition of MAPKs and Cdk5 with specific inhibitors, totally or partially impaired the ^{32}P-ortophosphate incorporation into N-terminal located sites of NFL, directly targeted by PKA and PKC. Conversely PKC inhibition totally impaired NFM and NFH phosphorylation in sites targeted by MAPKs and Cdk5. While the exact signaling mechanisms regulating NF phosphorylation in

QUIN-treated neurons remains elusive, these findings suggest the complexity of the signaling pathways implicated in these actions.

Even though QUIN is classically considered a NMDA agonist, its action on the cytoskeletal proteins of neural cells *in vivo* and *ex-vivo* (Pierozan et al., 2010, 2012) as well as our present findings cannot be fully explained by activation of NMDA receptors. In fact, cytoskeletal disruption in QUIN-treated primary neurons can be related to increased Ca^{2+} influx through L-VDCC in addition to NMDA, and to mGluR1 activation. In this context, enhanced Ca^{2+} influx through NMDA and L-VDCC in striatal neurons in culture support the role of Ca^{2+}-mediated neurotoxicity in the aberrant phosphorylation of NFs associated with QUIN exposure and is consistent with previous results in striatal slices (Pierozan et al., 2012). Also, VDCCs can be regulated by a G protein-mediated pathway (Hille, 1994) or by protein kinases such as PKA, PKC, and PKCaMII (Catterall, 1997). These protein kinases, together with casein kinase 1 (CK1) are able to phosphorylate and activate Ca^{2+} channels (Catterall, 1997). Therefore, it is probable that in cultured neurons, PKA, PKC and Cdk5 reinforces Ca^{2+}-mediated excitotoxicity in response to QUIN, contributing to disruption of the cytoskeleton, thereby causing more damage to neurons.

Taking into account our previous findings in striatal slices (Pierozan et al., 2012), we could propose that in QUIN-treated neurons mGluR1 is upstream of phospholipase C (PLC) which, in turn, produced diacylglycerol (DAG) and inositol 3,4,5 triphosphate (IP3). DAG is important to activate PKC and phosphorylate NFL, while IP3 contributed to Ca^{2+} release from internal stores promoting hyperphosphorylation of KSP repeats on the tail domain of NFM and NFH. These

mechanisms then set off interacting cascades of events culminating with aberrantly phosphorylated NFs and disrupted axonal cytoskeleton.

It is important to note that in our present data the misregulated signaling mechanisms modulating kinase activities and morphological alterations in neurons were prevented in the presence of astrocyte-conditioned medium or astrocyte-neuron co-culture. This is in line with current evidence indicating that astrocytes influence neuronal development and the activity of neurons at several levels through direct cell-to-cell contacts and via a variety of soluble factors (Schmalenbach and Muller, 1993, Nakayama et al., 2003, Nedergaard et al., 2003, Villegas et al., 2003, Kornyei et al., 2005). Otherwise, neurons are able to facilitate glial communication and contribute to neuroglial interaction, which play a role in neuroprotection (Rouach et al., 2002). Thus it is feasible that in our experimental conditions, striatal astrocytes secrete factors which promote neurite formation and extension and provide a cellular microenvironment where astrocyte/neuron interactions reciprocally protect themselves against QUIN insult, so that the homeostasis of the cytoskeleton and morphological features are preserved.

In addition, a number of studies have contributed to demonstrate that neurons and astrocytes tightly and actively interact and astrocytic gap junctions represent a target for the interactions occurring between neurons and astrocytes (Rouach et al., 2002). In fact, astrocytes may play a complex role in neuronal survival by exerting either a neuroprotective or a neurotoxic influence (Mattson et al., 1997). Otherwise, neurons release bioactive molecules, including neurotransmitters, peptides and lipids, which activate astrocytic receptors and modify the activity and/or the expression of gap junction channels (Giaume and McCarthy, 1996, Rouach et al., 2002). An important

consequence of the upregulation of astrocytic gap functions by neurons is the increase in the propagation of intercellular Ca^{2+} waves (Rouach et al., 2000). Indeed, astrocytes respond to neuronal activity by an elevation in $[Ca^{2+}]i$, which triggers the release of gliotransmitters and in turn contributes to the regulation of synaptic activity (Araque et al., 1999, Rouach et al., 2000). The magnitude of these neuroglial interactions regulates several aspects of cell function, including extracellular and intracellular homeostasis, trafficking and supply of energy metabolites, protection of neurons against oxidative stress, and propagation of death signals (Bruzzone and Giaume, 1999).

Conclusion

In summary, this study provides consistent evidence that the cytoskeletal is a critical target of the actions of QUIN in isolated striatal neurons and highlights the role for secreted factors and for reciprocal interactions between astrocytes and neurons protecting themselves against the insult. It has been proposed that an imbalance in the kinurenine pathway leading to QUIN accumulation might be involved in the pathogenesis of neurodegenerative diseases, such as Huntington's disease (Sánchez et al., 2008). Therefore, the relationship between high QUIN levels and neurotoxicity is an intense subject of study. However, further investigation is required in order to elucidate the molecular mechanisms by which neurons undergo dynamic cytoskeletal alterations and their roles in neurite morphology in response to QUIN insult. In addition, the pathways of astrocyte/neuron interactions and their role in neuroprotection will be of great interest in the in understanding the actions of QUIN on neural cells.

Acknowledgements

This work was supported by grants of the Conselho Nacional de Desenvolvimento Científico e Tecnológico (CNPq), Fundação de Amparo à Pesquisa do Estado do Rio Grande do Sul (FAPERGS) and Pro-Reitoria de Pesquisa de Pós Graduação of Universidade Federal do Rio Grande do Sul (Propesq-UFRGS).

References

Ackerley S, Grierson AJ, Banner S, Perkinton MS, Brownlees J, Byers HL, Ward M, Thornhill P, Hussain K, Waby JS, Anderton BH, Cooper JD, Dingwall C, Leigh PN, Shaw CE, Miller CC (p38alpha stress-activated protein kinase phosphorylates neurofilaments and is associated with neurofilament pathology in amyotrophic lateral sclerosis. Mol Cell Neurosci 26:354-364.2004).

Araque A, Parpura V, Sanzgiri RP, Haydon PG (Tripartite synapses: glia, the unacknowledged partner. Trends Neurosci 22:208-215.1999).

Baranes K, Kollmar D, Chejanovsky N, Sharoni A, Shefi O (Interactions of neurons with topographic nano cues affect branching morphology mimicking neuron-neuron interactions. J Mol Histol 43:437-447.2012).

Bindokas VP, Miller RJ (Excitotoxic degeneration is initiated at non-random sites in cultured rat cerebellar neurons. J Neurosci 15:6999-7011.1995).

Bonfoco E, Krainc D, Ankarcrona M, Nicotera P, Lipton SA (Apoptosis and necrosis: two distinct events induced, respectively, by mild and intense insults with N-methyl-D-aspartate or nitric oxide/superoxide in cortical cell cultures. Proc Natl Acad Sci U S A 92:7162-7166.1995).

Braidy N, Grant R, Adams S, Brew BJ, Guillemin GJ (Mechanism for quinolinic acid cytotoxicity in human astrocytes and neurons. Neurotox Res 16:77-86.2009).

Bruzzone R, Giaume C (Connexins and information transfer through glia. Adv Exp Med Biol 468:321-337.1999).

Catterall WA (Modulation of sodium and calcium channels by protein phosphorylation and G proteins. Adv Second Messenger Phosphoprotein Res 31:159-181.1997).

Cha YK, Kim YH, Ahn YH, Koh JY (Epidermal growth factor induces oxidative neuronal injury in cortical culture. J Neurochem 75:298-303.2000).

Chong YH, Lee MJ (Effect of HIV-1 gp41 peptides on secretion of beta-amyloid precursor protein in human astroglial cell line, T98G. J Mol Neurosci 12:147-156.1999).

Copani A, Casabona G, Bruno V, Caruso A, Condorelli DF, Messina A, Di Giorgi Gerevini V, Pin JP, Kuhn R, Knopfel T, Nicoletti F (The metabotropic glutamate receptor mGlu5 controls the onset of developmental apoptosis in cultured cerebellar neurons. Eur J Neurosci 10:2173-2184.1998).

da Silva JS, Dotti CG (Breaking the neuronal sphere: regulation of the actin cytoskeleton in neuritogenesis. Nat Rev Neurosci 3:694-704.2002).

Dent EW, Gertler FB (Cytoskeletal dynamics and transport in growth cone motility and axon guidance. Neuron 40:209-227.2003).

Dong Y, Liu HD, Zhao R, Yang CZ, Chen XQ, Wang XH, Lau LT, Chen J, Yu AC (Ischemia activates JNK/c-Jun/AP-1 pathway to up-regulate 14-3-3gamma in astrocyte. J Neurochem 109 Suppl 1:182-188.2009).

Funchal C, de Almeida LM, Oliveira Loureiro S, Vivian L, de Lima Pelaez P, Dall Bello Pessutto F, Rosa AM, Wajner M, Pessoa Pureur R (In vitro phosphorylation of cytoskeletal proteins from cerebral cortex of rats. Brain Res Brain Res Protoc 11:111-118.2003).

Gallo G (The cytoskeletal and signaling mechanisms of axon collateral branching. Dev Neurobiol 71:201-220.2011).

Giasson BI, Mushynski WE (Study of proline-directed protein kinases involved in phosphorylation of the heavy neurofilament subunit. J Neurosci 17:9466-9472.1997).

Giaume C, McCarthy KD (Control of gap-junctional communication in astrocytic networks. Trends Neurosci 19:319-325.1996).

Greenwood SM, Connolly CN (Dendritic and mitochondrial changes during glutamate excitotoxicity. Neuropharmacology 53:891-898.2007).

Guillemin GJ, Cullen KM, Lim CK, Smythe GA, Garner B, Kapoor V, Takikawa O, Brew BJ (Characterization of the kynurenine pathway in human neurons. J Neurosci 27:12884-12892.2007).

Guillemin GJ, Wang L, Brew BJ (Quinolinic acid selectively induces apoptosis of human astrocytes: potential role in AIDS dementia complex. J Neuroinflammation 2:16.2005).

Hille B (Modulation of ion-channel function by G-protein-coupled receptors. Trends Neurosci 17:531-536.1994).

Hisanaga S, Gonda Y, Inagaki M, Ikai A, Hirokawa N (Effects of phosphorylation of the neurofilament L protein on filamentous structures. Cell Regul 1:237-248.1990).

Holmgren A, Bouhy D, Timmerman V (Neurofilament phosphorylation and their proline-directed kinases in health and disease. J Peripher Nerv Syst 17:365-376.2012).

Kao CQ, Goforth PB, Ellis EF, Satin LS (Potentiation of GABA(A) currents after mechanical injury of cortical neurons. J Neurotrauma 21:259-270.2004).

Kerr SJ, Armati PJ, Guillemin GJ, Brew BJ (Chronic exposure of human neurons to quinolinic acid results in neuronal changes consistent with AIDS dementia complex. AIDS 12:355-363.1998).

Kesavapany S, Pareek TK, Zheng YL, Amin N, Gutkind JS, Ma W, Kulkarni AB, Grant P, Pant HC (Neuronal nuclear organization is controlled by cyclin-dependent kinase 5 phosphorylation of Ras Guanine nucleotide releasing factor-1. Neurosignals 15:157-173.2006).

Kim JP, Choi DW (Quinolinate neurotoxicity in cortical cell culture. Neuroscience 23:423-432.1987).

Kornyei Z, Szlavik V, Szabo B, Gocza E, Czirok A, Madarasz E (Humoral and contact interactions in astroglia/stem cell co-cultures in the course of glia-induced neurogenesis. Glia 49:430-444.2005).

Kumar U (Somatostatin in medium-sized aspiny interneurons of striatum is responsible for their preservation in quinolinic acid and N-methyl-D-asparate-induced neurotoxicity. J Mol Neurosci 35:345-354.2008).

Kurusu S, Matsui K, Watanabe T, Tsunou T, Kawaminami M (The cytotoxic effect of bromoenol lactone, a calcium-independent phospholipase A2 inhibitor, on rat cortical neurons in culture. Cell Mol Neurobiol 28:1109-1118.2008).

Laemmli UK (Cleavage of structural proteins during the assembly of the head of bacteriophage T4. Nature 227:680-685.1970).

Lopez-Picon F, Puustinen N, Kukko-Lukjanov TK, Holopainen IE (Resistance of neurofilaments to degradation, and lack of neuronal death and mossy fiber sprouting after kainic acid-induced status epilepticus in the developing rat hippocampus. Neurobiol Dis 17:415-426.2004).

Loureiro SO, Romao L, Alves T, Fonseca A, Heimfarth L, Moura Neto V, Wyse AT, Pessoa-Pureur R (Homocysteine induces cytoskeletal remodeling and production of reactive oxygen species in cultured cortical astrocytes. Brain Res 1355:151-164.2010).

Lowry OH, Rosebrough NJ, Farr AL, Randall RJ (Protein measurement with the Folin phenol reagent. J Biol Chem 193:265-275.1951).

Maldonado H, Ramirez E, Utreras E, Pando ME, Kettlun AM, Chiong M, Kulkarni AB, Collados L, Puente J, Cartier L, Valenzuela MA (Inhibition of cyclin-dependent kinase 5 but not of glycogen synthase kinase 3-beta prevents neurite retraction and tau hyperphosphorylation caused by secretable products of human T-cell leukemia virus type I-infected lymphocytes. J Neurosci Res 89:1489-1498.2011).

Masmoudi O, Gandolfo P, Tokay T, Leprince J, Ravni A, Vaudry H, Tonon MC (Somatostatin down-regulates the expression and release of endozepines from cultured rat astrocytes via distinct receptor subtypes. J Neurochem 94:561-571.2005).

Mattson MP, Barger SW, Furukawa K, Bruce AJ, Wyss-Coray T, Mark RJ, Mucke L (Cellular signaling roles of TGF beta, TNF alpha and beta APP in brain injury responses and Alzheimer's disease. Brain Res Brain Res Rev 23:47-61.1997).

McLin JP, Thompson LM, Steward O (Differential susceptibility to striatal neurodegeneration induced by quinolinic acid and kainate in inbred, outbred and hybrid mouse strains. Eur J Neurosci 24:3134-3140.2006).

Moura Neto V, Mallat M, Jeantet C, Prochiantz A (Microheterogeneity of tubulin proteins in neuronal and glial cells from the mouse brain in culture. EMBO J 2:1243-1248.1983).

Myint AM (Kynurenines: from the perspective of major psychiatric disorders. FEBS J 279:1375-1385.2012).

Nakayama T, Momoki-Soga T, Inoue N (Astrocyte-derived factors instruct differentiation of embryonic stem cells into neurons. Neurosci Res 46:241-249.2003).

Nedergaard M, Ransom B, Goldman SA (New roles for astrocytes: redefining the functional architecture of the brain. Trends Neurosci 26:523-530.2003).

Omary MB, Ku NO, Tao GZ, Toivola DM, Liao J ("Heads and tails" of intermediate filament phosphorylation: multiple sites and functional insights. Trends Biochem Sci 31:383-394.2006).

Perez-De La Cruz V, Carrillo-Mora P, Santamaria A (Quinolinic Acid, an endogenous molecule combining excitotoxicity, oxidative stress and other toxic mechanisms. Int J Tryptophan Res 5:1-8.2012).

Perrot R, Eyer J (Neuronal intermediate filaments and neurodegenerative disorders. Brain Res Bull 80:282-295.2009).

Pessoa-Pureur R, Wajner M (Cytoskeleton as a potential target in the neuropathology of maple syrup urine disease: insight from animal studies. J Inherit Metab Dis 30:664-672.2007).

Pierozan P, Zamoner A, Soska AK, Silvestrin RB, Loureiro SO, Heimfarth L, Mello e Souza T, Wajner M, Pessoa-Pureur R (Acute intrastriatal administration of quinolinic acid provokes hyperphosphorylation of cytoskeletal intermediate filament proteins in astrocytes and neurons of rats. Exp Neurol 224:188-196.2010).

Pierozan P, Zamoner A, Soska AK, Silvestrin RB, Loureiro SO, Heimfarth L, Mello e Souza T, Wajner M, Pessoa-Pureur R (Acute intrastriatal administration of quinolinic acid

provokes hyperphosphorylation of cytoskeletal intermediate filament proteins in astrocytes and neurons of rats. Exp Neurol 224:188-196.2012).

Rahman A, Ting K, Cullen KM, Braidy N, Brew BJ, Guillemin GJ (The excitotoxin quinolinic acid induces tau phosphorylation in human neurons. PLoS One 4:e6344.2009).

Rouach N, Avignone E, Meme W, Koulakoff A, Venance L, Blomstrand F, Giaume C (Gap junctions and connexin expression in the normal and pathological central nervous system. Biol Cell 94:457-475.2002).

Rouach N, Glowinski J, Giaume C (Activity-dependent neuronal control of gap-junctional communication in astrocytes. J Cell Biol 149:1513-1526.2000).

Rudrabhatla P, Zheng YL, Amin ND, Kesavapany S, Albers W, Pant HC (Pin1-dependent prolyl isomerization modulates the stress-induced phosphorylation of high molecular weight neurofilament protein. J Biol Chem 283:26737-26747.2008).

Sánchez AME, Mejı´a-Toiber J, Massieu L (Excitotoxic Neuronal Death and the Pathogenesis of Huntington's Disease. Archives of Medical Research 39: 265e276
2008).

Schmalenbach C, Muller HW (Astroglia-neuron interactions that promote long-term neuronal survival. J Chem Neuroanat 6:229-237.1993).

Schwarcz R, Pellicciari R (Manipulation of brain kynurenines: glial targets, neuronal effects, and clinical opportunities. J Pharmacol Exp Ther 303:1-10.2002).

Schwarcz R, Whetsell WO, Jr., Mangano RM (Quinolinic acid: an endogenous metabolite that produces axon-sparing lesions in rat brain. Science 219:316-318.1983).

Sharma P, Veeranna, Sharma M, Amin ND, Sihag RK, Grant P, Ahn N, Kulkarni AB, Pant HC (Phosphorylation of MEK1 by cdk5/p35 down-regulates the mitogen-activated protein kinase pathway. J Biol Chem 277:528-534.2002).

Shea TB, Chan WK (Regulation of neurofilament dynamics by phosphorylation. Eur J Neurosci 27:1893-1901.2008).

Shea TB, Zheng YL, Ortiz D, Pant HC (Cyclin-dependent kinase 5 increases perikaryal neurofilament phosphorylation and inhibits neurofilament axonal transport in response to oxidative stress. J Neurosci Res 76:795-800.2004).

Sihag RK, Jaffe H, Nixon RA, Rong X (Serine-23 is a major protein kinase A phosphorylation site on the amino-terminal head domain of the middle molecular mass subunit of neurofilament proteins. J Neurochem 72:491-499.1999).

Sihag RK, Nixon RA (Identification of Ser-55 as a major protein kinase A phosphorylation site on the 70-kDa subunit of neurofilaments. Early turnover during axonal transport. J Biol Chem 266:18861-18867.1991).

Stone TW (Neuropharmacology of quinolinic and kynurenic acids. Pharmacol Rev 45:309-379.1993).

Stone TW, Behan WM, Jones PA, Darlington LG, Smith RA (The role of kynurenines in the production of neuronal death, and the neuroprotective effect of purines. J Alzheimers Dis 3:355-366.2001).

Takagi N, Besshoh S, Marunouchi T, Takeo S, Tanonaka K (Metabotropic glutamate receptor 5 activation enhances tyrosine phosphorylation of the N-methyl-D-aspartate (NMDA) receptor and NMDA-induced cell death in hippocampal cultured neurons. Biol Pharm Bull 35:2224-2229.2012).

Tang M, Xing T, Zeng J, Wang H, Li C, Yin S, Yan D, Deng H, Liu J, Wang M, Chen J, Ruan DY (Unmodified CdSe quantum dots induce elevation of cytoplasmic calcium levels and impairment of functional properties of sodium channels in rat primary cultured hippocampal neurons. Environ Health Perspect 116:915-922.2008).

Tavares RG, Tasca CI, Santos CE, Alves LB, Porciuncula LO, Emanuelli T, Souza DO (Quinolinic acid stimulates synaptosomal glutamate release and inhibits glutamate uptake into astrocytes. Neurochem Int 40:621-627.2002).

Thomsen R, Daugaard TF, Holm IE, Nielsen AL (Alternative mRNA splicing from the glial fibrillary acidic protein (GFAP) gene generates isoforms with distinct subcellular mRNA localization patterns in astrocytes. PLoS One 8:e72110.2013).

Tymianski M, Spigelman I, Zhang L, Carlen PL, Tator CH, Charlton MP, Wallace MC (Mechanism of action and persistence of neuroprotection by cell-permeant Ca2+ chelators. J Cereb Blood Flow Metab 14:911-923.1994).

Uchida A, Alami NH, Brown A (Tight functional coupling of kinesin-1A and dynein motors in the bidirectional transport of neurofilaments. Mol Biol Cell 20:4997-5006.2009).

Villegas SN, Poletta FA, Carri NG (GLIA: A reassessment based on novel data on the developing and mature central nervous system. Cell Biol Int 27:599-609.2003).

Whetsell WO, Jr., Schwarcz R (Prolonged exposure to submicromolar concentrations of quinolinic acid causes excitotoxic damage in organotypic cultures of rat corticostriatal system. Neurosci Lett 97:271-275.1989).

Yuan Y, Jiang CY, Xu H, Sun Y, Hu FF, Bian JC, Liu XZ, Gu JH, Liu ZP (Cadmium-induced apoptosis in primary rat cerebral cortical neurons culture is mediated by a calcium signaling pathway. PLoS One 8:e64330.2013).

Zamoner A, Pessoa-Pureur R (Nongenomic actions of thyroid hormones: every why has a wherefore. Immunology, Endocrine & Metabolic Agents in Medical Chemistry 11(3):165-178.2011).

Zhou J, Wang H, Feng Y, Chen J (Increased expression of cdk5/p25 in N2a cells leads to hyperphosphorylation and impaired axonal transport of neurofilament proteins. Life Sci 86:532-537.2010).

Legends

Figure 1. Effect of QUIN on neuron viability. Striatal neurons of rats were cultured for 7 days in Neurobasal medium. Apoptotic and necrotic detection was carried out with Annexin V-FITC and propidium iodide (Pi) assay in the presence or absence of 10, 25, 50, 100 and 500 μM QUIN for 24 h. Cells labeled with FITC-labeled annexin V ($Anexin^{+}Pi^{-}$) detects early apoptotic cells, with propidium iodide ($Annexin^{-}Pi^{+}$) detects necrosis, with annexin plus Pi ($Annexin^{+}Pi^{+}$) detects cells that underwent apoptosis followed by necrosis and cells without labeled ($Annexin^{-}Pi^{-}$) to life cells.Data are reported as means ± S.D. of four independent experiments performed in triplicate. Results were statistically analyzed by one way ANOVA followed by Tukey-Kramer multiple analysis are indicated: $^{a}p<0.001$ compared with $Annexin^{-}Pi^{-}$ of control; $^{b}p<0.001$ compared with $Anexin^{+}Pi^{-}$ of control; $^{c}p<0.05$ compared with $Annexin^{-}Pi^{+}$ of control and $^{d}p<0.001$ compared with $Annexin^{+}Pi^{+}$ of control.

Figure 2. (A) Effect of QUIN on the phosphorylation of NFL, NFM and NFH subunits in the cytoskeletal fraction from primary neurons in culture. Data are reported as mean± S.D. of four different experiments and expressed as percent of controls. Statistically significant differences from controls, as determined by one-way ANOVA followed by Tukey–Kramer multiple comparison test are indicated: ***p< 0.001 and *p<0.05 compared with control. B) Coomassie blue stained molecular weight standards, representative stained gel of a control and treated samples, corresponding autoradiograph, and Western blot for NFL, NFM and NFH. Equal amounts of the cytoskeletal fraction (50 μg) from control (C) and treated (T) samples were run in 7.5% polyacrylamide gel electrophoresis. MW: molecular weight standard proteins; WB: Western blot. C) Western blot analysis of NFL, NFM and NFH protein content in cell homogenate. All lanes received equivalent amounts (30 μg) of total protein from cell

extract. Immunoblotting was carried out with monoclonal anti-NFL, anti-NFM and anti-NFH antibodies. The blots were developed using an ECL kit. Anti-β-actin was used as an internal control since its level is not affected by the experimental treatments. Representative immunological reactions are shown below. Data are reported as means ± S.D. of four different experiments. Results were statistically analyzed by one-way ANOVA followed by Tukey-kramer test. D) Representative immunoblots.

Figure 3. Involvement of protein kinases on QUIN-induced IF hyperphosphorylation. (A) Participation of second messenger dependent protein kinases PKA, PKCaMII and PKC was tested by using the specific inhibitors 20 μM H89, 10 μM KN93 and 10 nM staurosporina, respectively. (B) Participation of MEK/ERK, JNK, p38MAPK and Cdk5 was tested using the specific inhibitors 10 μM PD9859, 10 μM SP600125, 3 μM p38 MAPK inhibitor and 10 μM roscovitine, respectively. Data are reported as means ± S.D. of four different experiments and expressed as % of control. Statistically significant differences from controls, as determined by one-way ANOVA followed by Tukey–Kramer multiple comparison test are indicated: ***p<0.001and *p<0.05 compared with control group; ###p<0.001 and #p<0.05 compared with QUIN group.

Figure 4. (A) Involvement of glutamate receptors on QUIN-induced IF hyperphosphorylation in primary neurons in culture. Participation of NMDA and non-NMDA receptors, mRGlu1 and mRGlu5 was tested using the blockers 50 μM DL-AP5, CNQX, 100 μM MPEP and 10 μM 4C3HPG, respectively. Data are reported as means ± S.D. of four different experiments and expressed as percent of control. Statistically significant differences as determined by one-way ANOVA followed by Tukey-kramer multiple comparision test are indicated: ***p<0.001 compared with control and ###p<0.001 compared with QUIN group. B) Involvement of intra and extracellular Ca^{2+}

on QUIN-induced IF *in vitro* phosphorylation. Cultures were preincubated with BAPTA-AM, EGTA and verapamil to test the involvement of intra and extracellular Ca^{2+}, and L-VDCC. Data are reported as means ± S.D. of four different experiments and expressed as percent of control. Statistically significant differences as determined by one-way ANOVA followed by Tukey-Kramer multiple comparision test are indicated: ***p<0.001 and *p<0.05 compared with control and ###p<0.001 compared with QUIN group.

Figure 5. Effect of QUIN on neuronal cytoskeleton. Neuronal cells were cultured in Neurobasal medium supplemented with glutamine for 7 days. After, the cells were treated with 10, 25 and 100 µM QUIN for additional 24 h. The neurite length and neurite/neuron ratio were analyzed by using the Image J Software. A) Representative images of QUIN treated cells immunostained with anti-β-III tubulin (green), anti-MAP2 (red) and DAPI (blue) showing that treatments alter the neurites/neuron ratio (B) and the neurite lengths (C). Scale bar=50µm. Four independent experiments were performed in triplicate, encompassing ten fields randomly chosen in each group. The data were stored and morphometric analysis were carried out using the GraphPad Prism. Data were statistically analyzed by one-way ANOVA. Statistically significant differences from controls are indicated: ***p<0.001; **p<0.01 and *p< 0.05. (For interpretation of the references to color in this figure legend, the reader is referred to the web version of this article.)

Figure 6. Effect of conditioned medium of control and QUIN treated astrocytes on neuronal cytoskeleton. Neuronal cells were cultured in Neurobasal medium supplemented with glutamine for 7 days. After, cells were treated with conditioned medium of control or 10, 25 and 100 µM QUIN-treated astrocytes for 24 h. (A)

Representative images of cells immunostained with anti-β-III tubulin (green), anti-MAP2 (red) and DAPI (blue) showing that conditioned medium prevented the effects of QUIN. Scale bar= 30 µm. Analysis of neurite length (B) and neurites/neuron (C) of neurons treated with conditioned medium. The length of the neurites of each cell immunostained for β-III tubulin and MAP2 was analyzed using the Image J Software. Four independent experiments were performed, encompassing 10 fields randomly chosen on each group. Data were statistically analyzed by one-way ANOVA followed by Tukey-kramer test.

Figure 7. Effect of conditioned medium of control and QUIN treated astrocytes on the phosphorylation of NFL, NFM and NFH subunits in the cytoskeletal fraction from primary neurons in culture. Neuronal cells were cultured in Neurobasal medium supplemented with glutamine for 7 days. After, cells were treated with conditioned medium of control or 10, 25 and 100 µM QUIN-treated astrocytes for 24 h. Data are reported as mean ± S.D. of four different experiments and expressed as percent of controls. Statistically significant differences from controls, as determined by one-way ANOVA followed by Tukey–Kramer multiple comparison test. B) Representative Coomassie blue stained 7.5% SDS-PAGE of the cytoskeketal fraction of (50 µg) control (C) and (10, 25 and 100 µM) QUIN-treated neurons with corresponding autoradiograph. MW = molecular weight standards; WB = Western blot standards for NF-L, NF-M and NF-H.

Figure 8. Effect of QUIN treatments on the neurite length and neurite/neuron of neuron/astrocyte co-cultures. After astrocytes reach semi-confluence in DMEM/F12/10% FBS, neurons were plated onto astrocyte monolayers and cultured for 7 days. After, the cells were treated with 10, 25 and 100 µM QUIN for additional 24 h.

(A) Representative images of QUIN treated cells immunostained with anti-β-III tubulin (green), anti-GFAP (red) and DAPI (blue), showing that treatment did not alter neurite extension(B), neurite/neuron (C), cytoplasmic area (D) and cytoplasmic/nucleus ratio (D) of astrocytes. Scale bar= 50µm. Analysis of neurite length of neurons immunostained for β-III tubulin, and cytoplasmic area and cytoplasmic/nucleus ratio of astrocytes immunostained for GFAP was carried out using the Image J Software. Four independent experiments were performed in triplicate, encompassing 10 fields randomly chosen on each group. Data were statistically analyzed by one-way ANOVA.

Figure 9. Effect of QUIN exposure on the phosphorylation level of IF proteins in the cytoskeletal fraction from neuron/astrocyte co-cultures. After astrocytes reach semi-confluence in DMEM/F12/10% FBS, neurons were plated onto astrocyte monolayers and cultured for 7 days. After, the cells were treated with 10, 25 and 100 µM QUIN for additional 24 h. Data are reported as mean± S.D. of four different experiments and expressed as percent of controls. Statistically significant differences from controls, as determined by one-way ANOVA followed by Tukey–Kramer multiple comparison test. B) Coomassie blue stained molecular weight standards, representative stained gel of a control and treated samples, corresponding autoradiograph, and western blot for VIM, GFAP, NFL, NFM and NFH. Equal amounts of the cytoskeletal fraction (50 µg) from control (C) and treated (T) samples were run in 7.5% polyacrylamide gel electrophoresis. MW: molecular weight standard proteins; WB: Western blotting.

Figure 1

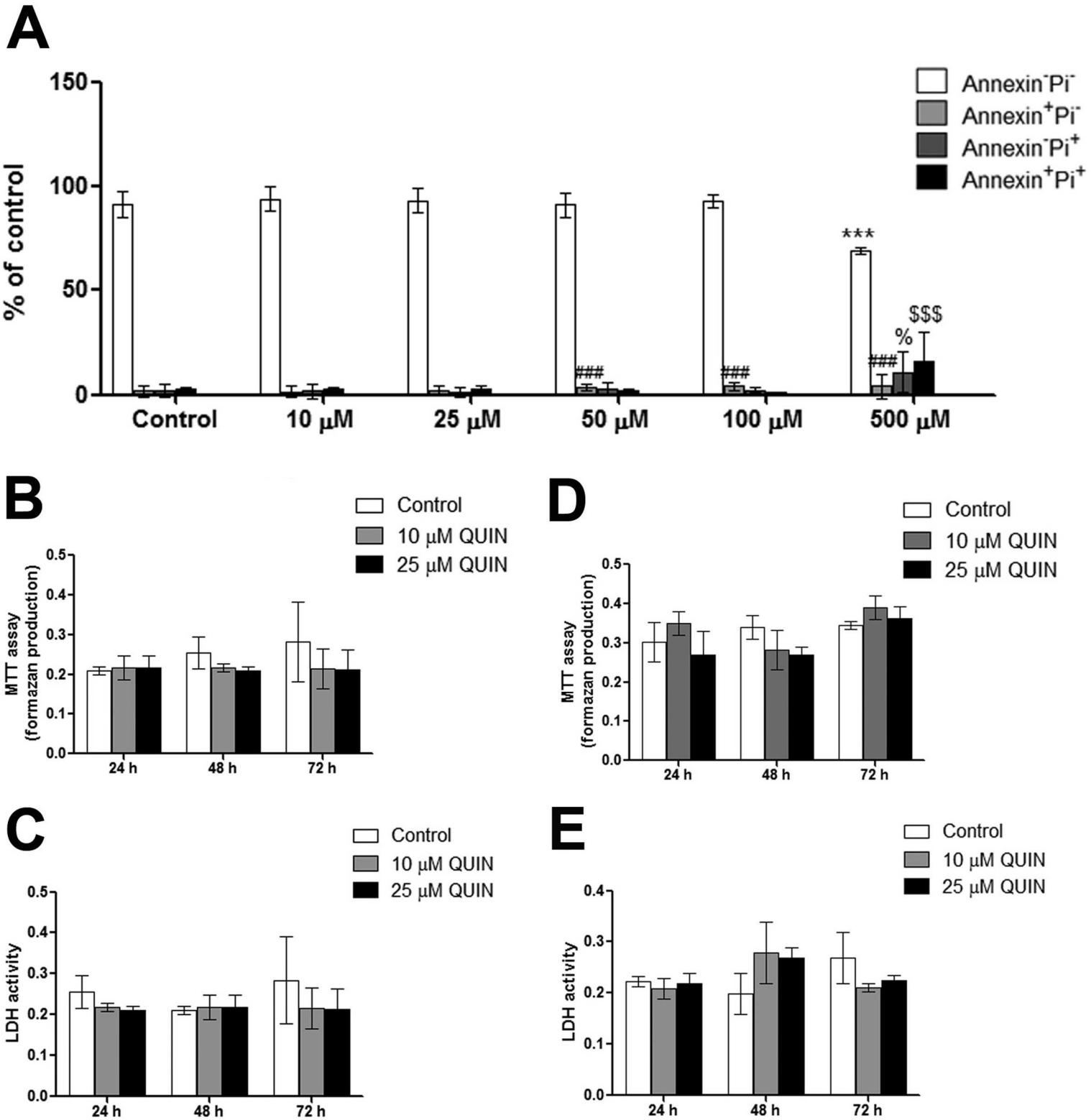
A
Annexin⁻Pi⁻
Annexin⁺Pi⁻
Annexin⁻Pi⁺
Annexin⁺Pi⁺
% of control
150
100
50
0
***
###
###
%
$$$
Control
10 μM
25 μM
50 μM
100 μM
500 μM
B
Control
10 μM QUIN
25 μM QUIN
MTT assay (formazan production)
0.5
0.4
0.3
0.2
0.1
0.0
24 h
48 h
72 h
D
Control
10 μM QUIN
25 μM QUIN
MTT assay (formazan production)
0.5
0.4
0.3
0.2
0.1
0.0
24 h
48 h
72 h
C
Control
10 μM QUIN
25 μM QUIN
LDH activity
0.5
0.4
0.3
0.2
0.1
0.0
24 h
48 h
72 h
E
Control
10 μM QUIN
25 μM QUIN
LDH activity
0.4
0.3
0.2
0.1
0.0
24 h
48 h
72 h

Figure 2

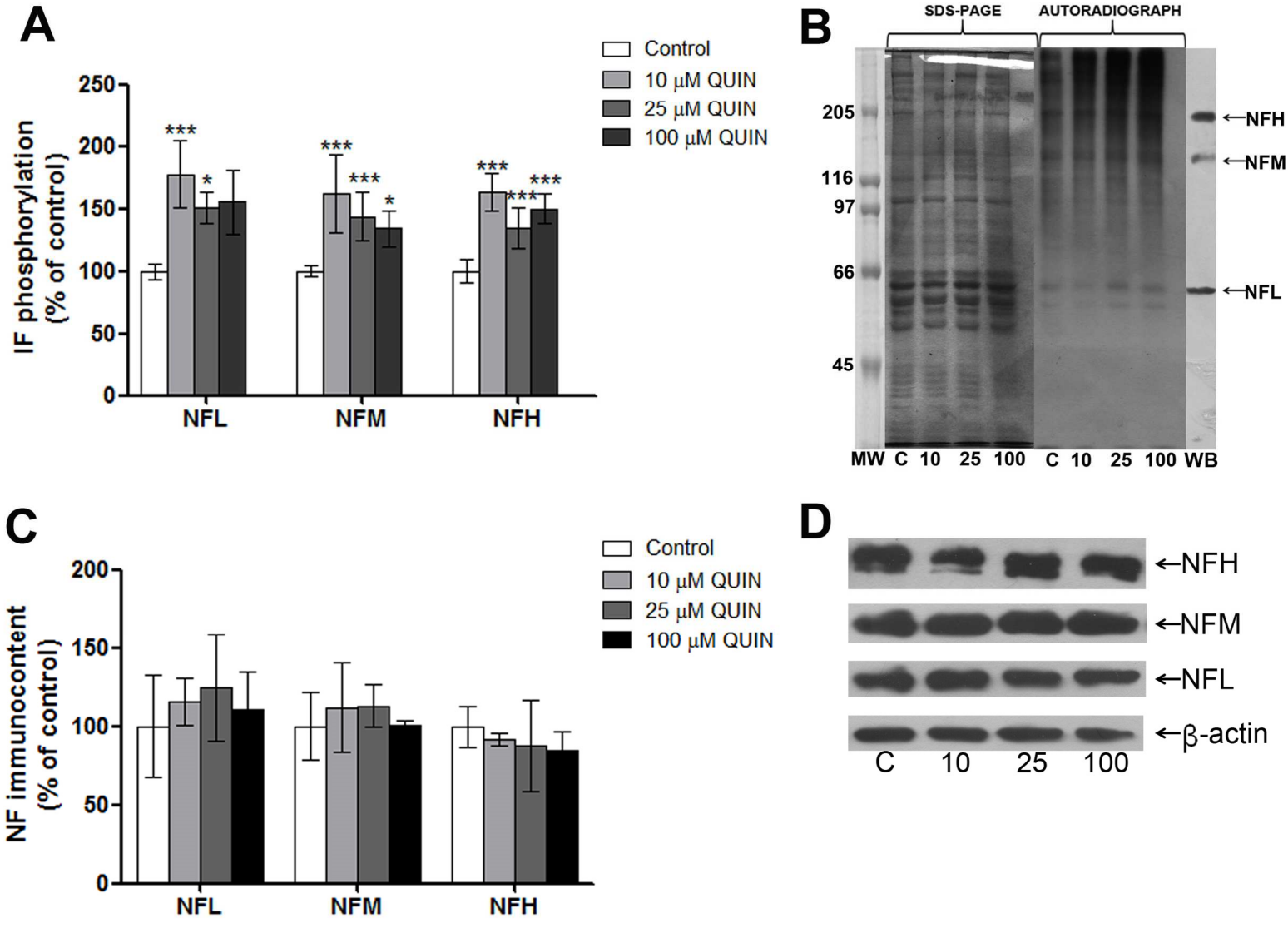
A
Control
10 μM QUIN
25 μM QUIN
100 μM QUIN
IF phosphorylation (% of control)
250
200
150
100
50
0
***
*
***
***
*
***
***
***
NFL
NFM
NFH
B
SDS-PAGE
AUTORADIOGRAPH
205
116
97
66
45
←NFH
←NFM
←NFL
MW C 10 25 100 C 10 25 100 WB
C
Control
10 μM QUIN
25 μM QUIN
100 μM QUIN
NF immunocontent (% of control)
200
150
100
50
0
NFL
NFM
NFH
D
←NFH
←NFM
←NFL
←β-actin
C 10 25 100

Figure 3

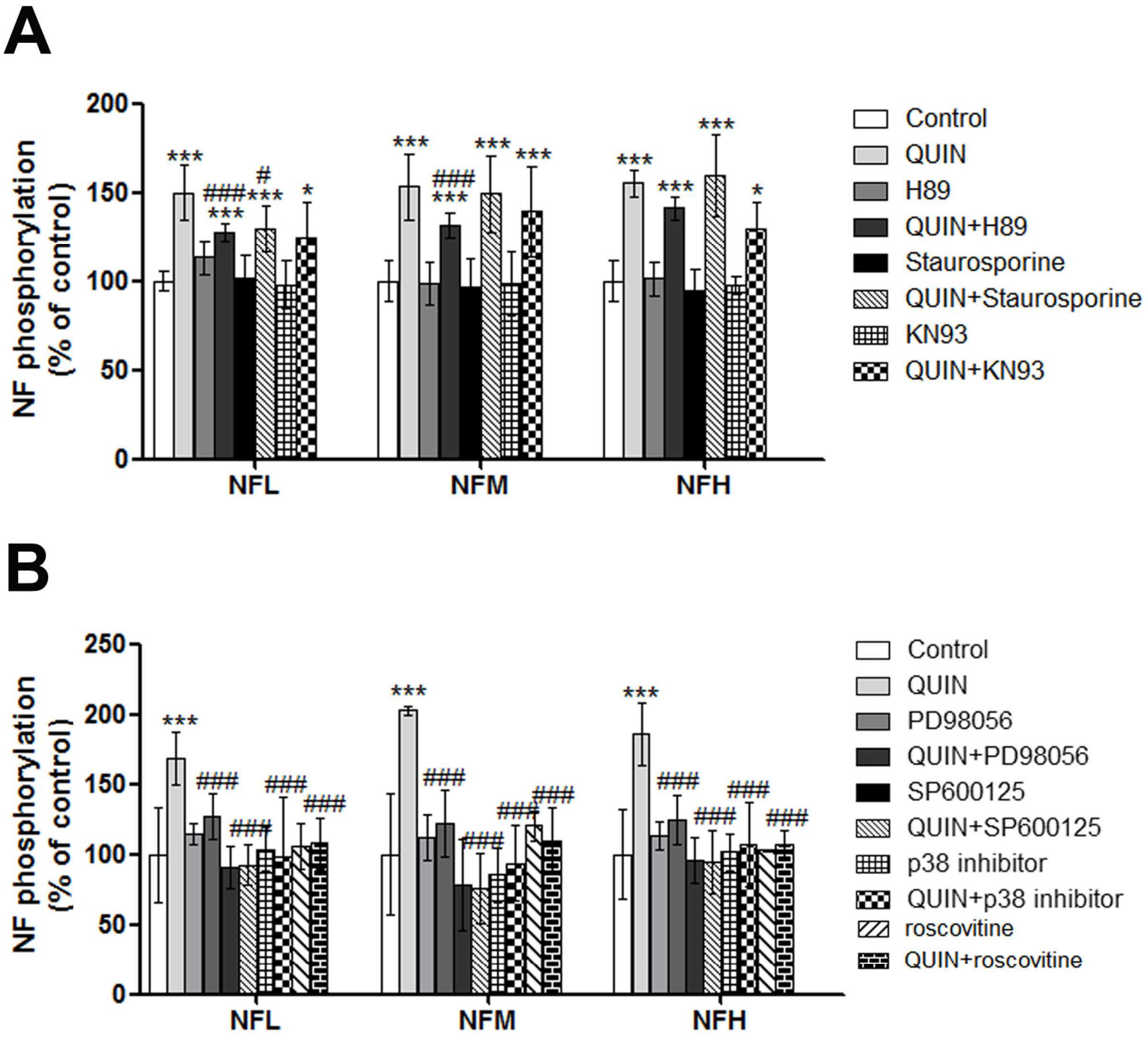
A
NF phosphorylation (% of control)
200
150
100
50
0
NFL
NFM
NFH
Control
QUIN
H89
QUIN+H89
Staurosporine
QUIN+Staurosporine
KN93
QUIN+KN93
B
NF phosphorylation (% of control)
250
200
150
100
50
0
NFL
NFM
NFH
Control
QUIN
PD98056
QUIN+PD98056
SP600125
QUIN+SP600125
p38 inhibitor
QUIN+p38 inhibitor
roscovitine
QUIN+roscovitine

Figure 4

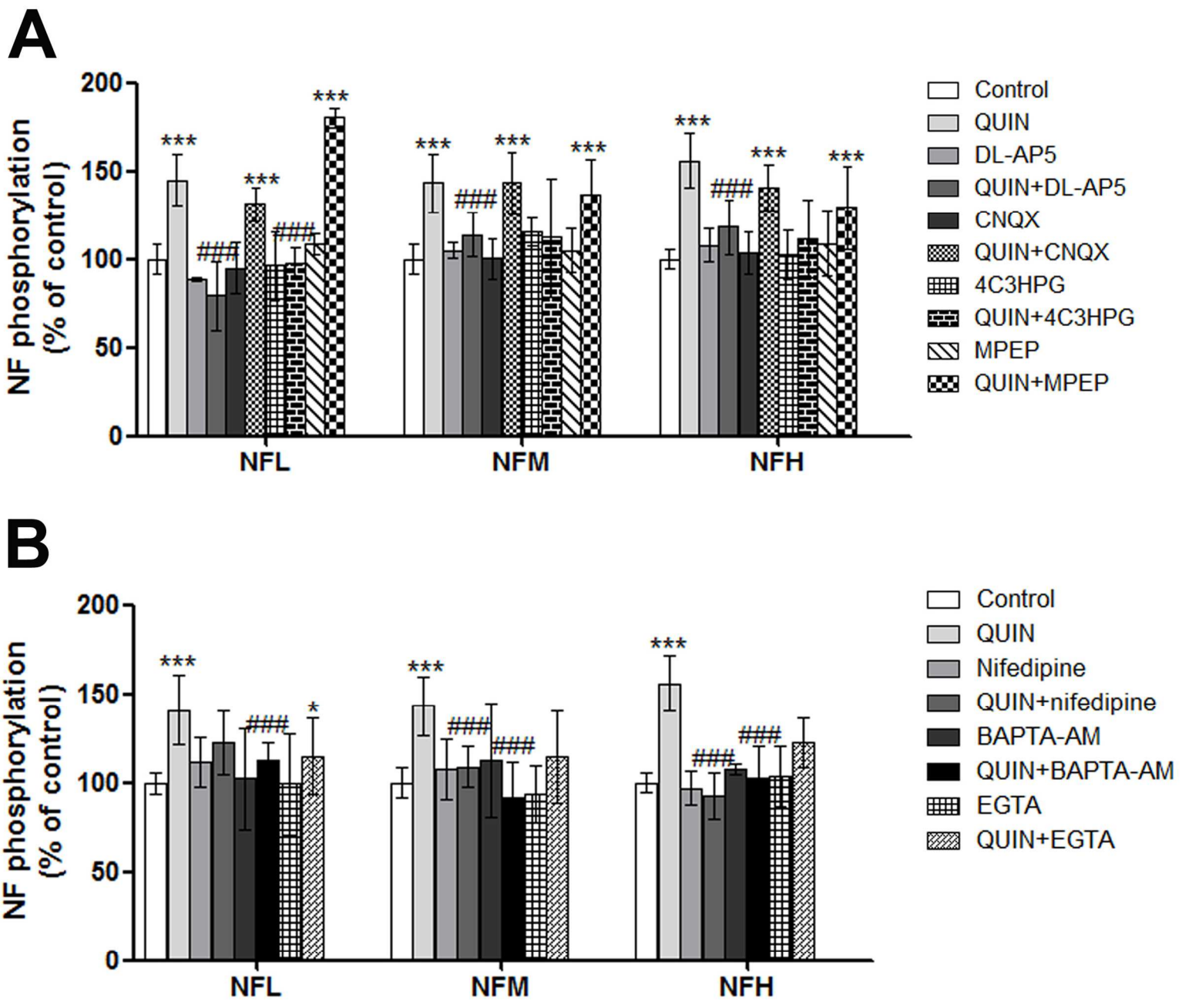
A
NF phosphorylation (% of control)
200
150
100
50
0
***
###
NFL
NFM
NFH
Control
QUIN
DL-AP5
QUIN+DL-AP5
CNQX
QUIN+CNQX
4C3HPG
QUIN+4C3HPG
MPEP
QUIN+MPEP
B
NF phosphorylation (% of control)
*
Nifedipine
QUIN+nifedipine
BAPTA-AM
QUIN+BAPTA-AM
EGTA
QUIN+EGTA

Figure 5

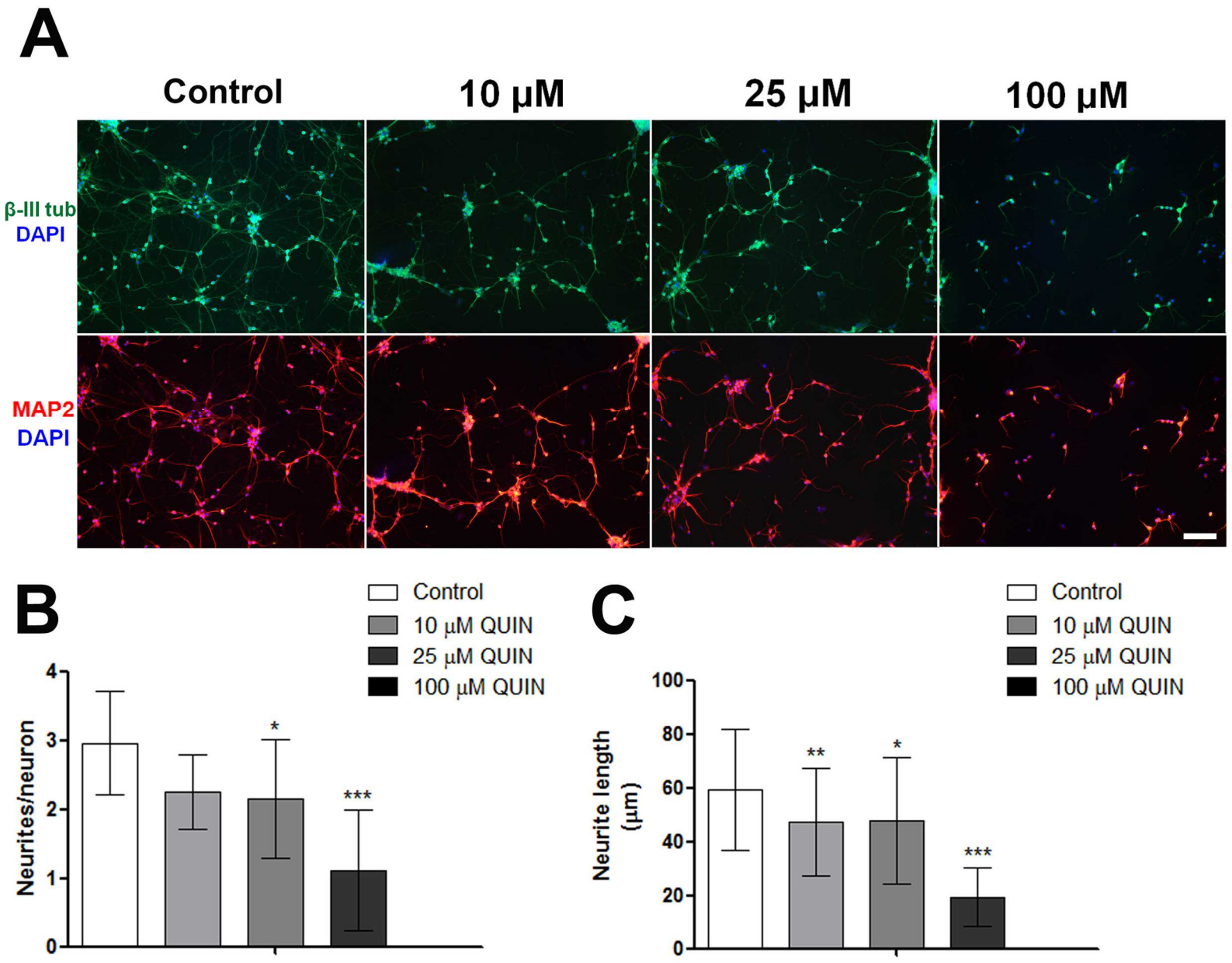
A
Control
10 µM
25 µM
100 µM
β-III tub
DAPI
MAP2
DAPI
B
Control
10 µM QUIN
25 µM QUIN
100 µM QUIN
Neurites/neuron
0
1
2
3
4
*
***
C
Control
10 µM QUIN
25 µM QUIN
100 µM QUIN
Neurite length (µm)
0
20
40
60
80
100
**
*
***

Figure 6

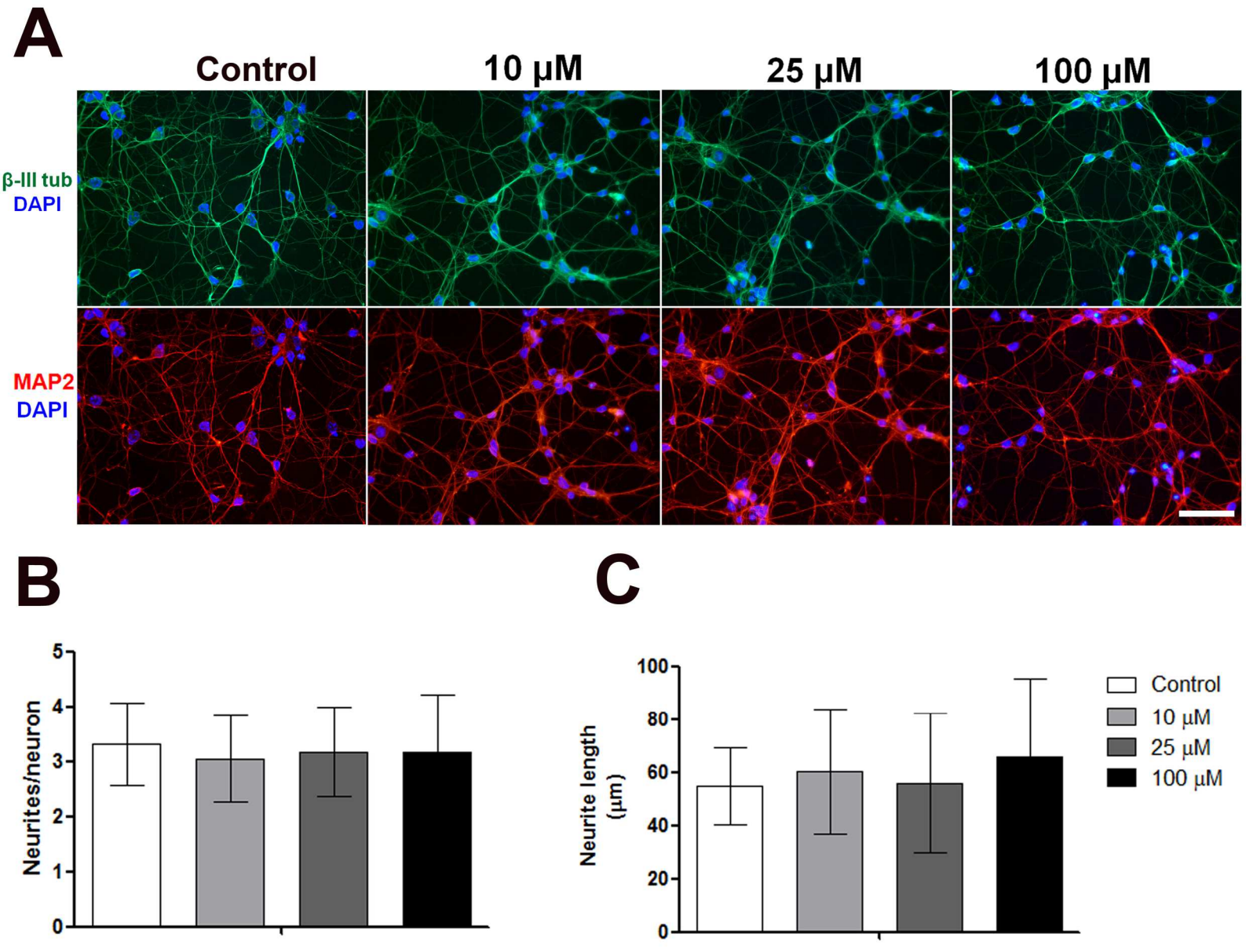
A
Control
10 μM
25 μM
100 μM
β-III tub
DAPI
MAP2
DAPI
B
Neurites/neuron
0
1
2
3
4
5
C
Neurite length (μm)
0
20
40
60
80
100
Control
10 μM
25 μM
100 μM

Figure 7

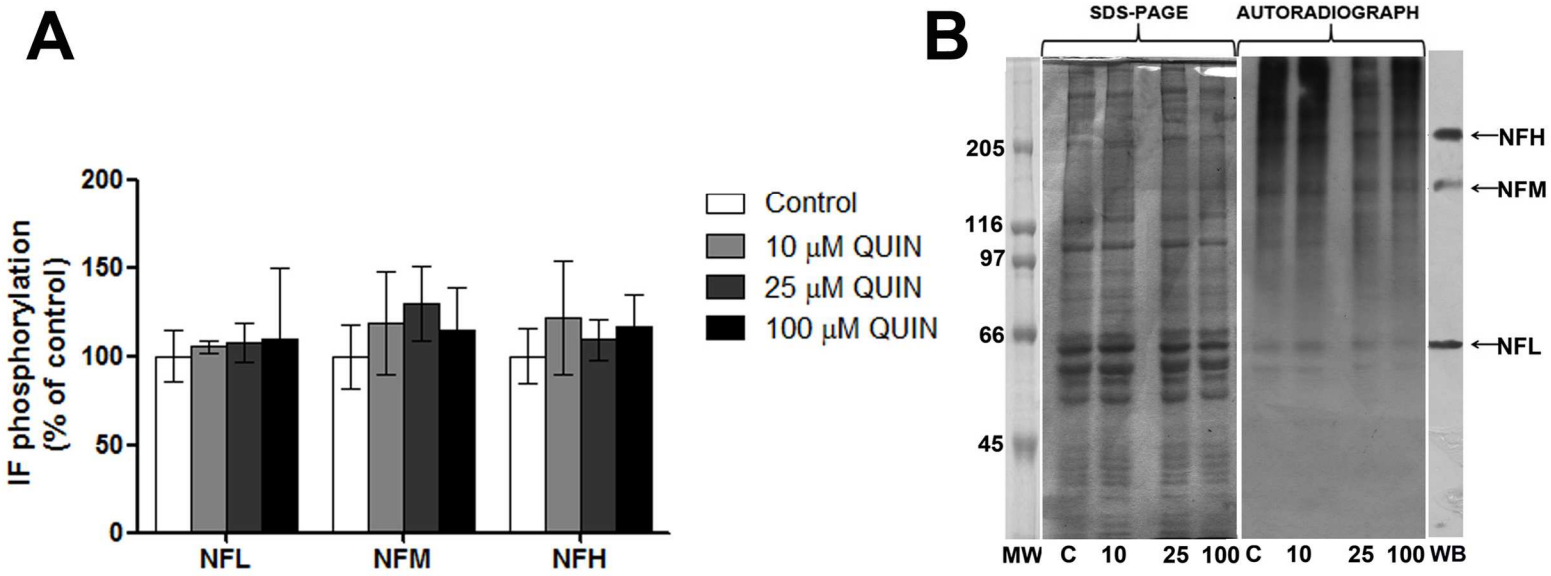
A
IF phosphorylation (% of control)
200
150
100
50
0
NFL
NFM
NFH
Control
10 μM QUIN
25 μM QUIN
100 μM QUIN
B
SDS-PAGE
AUTORADIOGRAPH
205
116
97
66
45
NFH
NFM
NFL
MW C 10 25 100 C 10 25 100 WB

Figure 8

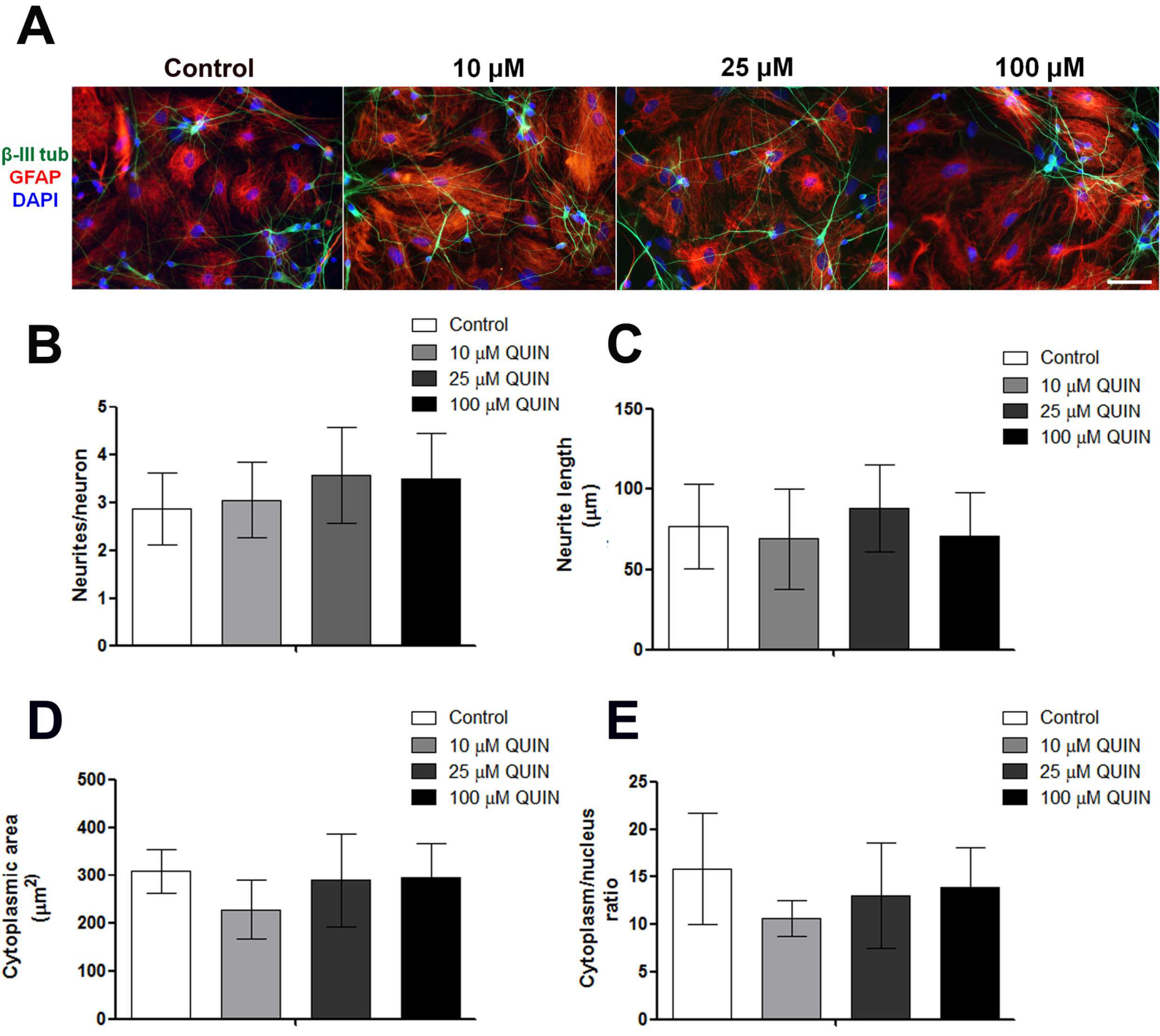
A
Control
10 µM
25 µM
100 µM
β-III tub
GFAP
DAPI
B
Control
10 µM QUIN
25 µM QUIN
100 µM QUIN
Neurites/neuron
0
1
2
3
4
5
C
Control
10 µM QUIN
25 µM QUIN
100 µM QUIN
Neurite length (µm)
0
50
100
150
D
Control
10 µM QUIN
25 µM QUIN
100 µM QUIN
Cytoplasmic area (µm2)
0
100
200
300
400
500
E
Control
10 µM QUIN
25 µM QUIN
100 µM QUIN
Cytoplasm/nucleus ratio
0
5
10
15
20
25

Figure 9

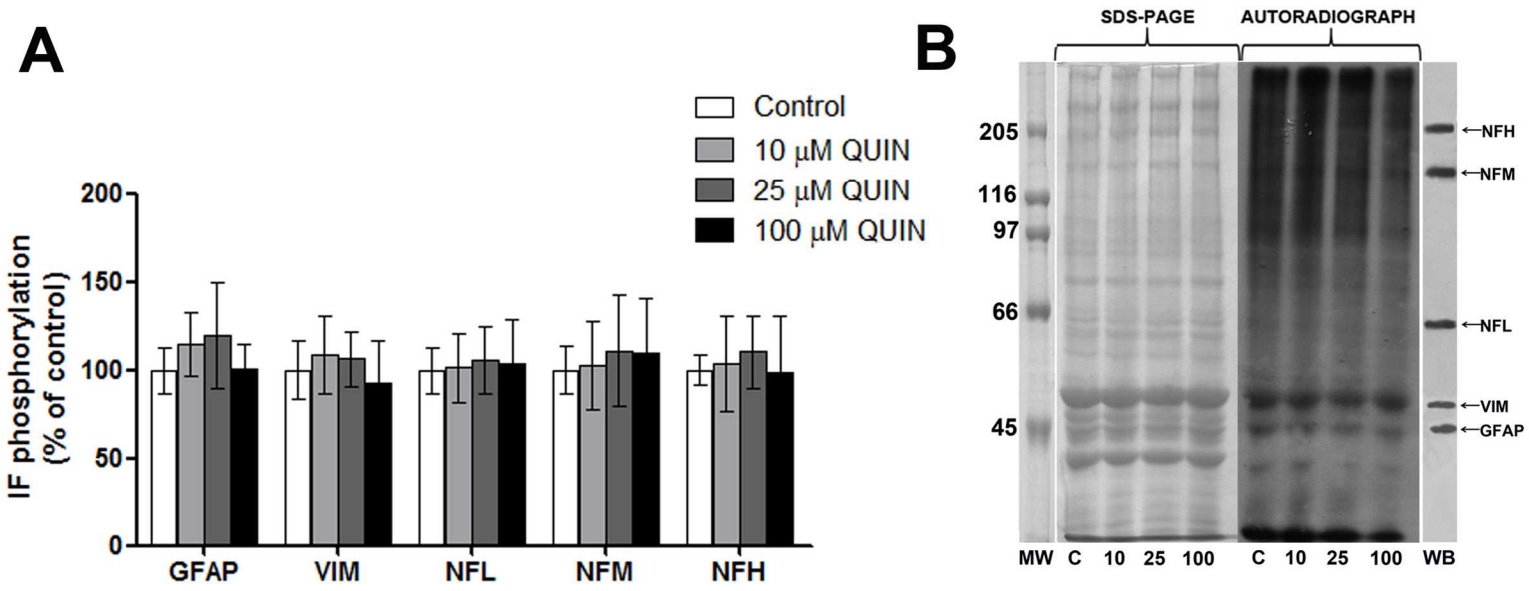
A
Control
10 μM QUIN
25 μM QUIN
100 μM QUIN
IF phosphorylation (% of control)
200
150
100
50
0
GFAP
VIM
NFL
NFM
NFH
B
SDS-PAGE
AUTORADIOGRAPH
205
116
97
66
45
←NFH
←NFM
←NFL
←VIM
←GFAP
MW C 10 25 100 C 10 25 100 WB

PARTE III

1. DISCUSSÃO

O foco deste trabalho foi acompanhar a evolução dos danos celulares causados pelo QUIN durante as primeiras semanas após o insulto excitotóxico. Atenção especial foi dada aos mecanismos moleculares direcionados para o citoesqueleto neural de ratos jovens e à relação entre o rompimento da homeostase do citoesqueleto e o dano celular excitotóxico causado pelo QUIN. Para isto, utilizamos 3 desenhos experimentais: o primeiro (desenho experimental 1) foi uma abordagem *in vivo*, a qual consistiu numa injeção intraestriatal do metabólito em ratos de 30 dias de idade mimetizando um modelo animal para a DHJ. Nesta abordagem investigamos a evolução das ações deste metabólito sobre o citoesqueleto e sobre alterações comportamentais e histopatológicas durante três semanas após a injeção, relacionando esses achados com os danos celulares e alterações comportamentais de humanos com DHJ. No segundo desenho experimental (desenho experimental 2) utilizamos fatias estriatais provenientes de ratos de 30 dias de idade tratadas agudamente com QUIN. Nesta abordagem verificamos os mecanismos moleculares direcionados para o citoesqueleto, por ser o estriado uma das principais regiões afetadas por este metabólito, constituindo este um estudo *ex vivo*. Este desenho experimental nos permite investigar mais profundamente as vias de sinalização direcionadas ao citoesqueleto que participam das ações desta excitotoxina. O terceiro desenho experimental (desenho experimental 3), considerado uma abordagem *in vitro*, utiliza células neurais, astrócitos e neurônios estriatais em cultura primária, na tentativa de verificar as respostas das células isoladas às altas concentraçãoes de QUIN, permitindo estabelecer uma relação entre a perda de homeostase do sistema fosforilante e o rompimento do citoesqueleto. Além disso, co-culturas de astrócitos e neurônios

constituiram uma importante abordagem que nos permitiu evidenciar as relações intercelulares de proteção ao insulto excitotóxico.

1.1. Desenho experimental 1: Alterações neuroquímicas, histopatológicas e comportamentais causadas pelo QUIN em ratos jovens - participação do citoesqueleto

Nesta abordagem experimental estudamos os efeitos de uma única injeção intraestriatal de QUIN sobre a excitotoxicidade, alterações comportamentais, homeostase do citoesqueleto e alterações histopatológicas de diferentes regiões cerebrais de ratos jovens. Animais de 30 dias de idade foram submetidos a uma única injeção de 150 nmol de QUIN no estriado, e os parâmetros determinados foram analisados 1, 7, 14 e 21 dias após a injeção. Um estudo prévio do nosso grupo já havia demonstrado que a injeção de QUIN provoca um efeito a curto prazo sobre a homeostase do citoesqueleto, observado 30 minutos após a administração da excitotoxina, levando a um desequilíbrio do sistema fosforilante associado ao citoesqueleto neural estriatal, causando hiperfosforilação dos FI gliais e neuronais mediada pela ativação de receptores NMDA e estresse oxidativo (Pierozan et al., 2010). No entanto, consideramos importante estender esse estudo para um período mais longo, abrangendo as três primeiras semanas após o insulto, o que nos permite avaliar melhor a participação do citoesqueleto na evolução do dano celular causado pelo QUIN.

Os resultados obtidos mostraram diferentes padrões de alterações dependendo da região cerebral. O espalhamento da onda excitotóxica da zona de lesão para outras regiões cerebrais sugere um dano espaço-temporal evocado pelo QUIN até três semanas

após a lesão. Os eventos excitotóxicos desencadeados pelo QUIN no estriado se mostraram rápidos e transitórios, iniciando-se 30 min após a injeção e restaurando os níveis basais de glutamato e Ca^{2+} após 24 horas. Estes efeitos foram seguidos de gliose reativa e alterações na homeostase do citoesqueleto neural, que ocorreram 24 horas após a lesão. Mais tardiamente, entre 7 e 14 dias após a injeção, houve o aparecimento de morte neuronal. No córtex cerebral, a excitotoxicidade mostrou-se de início rápido, porém com uma duração de intermediária (no caso da captação de glutamato) a persistente (no caso da captação de Ca^{2+}). Nesta estrutura cerebral a astrogliose, alteração do citoesqueleto e neurodegeneração ocorreram mais tardiamente, 7 (no caso da astrogliose) e 14 dias (no caso da neurodegeneração e alteração do citoesqueleto) após a lesão. Por outro lado, apesar dos efeitos excitotóxicos causados pelo QUIN no hipocampo serem de início rápido e persistente, não se observou astrogliose e neurodegeneração no período estudado, enquanto que as alterações no citoesqueleto apareceram mais tardiamente, 21 dias após a lesão.

As concentrações extracelulares de glutamato são altamente reguladas através de transportadores específicos localizados principalmente nas células gliais, mas também nos neurônios. O glutamato é captado pelas células gliais e metabolizado à glutamina, que por sua vez é liberada para o espaço extracelular e captada pelos neurônios, sendo novamente convertida a glutamato para reabastecer o *pool* de neurotransmissor (McKenna, 2007). A falha na remoção do glutamato após sua liberação leva ao seu acúmulo na fenda sináptica e à ativação prolongada de receptores glutamatérgicos, podendo causar uma mudança nas concentrações intracelulares de íons, especialmente o Ca^{2+}. O aumento excessivo de Ca^{2+} intracelular pode iniciar cascatas de sinalização que irão levar à morte celular (Arundine and Tymianski, 2003). Além disso, modificações em alguns componentes da neurotransmissão glutamatérgica têm sido reportadas em

estudos *post mortem* de pacientes com a DH e em modelos transgênicos da doença, sugerindo que a transmissão glutamatérgica pode culminar no desenvolvimento de um mecanismo excitotóxico nesta doença (Faideau et al., 2010, Marco et al., 2013). Nesse sentido, podemos propor que as alterações na captação de glutamato e de Ca^{2+} observadas nos animais tratados com QUIN possam estar causando um quadro de excitotoxicidade nas 3 estruturas estudadas, e é provável que a excitotoxicidade seja um dos primeiros eventos que o QUIN desencadeia no cérebro, culminando em astrogliose, alterações do citoesqueleto e morte neuronal, sendo que estes achados podem estar relacionados com as alterações comportamentais vistas no estudo.

A astrogliose é um processo desencadeado quando há um dano ao SNC, na tentativa de restaurar a homeostase cerebral durante a injúria (Pekny and Nilsson, 2005). Isso ocorre através de importantes funções que incluem a formação de cicatrizes gliais, regulação da resposta imune, modulação da sobrevivência neural e crescimento de neuritos (Sofroniew, 2009). A gliose reativa é um processo de astrogliose que causa várias mudanças moleculares e morfológicas nos astrócitos, incluindo hipertrofia, estrelação e proliferação celular, além de superexpressão de GFAP. O conjunto das alterações astrocitárias pode levar a alteração nas funções e na viabilidade neuronal (Pekny and Nilsson, 2005). Essas alterações podem ser benéficas ou prejudiciais aos neurônios, sendo que as consequências dependem de diversos fatores, como a idade do organismo, o tipo e a extensão da lesão (Sofroniew, 2009). Os resultados obtidos neste trabalho mostraram que os níveis alterados de fosforilação da GFAP foram acompanhados de aumento no imunocoteúdo dessa proteína no estriado e córtex cerebral, mas não no hipocampo. Esses resultados estão de acordo com a análise imunohistoquímica que mostrou astrogliose no estriado e no córtex 24 horas e 7 dias, respectivamente, depois da injeção com QUIN, e ausência de astrogliose no hipocampo

até 21 dias depois da lesão. Visto que os astrócitos foram rapidamente ativados, especialmente no estriado, e a morte neuronal ocorreu mais tardiamente em resposta ao dano excitotóxico provocado pela injeção com QUIN, é possível que os astrócitos estejam produzindo fatores solúveis tóxicos para os neurônios, contribuindo para a neurodegeneração vista nos animais injetados com QUIN.

Com relação aos efeitos do QUIN sobre a GFAP, nossos resultados mostraram que houve um aumento no imunoconteúdo dessa proteína, concomintante com aumento da fosforilação 24 horas após a injeção de QUIN, no estriado. Nós não podemos descartar que o aumento da fosforilação se deu pelo aumento na expressão da proteína, uma vez que no estudo *in vivo* não foi possivel usar ferramentas farmacológicas capazes de esclarecer se o aumento do imunoconteúdo está relacionado com expressão proteica aumentada. Por outro lado, o aumento do imunoconteúdo no córtex 14 dias após a injeção foi acompanhado de hipofosforilação da GFAP, fato que não era esperado. Embora ainda não tenhamos a explicação para esta evidência experimental, nossos resultados podem ser um indicativo de gliose reativa, que é um processo complexo que pode variar de célula para célula e de região para região no cérebro, de acordo com a intensidade e duração do insulto (McGraw et al., 2001, Sofroniew, 2005).

Os nossos resultados mostraram que a injeção intraestriatal de QUIN causou hiperfosforilação da Ser55 e Ser57 localizados na região amino-terminal da subunidade NFL, 24 horas e 21 dias no estriado e hipocampo, respectivamente. Considerando que os sítios Ser55 e Ser57 são fosforilados principalmente pela PKA e PKCaMII (Sihag et al., 2007), respectivamente, no interior do axônio, é possível que estas cinases estejam mediando a hiperfosforilação da subunidade NFL nessas regiões cerebrais em resposta á injeção com QUIN. O nível de fosforilação desta subunidade regula a capacidade de polimerização/despolimerização dos NFs propriamente ditos e consequentemente o

equilíbrio entre a fase solúvel, representado pelas subunidades em sua forma livre ou de pequenos agregados e a fase insolúvel, representada pelas subunidades associadas em filamentos. A hiperfosforilação de sítios específicos pode causar um desequilíbrio no sentido das subunidades solúveis, prejudicando sua associação em filamentos, com consequente prejuízo na formação da citoarquitetura axonal (Sihag and Nixon, 1990). Podemos então propor que o QUIN esteja interferindo na homeostase dos NF nos axônios *in vivo* o que pode afetar a fisiologia da região cerebral afetada.

A maior parte dos sítios de fosforilação da região carboxi-terminal dos NF está localizada na sequência de repetição dos aminoácidos lisina, serina e prolina (KSP) na região carboxi-terminal das subunidades NFM e NFH (Geisler et al., 1987, Xu et al., 1992), sendo que as cinases independentes de segundos mensageiros Cdk5 e MAPKs são as principais enzimas que fosforilam estes sítios (Jaffe et al., 1998, Veeranna et al., 2000). Evidências mostram que a fosforilação dos sítios KSP pode ser regulada por cascatas de sinalização que envolvem influxo de Ca^{2+} (Li et al., 1999), integrinas (Li et al., 2000) e fatores gliais (Dashiell et al., 2002). Cabe salientar que os NF quando são sintetizados no corpo celular não são fosforilados. Eles começam a ser fosforilados quando entram nos axônios e tornam-se progressivamente mais fosforilados a medida em que são transportados anterogradamente em direção aos terminais nervosos. Os NFs aberrantemente fosforilados nos KSP *repeats* perdem a capacidade de interagir com as cinesinas, que são as proteinas motoras responsáveis pelo transporte anterógrado e passam a agregar-se no interior do axônio levando à degeneração e morte neuronal (Yabe et al., 2001a, Yabe et al., 2001b).

Os nossos resultados mostraram que o QUIN ativou a Cdk5 no estriado e a via das MAPK no hipocampo, causando hiperfosforilação dos FI neuronais e dos KPS *repeats*. Estes resultados sugerem que o QUIN pode estar promovendo a agregação

entre os NF e causando a formação de aglomerados citotóxicos. Além disso, é descrito que a ativação da JNK inibe a translocação dos NF nos neuritos em crescimento causando acúmulo de fosfo-NF no corpo neuronal (DeFuria et al., 2006).

As proteínas fosfatases mais envolvidas na modulação da fosforilação dos FI são a PP1, PP2A e PP2B (Heimfarth et al., 2012). O QUIN induziu ativação da PP1 e PP2B no córtex cerebral 14 dias após a injeção, causando hipofosforilação dos FI neurais. A PP2B está envolvida na regulação do citoesqueleto neuronal em resposta a sinais extracelulares que aumentam o Ca^{2+} (Ferreira et al., 1993, Letourneau, 1996, Kayyali et al., 1997), enquanto que a PP1 pode ser regulada pela DARPP-32, cujos efeitos bioquímicos são dependentes dos níveis de fosforilação de sítios específicos (Hakansson et al., 2004, Heimfarth et al., 2012). Considerando que o aumento da fosforilação dos NF protege contra a ação da calpaina, uma importante protease que degrada os FI nos terminais nervosos, a desfosforilação destas estruturas poderá estar envolvida com sua proteólise prematura (Goldstein et al., 1987, Pant, 1988).

Visto que as alterações no citoesqueleto são respostas iniciais da disfunção celular, pode-se propor que a neurodegeneração vista no estriado e córtex cerebral seja uma resposta tanto à excitotoxicidade e astrogliose causadas pela injeção de QUIN, quanto à alteração na homeostase do citoesqueleto. Além disso, a agregação dos NF também pode estar relacionada com um aumento dos níveis de Ca^{2+} citosólico e morte celular induzida pela ativação dos receptores NMDA, deixando os neurônios mais susceptíveis ao dano excitotóxico (Sanelli et al., 2007).

As alterações no citoesqueleto hipocampal ocorreram mais tardiamente que nas outras estruturas. Além disso, houve ativação das MAPK 21 dias após a injeção no hipocampo. Visto que a p38MAPK é ativada em processos de morte celular e que a

ERK contribui para o processo de astrogliose (Che et al., 2001, Ito et al., 2009), é possível que as alterações no citoesqueleto e a ativação da via das MAPK estejam iniciando etapas de morte neuronal e astrogliose tardia no hipocampo, que não estão sendo detectadas nas primeiras semanas após a injeção intraestriatal com QUIN.

Com respeito a estas diferenças entre as regiões cerebrais, é possível que o QUIN cause diferentes tipos de estímulos dependendo do tecido cerebral, o que pode culminar em diferentes combinações de influxo e liberação de Ca^{2+}, levando a diferentes mecanismos de aumento de Ca^{2+} intracelular dependendo do tipo celular. Por exemplo, ele pode estar agindo não somente através dos receptores NMDA, mas também através dos canais L-VDCC, além dos receptores rianodina e IP3 do RE, que causam a liberação de Ca^{2+} dos estoques internos. Isto pode explicar porque o Ca^{2+} se mantém alterado no córtex cerebral e no hipocampo durante todo o período de estudo, apesar das oscilações de glutamato vistas nestas regiões. Além disso, a longa duração dos efeitos do QUIN pode não ser apenas por efeitos diretos, mas sim pela prolongada liberação de glutamato pelos astrócitos, o que poderia contribuir para o aumento do Ca^{2+} intracelular. Outro fator importante a ser considerado é que o Ca^{2+} pode ativar tanto cinases, como observado no estriado e no hipocampo, quanto fosfatases, como observado no córtex cerebral. Esses efeitos antagônicos podem ser explicados pelos diferentes padrões de flutuações das ondas de Ca^{2+} nas células estimuladas, gerando a ativação de diferentes vias de sinalização com consequentes respostas celulares (Berridge et al., 2003).

Além da perda seletiva e progressiva da homeostase do citoesqueleto, nossos resultados mostraram uma morte neuronal mais tardia em ratos jovens se comparado com os estudos em animais adultos. Em ratos adultos, o QUIN causa um dano neuronal massivo na região da lesão entre 30 minutos e 24 horas após a injeção, seguido por um dano neuronal progressivo que se estende até 14 dias após a administração de QUIN

(Beal et al., 1986, Brickell et al., 1999). Os efeitos da idade do animal na vulnerabilidade ao QUIN podem ser devidos a diferenças na expressão tanto dos receptores glutamatérgicos NMDA quanto não-NMDA durante a maturação cerebral (Haberny et al., 2002), além de mudanças na configuração de suas subunidades (Monyer et al., 1991, Williams et al., 1993, Benke et al., 1995), propriedades de condutância (Hestrin, 1992) e mudanças na densidade de receptores (Wenk et al., 1991, Pagliusi et al., 1994) que ocorrem em diversas regiões cerebrais de ratos e primatas na juventude e na idade adulta. Estas diferenças regionais na maturação e diferenciação dos receptores também podem explicar por que o hipocampo não apresentou neurodegeneração durante o período de estudo. Além disso, estes resultados são consistentes com os achados de outros estudos que mostraram que o hipocampo parece ser mais resistente à injúria tanto em modelos genéticos da DHJ (Shelbourne et al., 2007) quanto nos primeiros estágios da doença em humanos (van den Bogaard et al., 2011). Se realmente há um envolvimento excitotóxico na patogênese da DH e da DHJ, uma diferença na sensibilidade dos diferentes tipos neuronais relacionados com a idade do indivíduo pode contribuir para o entendimento dos diversos quadros fenotípicos vistos na doença juvenil e na doença na fase adulta.

Nossos achados histopatológicos sugerem que a morte neuronal não é necessária para desencadear o início dos sintomas cognitivos, visto que não houve neurodegeneração corticoestriatal antes de 7 dias após a lesão, e a disfunção cognitiva apareceu 24 h após a lesão. Talvez o quadro excitotóxico observado nas três estruturas estudadas seja condição suficiente para desencadear o déficit cognitivo encontrado nos animais lesionados. Por outro lado, as alterações motoras parecem ser consequência da neurodegeneração, visto que o déficit motor observado nos animais foi detectado somente após a neurodegeneração corticoestriatal. Isto é consistente com a hipótese de

que alterações motoras resultam de uma perda de neurônios estriatais (Albin et al., 1990, Kantor et al., 2006).

Estes resultados contribuem com novos conhecimentos a respeito dos mecanismos moleculares e comportamentais desencadeados pelo QUIN em ratos jovens. Os déficits cognitivos precederam as alterações motoras, enquanto que uma seletiva e progressiva gliose reativa, alteração no citoesqueleto e morte neuronal se iniciaram no estriado e se propagaram para o córtex e hipocampo. Nós propomos que os efeitos deletérios do QUIN podem interferir com os mecanismos de sinalização altamente regulados no cérebro imaturo. Uma questão central no entendimento da patogênese da DH é determinar as alterações moleculares, celulares e sinápticas que constituem a base das mudanças comportamentais e neuropatológicas. Embora existam vários estudos mostrando diversos mecanismos de disfunções moleculares que ocorrem na doença, os exatos mecanismos que iniciam as cascatas de sinalização deletéria que irão culminar nas disfunções celulares, teciduais e comportamentais ainda permanecem incertos. Este é um dos primeiros estudos que descreve as alterações bioquímicas, histopatológicas e comportamentais que ocorrem nas primeiras semanas após a administração intraestriatal de QUIN em animais jovens. Modelos animais que mimetizem os sintomas clínicos e neurobiológicos da DHJ podem prover novas abordagens para o estudo da patofisiologia da doença, e com isso permitir o desenvolvimento de novas terapias. Esperamos que nossos achados possam servir como uma importante ferramenta para o melhor entendimento da neurodegeneração precoce que ocorre na doença humana.

Para melhor comparação e integração entre as disfunções enzimáticas direcionadas para o citoesqueleto e o dano celular nas diferentes regiões cerebrais estudadas, o conjunto dos resultados obtidos em estriado, cortex cerebral e hipocampo de ratos injetados com QUIN estão representados na Figura 7.

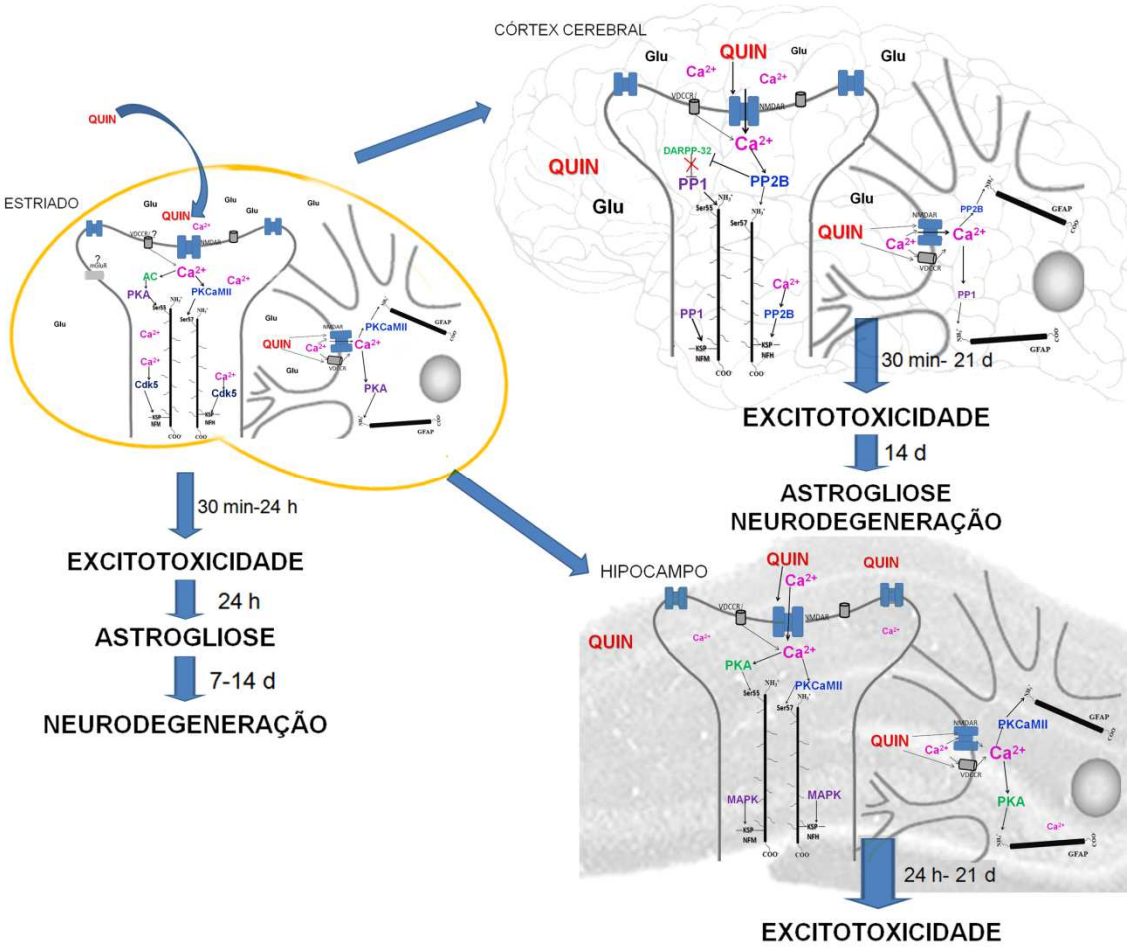

Figura 7. Mecanismos que levam a alterações do citoesqueleto e sua relação com o dano celular causados pelo QUIN *in vivo*. Um dos principais mecanismos da toxicidade do QUIN é através da superestimulação dos receptores NMDA. Adicionalmente, o QUIN causa diminuição da captação de glutamato do espaço extracelular, aumentando o quadro de excitotoxicidade e causando aumento das concentrações de Ca^{2+} intracelular. O Ca^{2+} é um elemento chave nos efeitos do QUIN sobre o citoesqueleto neural. No estriado e hipocampo, ele ativa a PKCaMII e a PKA, causando aumento da fosforilação dos sítios Ser55 e Ser57 da subunidade NFL e da região amino-terminal da GFAP. A Cdk5 também é ativada por Ca^{2+} no estriado, fosforilando os sítios KSP *repeats* das subunidades NFM/H. No hipocampo, esses sítios são fosforilados pela via das MAPK. No córtex, o Ca^{2+} ativa a proteína PP2B (calcineurina), que por sua vez inativa a DARPP-32, deixando a PP1 ativa. Essas duas enzimas desfoforilam os sítios Ser55 e Ser57 da NFL e os sítios KPS *repeats* da NFM/H, além da região amino-terminal da GFAP. Esquema geral dos efeitos da injeção intraestriatal com QUIN sobre o estriado, córtex cerebral e hipocampo de ratos de 30 dias de idade.

1.2. Desenho experimental 2 - mecanismos moleculares das alterações no citoesqueleto causadas pelo QUIN

Considerando que o QUIN altera a homeostase do citoesqueleto neural de ratos jovens *in vivo* e que este efeito pode estar relacionado com a neurodegeneração encontrada, procuramos entender um pouco melhor os mecanismos moleculares pelos quais este metabólito age no citoesqueleto. Uma vez que o corpo estriado é uma estrutura bastante susceptível às ações do QUIN e é a principal estrutura cerebral afetada na DH, nós verificamos o efeito de uma exposição *ex vivo,* utilizando fatias de tecido expostas ao QUIN, sobre a fosforilação dos FI neuronais e gliais no estriado de ratos jovens, determinando as cascatas de sinalização envolvidas na ruptura da homeostase do citoesqueleto**.**

Os resultados mostraram que 100 μM QUIN adicionado diretamente sobre fatias de estriado durante 50 minutos causou hiperfosforilação de GFAP e das subunidades dos NF em animais de 30 dias de idade. Isso está de acordo com os nossos resultados *in vivo*, que mostraram hiperfosforilação dos FI no estriado 30 min (Pierozan et al, 2010) e 24 horas após a injeção intraestriatal com QUIN.

Os efeitos do QUIN sobre o citoesqueleto estriatal foram principalmente, mas não exclusivamente, dependentes de receptores glutamatérgicos havendo algumas diferenças dependendo do tipo celular. Nos astrócitos, as ações do QUIN foram dependentes principalmente da ativação de receptores NMDA e dos canais L-VDCC. Já nos neurônios, o QUIN ativou os receptores NMDA, os mGluR do tipo 1 (mGluR1) e mGluR5, além de canais L-VDCC. Esses achados sustentam a hipótese de que o QUIN age em diferentes vias de sinalização dependendo do tipo celular afetado. A ativação

dos receptores mGluR1 pelo QUIN é consistente com o importante papel destes receptores no estriado, sendo que a ativação dos receptores mGluR1 e 5 exercem ações distintas dependendo do subtipo neuronal afetado (Bonsi et al., 2008).

Os receptores NMDA estão envolvidos nos efeitos desencadeados pelo QUIN tanto nos neurônios quanto nos astrócitos. A ativação sustentada dos receptores NMDA leva a um aumento excessivo no influxo de íons Ca^{2+}, causando excitotoxicidade, que por sua vez pode iniciar diversos tipos de cascatas neurotóxicas, incluindo vias de sinalização formadas pela ativação de cinases (Szydlowska and Tymianski, 2010).

É importante ressaltar que os receptores VDCC regulam a atividade elétrica neuronal, modulam a abertura de outros canais e controlam numerosos processos celulares, como a liberação de NT, sobrevivência neuronal, ativação de cinases, crescimento de neuritos e trancrição gênica através do influxo de Ca^{2+} extracelular, seguido de despolarização da membrana (Dolmetsch et al., 2001, Lipscombe et al., 2004). Em processos patológicos relacionados com a excitotoxicidade, a ativação desses receptores pode contribuir para o influxo massivo de Ca^{2+} para o citoplasma, além de contribuir para a ativação dos receptores NMDA e AMPA (Freund and Reddig, 1994, Akopian and Walsh, 2002).

Entre as múltiplas ações do Ca^{2+} no SNC, há também a modulação de sistemas enzimáticos de fosforilação de proteinas do citoesqueleto (Zamoner et al., 2008, Loureiro et al., 2009, Heimfarth et al., 2012). Utilizando um bloqueador de receptores L-VDCC e quelantes intra e extracelulares de Ca^{2+}, nós observamos que houve uma prevenção dos efeitos causados pelo QUIN sobre a fosforilação dos FI em fatias estriatais, mostrando a relevância deste segundo mensageiro nos efeitos desencadeados pelo QUIN tanto em astrócitos quanto em neurônios *ex vivo*.

Interessantemente, o bloqueio da liberação de Ca^{2+} pelo RE através dos receptores rianodina preveniu os efeitos do QUIN nos neurônios, mas não em astrócitos estriatais. Os receptores rianodina contribuem para a plasticidade sináptica, em mecanismos de aprendizado e memória e em processos de apoptose (Chavis et al., 1996, Schwab et al., 2001, Galeotti et al., 2008). Com base nesses resultados, podemos concluir que o QUIN causa aumento de Ca^{2+} intracelular nas células neuronais pelo influxo deste íon através dos receptores NMDA, canais L-VDCC e liberação dos estoques internos, reforçando o papel do Ca^{2+} nas ações do QUIN sobre o citoesqueleto.

O aumento de Ca^{2+} intracelular proveniente dos receptores NMDA e L-VDCC causado pelo QUIN nos astrócitos pode formar diferentes padrões de oscilação comparado com os causados nos neurônios, através do influxo de Ca^{2+} pelos canais NMDA, L-VDCC, mGluR5 e rianodina. Isto poderia explicar as diferentes respostas observadas nos dois tipos celulares devido à exposição ao QUIN *ex vivo*. Uma alteração na homeostase do Ca^{2+} leva a uma ativação direta ou indireta de cinases e fosfatases, que, por sua vez, regulam o equilíbrio de fosforilação/desfosforilação dos FI gliais e neuronais. Em processos patológicos, a habilidade dos neurônios e astrócitos em controlar o influxo de Ca^{2+} e restaurar seus níveis basais está comprometida, levando a um rompimento da homeostase desse íon e desencadeando a hiperativação de enzimas e de vias de morte celular (Mattson, 2007).

A transdução de sinais no SNC é muito dependente de três serina/treonina cinases: a PKA, a PKCaMII e a PKC (Scott and Soderling, 1992). A PKA pode ser ativada pelo aumento do AMPc formado pela enzima adenilato ciclase (AC). Existem diversos tipos de AC neurais que são ativadas por Ca^{2+} (Steiner et al., 2006). O sistema AMPc/PKA têm um grande papel integrativo nas células animais, é altamente expresso em neurônios, e representa uma via de sinalização crítica no processo de aprendizado e

memória (Drain et al., 1991, Malenka, 1994). A PKCaMII é uma cinase dependente de Ca^{2+} e calmodulina que está envolvida com a plasticidade neuronal e no aprendizado e memória, sendo o maior mediador de glutamato nesses eventos (Malenka and Nicoll, 1999). Além disso, ela pode participar da regulação tanto da morte neuronal, através do aumento da condutância do receptor AMPA (Oh and Derkach, 2005), quanto da sobrevivência neuronal, através da inibição da óxido nítrico sintase (NOS) (Komeima et al., 2000). Por sua vez, a PKC regula eventos de curta duração no cérebro, como fluxo de íons e liberação de NT, de média duração, como modulação de receptores e de longa duração, como remodelamento sináptico e expressão gênica (RamaRao and Bhattacharya, 2012). Vários estudos têm relacionado a PKC com injúria ao SNC (Felipo et al., 1993, Krieger et al., 1996). A PKA, PKCaMII e PKC também estão envolvidas com a fosforilação da região amino-terminal dos FI (Omary et al., 2006, Pierozan et al., 2010, Heimfarth et al., 2012, Pierozan et al., 2012).

A fosforilação da região amino-terminal dos FI é conhecida por regular a associação/desassociação dos FI e tem um papel importante na divisão celular. Ainda, desregulação na fosforilação de sítios dessa região pode levar à desassociação dos FI e contribuir para o desequilíbrio da homeostase do citoesqueleto (Gill et al., 1990, Heins et al., 1993). O aumento dos níveis intracelulares de Ca^{2+} pode ativar a PKCaMII e a PKA. Nos neurônios, estas enzimas fosforilam a Ser57 e Ser55, respectivamente, localizados na região amino-terminal da NFL (Omary et al., 2006). O papel da fosforilação da região amino-terminal nos NF está relacionado com a formação do NF heteropolimérico (Ching and Liem, 1999). Em astrócitos, a fosforilação dos domínios amino-terminais de vimentina e GFAP é importante para a associação dos filamentos, tendo um importante papel na divisão celular. A fosforilação anormal destes sítios nessas proteínas pode causar desassociação dos FI, contribuindo para o desequilíbrio da

homeostase celular (Gill et al., 1990, Heins et al., 1993). O estudo *in vitro* com QUIN mostrou que este metabólito é capaz de ativar a PKA e a PKCaMII nos neurônios e astrócitos, através do aumento de Ca^{2+} intracelular. Estas enzimas, por sua vez, fosforilam os sítios Ser55 e Ser 57 da subunidade NFL e a região amino-terminal da GFAP. Estes resultados sugerem, portanto, que a toxicidade do QUIN *ex vivo* pode incluir desestabilização da rede de FI tanto nas células neuronais quanto astrocitárias.

Por outro lado, a PKC foi ativada apenas nos neurônios, contribuindo para as ações do QUIN neste tipo celular. Essa enzima é ativada principalmente por diacilglicerol (DAG), através da ativação de receptores ou pela despolarização da membrana celular (Majewski and Iannazzo, 1998). O DAG pode ser gerado através da hidrólise de fosfatidilinositídios ou de fosfatidilcolina da membrana plasmática, através da ação da fosfolipase C (PLC) (Huang, 1989). A hidrólise destes lipídios de membrana pela PLC causa um aumento transitório de IP3 e DAG. O IP3 abre canais de Ca^{2+} do RE, enquanto que o DAG é um ativador da PKC (Berridge, 1987). Em particular, no SNC, os mGluR1 podem causar ativação da PLC, com consequente ativação da PKC (Hermans and Challiss, 2001). Levando em consideração que a fosforilação da NFL foi parcialmente prevenida por um antagonista de receptores mGluR1, por inibição da PLC e por inibição da PKC, podemos propor que esta via de sinalização está implicada nas ações do QUIN sobre os NFs.

Além das cinases dependentes de segundos mensageiros, os FI podem ser fosforilados por cinases independentes de segundos mensageiros, como a ERK1/2, a JNK, a p38MAPK e a Cdk5. Estas enzimas fosforilam a região carboxi-terminal dos FI, regulando a sua interação com outros FI e com outras proteínas do citoesqueleto (Geisler et al., 1987, Omary et al., 2006, Holmgren et al., 2012). Os nossos resultados mostraram que a Cdk5 está envolvida na hiperfosforilação dos sítios KSP *repeats*

causada pelo QUIN, e que a JNK está apenas parcialmente envolvida na fosforilação da subunidade NFM. A Cdk5 é um membro da família das cinases dependentes de ciclina. A sua atividade está restrita ao SNC e ela é ativada pelas proteínas p35 e p39, as quais possuem padrões neuronais específicos. Nos últimos anos, tem se verificado que a Cdk5 possui distintos papéis no SNC, funcionando como uma enzima integradora em diversas vias de transdução de sinais. Além do seu papel fisiológico, ela vem sendo implicada em várias desordens neurodegenerativas (Kesavapany et al., 2004). Estudos mostraram que a p35 pode ser clivada por uma protease dependente de Ca^{2+} (calpaina) produzindo um fragmento mais ativo, a proteína p25. Esta proteína transloca através da membrana e causa hiperativação, perda de compartimentalização e especifidade ao substrato da Cdk5 (Patrick et al., 1999). Insultos neurotóxicos, como excitotoxicidade, causam ativação da calpaína, níveis aumentados da p25 e hiperativação da Cdk5. Isto pode levar à fosforilação aberrante de componentes do citoesqueleto, como a proteína tau, proteinas associadas aos microtúbulos (MAPs) e NFs, podendo desencadear processos de morte neuronal (Patrick et al., 1999, Lee et al., 2000). É sabido que a fosforilação da porção carboxi-terminal da NFH restringe a sua associação com a cinesina, uma proteína do transporte anterógrado axonal, e estimula sua interação com a dineína, uma proteína do transporte retrógrado axonal resultando na diminuição da velocidade do transporte axonal de NF (Motil et al., 2006). Podemos então propor que o NFM e NFH hiperfosforilados na região carboxi-terminal podem formar agregados proteicos no interior dos axônios contribuindo para o dano celular causado pelo QUIN.

Podemos concluir, portanto, através dos resultados *ex vivo* que o rompimento da homeostase do citoesqueleto causada pelo QUIN é um processo complexo iniciado pela ativação de mGluRs e iGluR, além da ativação dos canais L-VDCC. Esses receptores de membrana ativam a via DAG/IP3/PLC e a liberação de Ca^{2+} do RE, levando a um

aumento do Ca^{2+} citosólico, que por sua vez irá desencadear uma cascata de eventos, incluindo a ativação de proteínas cinases dependentes e independentes de segundos mensageiros. Estas enzimas irão fosforilar sítios específicos das subunidades da GFAP e dos NF, desestabilizando o citoesqueleto tanto de neurônios quanto de astrócitos.

Os resultados *ex vivo* mostrando a ativação aberrante de diferentes cascatas de sinalização em resposta ao aumento do Ca^{2+} intracelular e rompimento da homeostase de proteinas do citoesqueleto no estriado podem estar associados à perda da homeostase celular, astrogliose e morte neuronal observados no animais tratados com QUIN. Estes resultados reforçam a hipótese de que a perda da homeostase do citoesqueleto faz parte do conjunto de processos característicos da injúria celular.

1.3. Desenho experimental 3 - Resposta de astrócitos e neurônios isolados ao QUIN e interação neurônio-astrócito

O isolamento e a cultura de células são ferramentas essenciais no estudo das funções celulares. As células isoladas e mantidas em condições controladas podem ser manipuladas e observadas em um nível que não seria possível utilizando o tecido intacto (Zhang and Kuhn, 2013). Além disso, a utilização de co-culturas possibilita a obtenção de dados sobre as interações neurônio-astrócito tanto em situação fisiológica quanto patológica. Considerando que tanto no modelo *in vivo* quanto no modelo *ex vivo* utilizando o QUIN como agente excitotóxico houve um desequilíbrio do sistema fosforilante associado ao citoesqueleto neural, e que este desequilíbrio pode estar associado com alterações morfológicas e dano celular, decidimos estudar os efeitos do QUIN sobre o citoesqueleto de astrócitos e neurônios primários isolados do estriado,

com enfoque na relação entre os níveis de fosforilação dos FI e a reorganização do citoesqueleto. Além disso, utilizamos co-cultura neurônio-astrócito estriatal para avaliar a contribuição dessa interação sobre os efeitos desencadeados pelo QUIN.

Observamos que o QUIN afetou o sistema fosforilante associado aos FI nas culturas neuronais e astrocitárias isoladas. Esses resultados estão de acordo com os estudos *in vivo* e *ex vivo* anteriormente discutidos, nos quais observamos uma alteração na fosforilação dos FI neurais. Além disso, a hiperfoforilação dos FI estriatais causou uma reorganização do citoesqueleto e alterações morfológicas em astrócitos e neurônios 24 horas após a exposição ao QUIN.

Os astrócitos são células multifuncionais que, além de terem um papel essencial no controle da homeostase cerebral e contribuir para o processamento de informações, são capazes de produzir respostas a um infindável número de insultos ao SNC (Buffo et al., 2009). Além disso, durante uma resposta à injúria cerebral, os astrócitos migram para o sítio da injúria, onde eles contribuem no reparo do tecido danificado criando uma cicatriz glial protetora além de responder à injúria removendo restos celulares e secretando fatores tróficos. Porém, essa resposta de emergência pode ser tanto benéfica quanto deletéria para o SNC. Alterações da funcionalidade das células gliais, incluindo mudanças na sua morfologia e atividade proliferativa são um achado comum em neuropatologias (Sofroniew, 2005, 2009). Durante a inflamação cerebral associada com a DH, por exemplo, os astrócitos são ativados, levando à hipertrofia e/ou proliferação celular (Guncova et al., 2010, Oliveira, 2010). Saber qual o papel que os astrócitos exercem nas doenças que acometem o SNC, se benéfico ou deletério, pode ter uma grande contribuição para o entendimento da patofisiologia destas doenças. Nesse sentido, os astrócitos em cultura são modelos úteis para avaliar a resposta a injúrias neurotóxicas.

Uma vez ativados, os astrócitos respondem tipicamente a uma injúria com hipertrofia e proliferação celular, superexpressão de nestina, vimentina e GFAP (Silver and Miller, 2004). Essas respostas podem levar a efeitos reparadores ou destrutivos, dependendo do contexto em que a lesão ocorre, como a intensidade, o tempo (crônico versus agudo) e o tipo de injúria. Embora o QUIN não tenha induzido superexpressão de vimentina ou GFAP nos astrócitos isolados durante as 24 horas de exposição, nós podemos supor que todas essas respostas representam passos iniciais de uma astrogliose programada, visto que a dinâmica das respostas astrocitárias à injúria são dependentes do grau de dano neurológico (Buffo et al., 2010).

Os receptores iGluR, em particular o NMDA, têm um importante papel na sinalização glial. A sinalização glutamatérgica astrocitária envolve a indução de ondas intracelulares de Ca^{2+}, que pode ser uma resposta a NT liberados tanto por neurônios quanto por outros astrócitos (Cornell-Bell et al., 1990). Enquanto que nos neurônios os canais de sódio são os maiores receptores envolvidos na despolarização da membrana, nos astrócitos podem ocorrer diferentes formas de sinalização, que irão culminar em ondas de Ca^{2+} intracelulares. Nos astrócitos, os receptores AMPA e mGluR são os principais receptores envolvidos na facilitação da entrada do Ca^{2+} para o citoplasma. No entanto, recentes estudos revelaram que a ativação dos receptores NMDA também pode ser importante para os mecanismos de influxo de Ca^{2+}, visto que estes canais iônicos apresentam uma permeabilidade muito maior a este íon que os receptores AMPA (Schipke et al., 2001). As vias de sinalização ativadas pelo aumento de Ca^{2+} intracelular nos astrócitos ainda não são bem compreendidas. Evidências prévias mostraram que o Ca^{2+} extracelular pode liberar os estoques internos de Ca^{2+} através da via DAG/IP3 após ativação dos receptores mGluRs. No entanto, este mecanismo parece ser dependente de

ativação prévia dos receptores NMDA (Benarroch, 2005). Portanto, é provável que tanto os mGluR quanto os iGluR estejam envolvidos na sinalização glial.

Nossos resultados mostraram que o aumento do influxo de Ca^{2+} causado pela exposição ao QUIN foi dependente dos receptores NMDA. A utilização de quelantes intra e extracelulares de Ca^{2+} mostrou que a hiperfosforilação da GFAP/Vim causada pelo QUIN é dependente do aumento nas concentrações de Ca^{2+} intracelulares. A estreita correlação entre as ações do QUIN e os níveis citosólicos de Ca^{2+} foi comprovada pela marcação dos astrócitos com o FURA-2AM, um indicador do aumento de Ca^{2+} intracelular, demonstrando que o aumento no Ca^{2+} citosólico através dos receptores NMDA é um dos primeiros eventos desencadeantes dos mecanismos de sinalização que tem o citoesqueleto astroglial como alvo.

Interessantemente, os resultados obtidos através dos experimentos com FURA-2AM mostraram que os receptores AMPA também estão envolvidos no aumento do Ca^{2+} intracelular desencadeado pelo QUIN. Os receptores AMPA são proteínas hetero-oligoméricas formadas por 4 subunidades (A1-4), sendo que cada subunidade interage com proteínas citoplasmáticas específicas (Hollmann and Heinemann, 1994). Uma explicação para a participação dos receptores AMPA nos efeitos do QUIN pode se dar pelo fato de que a subunidade GluA2 do receptor AMPA deixa o canal menos permeável ao Ca^{2+}, e a maioria das células gliais não expressa essa subunidade, resultando em receptores AMPA astrogliais mais permeáveis a este íon (Burnashev, 1998). Isto está de acordo com nossos achados, mostrando que o CNQX preveniu a entrada de Ca^{2+} causada pelo QUIN em astrócitos estriatais.

Surpreendentemente, apesar da relevância do aumento dos níveis de Ca^{2+} nos efeitos do QUIN sobre os FI, a fosforilação da GFAP/Vim não teve a participação da

PKCaMII. Esses achados podem ser um indício da importância da comunicação neurônio-astrócito na sinalização desencadeada pelo QUIN, visto que nos outros desenhos experimentais essa enzima participou dos eventos desencadeados pelo metabólito em astrócitos. Por outro lado, a hiperfosforilação da GFAP/Vim nos astrócitos em cultura foi mediada por PKA. Visto que as isoformas neurais da AC podem ser ativadas por Ca^{2+} (Steiner et al., 2006), provavelmente o aumento do Ca^{2+} citosólico desencadeado pelo QUIN causou a ativação da PKA. A PKC também teve participação nos efeitos desencadeados pelo QUIN em astrócitos isolados. A ativação da PKC pode ser mediada pela ativação dos receptores mGluR via DAG/IP3/PLC, como discutido anteriormente (Wang et al., 2012), portanto a ativação dos mGluR1 e 5 pelo QUIN provavelmente causou a ativação da PKC em astrócitos.

Alterações no citoesqueleto de actina em resposta a sinais celulares podem ocasionar complicações relevantes em diversas funções astrocitárias, como motilidade celular, suporte metabólico, excitotoxicidade e estresse oxidativo (Aschner, 2000, Hazrati et al., 2008). Considerando as alterações na dinâmica do citoesqueleto celular, observamos que os astrócitos apresentaram retração no citoplasma com redistribuição dos filamentos de GFAP e actina após 24 horas de tratamento com QUIN. Essa redistribuição não foi acompanhada de aumento no imunoconteúdo dessas proteínas, sugerindo que o metabólito causa uma reorganização dos FIs em astrócitos isolados, sem alterar a expressão de suas subunidades. O remodelamento do citoesqueleto de actina e GFAP pode explicar as alterações morfológicas observadas, sugerindo um papel para as proteínas do citoesqueleto na resposta dos astrócitos às ações deletérias do QUIN.

O citoesqueleto de actina é considerado um dos reguladores-chave da sobrevivência ou morte celular. A extrema dinâmica dos filamentos de actina pode

promover a longevidade celular, enquanto que a indução da estabilização desses filamentos está associada a vias de apoptose (Gourlay and Ayscough, 2005, Boldogh and Pon, 2006). Embora os mecanismos exatos que desencadeiam esses efeitos ainda não sejam bem compreendidos, estudos prévios sugerem que a estabilização da actina pode alterar as funções mitocondriais, levando à apoptose (Martin and Leder, 2001). Isso está de acordo com os nossos achados, mostrando ausência de morte celular em todas as concentrações utilizadas, concomitante com a desestabilização do citoesqueleto de actina. Também está de acordo com outros achados do nosso grupo, onde astrócitos corticais tratados com homocisteína e prolina tiveram desregulação do sistema fosforilante e remodelamento do citoesqueleto, com ausência de morte celular (Loureiro et al., 2010b, Loureiro et al., 2013).

Por outro lado, um estudo prévio utilizando astrócitos humanos fetais evidenciou que 50 nM de QUIN foram suficientes para causar apoptose astrocitária (Guillemin et al., 2005). Além disso, Braidy e colaboradores (Braidy et al., 2009) mostraram que houve um aumento da atividade da LDH em astrócitos humanos expostos a 1-1000 μM de QUIN por 24 horas. Os mecanismos de toxicidade que o QUIN desencadeia em astrócitos humanos envolveu a ativação de receptores NMDA e produção de NO• (Braidy et al., 2009). Com base nesses resultados, consideramos importante desenvolver estudos subsequentes para melhor elucidar nossos achados. Porém, deve ser considerado o papel dos receptores mGluR1 e 5 na toxicidade evocada pelo QUIN nos astrócitos primários de ratos, visto que evidências sugerem que a ativação destes receptores protege os astrocitos corticais de morte induzida por isquemia (Liu et al., 2013).

É possível que o desequilíbrio dos sistemas de fosforilação em resposta ao QUIN, além de provocar hiperfosforilação dos FI, possa levar à perda da homeostase do

citoesqueleto de actina nos astrócitos em cultura. Essa possibilidade é reforçada pela evidência de que a reorganização da actina é controlada por proteínas associadas, as quais, por sua vez, são reguladas por cascatas de fosforilação. Dentre essas proteínas, a cofilina é a mais importante proteína associada à actina, estando implicada na migração celular e reorganização do citoesqueleto de actina (Van Troys et al., 2008). Os efeitos da cofilina na dinâmica da actina são diversos e a sua regulação é complexa. Nas células ativadas, múltiplas vias de sinalização podem ser iniciadas através de mecanismos de fosforilação, resultando em diferentes tipos de ativação/desativação que controlam a sua atividade. A fosforilação/desfosforilação da cofilina é um modulador crucial da dinâmica dos filamentos de actina, sendo que sua fosforilação na Ser3 causa inativação por inibição da ligação da actina G e F (Bamburg and Wiggan, 2002).

Duas famílias de cinases são responsáveis pela inativação da cofilina por fosforilação: as LIM cinases e as TESK cinases (Scott and Olson, 2007), sendo que as LIM cinases se mostraram reguladores essenciais para reorganização do citoesqueleto de actina (Sumi et al., 1999). Além disso, um estudo recente mostrou o papel da SSH fosfatase, um membro da família Slingshot (SSH) 1L de proteínas fosfatases, na desfosforilação da cofilina mediada por Ca^{2+} (Nishita et al., 2004). Neste contexto, flutuações nas concentrações intracelulares de Ca^{2+} (Van Troys et al., 2008) bem como alterações da via AMPc/PKA têm a capacidade de modular o citoesqueleto de actina através da fosforilação/desfosforilação de cofilina. O Ca^{2+} atua ativando a calcineurina (PP2B), que desfosforila a SSH1, ativando-a. A SSH1 ativa desfosforila a cofilina (Nishita et al., 2004). A PKA ativada, por sua vez, fosforila a LIM cinase, que fosforila a cofilina na Ser3 (Meberg et al., 1998, Nadella et al., 2009). Portanto, é possível que nos astrócitos tratados com QUIN, a sinalização glutamatérgica esteja causando uma reorganização do citoesqueleto de actina concomitante com a rede de GFAP/Vim

através da ativação de cascatas de fosforilação, que irão interferir na cascata de sinalização das proteínas associadas á actina. Apesar do conjunto de evidências mostrando a importância da cofilina, novos experimentos serão necessários para verificar sua participação na regulação da dinâmica dos filamentos de actina em astrócitos isolados expostos ao QUIN.

É interessante salientar que 24 horas após a remoção do QUIN das culturas primárias, os níveis de fosforilação dos FI, bem como a reorganização do citoesqueleto de actina e GFAP, assim como a morfologia celular, voltaram a suas condições basais, indicando a reversibilidade das ações causadas pelo QUIN no citoesqueleto astrocitário. Com base nesses achados, nós podemos propor que, nos astrócitos tratados com QUIN, o desequilíbrio do sistema fosforilante associado ao citoesqueleto de GFAP/Vim foi capaz de mediar a reorganização da rede citoesquelética, alterando a plasticidade celular. Este efeito foi desencadeado por mecanismos glutamatérgicos e Ca^{2+}, ativação da PKA e PKC que, junto com o remodelamento da rede de actina, foram responsáveis por alterar o citoesqueleto astrocitário. As ações do QUIN no citoesqueleto podem representar um dano ao astrócito por induzir a desestabilização do citoesqueleto com consequências na plasticidade e função celular. Estes resultados somam-se aos obtidos nas abordagens *in vivo* e *ex-vivo*, mostrando que a perda da homeostase do citoesqueleto pode ser um dos mecanismos implicados na toxicidade do QUIN em astrócitos.

A exposição crônica dos neurônios humanos ao QUIN pode causar efeitos deletérios a estas células, podendo levar a sua morte. O QUIN causa mudanças estruturais significativas nos neurônios, incluindo alterações dendríticas, ruptura dos microtúbulos e diminuição de organelas (Whetsell and Schwarcz, 1989). Além disso, evidências do nosso grupo (Pierozan et al., 2010, Pierozan et al., 2012) e de outros (Kerr et al., 1998, Braidy et al., 2009) mostraram que o rompimento do citoesqueleto de

células neurais é um dos alvos das ações do QUIN tanto *ex-vivo* quanto *in vivo*. As alterações no citoesqueleto neural representam um dos primeiros eventos desencadeados por este metabólito, em que a excitotoxicidade e o dano oxidativo estão envolvidos (Perez-De La Cruz et al., 2012).

Nós observamos que o QUIN se mostrou tóxico aos neurônios estriatais em cultura, induzindo morte celular por apoptose em altas concentrações. Estes dados estão de acordo com estudos prévios, mostrando que 300 μM QUIN causou morte significativa de neurônios espinhais médios estriatais e 1 mM causou aumento de liberação de LDH em neurônios corticais (Kim and Choi, 1987, Kumar, 2008). Em concentrações menores (10 μM), o QUIN causou alteração da homeostase do citoesqueleto neuronal através da hiperfosforilação das subunidades dos NF, além de alterar parâmetros morfométricos neuronais, como a razão neurônio/neurito e o comprimento dos neuritos, sem indução de morte.

Os NF desempenham um importante papel estrutural em neurônios e, junto com os MT e as proteínas associadas aos MT, sustentam a rede axonal e dendrítica, além de promoverem o crescimento e/ou espessamento axonal (Kesavapany et al., 2006). Nesse sentido, é de grande importância avaliar a correlação entre a alteração do sistema fosforilante associado ao citoesqueleto e as prováveis alterações morfológicas nos neurônios em diversas patologias, incluindo processos que desencadeiam quadros de excitotoxicidade.

O desequilíbrio na homeostase do sistema fosforilante associado ao citoesqueleto neuronal foi dependente do influxo de Ca^{2+} através da ativação de receptores NMDA, dos L-VDCC e da ativação dos receptores mGluR1. Estes resultados estão consistentes com os outros desenhos experimentais que mostraram excitotoxicidade através do

aumento do Ca^{2+} intracelular e sinalização glutamatérgica (Pierozan et al., 2010, Pierozan et al., 2012). A fosforilação aberrante das subunidades dos NF resultante de uma desregulação na atividade de cinases/fosfatases pode causar estresse celular induzido por alteração nos NF e causar dano neuronal (Shea and Chan, 2008, Holmgren et al., 2012). Nós demonstramos que as subunidades dos NF de neurônios estriatais em cultura estão hiperfosforiladas em resposta a 10 μM QUIN, e que PKA, PKC, bem como MAPKs e Cdk5 estão envolvidas nestes mecanismos. Como discutido anteriormente, a fosforilação das subunidades da NFL pela PKA ou PKC previne a associação da subunidade NFL e desassocia filamentos previamente formados (Hisanaga et al., 1990), interferindo, portanto, com a rede axonal. Visto que os receptores NMDA, e L-VDCC estão envolvidos nos efeitos desencadeados pelo QUIN nos neurônios em cultura e que utilizando tampões intra e extracelulares de Ca^{2+} este efeito foi prevenido, podemos concluir que a ativação da PKA se deu através do aumento de Ca^{2+} intracelular. Da mesma forma que nos astrócitos, a ativação da PKC se deu através da ativação dos receptores mGluR1 e da via DAG/IP3/PLC, enquanto que não houve a participação da PKCaMII nestes efeitos.

Além disso, o QUIN ativou a ERK1/2, JNK e p38MAPK, bem como a Cdk5, sugerindo desregulação do citoesqueleto axonal e disfunção celular (Perrot and Eyer, 2009). Interessantemente, nossos resultados demonstraram que a inibição das MAPK e Cdk5 preveniu a fosforilação da NFL, ao mesmo tempo em que a inibição da PKC preveniu a fosforilação da NFM. Visto que estes não são os sítios tipicamente fosforilados por estas enzimas, nós podemos supor que vias de sinalização complexas estão implicadas nas ações do QUIN sobre o citoesqueleto neuronal.

O crescimento dos processos neuronais é dependente de mudanças na dinâmica e nas propriedades do citoesqueleto (da Silva and Dotti, 2002, Dent and Gertler, 2003).

Os resultados do nosso estudo mostraram que os neurônios tratados com QUIN apresentaram redução da razão neurito/neurônio e do comprimento dos neuritos, sendo esse efeito dependente da concentração de QUIN. As alterações morfológicas que nós encontramos nos neurônios tratados com QUIN parecem estar envolvidas com a desregulação dos mecanismos de sinalização relacionados com a homeostase dos NF. Os dendritos são considerados particularmente vulneráveis à injúria excitotóxica, visto que os contatos sinápticos excitatórios estão predominantemente na árvore dendrítica. Por este motivo, os dendritos têm sido propostos como sítios iniciais de injúria causada por excitotoxicidade (Bindokas and Miller, 1995). Portanto, o desequilíbrio na homeostase do citoesqueleto neuronal causado pelo QUIN pode representar, ao menos em parte, uma injúria excitotóxica dendrítica (Greenwood and Connolly, 2007), podendo resultar em uma rápida necrose ou em apoptose tardia do neurônio, dependendo da severidade do insulto (Bonfoco et al., 1995).

Interações entre neurônios e astrócitos são eventos críticos para a sinalização, metabolismo energético, homeostase extracelular de íons, regulação do volume celular, além de neuroproteção no SNC. Os astrócitos estão altamente relacionados com a funcionalidade das sinapses, e formam uma extensa rede interconectada por junções *gap*. Eles expressam diversas proteínas de membrana e enzimas que são criticas para a captação de glutamato nas sinapses, detoxificação da amônia e tamponamento do K^+ extracelular. Eles também participam da detecção, propagação e modulação dos sinais excitatórios nas sinapses, provendo suporte metabólico para os neurônios ativos, e contribuindo para o funcionamento do tecido cerebral (Perea and Araque, 2005, Halassa and Haydon, 2010). Distúrbios dessas interações neurônio-astrócito estão relacionados com diversas doenças neurológicas, incluindo isquemia cerebral, neurodegeneração e encefalopatia hepática (Albrecht et al., Mizuno, 2011, Kang et al., 2012).

Considerando que os insultos gerados pelo QUIN provocaram reorganização do citoesqueleto das células gliais e neuronais isoladas e que o citoesqueleto neuronal foi mais susceptível que o astrocitário às ações desencadeadas pelo QUIN, (foi necessário uma concentração 10 vezes maior para alterar o sistema fosforilante associado ao citoesqueleto de astrócitos), avaliamos a fosforilação dos FI, bem como a organização do citoesqueleto neural em co-cultura neurônio/astrócito, com o objetivo de verificar as consequências dessa interação sobre a resposta de cada tipo celular.

Inicialmente observamos que neurônios expostos ao meio condicionado de astrócitos tratados com QUIN não apresentaram alteração de nenhum dos parâmetros relativos à homeostase do citoesqueleto neuronal. Estes achados sugerem que os astrócitos ativados pelo QUIN podem secretar fatores protetores capazes de modular os mecanismos de sinalização que tem o citoesqueleto neuronal como alvo.

É bem estabelecido que os astrócitos secretam diferentes gliotransmissores como glutamato, d-serina, TNF-α e ATP. Alguns desses metabólitos são liberados de maneira Ca^{2+}-dependente (Volterra and Meldolesi, 2005), e constituem sinais de *feedback* dos astrócitos para modular a excitabilidade neuronal e a transmissão sináptica (Araque et al., 1998, Araque et al., 2000, Takano et al., 2002). A regressão dos neuritos e a neurodegeneração são achados comuns nas desordens neurodegenerativas, sendo que os fatores de crescimento e os neurotransmissores excitatórios têm um papel chave nos processos neurodegenerativos. Um grande número de fatores de crescimento podem atuar no desenvolvimento do SNC e na resposta à injúria, tendo um importante papel durante um quadro de excitotoxicidade, por estimular o reparo ao SNC (Mattson and Scheff, 1994). Os mais importantes fatores de crescimento incluem o fator de crescimento neurotrófico (NGF), o fator de crescimento de fibroblastos (FGF), fator neurotrófico derivado do cérebro (BDNF) e o fator neurotrófico ciliar (CNTF) (Mattson

and Scheff, 1994). Neste contexto, um estudo de Figueiredo e colaboradores (Figueiredo et al., 2008) demonstrou que os astrócitos protegeram neurônios cerebelares granulares de um insulto com QUIN pela secreção de FGF-2. O FGF-2 é um fator de crescimento envolvido em processos de neurogênese após um estresse agudo, sendo que vários estudos mostraram que o estresse agudo aumenta a expressão e liberação de FGF-2 pelas células astrocitárias (Figueiredo et al., 2008, Kirby et al., 2013, Xia et al., 2013). Outro estudo mostrou que o CNF protegeu os neurônios estriatais de uma injeção intraestriatal com QUIN, por aumentar a atividade dos transportadores glutamatérgicos gliais (Beurrier et al., 2010). Embora no nosso estudo não tenhamos avaliado qual fator é o responsável pela proteção dos neurônios pelos astrócitos, é possível que o QUIN promova a liberação de algum fator protetor pelos astrócitos, que estaria protegendo os neurônios dos efeitos desencadeados pelo QUIN sobre o citoesqueleto neuronal.

Na tentativa de investigar mais a fundo a interação célula/célula na injúria excitotóxica causada pelo QUIN, nós avaliamos os efeitos desencadeados por concentrações crescentes de QUIN sobre a co-cultura astrócito/neurônio. Surpreendentemente, nossos resultados mostraram que os dois tipos celulares interagem ativamente protegendo-se mutuamente contra os insultos causados pelo metabólito, visto que ambos os tipos celulares preservaram a sua organização citoesquelética e morfologia, além de manter intacto o sistema fosforilante associado aos FI.

Sabe-se que os astrócitos influenciam o desenvolvimento e a atividade neuronal não apenas pela liberação de fatores solúveis, mas também através da interação célula-célula (Schmalenbach and Muller, 1993, Nedergaard et al., 2003, Villegas et al., 2003, Kornyei et al., 2005). A existência de uma sinalização bi-direcional entre os astrócitos e os neurônios tem revelado o importante papel dos astrócitos na fisiologia do SNC. Como consequência, há um novo conceito de fisiologia sináptica: a sinapse “tripartite”,

onde os astrócitos trocam informação com os elementos pré e pós-sinápticos neuronais e participam de elementos regulatórios dinâmicos na neurotransmissão. A habilidade dos astrócitos em responder à atividade neuronal, discriminar entre a atividade de diferentes sinapses, e modular a excitabilidade astrocítica através da atividade sináptica, indica que os astrócitos são dotados de características que permitem o processamento de informações sinápticas (Perea and Araque, 2005).

Por outro lado, os neurônios também podem modular a atividade astrocitária, facilitando a comunicação glial e contribuindo para a interação neuroglial (Rouach et al., 2002). Eles secretam moléculas bioativas, como NTs, peptídeos e lipídeos, que ativam os receptores astrogliais e modificam a sua atividade ou a expressão de proteínas das junções *gap* (Giaume and McCarthy, 1996, Rouach et al., 2002). Uma consequência importante dessa regulação é o aumento na propagação das ondas intercelulares de Ca^{2+} astroglial (Rouach et al., 2002). Nesse sentido, um estudo mostrou que os neurônios aumentam a expressão das junções *gap* dos astrócitos, por aumentar a expressão de uma das proteínas transmembrana mais importantes que constituem as junções *gap* em astrócitos, a conexina 43 (Rouach et al., 2000). Este estudo está de acordo com observações prévias de que os neurônios facilitam a comunicação glial em co-cultura cerebelar (Fischer and Kettenmann, 1985). Esses e outros trabalhos têm indicado que a comunicação através das junções *gap* e/ou a expressão de conexinas nos astrócitos são controladas pelos neurônios (Rouach et al., 2004). Além disso, parece que em patologias caracterizadas por disfunção neuronal, as junções *gap* astrocíticas representam um alvo para as interações neurogliais (Rohlmann et al., 1993, Hanani et al., 2002).

Com base no exposto acima, se torna possível afirmar que existe uma regulação mútua de ambos os tipos celulares. Essa regulação mútua pode envolver a modulação da

transmissão sináptica em neurônios e a comunicação via junções *gap* em astrócitos. Esse controle mútuo reforça o conceito de uma estreita colaboração entre a rede neuronal e astrocitária no processamento da informação (Smith, 1994). Além disso, devido a várias linhas de estudo terem demonstrado que os neurônios regulam a expressão de conexinas nas junções *gap* astrocitárias, podemos supor que, na co-cultura tratada com QUIN, os neurônios estejam contribuindo para o aumento destas junções nos astrócitos, enquanto que os astrócitos estariam secretando fatores protetores para os neurônios, levando a uma proteção recíproca contra as ações deletérias do QUIN sobre as vias de sinalização direcionadas ao citoesqueleto neural.

Concluindo, a abordagem em células isoladas fornece consistentes evidências de que o citoesqueleto neural é um alvo crítico para as ações do QUIN em culturas de neurônios e astrócitos isolados, modificando as suas morfologias, e provavelmente suas funções. Além disso, houve uma recíproca proteção entre astrócitos e neurônios contra os insultos provocados pelo QUIN. No entanto, mais pesquisas devem ser feitas para elucidar a relação entre as alterações na dinâmica e na morfologia do citoesqueleto neural e prováveis mudanças nas funções celulares em resposta ao QUIN. Além disso, um intenso estudo entre as interações astrócitos/neurônios e seu papel na neuroproteção pode ser de grande interesse para o entendimento das ações do QUIN nas células neurais.

1.4. Considerações finais

Considerando o conjunto dos nossos resultados, podemos dizer que o QUIN é um composto neurotóxico capaz de afetar a sinalização celular e a dinâmica do citoesqueleto de diferentes estruturas cerebrais como o corpo estriado, córtex cerebral e

hipocampo. Entretanto, os seus efeitos vão depender das características de cada estrutura e do tipo celular.

Analisando os resultados dos três desenhos experimentais, podemos concluir que as ações do QUIN sobre o citoesqueleto neural baseiam-se fundamentalmente no desenvolvimento de um quadro excitotóxico, através da ativação do sistema glutamatérgico e aumento de Ca^{2+} intracelular, com consequente ativação de cascatas de fosforilação. Essa ativação das cascatas causa alteração na fosforilação dos FI neurais, além de alteração na organização do citoesqueleto de astrócitos e neurônios.

Levando-se em conta apenas o estriado, encontramos algumas diferenças dependendo do modelo experimental utilizado. Como mostrado na Tabela 1, os modelos *in vivo* e *ex vivo* apresentam grande semelhança nas vias de sinalização envolvidas, embora o modelo *in vivo* não nos dê condições de explorar mais a fundo a sinalização desencadeada pelo QUIN, como a participação dos receptores mGluR 1 e 5 e dos canais L-VDCC. Também podemos verificar algumas diferenças entre os mecanismos de ação desencadeados pelo QUIN em fatias estriatais e em cultura de células. Uma provável explicação para estas diferenças é que as células isoladas muitas vezes respondem a estímulos externos diferentemente de fatias, onde há diversos tipos celulares interagindo, e do cérebro intacto, onde as conexões entre as estruturas cerebrais estão preservadas. Os tipos celulares neurais comunicam-se entre si, através da liberação de fatores e neurotransmissores, além do contato célula-célula, modificando as respostas que a célula teria isoladamente.

Tabela 1. Resumo dos efeitos do QUIN sobre o sistema fosforilante associado ao citoesqueleto estriatal nas diferentes abordagens experimentais.

Abordagem	**Neurônios**	**Astrócitos**
In vivo	Aumento de fosforilação dos NF pela ativação de PKA,	Aumento de fosforilação da GFAP pela ativação de

	PKCaMII e Cdk5	PKA e PKCamII
Ex vivo	Aumento de fosforilação dos NF pela ativação dos receptores NMDA, mGluR1 e 5 e canais L-VDCC. Aumento de influxo de Ca^{2+} extracelular e liberação dos estoques extracelulares. Ativação da PKA, PKCaMII, PKC e Ckd5	Aumento da fosforilação da GFAP pela ativação dos receptores NMDA e canais L-VDCC. Aumento do influxo de Ca^{2+} extracelular e ativação da PKA e PKCaMII
In vitro	Aumento da fosforilação dos NF através da ativação dos receptores NMDA, mGluR1 e canais L-VDCC. Aumento de influxo de Ca^{2+} e ativação da PKA, PKC, MAPK e Cdk5	Aumento da fosforilação da GFAP pela ativação de receptores NMDA, AMPA e mGluR1 e 5. Aumento do influxo de Ca^{2+} e ativação da PKA e PKC

Um dado importante que comprova o exposto acima é o resultado da proteção mútua que nós demonstramos nas co-culturas neurônio-astrócito tratados com QUIN. Esta neuroproteção não foi observada no modelo *in vivo* e no estudo *ex vivo*. Quando houve a interação apenas do neurônio com o astrócitos, estes dois tipos celulares desenvolveram mecanismos de proteção mútua que os pouparam dos efeitos excitotóxicos do QUIN. Porém, nas fatias estriatais e no cérebro intacto, houve um terceiro elemento que impediu essa proteção, causando dano tanto neuronal quanto astroglial.

As células da microglia são as células imunes residentes no cérebro que após mudanças patológicas, como injúria excitotóxica, se tornam ativadas e rapidamente mudam sua morfologia (van Rossum and Hanisch, 2004). Esta mudança é acompanhada de liberação de citocinas pró-inflamatórias e produção de altos níveis de QUIN e glutamato (Tikka and Koistinaho, 2001), sendo que todos esses fatores podem contribuir para o quadro de excitotoxicidade. A microglia ativada exerce seus efeitos nos neurônios e em astrócitos, através da liberação de substâncias citotóxicas como

radicais livres de oxigênio, óxido nítrico, glutamato e proteases (van Rossum and Hanisch, 2004). Os efeitos da microglia também são modulados por astrócitos e neurônios através de citocinas e NT, dando origem a uma complexa interação microglia-neurônio-astrócito que é denominada neuroinflamação. A neuroinflamação é um elemento importante de doenças neurodegenerativas (Glass et al., 2010) e é considerada uma consequência da ativação microglial (Kalaria, 1999, Mennicken et al., 1999). Há um grande número de evidências mostrando que um importante componente da resposta microglial à injúria ou doenças do SNC é a ativação da RQ.

Como falado anteriormente, em condições de neuroinflamação os macrófagos e a microglia podem produzir altas quantidades de QUIN, que podem ser tóxicas ao SNC (Heyes, 1993). O rápido recrutamento das células microgliais ao sítio de injúria é bem documentado após excitotoxicidade (McGeer et al., 1993, Akiyama et al., 1994). Embora se saiba que a microglia ativada nas imediações do sítio de injúria está envolvida na remoção dos restos de neurônios em degeneração (Rozemuller et al., 1989), a exata contribuição da ativação microglial na recuperação e remodelamento neuronal ainda não está bem clara. As células microgliais aumentam consideravelmente no cérebro de pacientes com HD e estas células expressam quantidades aumentadas de QUIN. Nesse sentido, um estudo de Sapp e colaboradores (Sapp et al., 2001) mostrou mudanças microgliais no estriado, córtex cerebral e globo pálido de pacientes com DH. Além disso, Pavese e colaboradores (Pavese et al., 2006) mostraram que a ativação microglial na DH está relacionada com a progressão da doença. Interessantemente, estudo utilizando a injeção intraestriatal de QUIN como modelo para a DH demonstrou que a infusão do metabólito causa uma resposta microglial que acompanha a injúria excitotóxica (Topper et al., 1993), produzindo lesões acompanhadas de resposta inflamatória, que envolvem aumento de ativação e proliferação da microglia (Ryu et al.,

2005). Ou seja, o QUIN ativa a microglia, e esta ativada produz mais QUIN em quantidades neurotóxicas, alimentando a injúria excitotóxica.

Com base no exposto acima e nos resultados encontrados em co-cultura astrócito-neurônio, podemos propor que a microglia contribui para produzir o dano excitotóxico desencadeado pelo QUIN. O QUIN tem a capacidade de ativar a microglia, sendo que estas células ativadas irão liberar fatores citotóxicos deletérios para as células, além de produzir mais QUIN, alimentando assim o quadro excitotóxico.

2. CONCLUSÃO

Células neurais do corpo estriado, córtex cerebral e hipocampo são susceptíveis á ações excitotóxicas desencadeadas pelo QUIN. Insultos com QUIN em ratos jovens podem causar um quadro neurotóxico bastante semelhante ao encontrado na DHJ. Os experimentos *in vivo* com ratos jovens demonstraram que o QUIN pode ser um bom modelo para o estudo da DHJ. Além disso, o citoesqueleto neural é um importante alvo para as ações do QUIN no cérebro de ratos jovens, como demonstrado em culturas celulares tratadas com QUIN.

As ações do QUIN sobre o citoesqueleto são dependentes de sinalização glutamatérgica, do aumento do Ca^{2+} intracelular e da ativação de cascatas de sinalização. Além disso, os efeitos sobre os FI são dependentes da estrutura cerebral e do modelo experimental. Portanto, as alterações do citoesqueleto cerebral podem estar envolvidas, pelo menos em parte, com a neurotoxicidade do QUIN.

3. PERSPECTIVAS

Os resultados obtidos nesse trabalho vislumbram novas possibilidades de estudos com a finalidade de elucidar melhor as respostas celulares às ações desencadeadas pelo QUIN, além de investigar possíveis mecanismos de proteção contra esses efeitos. Dessa maneira, nossas perspectivas são:

3.1. Avaliar o papel da neuroinflamação nos efeitos desencadeados pelo QUIN sobre o citoesqueleto neural, utilizando diversos tipos de agentes anti-inflamatórios.

3.2. Verificar o efeito neuroprotetor da quinurenina nas ações do QUIN *in vivo*, *ex vivo* e *in vitro*.

3.3. Estudar os mecanismos pelos quais os astrócitos e neurônios em cultura se protegem dos efeitos causados pelo QUIN, avaliando possíveis fatores solúveis e proteínas formadoras das junções *gap* nessa neuroproteção.

3.4. Analisar o papel da microglia nos efeitos desencadeados pelo QUIN.

4. REFERÊNCIAS

Ackerley S, Grierson AJ, Banner S, Perkinton MS, Brownlees J, Byers HL, Ward M, Thornhill P, Hussain K, Waby JS, Anderton BH, Cooper JD, Dingwall C, Leigh PN, Shaw CE, Miller CC (p38alpha stress-activated protein kinase phosphorylates neurofilaments and is associated with neurofilament pathology in amyotrophic lateral sclerosis. Mol Cell Neurosci 26:354-364.2004).

Ackerley S, Grierson AJ, Brownlees J, Thornhill P, Anderton BH, Leigh PN, Shaw CE, Miller CC (Glutamate slows axonal transport of neurofilaments in transfected neurons. J Cell Biol 150:165-176.2000).

Ackerley S, Thornhill P, Grierson AJ, Brownlees J, Anderton BH, Leigh PN, Shaw CE, Miller CC (Neurofilament heavy chain side arm phosphorylation regulates axonal transport of neurofilaments. J Cell Biol 161:489-495.2003).

Akiyama H, Tooyama I, Kondo H, Ikeda K, Kimura H, McGeer EG, McGeer PL (Early response of brain resident microglia to kainic acid-induced hippocampal lesions. Brain Res 635:257-268.1994).

Akopian G, Walsh JP (Corticostriatal paired-pulse potentiation produced by voltage-dependent activation of NMDA receptors and L-type Ca(2+) channels. J Neurophysiol 87:157-165.2002).

Alberts B, Johnson A, Lewis J, Raff M, Roberts K, Walter PO (Citoesqueleto. In: Biologia molecular da célula 6 ed.:907-982.2008).

Albin RL, Reiner A, Anderson KD, Penney JB, Young AB (Striatal and nigral neuron subpopulations in rigid Huntington's disease: implications for the functional anatomy of chorea and rigidity-akinesia. Ann Neurol 27:357-365.1990).

Albrecht J, Zielinska M, Norenberg MD (Glutamine as a mediator of ammonia neurotoxicity: A critical appraisal. Biochem Pharmacol 80:1303-1308).

Ali SS, Xiong C, Lucero J, Behrens MM, Dugan LL, Quick KL (Gender differences in free radical homeostasis during aging: shorter-lived female C57BL6 mice have increased oxidative stress. Aging Cell 5:565-574.2006).

Anderson RM, Bitterman KJ, Wood JG, Medvedik O, Cohen H, Lin SS, Manchester JK, Gordon JI, Sinclair DA (Manipulation of a nuclear NAD+ salvage pathway delays aging without altering steady-state NAD+ levels. J Biol Chem 277:18881-18890.2002).

Araque A, Li N, Doyle RT, Haydon PG (SNARE protein-dependent glutamate release from astrocytes. J Neurosci 20:666-673.2000).

Araque A, Sanzgiri RP, Parpura V, Haydon PG (Calcium elevation in astrocytes causes an NMDA receptor-dependent increase in the frequency of miniature synaptic currents in cultured hippocampal neurons. J Neurosci 18:6822-6829.1998).

Arundine M, Tymianski M (Molecular mechanisms of calcium-dependent neurodegeneration in excitotoxicity. Cell Calcium 34:325-337.2003).

Aschner M (Astrocytic swelling, phospholipase A2, glutathione and glutamate: interactions in methylmercury-induced neurotoxicity. Cell Mol Biol (Noisy-le-grand) 46:843-854.2000).
Bamburg JR, Wiggan OP (ADF/cofilin and actin dynamics in disease. Trends Cell Biol 12:598-605.2002).
Bartos A, Fialova L, Svarcova J, Ripova D (Patients with Alzheimer disease have elevated intrathecal synthesis of antibodies against tau protein and heavy neurofilament. J Neuroimmunol 252:100-105.2012).
Beal MF, Kowall NW, Ellison DW, Mazurek MF, Swartz KJ, Martin JB (Replication of the neurochemical characteristics of Huntington's disease by quinolinic acid. Nature 321:168-171.1986).
Beaulieu JM, Robertson J, Julien JP (Interactions between peripherin and neurofilaments in cultured cells: disruption of peripherin assembly by the NF-M and NF-H subunits. Biochem Cell Biol 77:41-45.1999).
Benarroch EE (Neuron-astrocyte interactions: partnership for normal function and disease in the central nervous system. Mayo Clin Proc 80:1326-1338.2005).
Benke D, Wenzel A, Scheuer L, Fritschy JM, Mohler H (Immunobiochemical characterization of the NMDA-receptor subunit NR1 in the developing and adult rat brain. J Recept Signal Transduct Res 15:393-411.1995).
Berridge MJ (Inositol trisphosphate and diacylglycerol: two interacting second messengers. Annu Rev Biochem 56:159-193.1987).
Berridge MJ, Bootman MD, Roderick HL (Calcium signalling: dynamics, homeostasis and remodelling. Nat Rev Mol Cell Biol 4:517-529.2003).
Berridge MJ, Lipp P, Bootman MD (The versatility and universality of calcium signalling. Nat Rev Mol Cell Biol 1:11-21.2000).
Beurrier C, Faideau M, Bennouar KE, Escartin C, Kerkerian-Le Goff L, Bonvento G, Gubellini P (Ciliary neurotrophic factor protects striatal neurons against excitotoxicity by enhancing glial glutamate uptake. PLoS One 5:e8550.2010).
Bindokas VP, Miller RJ (Excitotoxic degeneration is initiated at non-random sites in cultured rat cerebellar neurons. J Neurosci 15:6999-7011.1995).
Boldogh IR, Pon LA (Interactions of mitochondria with the actin cytoskeleton. Biochim Biophys Acta 1763:450-462.2006).
Bonfoco E, Krainc D, Ankarcrona M, Nicotera P, Lipton SA (Apoptosis and necrosis: two distinct events induced, respectively, by mild and intense insults with N-methyl-D-aspartate or nitric oxide/superoxide in cortical cell cultures. Proc Natl Acad Sci U S A 92:7162-7166.1995).
Bonsi P, Platania P, Martella G, Madeo G, Vita D, Tassone A, Bernardi G, Pisani A (Distinct roles of group I mGlu receptors in striatal function. Neuropharmacology 55:392-395.2008).
Bootman MD, Lipp P, Berridge MJ (The organisation and functions of local Ca(2+) signals. J Cell Sci 114:2213-2222.2001).
Braidy N, Grant R, Adams S, Brew BJ, Guillemin GJ (Mechanism for quinolinic acid cytotoxicity in human astrocytes and neurons. Neurotox Res 16:77-86.2009).

Brickell KL, Nicholson LF, Waldvogel HJ, Faull RL (Chemical and anatomical changes in the striatum and substantia nigra following quinolinic acid lesions in the striatum of the rat: a detailed time course of the cellular and GABA(A) receptor changes. J Chem Neuroanat 17:75-97.1999).

Buffo A, Rolando C, Ceruti S (Astrocytes in the damaged brain: molecular and cellular insights into their reactive response and healing potential. Biochem Pharmacol 79:77-89.2009).

Buffo A, Rolando C, Ceruti S (Astrocytes in the damaged brain: molecular and cellular insights into their reactive response and healing potential. Biochem Pharmacol 79:77-89.2010).

Burnashev N (Calcium permeability of ligand-gated channels. Cell Calcium 24:325-332.1998).

Campellone KG, Welch MD (A nucleator arms race: cellular control of actin assembly. Nat Rev Mol Cell Biol 11:237-251.2010).

Carraway CAC (The cytoskeleton in transduction of signal and regulation of cellular function. In: Carraway, KL and Carraway, CAC Cytoskeleton: Signalling and cellular regulation New York, Oxford University Press.2000).

Caudle WM, Zhang J (Glutamate, excitotoxicity, and programmed cell death in Parkinson disease. Exp Neurol 220:230-233.2009).

Chang L, Goldman RD (Intermediate filaments mediate cytoskeletal crosstalk. Nat Rev Mol Cell Biol 5:601-613.2004).

Chavis P, Fagni L, Lansman JB, Bockaert J (Functional coupling between ryanodine receptors and L-type calcium channels in neurons. Nature 382:719-722.1996).

Che Y, Yu YM, Han PL, Lee JK (Delayed induction of p38 MAPKs in reactive astrocytes in the brain of mice after KA-induced seizure. Brain Res Mol Brain Res 94:157-165.2001).

Ching GY, Liem RK (Analysis of the roles of the head domains of type IV rat neuronal intermediate filament proteins in filament assembly using domain-swapped chimeric proteins. J Cell Sci 112 (Pt 13):2233-2240.1999).

Cornell-Bell AH, Finkbeiner SM, Cooper MS, Smith SJ (Glutamate induces calcium waves in cultured astrocytes: long-range glial signaling. Science 247:470-473.1990).

Cote F, Collard JF, Julien JP (Progressive neuronopathy in transgenic mice expressing the human neurofilament heavy gene: a mouse model of amyotrophic lateral sclerosis. Cell 73:35-46.1993).

da Silva JS, Dotti CG (Breaking the neuronal sphere: regulation of the actin cytoskeleton in neuritogenesis. Nat Rev Neurosci 3:694-704.2002).

Dashiell SM, Tanner SL, Pant HC, Quarles RH (Myelin-associated glycoprotein modulates expression and phosphorylation of neuronal cytoskeletal elements and their associated kinases. J Neurochem 81:1263-1272.2002).

DeFuria J, Chen P, Shea TB (Divergent effects of the MEKK-1/JNK pathway on NB2a/d1 differentiation: some activity is required for outgrowth and

stabilization of neurites but overactivation inhibits both phenomena. Brain Res 1123:20-26.2006).
Dent EW, Gertler FB (Cytoskeletal dynamics and transport in growth cone motility and axon guidance. Neuron 40:209-227.2003).
DiProspero NA, Chen EY, Charles V, Plomann M, Kordower JH, Tagle DA (Early changes in Huntington's disease patient brains involve alterations in cytoskeletal and synaptic elements. J Neurocytol 33:517-533.2004).
Dolmetsch RE, Pajvani U, Fife K, Spotts JM, Greenberg ME (Signaling to the nucleus by an L-type calcium channel-calmodulin complex through the MAP kinase pathway. Science 294:333-339.2001).
Drain P, Folkers E, Quinn WG (cAMP-dependent protein kinase and the disruption of learning in transgenic flies. Neuron 6:71-82.1991).
Eng LF, Ghirnikar RS (GFAP and astrogliosis. Brain Pathol 4:229-237.1994).
Eriksson JE, Dechat T, Grin B, Helfand B, Mendez M, Pallari HM, Goldman RD (Introducing intermediate filaments: from discovery to disease. J Clin Invest 119:1763-1771.2009).
Estrada Sanchez AM, Mejia-Toiber J, Massieu L (Excitotoxic neuronal death and the pathogenesis of Huntington's disease. Arch Med Res 39:265-276.2008).
Faideau M, Kim J, Cormier K, Gilmore R, Welch M, Auregan G, Dufour N, Guillermier M, Brouillet E, Hantraye P, Deglon N, Ferrante RJ, Bonvento G (In vivo expression of polyglutamine-expanded huntingtin by mouse striatal astrocytes impairs glutamate transport: a correlation with Huntington's disease subjects. Hum Mol Genet 19:3053-3067.2010).
Felipo V, Grau E, Minana MD, Grisolia S (Hyperammonemia decreases protein-kinase-C-dependent phosphorylation of microtubule-associated protein 2 and increases its binding to tubulin. Eur J Biochem 214:243-249.1993).
Ferreira A, Kincaid R, Kosik KS (Calcineurin is associated with the cytoskeleton of cultured neurons and has a role in the acquisition of polarity. Mol Biol Cell 4:1225-1238.1993).
Figueiredo C, Pais TF, Gomes JR, Chatterjee S (Neuron-microglia crosstalk up-regulates neuronal FGF-2 expression which mediates neuroprotection against excitotoxicity via JNK1/2. J Neurochem 107:73-85.2008).
Figueredo-Cardenas G, Chen Q, Reiner A (Age-dependent differences in survival of striatal somatostatin-NPY-NADPH-diaphorase-containing interneurons versus striatal projection neurons after intrastriatal injection of quinolinic acid in rats. Exp Neurol 146:444-457.1997).
Fischer G, Kettenmann H (Cultured astrocytes form a syncytium after maturation. Exp Cell Res 159:273-279.1985).
Foster AC, White RJ, Schwarcz R (Synthesis of quinolinic acid by 3-hydroxyanthranilic acid oxygenase in rat brain tissue in vitro. J Neurochem 47:23-30.1986).
Freund WD, Reddig S (AMPA/Zn(2+)-induced neurotoxicity in rat primary cortical cultures: involvement of L-type calcium channels. Brain Res 654:257-264.1994).

Friede RL, Samorajski T (Axon caliber related to neurofilaments and microtubules in sciatic nerve fibers of rats and mice. Anat Rec 167:379-387.1970).
Fuchs E (Intermediate filaments and disease: mutations that cripple cell strength. J Cell Biol 125:511-516.1994).
Fuchs E, Cleveland DW (A structural scaffolding of intermediate filaments in health and disease. Science 279:514-519.1998).
Galeotti N, Quattrone A, Vivoli E, Norcini M, Bartolini A, Ghelardini C (Different involvement of type 1, 2, and 3 ryanodine receptors in memory processes. Learn Mem 15:315-323.2008).
Geisler N, Vandekerckhove J, Weber K (Location and sequence characterization of the major phosphorylation sites of the high molecular mass neurofilament proteins M and H. FEBS Lett 221:403-407.1987).
Giaume C, McCarthy KD (Control of gap-junctional communication in astrocytic networks. Trends Neurosci 19:319-325.1996).
Gill SR, Wong PC, Monteiro MJ, Cleveland DW (Assembly properties of dominant and recessive mutations in the small mouse neurofilament (NF-L) subunit. J Cell Biol 111:2005-2019.1990).
Glass CK, Saijo K, Winner B, Marchetto MC, Gage FH (Mechanisms underlying inflammation in neurodegeneration. Cell 140:918-934.2010).
Goda K, Kishimoto R, Shimizu S, Hamane Y, Ueda M (Quinolinic acid and active oxygens. Possible contribution of active Oxygens during cell death in the brain. Adv Exp Med Biol 398:247-254.1996).
Goedert M (Neurofibrillary pathology of Alzheimer's disease and other tauopathies. Prog Brain Res 117:287-306.1998).
Goldstein ME, Sternberger NH, Sternberger LA (Phosphorylation protects neurofilaments against proteolysis. J Neuroimmunol 14:149-160.1987).
Gonzalez-Alegre P, Afifi AK (Clinical characteristics of childhood-onset (juvenile) Huntington disease: report of 12 patients and review of the literature. J Child Neurol 21:223-229.2006).
Goto H, Kosako H, Tanabe K, Yanagida M, Sakurai M, Amano M, Kaibuchi K, Inagaki M (Phosphorylation of vimentin by Rho-associated kinase at a unique amino-terminal site that is specifically phosphorylated during cytokinesis. J Biol Chem 273:11728-11736.1998).
Gotow T (Neurofilaments in health and disease. Med Electron Microsc 33:173-199.2000).
Gotow T, Takeda M, Tanaka T, Hashimoto PH (Macromolecular structure of reassembled neurofilaments as revealed by the quick-freeze deep-etch mica method: difference between NF-M and NF-H subunits in their ability to form cross-bridges. Eur J Cell Biol 58:331-345.1992).
Gourlay CW, Ayscough KR (A role for actin in aging and apoptosis. Biochem Soc Trans 33:1260-1264.2005).
Green KJ, Bohringer M, Gocken T, Jones JC (Intermediate filament associated proteins. Adv Protein Chem 70:143-202.2005).

Greenwood SM, Connolly CN (Dendritic and mitochondrial changes during glutamate excitotoxicity. Neuropharmacology 53:891-898.2007).
Guidetti P, Luthi-Carter RE, Augood SJ, Schwarcz R (Neostriatal and cortical quinolinate levels are increased in early grade Huntington's disease. Neurobiol Dis 17:455-461.2004).
Guidetti P, Schwarcz R (3-Hydroxykynurenine and quinolinate: pathogenic synergism in early grade Huntington's disease? Adv Exp Med Biol 527:137-145.2003).
Guillemin GJ, Wang L, Brew BJ (Quinolinic acid selectively induces apoptosis of human astrocytes: potential role in AIDS dementia complex. J Neuroinflammation 2:16.2005).
Guncova I, Latr I, Mazurova Y (The neurodegenerative process in a neurotoxic rat model and in patients with Huntington's disease: histopathological parallels and differences. Acta Histochem 113:783-792.2010).
Haberny KA, Paule MG, Scallet AC, Sistare FD, Lester DS, Hanig JP, Slikker W, Jr. (Ontogeny of the N-methyl-D-aspartate (NMDA) receptor system and susceptibility to neurotoxicity. Toxicol Sci 68:9-17.2002).
Hakansson K, Lindskog M, Pozzi L, Usiello A, Fisone G (DARPP-32 and modulation of cAMP signaling: involvement in motor control and levodopa-induced dyskinesia. Parkinsonism Relat Disord 10:281-286.2004).
Halassa MM, Haydon PG (Integrated brain circuits: astrocytic networks modulate neuronal activity and behavior. Annu Rev Physiol 72:335-355.2010).
Hanani M, Huang TY, Cherkas PS, Ledda M, Pannese E (Glial cell plasticity in sensory ganglia induced by nerve damage. Neuroscience 114:279-283.2002).
Hanisch UK, Kettenmann H (Microglia: active sensor and versatile effector cells in the normal and pathologic brain. Nat Neurosci 10:1387-1394.2007).
Hazrati LN, Kleinschmidt-DeMasters BK, Handler MH, Smith ML, Ochi A, Otsubo H, Rutka JT, Go C, Weiss S, Hawkins CE (Astrocytic inclusions in epilepsy: expanding the spectrum of filaminopathies. J Neuropathol Exp Neurol 67:669-676.2008).
Heimfarth L, Loureiro SO, Reis KP, de Lima BO, Zamboni F, Lacerda S, Soska AK, Wild L, da Rocha JB, Pessoa-Pureur R (Diphenyl ditelluride induces hypophosphorylation of intermediate filaments through modulation of DARPP-32-dependent pathways in cerebral cortex of young rats. Arch Toxicol 86:217-230.2012).
Heins S, Wong PC, Muller S, Goldie K, Cleveland DW, Aebi U (The rod domain of NF-L determines neurofilament architecture, whereas the end domains specify filament assembly and network formation. J Cell Biol 123:1517-1533.1993).
Helfand BT, Chou YH, Shumaker DK, Goldman RD (Intermediate filament proteins participate in signal transduction. Trends Cell Biol 15:568-570.2005).
Hermans E, Challiss RA (Structural, signalling and regulatory properties of the group I metabotropic glutamate receptors: prototypic family C G-protein-coupled receptors. Biochem J 359:465-484.2001).

Herrmann H, Aebi U (Intermediate filaments and their associates: multi-talented structural elements specifying cytoarchitecture and cytodynamics. Curr Opin Cell Biol 12:79-90.2000).
Herrmann H, Bar H, Kreplak L, Strelkov SV, Aebi U (Intermediate filaments: from cell architecture to nanomechanics. Nat Rev Mol Cell Biol 8:562-573.2007).
Hestrin S (Developmental regulation of NMDA receptor-mediated synaptic currents at a central synapse. Nature 357:686-689.1992).
Heyes MP (Quinolinic acid and inflammation. Ann N Y Acad Sci 679:211-216.1993).
Heyes MP, Saito K, Chen CY, Proescholdt MG, Nowak TS, Jr., Li J, Beagles KE, Proescholdt MA, Zito MA, Kawai K, Markey SP (Species heterogeneity between gerbils and rats: quinolinate production by microglia and astrocytes and accumulations in response to ischemic brain injury and systemic immune activation. J Neurochem 69:1519-1529.1997).
Hisanaga S, Gonda Y, Inagaki M, Ikai A, Hirokawa N (Effects of phosphorylation of the neurofilament L protein on filamentous structures. Cell Regul 1:237-248.1990).
Hollenbeck P (Cytoskeleton: Microtubules get the signal. Curr Biol 11:R820-823.2001).
Hollmann M, Heinemann S (Cloned glutamate receptors. Annu Rev Neurosci 17:31-108.1994).
Holmgren A, Bouhy D, Timmerman V (Neurofilament phosphorylation and their proline-directed kinases in health and disease. J Peripher Nerv Syst 17:365-376.2012).
Huang KP (The mechanism of protein kinase C activation. Trends Neurosci 12:425-432.1989).
Iino M, Goto K, Kakegawa W, Okado H, Sudo M, Ishiuchi S, Miwa A, Takayasu Y, Saito I, Tsuzuki K, Ozawa S (Glia-synapse interaction through Ca2+-permeable AMPA receptors in Bergmann glia. Science 292:926-929.2001).
Inada H, Togashi H, Nakamura Y, Kaibuchi K, Nagata K, Inagaki M (Balance between activities of Rho kinase and type 1 protein phosphatase modulates turnover of phosphorylation and dynamics of desmin/vimentin filaments. J Biol Chem 274:34932-34939.1999).
Inagaki M, Gonda Y, Nishizawa K, Kitamura S, Sato C, Ando S, Tanabe K, Kikuchi K, Tsuiki S, Nishi Y (Phosphorylation sites linked to glial filament disassembly in vitro locate in a non-alpha-helical head domain. J Biol Chem 265:4722-4729.1990).
Ito M, Natsume A, Takeuchi H, Shimato S, Ohno M, Wakabayashi T, Yoshida J (Type I interferon inhibits astrocytic gliosis and promotes functional recovery after spinal cord injury by deactivation of the MEK/ERK pathway. J Neurotrauma 26:41-53.2009).
Jaffe H, Veeranna, Pant HC (Characterization of serine and threonine phosphorylation sites in beta-elimination/ethanethiol addition-modified proteins by electrospray tandem mass spectrometry and database searching. Biochemistry 37:16211-16224.1998).

Johnson LN (The regulation of protein phosphorylation. Biochem Soc Trans 37:627-641.2009).
Julien JP (Neurofilament functions in health and disease. Curr Opin Neurobiol 9:554-560.1999).
Jung C, Yabe JT, Lee S, Shea TB (Hypophosphorylated neurofilament subunits undergo axonal transport more rapidly than more extensively phosphorylated subunits in situ. Cell Motil Cytoskeleton 47:120-129.2000).
Juranek JK, Geddis MS, Rosario R, Schmidt AM (Impaired slow axonal transport in diabetic peripheral nerve is independent of RAGE. Eur J Neurosci 38:3159-3168.2013).
Kalaria RN (Cerebral endothelial activation and signal transduction mechanisms during inflammation and infectious disease. Am J Pathol 154:1311-1314.1999).
Kang SS, Keasey MP, Cai J, Hagg T (Loss of neuron-astroglial interaction rapidly induces protective CNTF expression after stroke in mice. J Neurosci 32:9277-9287.2012).
Kantor O, Temel Y, Holzmann C, Raber K, Nguyen HP, Cao C, Turkoglu HO, Rutten BP, Visser-Vandewalle V, Steinbusch HW, Blokland A, Korr H, Riess O, von Horsten S, Schmitz C (Selective striatal neuron loss and alterations in behavior correlate with impaired striatal function in Huntington's disease transgenic rats. Neurobiol Dis 22:538-547.2006).
Kayyali US, Zhang W, Yee AG, Seidman JG, Potter H (Cytoskeletal changes in the brains of mice lacking calcineurin A alpha. J Neurochem 68:1668-1678.1997).
Kerr SJ, Armati PJ, Guillemin GJ, Brew BJ (Chronic exposure of human neurons to quinolinic acid results in neuronal changes consistent with AIDS dementia complex. AIDS 12:355-363.1998).
Kesavapany S, Amin N, Zheng YL, Nijhara R, Jaffe H, Sihag R, Gutkind JS, Takahashi S, Kulkarni A, Grant P, Pant HC (p35/cyclin-dependent kinase 5 phosphorylation of ras guanine nucleotide releasing factor 2 (RasGRF2) mediates Rac-dependent Extracellular Signal-regulated kinase 1/2 activity, altering RasGRF2 and microtubule-associated protein 1b distribution in neurons. J Neurosci 24:4421-4431.2004).
Kesavapany S, Pareek TK, Zheng YL, Amin N, Gutkind JS, Ma W, Kulkarni AB, Grant P, Pant HC (Neuronal nuclear organization is controlled by cyclin-dependent kinase 5 phosphorylation of Ras Guanine nucleotide releasing factor-1. Neurosignals 15:157-173.2006).
Kim JP, Choi DW (Quinolinate neurotoxicity in cortical cell culture. Neuroscience 23:423-432.1987).
Kirby ED, Muroy SE, Sun WG, Covarrubias D, Leong MJ, Barchas LA, Kaufer D (Acute stress enhances adult rat hippocampal neurogenesis and activation of newborn neurons via secreted astrocytic FGF2. Elife 2:e00362.2013).
Kirkpatrick LL, Brady ST (Cytoskeleton of neurons and glia. Basic neurochemistry-Molecular, celular and medical aspects 6 ed.:155-173.1999).
Koenig E (Cell Biology of the axon. Springer Berlin Heidelberg, 2009.2009).

Kohler C, Eriksson LG, Okuno E, Schwarcz R (Localization of quinolinic acid metabolizing enzymes in the rat brain. Immunohistochemical studies using antibodies to 3-hydroxyanthranilic acid oxygenase and quinolinic acid phosphoribosyltransferase. Neuroscience 27:49-76.1988).

Komeima K, Hayashi Y, Naito Y, Watanabe Y (Inhibition of neuronal nitric-oxide synthase by calcium/ calmodulin-dependent protein kinase IIalpha through Ser847 phosphorylation in NG108-15 neuronal cells. J Biol Chem 275:28139-28143.2000).

Konur S, Ghosh A (Calcium signaling and the control of dendritic development. Neuron 46:401-405.2005).

Kornyei Z, Szlavik V, Szabo B, Gocza E, Czirok A, Madarasz E (Humoral and contact interactions in astroglia/stem cell co-cultures in the course of glia-induced neurogenesis. Glia 49:430-444.2005).

Krieger C, Lanius RA, Pelech SL, Shaw CA (Amyotrophic lateral sclerosis: the involvement of intracellular Ca2+ and protein kinase C. Trends Pharmacol Sci 17:114-120.1996).

Kumar U (Somatostatin in medium-sized aspiny interneurons of striatum is responsible for their preservation in quinolinic acid and N-methyl-D-asparate-induced neurotoxicity. J Mol Neurosci 35:345-354.2008).

Lafon-Cazal M, Pietri S, Culcasi M, Bockaert J (NMDA-dependent superoxide production and neurotoxicity. Nature 364:535-537.1993).

Lee MK, Cleveland DW (Neuronal intermediate filaments. Annu Rev Neurosci 19:187-217.1996).

Lee MS, Kwon YT, Li M, Peng J, Friedlander RM, Tsai LH (Neurotoxicity induces cleavage of p35 to p25 by calpain. Nature 405:360-364.2000).

Letourneau PC (The cytoskeleton in nerve growth cone motility and axonal pathfinding. Perspect Dev Neurobiol 4:111-123.1996).

Li BS, Veeranna, Grant P, Pant HC (Calcium influx and membrane depolarization induce phosphorylation of neurofilament (NF-M) KSP repeats in PC12 cells. Brain Res Mol Brain Res 70:84-91.1999).

Li BS, Zhang L, Gu J, Amin ND, Pant HC (Integrin alpha(1) beta(1)-mediated activation of cyclin-dependent kinase 5 activity is involved in neurite outgrowth and human neurofilament protein H Lys-Ser-Pro tail domain phosphorylation. J Neurosci 20:6055-6062.2000).

Lipscombe D, Helton TD, Xu W (L-type calcium channels: the low down. J Neurophysiol 92:2633-2641.2004).

Liu B, Dong Q, Zhang S, Su D, Yang Z, Lv M (mGluR1,5 activation protects cortical astrocytes and GABAergic neurons from ischemia-induced impairment. Neurosci Res 75:160-166.2013).

Loureiro SO, Heimfarth L, Lacerda BA, Vidal LF, Soska A, dos Santos NG, de Souza Wyse AT, Pessoa-Pureur R (Homocysteine induces hypophosphorylation of intermediate filaments and reorganization of actin cytoskeleton in C6 glioma cells. Cell Mol Neurobiol 30:557-568.2010a).

Loureiro SO, Heimfarth L, Pelaez Pde L, Lacerda BA, Vidal LF, Soska A, Santos NG, Andrade C, Tagliari B, Scherer EB, Guma FT, Wyse AT, Pessoa-Pureur R (Hyperhomocysteinemia selectively alters expression and stoichiometry of intermediate filament and induces glutamate- and calcium-mediated mechanisms in rat brain during development. Int J Dev Neurosci 28:21-30.2009).

Loureiro SO, Heimfarth L, Scherer EB, da Cunha MJ, de Lima BO, Biasibetti H, Pessoa-Pureur R, Wyse AT (Cytoskeleton of cortical astrocytes as a target to proline through oxidative stress mechanisms. Exp Cell Res 319:89-104.2013).

Loureiro SO, Romao L, Alves T, Fonseca A, Heimfarth L, Moura Neto V, Wyse AT, Pessoa-Pureur R (Homocysteine induces cytoskeletal remodeling and production of reactive oxygen species in cultured cortical astrocytes. Brain Res 1355:151-164.2010b).

Ludin B, Matus A (The neuronal cytoskeleton and its role in axonal and dendritic plasticity. Hippocampus 3 Spec No:61-71.1993).

Magin TM, Hesse M, Meier-Bornheim R, Reichelt J (Developing mouse models to study intermediate filament function. Methods Cell Biol 78:65-94.2004).

Majewski H, Iannazzo L (Protein kinase C: a physiological mediator of enhanced transmitter output. Prog Neurobiol 55:463-475.1998).

Malenka RC (Synaptic plasticity in the hippocampus: LTP and LTD. Cell 78:535-538.1994).

Malenka RC, Nicoll RA (Long-term potentiation--a decade of progress? Science 285:1870-1874.1999).

Marco S, Giralt A, Petrovic MM, Pouladi MA, Martinez-Turrillas R, Martinez-Hernandez J, Kaltenbach LS, Torres-Peraza J, Graham RK, Watanabe M, Lujan R, Nakanishi N, Lipton SA, Lo DC, Hayden MR, Alberch J, Wesseling JF, Perez-Otano I (Suppressing aberrant GluN3A expression rescues synaptic and behavioral impairments in Huntington's disease models. Nat Med 19:1030-1038.2013).

Martin SS, Leder P (Human MCF10A mammary epithelial cells undergo apoptosis following actin depolymerization that is independent of attachment and rescued by Bcl-2. Mol Cell Biol 21:6529-6536.2001).

Massudi H, Grant R, Braidy N, Guest J, Farnsworth B, Guillemin GJ (Age-associated changes in oxidative stress and NAD+ metabolism in human tissue. PLoS One 7:e42357.2012).

Mattson MP (Cellular signaling mechanisms common to the development and degeneration of neuroarchitecture. A review. Mech Ageing Dev 50:103-157.1989).

Mattson MP (Calcium and neurodegeneration. Aging Cell 6:337-350.2007).

Mattson MP, Scheff SW (Endogenous neuroprotection factors and traumatic brain injury: mechanisms of action and implications for therapy. J Neurotrauma 11:3-33.1994).

McGeer PL, Kawamata T, Walker DG, Akiyama H, Tooyama I, McGeer EG (Microglia in degenerative neurological disease. Glia 7:84-92.1993).
McGraw J, Hiebert GW, Steeves JD (Modulating astrogliosis after neurotrauma. J Neurosci Res 63:109-115.2001).
McKenna MC (The glutamate-glutamine cycle is not stoichiometric: fates of glutamate in brain. J Neurosci Res 85:3347-3358.2007).
Meberg PJ, Ono S, Minamide LS, Takahashi M, Bamburg JR (Actin depolymerizing factor and cofilin phosphorylation dynamics: response to signals that regulate neurite extension. Cell Motil Cytoskeleton 39:172-190.1998).
Meldrum BS (Glutamate as a neurotransmitter in the brain: review of physiology and pathology. J Nutr 130:1007S-1015S.2000).
Mennicken F, Maki R, de Souza EB, Quirion R (Chemokines and chemokine receptors in the CNS: a possible role in neuroinflammation and patterning. Trends Pharmacol Sci 20:73-78.1999).
Middeldorp J, Hol EM (GFAP in health and disease. Prog Neurobiol 93:421-443.2011).
Miller CC, Ackerley S, Brownlees J, Grierson AJ, Jacobsen NJ, Thornhill P (Axonal transport of neurofilaments in normal and disease states. Cell Mol Life Sci 59:323-330.2002).
Mizuno T ([Disruption of interactions between immunocytes, glia and neurons in demyelinating diseases: a view from neuroscience]. Rinsho Shinkeigaku 51:892-893.2011).
Montero M, Alonso MT, Carnicero E, Cuchillo-Ibanez I, Albillos A, Garcia AG, Garcia-Sancho J, Alvarez J (Chromaffin-cell stimulation triggers fast millimolar mitochondrial Ca2+ transients that modulate secretion. Nat Cell Biol 2:57-61.2000).
Monyer H, Seeburg PH, Wisden W (Glutamate-operated channels: developmentally early and mature forms arise by alternative splicing. Neuron 6:799-810.1991).
Morris JR, Lasek RJ (Monomer-polymer equilibria in the axon: direct measurement of tubulin and actin as polymer and monomer in axoplasm. J Cell Biol 98:2064-2076.1984).
Motil J, Chan WK, Dubey M, Chaudhury P, Pimenta A, Chylinski TM, Ortiz DT, Shea TB (Dynein mediates retrograde neurofilament transport within axons and anterograde delivery of NFs from perikarya into axons: regulation by multiple phosphorylation events. Cell Motil Cytoskeleton 63:266-286.2006).
Munoz-Sanjuan I, Bates GP (The importance of integrating basic and clinical research toward the development of new therapies for Huntington disease. J Clin Invest 121:476-483.2011).
Nadella KS, Saji M, Jacob NK, Pavel E, Ringel MD, Kirschner LS (Regulation of actin function by protein kinase A-mediated phosphorylation of Limk1. EMBO Rep 10:599-605.2009).
Nakamura Y, Takeda M, Aimoto S, Hojo H, Takao T, Shimonishi Y, Hariguchi S, Nishimura T (Assembly regulatory domain of glial fibrillary acidic protein. A

single phosphorylation diminishes its assembly-accelerating property. J Biol Chem 267:23269-23274.1992).
Nance MA, Myers RH (Juvenile onset Huntington's disease--clinical and research perspectives. Ment Retard Dev Disabil Res Rev 7:153-157.2001).
Nedergaard M, Ransom B, Goldman SA (New roles for astrocytes: redefining the functional architecture of the brain. Trends Neurosci 26:523-530.2003).
Nishita M, Wang Y, Tomizawa C, Suzuki A, Niwa R, Uemura T, Mizuno K (Phosphoinositide 3-kinase-mediated activation of cofilin phosphatase Slingshot and its role for insulin-induced membrane protrusion. J Biol Chem 279:7193-7198.2004).
Oh MC, Derkach VA (Dominant role of the GluR2 subunit in regulation of AMPA receptors by CaMKII. Nat Neurosci 8:853-854.2005).
Oliveira JM (Mitochondrial bioenergetics and dynamics in Huntington's disease: tripartite synapses and selective striatal degeneration. J Bioenerg Biomembr 42:227-234.2010).
Omary MB, Coulombe PA, McLean WH (Intermediate filament proteins and their associated diseases. N Engl J Med 351:2087-2100.2004).
Omary MB, Ku NO, Tao GZ, Toivola DM, Liao J ("Heads and tails" of intermediate filament phosphorylation: multiple sites and functional insights. Trends Biochem Sci 31:383-394.2006).
Ozawa S, Kamiya H, Tsuzuki K (Glutamate receptors in the mammalian central nervous system. Prog Neurobiol 54:581-618.1998).
Pagliusi SR, Gerrard P, Abdallah M, Talabot D, Catsicas S (Age-related changes in expression of AMPA-selective glutamate receptor subunits: is calcium-permeability altered in hippocampal neurons? Neuroscience 61:429-433.1994).
Pant HC (Dephosphorylation of neurofilament proteins enhances their susceptibility to degradation by calpain. Biochem J 256:665-668.1988).
Patrick GN, Zukerberg L, Nikolic M, de la Monte S, Dikkes P, Tsai LH (Conversion of p35 to p25 deregulates Cdk5 activity and promotes neurodegeneration. Nature 402:615-622.1999).
Pavese N, Gerhard A, Tai YF, Ho AK, Turkheimer F, Barker RA, Brooks DJ, Piccini P (Microglial activation correlates with severity in Huntington disease: a clinical and PET study. Neurology 66:1638-1643.2006).
Pekny M, Johansson CB, Eliasson C, Stakeberg J, Wallen A, Perlmann T, Lendahl U, Betsholtz C, Berthold CH, Frisen J (Abnormal reaction to central nervous system injury in mice lacking glial fibrillary acidic protein and vimentin. J Cell Biol 145:503-514.1999).
Pekny M, Nilsson M (Astrocyte activation and reactive gliosis. Glia 50:427-434.2005).
Pekny M, Pekna M (Astrocyte intermediate filaments in CNS pathologies and regeneration. J Pathol 204:428-437.2004).
Pemberton LA, Kerr SJ, Brew BJ (HIV-1 gp120 does not induce Quinolinic acid production by macrophages. J Neurovirol 3:86-87.1997).

Perea G, Araque A (Glial calcium signaling and neuron-glia communication. Cell Calcium 38:375-382.2005).

Perez-De La Cruz V, Carrillo-Mora P, Santamaria A (Quinolinic Acid, an endogenous molecule combining excitotoxicity, oxidative stress and other toxic mechanisms. Int J Tryptophan Res 5:1-8.2012).

Perez-De La Cruz V, Konigsberg M, Santamaria A (Kynurenine pathway and disease: an overview. CNS Neurol Disord Drug Targets 6:398-410.2007).

Perrot R, Eyer J (Neuronal intermediate filaments and neurodegenerative disorders. Brain Res Bull 80:282-295.2009).

Petzold A (Neurofilament phosphoforms: surrogate markers for axonal injury, degeneration and loss. J Neurol Sci 233:183-198.2005).

Pierozan P, Zamoner A, Soska AK, de Lima BO, Reis KP, Zamboni F, Wajner M, Pessoa-Pureur R (Signaling mechanisms downstream of quinolinic acid targeting the cytoskeleton of rat striatal neurons and astrocytes. Exp Neurol 233:391-399.2012).

Pierozan P, Zamoner A, Soska AK, Silvestrin RB, Loureiro SO, Heimfarth L, Mello e Souza T, Wajner M, Pessoa-Pureur R (Acute intrastriatal administration of quinolinic acid provokes hyperphosphorylation of cytoskeletal intermediate filament proteins in astrocytes and neurons of rats. Exp Neurol 224:188-196.2010).

Puentes F, Topping J, Kuhle J, van der Star BJ, Douiri A, Giovannoni G, Baker D, Amor S, Malaspina A (Immune reactivity to neurofilament proteins in the clinical staging of amyotrophic lateral sclerosis. J Neurol Neurosurg Psychiatry 85:274-278.2014).

Ralton JE, Lu X, Hutcheson AM, Quinlan RA (Identification of two N-terminal non-alpha-helical domain motifs important in the assembly of glial fibrillary acidic protein. J Cell Sci 107 (Pt 7):1935-1948.1994).

RamaRao G, Bhattacharya BK (Multiple signal transduction pathways alterations during nerve agent toxicity. Toxicol Lett 208:16-22.2012).

Ransome MI, Renoir T, Hannan AJ (Hippocampal neurogenesis, cognitive deficits and affective disorder in Huntington's disease. Neural Plast 2012:874387.2012).

Rasmussen A, Macias R, Yescas P, Ochoa A, Davila G, Alonso E (Huntington disease in children: genotype-phenotype correlation. Neuropediatrics 31:190-194.2000).

Rohlmann A, Laskawi R, Hofer A, Dobo E, Dermietzel R, Wolff JR (Facial nerve lesions lead to increased immunostaining of the astrocytic gap junction protein (connexin 43) in the corresponding facial nucleus of rats. Neurosci Lett 154:206-208.1993).

Rouach N, Glowinski J, Giaume C (Activity-dependent neuronal control of gap-junctional communication in astrocytes. J Cell Biol 149:1513-1526.2000).

Rouach N, Koulakoff A, Giaume C (Neurons set the tone of gap junctional communication in astrocytic networks. Neurochem Int 45:265-272.2004).

Rouach N, Tence M, Glowinski J, Giaume C (Costimulation of N-methyl-D-aspartate and muscarinic neuronal receptors modulates gap junctional communication in striatal astrocytes. Proc Natl Acad Sci U S A 99:1023-1028.2002).

Rozemuller JM, Eikelenboom P, Pals ST, Stam FC (Microglial cells around amyloid plaques in Alzheimer's disease express leucocyte adhesion molecules of the LFA-1 family. Neurosci Lett 101:288-292.1989).

Ruddick JP, Evans AK, Nutt DJ, Lightman SL, Rook GA, Lowry CA (Tryptophan metabolism in the central nervous system: medical implications. Expert Rev Mol Med 8:1-27.2006).

Ryu JK, Choi HB, McLarnon JG (Peripheral benzodiazepine receptor ligand PK11195 reduces microglial activation and neuronal death in quinolinic acid-injected rat striatum. Neurobiol Dis 20:550-561.2005).

Sanchez C, Diaz-Nido J, Avila J (Phosphorylation of microtubule-associated protein 2 (MAP2) and its relevance for the regulation of the neuronal cytoskeleton function. Prog Neurobiol 61:133-168.2000).

Sanelli T, Ge W, Leystra-Lantz C, Strong MJ (Calcium mediated excitotoxicity in neurofilament aggregate-bearing neurons in vitro is NMDA receptor dependant. J Neurol Sci 256:39-51.2007).

Sapp E, Kegel KB, Aronin N, Hashikawa T, Uchiyama Y, Tohyama K, Bhide PG, Vonsattel JP, DiFiglia M (Early and progressive accumulation of reactive microglia in the Huntington disease brain. J Neuropathol Exp Neurol 60:161-172.2001).

Sattler R, Tymianski M (Molecular mechanisms of calcium-dependent excitotoxicity. J Mol Med (Berl) 78:3-13.2000).

Schipke CG, Ohlemeyer C, Matyash M, Nolte C, Kettenmann H, Kirchhoff F (Astrocytes of the mouse neocortex express functional N-methyl-D-aspartate receptors. FASEB J 15:1270-1272.2001).

Schmalenbach C, Muller HW (Astroglia-neuron interactions that promote long-term neuronal survival. J Chem Neuroanat 6:229-237.1993).

Schwab Y, Mouton J, Chasserot-Golaz S, Marty I, Maulet Y, Jover E (Calcium-dependent translocation of synaptotagmin to the plasma membrane in the dendrites of developing neurones. Brain Res Mol Brain Res 96:1-13.2001).

Schwarcz R, Bruno JP, Muchowski PJ, Wu HQ (Kynurenines in the mammalian brain: when physiology meets pathology. Nat Rev Neurosci 13:465-477.2012).

Schwarcz R, Guidetti P, Sathyasaikumar KV, Muchowski PJ (Of mice, rats and men: Revisiting the quinolinic acid hypothesis of Huntington's disease. Prog Neurobiol 90:230-245.2010).

Scott JD, Soderling TR (Serine/threonine protein kinases. Curr Opin Neurobiol 2:289-295.1992).

Scott RW, Olson MF (LIM kinases: function, regulation and association with human disease. J Mol Med (Berl) 85:555-568.2007).

Shea TB, Chan WK (Regulation of neurofilament dynamics by phosphorylation. Eur J Neurosci 27:1893-1901.2008).

Shelbourne P, Coote E, Dadak S, Cobb SR (Normal electrical properties of hippocampal neurons modelling early Huntington disease pathogenesis. Brain Res 1139:226-234.2007).

Sihag RK, Inagaki M, Yamaguchi T, Shea TB, Pant HC (Role of phosphorylation on the structural dynamics and function of types III and IV intermediate filaments. Exp Cell Res 313:2098-2109.2007).

Sihag RK, Nixon RA (Phosphorylation of the amino-terminal head domain of the middle molecular mass 145-kDa subunit of neurofilaments. Evidence for regulation by second messenger-dependent protein kinases. J Biol Chem 265:4166-4171.1990).

Silver J, Miller JH (Regeneration beyond the glial scar. Nat Rev Neurosci 5:146-156.2004).

Smith DG, Guillemin GJ, Pemberton L, Kerr S, Nath A, Smythe GA, Brew BJ (Quinolinic acid is produced by macrophages stimulated by platelet activating factor, Nef and Tat. J Neurovirol 7:56-60.2001).

Smith SJ (Neural signalling. Neuromodulatory astrocytes. Curr Biol 4:807-810.1994).

Sofroniew MV (Reactive astrocytes in neural repair and protection. Neuroscientist 11:400-407.2005).

Sofroniew MV (Molecular dissection of reactive astrogliosis and glial scar formation. Trends Neurosci 32:638-647.2009).

Sprengel R, Seeburg PH (The unique properties of glutamate receptor channels. FEBS Lett 325:90-94.1993).

Steiner D, Saya D, Schallmach E, Simonds WF, Vogel Z (Adenylyl cyclase type-VIII activity is regulated by G(betagamma) subunits. Cell Signal 18:62-68.2006).

Stipek S, Stastny F, Platenik J, Crkovska J, Zima T (The effect of quinolinate on rat brain lipid peroxidation is dependent on iron. Neurochem Int 30:233-237.1997).

Stone TW, Stoy N, Darlington LG (An expanding range of targets for kynurenine metabolites of tryptophan. Trends Pharmacol Sci 34:136-143.2013).

Su W, Chen HB, Li SH, Wu DY (Correlational study of the serum levels of the glial fibrillary acidic protein and neurofilament proteins in Parkinson's disease patients. Clin Neurol Neurosurg 114:372-375.2012).

Sumi T, Matsumoto K, Takai Y, Nakamura T (Cofilin phosphorylation and actin cytoskeletal dynamics regulated by rho- and Cdc42-activated LIM-kinase 2. J Cell Biol 147:1519-1532.1999).

Sun Z, Chen Q, Reiner A (Enkephalinergic striatal projection neurons become less affected by quinolinic acid than substance P-containing striatal projection neurons as rats age. Exp Neurol 184:1034-1042.2003).

Szeverenyi I, Cassidy AJ, Chung CW, Lee BT, Common JE, Ogg SC, Chen H, Sim SY, Goh WL, Ng KW, Simpson JA, Chee LL, Eng GH, Li B, Lunny DP, Chuon D, Venkatesh A, Khoo KH, McLean WH, Lim YP, Lane EB (The Human Intermediate Filament Database: comprehensive information on a gene family involved in many human diseases. Hum Mutat 29:351-360.2008).

Szydlowska K, Tymianski M (Calcium, ischemia and excitotoxicity. Cell Calcium 47:122-129.2010).

Takano H, Sul JY, Mazzanti ML, Doyle RT, Haydon PG, Porter MD (Micropatterned substrates: approach to probing intercellular communication pathways. Anal Chem 74:4640-4646.2002).

Takikawa O, Yoshida R, Kido R, Hayaishi O (Tryptophan degradation in mice initiated by indoleamine 2,3-dioxygenase. J Biol Chem 261:3648-3653.1986).

Tavares RG, Schmidt AP, Tasca CI, Souza DO (Quinolinic acid-induced seizures stimulate glutamate uptake into synaptic vesicles from rat brain: effects prevented by guanine-based purines. Neurochem Res 33:97-102.2008).

Tikka TM, Koistinaho JE (Minocycline provides neuroprotection against N-methyl-D-aspartate neurotoxicity by inhibiting microglia. J Immunol 166:7527-7533.2001).

Ting KK, Brew BJ, Guillemin GJ (Effect of quinolinic acid on human astrocytes morphology and functions: implications in Alzheimer's disease. J Neuroinflammation 6:36.2009).

Topper R, Gehrmann J, Schwarz M, Block F, Noth J, Kreutzberg GW (Remote microglial activation in the quinolinic acid model of Huntington's disease. Exp Neurol 123:271-283.1993).

Tymianski M (Cytosolic calcium concentrations and cell death in vitro. Adv Neurol 71:85-105.1996).

Tymianski M, Tator CH (Normal and abnormal calcium homeostasis in neurons: a basis for the pathophysiology of traumatic and ischemic central nervous system injury. Neurosurgery 38:1176-1195.1996).

Ubersax JA, Ferrell JE, Jr. (Mechanisms of specificity in protein phosphorylation. Nat Rev Mol Cell Biol 8:530-541.2007).

Unschuld PG, Edden RA, Carass A, Liu X, Shanahan M, Wang X, Oishi K, Brandt J, Bassett SS, Redgrave GW, Margolis RL, van Zijl PC, Barker PB, Ross CA (Brain metabolite alterations and cognitive dysfunction in early Huntington's disease. Mov Disord 27:895-902.2012).

van den Bogaard SJ, Dumas EM, Acharya TP, Johnson H, Langbehn DR, Scahill RI, Tabrizi SJ, van Buchem MA, van der Grond J, Roos RA (Early atrophy of pallidum and accumbens nucleus in Huntington's disease. J Neurol 258:412-420.2011).

van Rossum D, Hanisch UK (Microglia. Metab Brain Dis 19:393-411.2004).

Van Troys M, Huyck L, Leyman S, Dhaese S, Vandekerkhove J, Ampe C (Ins and outs of ADF/cofilin activity and regulation. Eur J Cell Biol 87:649-667.2008).

Veeranna, Shetty KT, Takahashi M, Grant P, Pant HC (Cdk5 and MAPK are associated with complexes of cytoskeletal proteins in rat brain. Brain Res Mol Brain Res 76:229-236.2000).

Villegas SN, Poletta FA, Carri NG (GLIA: A reassessment based on novel data on the developing and mature central nervous system. Cell Biol Int 27:599-609.2003).

Volterra A, Meldolesi J (Astrocytes, from brain glue to communication elements: the revolution continues. Nat Rev Neurosci 6:626-640.2005).

Vonsattel JP, DiFiglia M (Huntington disease. J Neuropathol Exp Neurol 57:369-384.1998).
Wang H, Jiang YW, Zhang WJ, Xu SQ, Liu HL, Yang WY, Lou JN (Differential activations of PKC/PKA related to microvasculopathy in diabetic GK rats. Am J Physiol Endocrinol Metab 302:E173-182.2012).
Wang LH, Qin ZH (Animal models of Huntington's disease: implications in uncovering pathogenic mechanisms and developing therapies. Acta Pharmacol Sin 27:1287-1302.2006).
Wenk GL, Walker LC, Price DL, Cork LC (Loss of NMDA, but not GABA-A, binding in the brains of aged rats and monkeys. Neurobiol Aging 12:93-98.1991).
Whetsell WO, Jr., Schwarcz R (Prolonged exposure to submicromolar concentrations of quinolinic acid causes excitotoxic damage in organotypic cultures of rat corticostriatal system. Neurosci Lett 97:271-275.1989).
Williams K, Russell SL, Shen YM, Molinoff PB (Developmental switch in the expression of NMDA receptors occurs in vivo and in vitro. Neuron 10:267-278.1993).
Wilson CJ, Chang HT, Kitai ST (Firing patterns and synaptic potentials of identified giant aspiny interneurons in the rat neostriatum. J Neurosci 10:508-519.1990).
Xia L, Zhai M, Wang L, Miao D, Zhu X, Wang W (FGF2 blocks PTSD symptoms via an astrocyte-based mechanism. Behav Brain Res 256:472-480.2013).
Xu ZS, Liu WS, Willard MB (Identification of six phosphorylation sites in the COOH-terminal tail region of the rat neurofilament protein M. J Biol Chem 267:4467-4471.1992).
Yabe JT, Chan WK, Chylinski TM, Lee S, Pimenta AF, Shea TB (The predominant form in which neurofilament subunits undergo axonal transport varies during axonal initiation, elongation, and maturation. Cell Motil Cytoskeleton 48:61-83.2001a).
Yabe JT, Wang FS, Chylinski T, Katchmar T, Shea TB (Selective accumulation of the high molecular weight neurofilament subunit within the distal region of growing axonal neurites. Cell Motil Cytoskeleton 50:1-12.2001b).
Zamoner A, Heimfarth L, Oliveira Loureiro S, Royer C, Mena Barreto Silva FR, Pessoa-Pureur R (Nongenomic actions of thyroxine modulate intermediate filament phosphorylation in cerebral cortex of rats. Neuroscience 156:640-652.2008).
Zhang S, Kuhn JR (Cell isolation and culture. WormBook 1-39.2013).